

Solution Properties of some Gaseous
Hydrocarbons in Water-Alkanol
Mixtures

by

Donald E Macphee BSc (HONS)

A thesis presented to the CNAA in
partial fulfilment of the
requirements for the degree of

Doctor of Philosophy

Dundee College of Technology

1983

Abstract of Thesis

The solubility of several hydrocarbon gases in water and in aqueous alcohol solvents has been measured in the temperature range 4-61 °C at a total pressure of one atmosphere, by a physical method based on the flowing film technique. Using standard procedures, $\Delta\bar{G}^\circ$, $\Delta\bar{H}^\circ$ and $\Delta\bar{S}^\circ$ of solution have been evaluated and expressed as functions of temperature and solvent composition. The observed variations in these functions and their dependence on temperature and alcohol concentration are then related to current theories of water structure also discussed here but with particular reference to hydrophobic interactions in the solution.

It is shown that the extent of these interactions can be observed in the isotherms of $\Delta\bar{H}^\circ$ and $\Delta\bar{S}^\circ$ at low concentrations of alcohol and a numerical method was used to estimate the magnitude of the hydrophobic contribution to the observed values of the functions themselves. The changes in these functions are then related to the sizes and shapes of the chosen solute molecules to provide a possible structural interpretation of the hydrophobic effect consistent with the observed experimental results.

TABLE OF CONTENTS

	Page
List of Tables	v
List of Figures	vii
List of Appendices	xi
Acknowledgements	xii
Abstract of Thesis	xiii
<u>Chapter 1</u> <u>INTRODUCTION</u>	2
Introduction	3
The Application of Gas Solubilities to Sturctural Studies	9
Choice of Solutes	12
<u>Chapter 2</u> <u>EXPERIMENTAL</u>	14
2.1 Types of Measurement	15
2.1.1 Extraction Methods	15
2.1.2 Saturation Methods	16
2.2 Equilibrium between the gas and its solution	16
2.2.1 Shaking a Mixture of the two	16
2.2.2 Flowing Thin Film of Solvent	16
2.2.3 Bubbling of Gas	17
2.2.4 Flowing the gas over a liquid held in a stationary support	17
2.3 Historical	17
2.4 The Flowing Film Technique	19
2.4.1 Principle of Operation	19
2.4.2 Apparatus Components and Functions	21
2.5 Recent Modifications	24
2.6 Purity of Materials	29

Table of Contents (Contd)

	Page
<u>Chapter 3</u> <u>THEORETICAL</u>	30
3.1 Symbols	31
3.2 Obtaining a Solubility Curve	33
3.3 Units and Treatment for Non-ideality	36
3.4 Relationship between $\log s_o$ and the Thermodynamic Functions	46
3.4.1 Standard States	47
3.4.2 Formulation of Thermodynamic Functions	47
3.5 Methods of Evaluation	51
<u>Chapter 4</u> <u>RESULTS</u>	57
4.1 Results	58
4.2 Solubility Curves	75
4.3 Solubility Isotherms	84
4.4 Thermodynamics Data	92
4.5 $\Delta \bar{G}^\circ$ Isotherms	105
4.6 $\Delta \bar{H}^\circ$ Isotherms	114
4.7 $\Delta \bar{S}^\circ$ Isotherms	123
<u>Chapter 5</u> <u>OBSERVATIONS</u>	132
5.1 General Observations	134
5.2 $\Delta \bar{H}^\circ$ and $\Delta \bar{S}^\circ$ Isotherms	143
<u>Chapter 6</u> <u>STRUCTURAL THEORIES OF WATER</u>	151
6.1 The Need for a Model	152
6.2 Models for the Structure of Liquid Water	154
6.2.1 Mixture Models	155
6.2.1.1 'Mixture of Structures' Model (1933)	155
6.2.1.2 'Mixture of States' Model (1962)	156
6.2.1.3 'Mixture of Structures' Model (1965)	158
6.2.2 The Continuum Model	159
6.2.3 The Band Model	161
6.2.4 Molecular Dynamics Calculations	163

Table of Contents (Contd)

	Page
6.3 The Hydrophobic Interaction	165
<u>Chapter 7</u> <u>DISCUSSION OF RESULTS</u>	182
7.1 Effect of Temperature	183
7.2 The Effect of the Alcohol	193
7.3 The Effect of the Solute	202
<u>Chapter 8</u> <u>CONCLUSIONS AND FUTURE DEVELOPMENTS</u>	212
 APPENDICES	 224
 REFERENCES	 235

LIST OF TABLES

		Page
<u>Chapter 3</u>	<u>THEORETICAL</u>	
Table 3.3.1	Calculation of BP, the deviation from ideality in the gas phase for some gaseous solutes at 277 K and 101.3 kPa	42
Table 3.3.2	Ratio of solute:solvent molecules in solution for each gas at conditions of highest solubility	45
Table 3.5.1	Numerical data to confirm the accuracy of a solubility curve	55
 <u>Chapter 4</u>	 <u>RESULTS</u>	
	Experimental Solubility Data for:	
Table 4.1.1	propane in mixtures of water and ethanol	59
Table 4.1.2	butane in mixtures of water and ethanol	61
Table 4.1.3	2-methylpropane in mixtures of water and ethanol	63
Table 4.1.4	2,2-dimethylpropane in mixtures of water and ethanol	65
Table 4.1.5	cyclopropane in mixtures of water and ethanol	67
Table 4.1.6	propene in mixtures of water and ethanol	69
Table 4.1.7	propane in mixtures of water and 2-methylpropan-2-ol	71
Table 4.1.8	butane in mixtures of water and 2-methylpropan-2-ol	73
	Tabulated Thermodynamic Data for the solubility of:	
Table 4.4.1	propane in water-ethanol solvents	93
Table 4.4.2	butane in water-ethanol solvents	95
Table 4.4.3	2-methylpropane in water-ethanol solvents	97
Table 4.4.4	2,2-dimethylpropane in water-ethanol solvents	98
Table 4.4.5	cyclopropane in water-ethanol solvents	99

List of Tables (Contd)

		Page
Table 4.4.6	propene in water-ethanol solvents	101
Table 4.4.7	propane in water-2-methylpropan-2-ol solvents	103
Table 4.4.8	butane in water-2-methylpropan-2-ol solvents	104
<u>Chapter 5</u>	<u>OBSERVATIONS</u>	
Table 5.1.1	Positions of graphical extrema on the solubility isotherms using aqueous ethanol	137
Table 5.1.2	Positions of graphical extrema on the solubility isotherms using aqueous ethanol and aqueous 2-methylpropan-2-ol	138
Table 5.1.3	Coefficients for fifth order polynomial to fit $\Delta\bar{G}^\circ$ isotherms	140
Table 5.1.4	Extent of graphical extrema	142
Table 5.2.1	Tabulated data to show the extent of unusual graphical features	148
<u>Chapter 7</u>	<u>DISCUSSION OF RESULTS</u>	
Table 7.1.1	$\Delta(\Delta\bar{X}^\circ)$ values from data of Cargill ^{3 22 27 28}	185
Table 7.1.2	$\Delta(\Delta\bar{X}^\circ)$ values for the solubility of the chosen hydrocarbons	186
Table 7.1.3	Calculated mole fractions of structured water as a fraction of temperature	188
Table 7.2.1	Mole fractions of ethanol for positions of extrema on the solubility isotherms for several gases	197
Table 7.2.2	$\Delta(\Delta\bar{X}^\circ)$ data for the solution of propane and butane in aqueous 2-methylpropan-2-ol	199
Table 7.3.1	Comparison of structure promoting ability of several solutes in water at 4.7 °C	204
Table 7.3.2	Calculated values of $\delta\Delta\bar{H}^\circ$ and $\delta\Delta\bar{S}^\circ$ for selected solutes in water	207

LIST OF FIGURES

	Page
<u>Chapter 2</u>	<u>EXPERIMENTAL</u>
Figure 2.4(i)	20
Figure 2.5(i)	26
<u>Chapter 3</u>	<u>THEORETICAL</u>
Figure 3.2(i)	34
Figure 3.2(ii)a	35
Figure 3.2(ii)b	35
Figure 3.5(i)	54
Figure 3.5(ii)	54
Plot of Volume of gas vs Mass of Solvent Solubility curve Solubility isotherms Plot of $\Delta \bar{H}^\circ$ vs T Plot of $\Delta \bar{H}_{290K}^\circ$, $\Delta \bar{H}_{310K}^\circ$, $\Delta \bar{C}_p < 300K$ and $\Delta \bar{C}_p > 300K$ all against solvent composition	
<u>Chapter 4</u>	<u>RESULTS</u>
Solubility curves for:	
Figure 4.2.1	76
Figure 4.2.2	77
Figure 4.2.3	78
Figure 4.2.4	79
Figure 4.2.5	80
Figure 4.2.6	81
Figure 4.2.7	82
Figure 4.2.8	83
Solubility isotherms for:	
Figure 4.3.1	85
Figure 4.3.2	86
Figure 4.3.3	87

List of Figures (Contd)

		Page
Figure 4.3.4	2,2-dimethylpropane in water-ethanol mixtures	88
Figure 4.3.5	cyclopropane in water-ethanol mixtures	89
Figure 4.3.6	propene in water-ethanol mixtures	90
Figure 4.3.7	propane and butane in 2-methylpropan-2-ol mixtures	91
	$\Delta \bar{G}^\circ$ isotherms for the solution of:	
Figure 4.5.1	propane in mixtures of water and ethanol	106
Figure 4.5.2	butane in mixtures of water and ethanol	107
Figure 4.5.3	2-methylpropane in mixtures of water and ethanol	108
Figure 4.5.4	2,2-dimethylpropane in mixtures of water and ethanol	109
Figure 4.5.5	cyclopropane in mixtures of water and ethanol	110
Figure 4.5.6	propene in mixtures of water and ethanol	111
Figure 4.5.7	propane in mixtures of water and 2-methylpropan-2-ol	112
Figure 4.5.8	butane in mixtures of water and 2-methylpropan-2-ol	113
	$\Delta \bar{H}^\circ$ isotherms for the solution of:	
Figure 4.6.1	propane in mixtures of water and ethanol	115
Figure 4.6.2	butane in mixtures of water and ethanol	116
Figure 4.6.3	2-methylpropane in mixtures of water and ethanol	117
Figure 4.6.4	2,2-dimethylpropane in mixtures of water and ethanol	118
Figure 4.6.5	cyclopropane in mixtures of water and ethanol	119
Figure 4.6.6	propene in mixtures of water and ethanol	120

List of Figures (Contd)

		Page
Figure 4.6.7	propane in mixtures of water and 2-methylpropan-2-ol	121
Figure 4.6.8	butane in mixtures of water and 2-methylpropan-2-ol	122
	$\Delta \bar{S}^\circ$ isotherms for the solution of:	
Figure 4.7.1	propane in mixtures of water and ethanol	124
Figure 4.7.2	butane in mixtures of water and ethanol	125
Figure 4.7.3	2-methylpropane in mixtures of water and ethanol	126
Figure 4.7.4	2,2-dimethylpropane in mixtures of water and ethanol	127
Figure 4.7.5	cyclopropane in mixtures of water and ethanol	128
Figure 4.7.6	propene in mixtures of water and ethanol	129
Figure 4.7.7	propane in mixtures of water and 2-methylpropan-2-ol	130
Figure 4.7.8	butane in mixtures of water and 2-methylpropan-2-ol	131
<u>Chapter 5</u>	<u>OBSERVATION</u>	
Figure 5.2.1	Models depicting the size and shape of the solute molecules	144
Figure 5.2.2	The effect of curvature or minima on the isotherms of $\Delta \bar{H}^\circ$	148
<u>Chapter 6</u>	<u>STRUCTURAL THEORIES FOR WATER</u>	
Figure 6.3.1	Schematic cross section of a hydrogen bonded water cluster near a hydrocarbon solute molecule	168
Figure 6.3.2	Schematic representation of the energy level changes occurring on transfer of water from the pure liquid to next to a non-polar solute	168

List of Figures (Contd)

	Page
Figure 6.3.3 Cyclic process to relate the hydrophobic effect to experimentally measured quantities	172
Figure 6.3.4 Variation of the strength of hydrophobic interaction with increasing ethanol concentration	172
Figure 6.3.5 Schematic process used to investigate intramolecular hydrophobic interactions	178
 <u>Chapter 7</u> <u>DISCUSSION OF RESULTS</u>	
Figure 7.1.1 Graphical illustration of the effect of temperature on water structure	189
Figure 7.1.2 Structural interpretation of the hydrophobic interaction	190
Figure 7.2 Typical $\Delta \bar{H}^\circ$ isotherm for high temperature showing effect of hydrophobic interactions	201

LIST OF APPENDICES

		Page
Appendix I	Data Collection Sheet	225
Appendix II	Applesoft program 'GRAPH' - used to evaluate solubilities	227
Appendix III(a)	Applesoft program 'MAKE CURVE' - used to construct a solubility curve	229
Appendix III(b)	Applesoft program 'CURVE TEST' - used to test the curve obtained in Appendix III(a)	230
Appendix IV	Algol program 'FINDH' - used to evaluate $\Delta \bar{H}^\circ$ for temperatures midway between integral $10^4/T$ values	232
Appendix V	Applesoft program 'CHECK DH' - used to calculate values $\Delta \bar{H}^\circ$, $\Delta \bar{C}_p^\circ$ and $\Delta \bar{G}^\circ$ at 290K, 310K, $P < 300K$ and $P > 300K$	233
Appendix VI	Algol program 'HYDRAL' - used to evaluate $\Delta \bar{G}^\circ$, $\Delta \bar{H}^\circ$, $\Delta \bar{S}^\circ$, K_H and x_{gas}	234

The programs in Appendices IV and VI were written by Dr R W Cargill.

Acknowledgements

I would like to take this opportunity to express my thanks to the following people, with out whose support this thesis could not have been completed:

Dr R W Cargill, my supervisor who was always available with friendly advice and encouragement throughout the term of the research project;

Prof P A H Wyatt, my second supervisor with whom I had several interesting and valuable discussions;

Mr M G Black, (for his work on the computer interfacing for the modified solubility apparatus), and the technical staff of the department of Molecular and Life Sciences;

The Staff of the Centre for Educational Development who kindly reproduced graphs;

Mrs Maureen Miller and my wife Jay, who accurately transcribed my handwritten manuscript into the typewritten form in which it is presented;

The Governors of Dundee College of Technology who provided financial assistance for the purchase of equipment; and

The British Gas Corporation from whom I received financial support in the form of a British Gas Research Scholarship.

Abstract of Thesis

The solubility of several hydrocarbon gases in water and in aqueous alcohol solvents has been measured in the temperature range 4-61 °C at a total pressure of one atmosphere, by a physical method based on the flowing film technique. Using standard procedures, $\Delta\bar{G}^\circ$, $\Delta\bar{H}^\circ$ and $\Delta\bar{S}^\circ$ of solution have been evaluated and expressed as functions of temperature and solvent composition. The observed variations in these functions and their dependence on temperature and alcohol concentration are then related to current theories of water structure also discussed here but with particular reference to hydrophobic interactions in the solution.

It is shown that the extent of these interactions can be observed in the isotherms of $\Delta\bar{H}^\circ$ and $\Delta\bar{S}^\circ$ at low concentrations of alcohol and a numerical method was used to estimate the magnitude of the hydrophobic contribution to the observed values of the functions themselves. The changes in these functions are then related to the sizes and shapes of the chosen solute molecules to provide a possible structural interpretation of the hydrophobic effect consistent with the observed experimental results.

To Jay

1. INTRODUCTION

1. INTRODUCTION

A solution may be defined as a homogeneous mixture of two or more substances, the composition of which can be varied within certain limits. When different substances are brought together, they either react chemically or simply mix and it is this latter situation, where there is no chemical action, which constitutes a true solution. The substances forming the solution are known as the solute and the solvent. Very often, it is difficult to know which is which but in general, the substance or component which is present in the greater quantity is labelled the solvent.

Of the three states of matter, the solvent is most commonly associated with the liquid state. Gaseous and solid solutions do exist but liquid solvents are more familiar with many of these being commercially available products such as paint strippers or plastic cements. The most common liquid solvent of them all is water which will dissolve anything, given time. This remarkable property has placed water closer than any other natural substance to being the universal chemical solvent.

This and other peculiar characteristics of water have attracted the attentions of many scientists who have attempted to explain the anomalies of liquid water from investigations of its structure. The solubility

characteristics of certain solutes in water and water-based solvents can also reveal information about structural changes within the solvent and it is in this way that the results from this study are to be analysed.

If we are to understand the world in which we live then we must attempt to understand water. This liquid is of fundamental importance to our environment and to our very survival. Many of its unusual properties are taken for granted in every day life and are not considered unusual at all, but they are important in our world and it is because of these that water plays such a vital role in our existence. To appreciate the extent of our reliance on water, it may be worthwhile to examine the distribution of this remarkable liquid in nature and note some of its peculiar characteristics on which we depend.

The water of the earth is found in lakes and rivers, icefields and glaciers, in the soil and life of the earth and in the strata and rocks for a considerable depth below the surface. Its unique solvent power is demonstrated in the largest aqueous solution of all - the sea. The oceans of the world cover 139 million square miles, 71% of the earth's surface and extend to depths in which Mt. Everest could be buried and still have thousands of feet to spare.

As rivers and streams flow over the land regions of the world, rocks and mountains are eroded, the washings dissolved and carried out to sea where thorough mixing occurs due to variations in temperature, tides and currents. The efficiency of mixing is such that a sample taken from the surface at any pollution-free region of the ocean would be representative of one taken anywhere else in the world.

The atmosphere, too, contains significant quantities of water in the form of vapour released from surface waters by the heat of the sun. Extending 200 miles above the earth's surface, the atmosphere contains several distinguishable layers. The first of these, the troposphere, is responsible for the world's weather and contains most of the atmospheric water in its 14,000 m. For the purpose of calculation though, it is assumed that the first 2,300 m contains half of the 4% moisture content associated with this whole layer¹. Above the tropopause, it is suspected that some water vapour is still present. Measurements of humidity in middle latitudes and dawn and twilight observations of clouds provide evidence of moisture at heights of up to 15 and 16 miles.

Below the surface, between the zone of weathering and a depth of about 800 m, subterranean waters supply

wells and springs from pores and fissures in the rock. Below 800 m and down to about 21,000 m¹ these sub-surface waters provide sources to hot springs, geysers and volcanic steam.

It is clear that water is present everywhere in the world, in some places more accessible than others, and it is not surprising that this remarkable liquid features so highly in our environment. Water is also of fundamental biological importance, from its role in the stabilisation of folded protein structures to its role in the construction of the basic unit of life. The cell consists largely of water which forms an aqueous solution of biologically active material within the membrane boundary. On a less microscopic scale, plants and animals require regular intakes of water to maintain a sufficient fluid level for survival, otherwise dehydration and death follows. In most mammals, dehydration causes water to be drawn from the blood, to replace water lost in perspiration, and the blood thickens to a point where it cannot circulate quickly enough to carry metabolic heat to the skin. The body temperature soars and death follows quickly. In extreme cases, a man will lose about 12% of his body weight in fluids. (If he could drink this amount of water at one time, he would die of water intoxication.)

In some regions of the world, water is very scarce and scorching daytime temperatures evaporate most of the available moisture. These regions, known as deserts, are very inhospitable environments for most of the earth's creatures where roasting days give way to bitterly cold nights as the heat of the day is radiated into a cloudless night sky. Unrelated as it may seem, the lack of moisture in the deserts is responsible for these drastic temperature variations. Water exhibits some remarkable thermal properties, one of which is its abnormally high heat capacity. This is a measure of a substance's ability to absorb and retain heat. In moderate climates, there are considerable quantities of water available to absorb the sun's heat during the day, slowly releasing it at night, thus maintaining a moderate temperature variation over a 24 hour period. In the desert, where there is very little moisture, temperature moderations of this kind cannot occur.

This heat-storage property of water is widely exploited. Central heating in many homes, schools and offices uses the heat transfer properties of water. As a coolant, water is used in many applications from power stations to the family car. Many unfortunate motorists are no doubt aware that without proper protection, this cooling water can freeze, in extreme winter conditions, with disastrous consequences. Water, along with bismuth,

is one of the few substances which expands on freezing. As the temperature decreases from 4°C , liquid water expands, this expansion becoming even more apparent below the freezing point. The force with which this occurs is sufficient to fracture the engine block in the motor car and burst pipes in domestic plumbing systems.

However, from an environmental point of view, this density variation with temperature is a fortunate one. Because of this, ice is less dense than water and therefore floats. Apart from the obvious advantage to fish and other forms of marine life, land bound creatures benefit also. If ice were heavier than water, lakes and seas would freeze from the bottom up. Only the surface layers would melt in the summer heat, the great bulk remaining solid throughout the whole year making life on the surface unbearably cold and extremely uncomfortable.

So we must appreciate the properties of water for they are necessary to our environment. The continuous cycle which water follows as it evaporates into the atmosphere, rains or snows onto the mountains and is led back to the sea in rivers and streams is a cycle which supports life in all forms, each of which has smaller but equally important water cycles itself. To understand water is a difficult task. The amazing properties of this liquid have not yet been fully explained and as yet,

no universally acceptable model for water structure is available. However, research continues and as more data are collected for water and aqueous systems, existing theories are supported or modified. The measurement of solubilities in this study is a contribution to the fast growing bank of experimental data on such systems and the aim is to use the thermodynamic descriptions of solution in order to reveal some features of water which may assist a fuller understanding of this very common but unusual liquid.

The Application of Gas Solubilities to Structural Studies

All gases are absorbed to some extent by all liquids, the amount absorbed varying with the nature of the gas and of the liquid. Dissolved gases are common in our environment. Fish breathe by extracting dissolved oxygen from water and many popular drinks contain dissolved carbon dioxide. The solubility characteristics of air in blood are painfully familiar to many deep sea divers and in industrial areas, gaseous pollutants dissolve in the water of the atmosphere to give "acidic rain".

The physical process of solubility of gases in liquids describes the transfer of molecules from the gas phase into the solution phase. Here the solute molecules adopt the properties of the corresponding liquified gas

but find themselves in an environment of solvent molecules. The ease with which this transfer process takes place must depend on the suitability of the solute molecules for inclusion among those of the solvent.

An ideal solution is one in which the solute molecules fit into the structure of the solvent and interact only with solvent molecules. In this situation, those molecules in the close environment of the solute particle are all of the same character, each influencing the molecules of the solute in the same way, producing a constant interaction around them. The presence of one solute molecule in the close vicinity of another will disturb this constancy of interaction and produce deviations from the ideal solution. These are reflected in deviations from Henry's Law of gas solubility which states that the amount of gas dissolved at a given temperature is proportional to its partial pressure. Theories of ideality and regularity sufficiently describe many non-aqueous solutions but when water is a component, the nature of this liquid makes it impossible to describe the resulting solution as either ideal or regular unless suitable experimental conditions are chosen.

In this study, the solutions of the dissolved gases are very dilute and under these conditions it is usually justifiable to assume an ideal dilute solution. The

molecular interpretation of this assumption is that in solution, the dissolved gas molecules are so few compared with the number of solvent molecules that the probability of two solute molecules interacting is negligibly small.

Thus the process of transfer of a solute molecule from the gas phase to the solution phase can be monitored thermodynamically. If the gas and its solution are at equilibrium with each other, the position of equilibrium for a given set of experimental conditions is given by the equilibrium constant, from which thermodynamic parameters related to structural changes in the solvent may be obtained. The procedure is not affected by the introduction of a co-solvent and in this study, an alcohol was introduced as co-solvent to water and its effect on the structure of water was observed.

This approach to structure elucidation has been adopted by several workers^{2,3} and has been used for some time. The measurement of gas solubilities is relatively easy experimentally, and details of the procedure are given in Chapter 2.

Choice of Solutes

In this study, the following gaseous hydrocarbons were used as solutes: propane, butane, 2-methylpropane, 2,2-dimethylpropane, cyclopropane and propene. These were chosen primarily to give a variation in molecular size and shape but because of the nature of their interaction with water, it was possible to estimate the so-called hydrophobic effect in the resulting aqueous solution. McAuliffe⁴ and others^{5,6} reported the solubility of these hydrocarbon gases in water some time ago. More recently Ben-Naim⁷ measured the solubilities of methane and ethane in aqueous ethanol solvents and this work encouraged the present study to begin with an investigation of the solubility characteristics of propane and butane in aqueous ethanol. On completion of this system, the solvent was replaced with aqueous t-butyl alcohol.

The effect of chain branching in solute molecules was then investigated by using 2-methylpropane and 2,2-dimethylpropane as solutes in the aqueous ethanol solvent. In contrast to the straight chain cylindrical molecules of ethane to butane, these branched chain aliphatic hydrocarbons have nearly spherical molecules, similar to a larger version of a methane molecule.

The solute 2,2-dimethylpropane liquifies at 9.5°C and this restricted the experimental temperature range slightly but nonetheless, a substantial array of data was obtained for these systems.

From the range of gases used, it was possible to obtain comparisons of the effects on the structure of water due to chain branching, chain length, double bonds and cyclic systems and to observe the effects of the hydrophobic interaction exhibited by the different types of solute chosen.

2. EXPERIMENTAL

2. EXPERIMENTAL

2.1 Types of Measurement

The solubility of a gas in a liquid is measured as the volume of gas which will dissolve in a fixed mass (or volume) of solvent at experimental conditions of temperature and pressure. This measurement relies on the assumption that the gas and its solution are at equilibrium with each other and this condition is therefore an essential factor in the design of any solubility measuring device.

The design of the apparatus also depends on the type of measuring process to be used, and these may be chemical or physical in nature. The chemical methods^{8,9} are accurate enough but are usually specific to a given solute - solvent system and are therefore not generally applicable. The physical methods are divided into two groups as follows.

2.1.1 Extraction Methods

These involve the extraction of a gas from a previously saturated solution under conditions where temperature, pressure and volume are known. Several workers have adopted techniques using these methods^{10,11} and high degrees of precision have been reported.

2.1.2 Saturation Methods

These involve the bringing of a degassed solvent into contact with the gas under conditions where temperature, pressure and volume are known. This type of process is also very common^{2,5,12} and it is one such process which was used in this study of solubilities.

2.2 Equilibrium between the gas and its solution

The experimental condition of equilibrium between the gas and its solution is of great importance in the measurement of gas solubilities and several techniques have been adopted to achieve it.

2.2.1 Shaking a Mixture of the two

This involves the containing of a gas and solvent in a chamber which can either be lifted and shaken or agitated using a mechanical or magnetic stirrer. The method was used successfully by Cook and Hanson¹³ and by Ben-Naim² who allowed about three hours for equilibrium to be reached.

2.2.2 Flowing Thin Film of Solvent

This is the technique of Morrison⁵ which involves the trapping of a gas in a cylinder, so that it is dissolved by the solvent which runs down the interior of the cylinder

in a thin film. Equilibrium is achieved very quickly and comparisons have been made with the measurements of Ben-Naim² to show good agreement to within experimental error.

2.2.3 Bubbling of Gas

Here, the gas is bubbled through the solvent¹⁴. This is a simple technique which is quite effective for systems where the solubility of the gas is high.

2.2.4 Flowing the gas over a liquid held in a stationary support

This is equivalent to the measurement of solubilities by gas-liquid chromatography. This is a specialised technique and one which has achieved high levels of precision^{4,15}. This method has also been used to determine properties of the solution phase¹⁶.

2.3 Historical

The measurement of gas solubilities in liquids has greatly improved in accuracy and technique since the early pioneers first attempted quantitative investigations. The evolution of solubility measuring devices has been widely documented in various reviews^{17,18} along with their reliability in terms of accuracy of measurement.

It is therefore not necessary to give detailed descriptions of developments in technique here because there is ample information available on this. However, a brief summary of the important historical stages in the development of the saturation process may serve as a foundation for the remainder of this chapter.

The work of Henry¹⁹ is one of the first serious attempts to report the solubility of gases in liquids to any degree of accuracy. However, due to the scarcity of pure materials, his overall accuracy was not particularly high but his ideas were incorporated in the technique developed by Bunsen²⁰. This saturation process employed the method of shaking to bring the gas and its solution to equilibrium. The complete apparatus was small enough to be lifted as a unit, making this a manual operation.

The method of Bunsen was almost entirely replaced by that of Ostwald²¹. The main advantage of this technique was the introduction of a gas burette to allow the accurate measurement of volume changes. Again the shaking method was employed and the reduction in gas pressure was compensated for by the introduction of mercury into the burette which replaced the dissolved gas.

It is interesting to note the changes which had occurred at the very early stages. Accurate volume changes were now recorded by the rising level of an 'inert'

fluid in a gas burette. This, in effect, is similar to many of the present day types of apparatus. The method of shaking (or stirring) and the use of an 'inert' fluid are still popular applications to the measurement of gas solubilities^{2,22,23}.

Other modern methods include the flowing film technique, discussed in the next section, gas-liquid chromatography¹⁶ and mass spectrometry²⁴.

2.4 The Flowing Film Technique

This is the now well-established technique of Morrison⁵ and, with a few modifications by Cargill³, it is the one used here. The technique employs a flow system in glass and stable pumping. The solubility of two gases can be measured simultaneously in a solvent of given composition and at a given temperature, the total pressure being kept constant at one atmosphere.

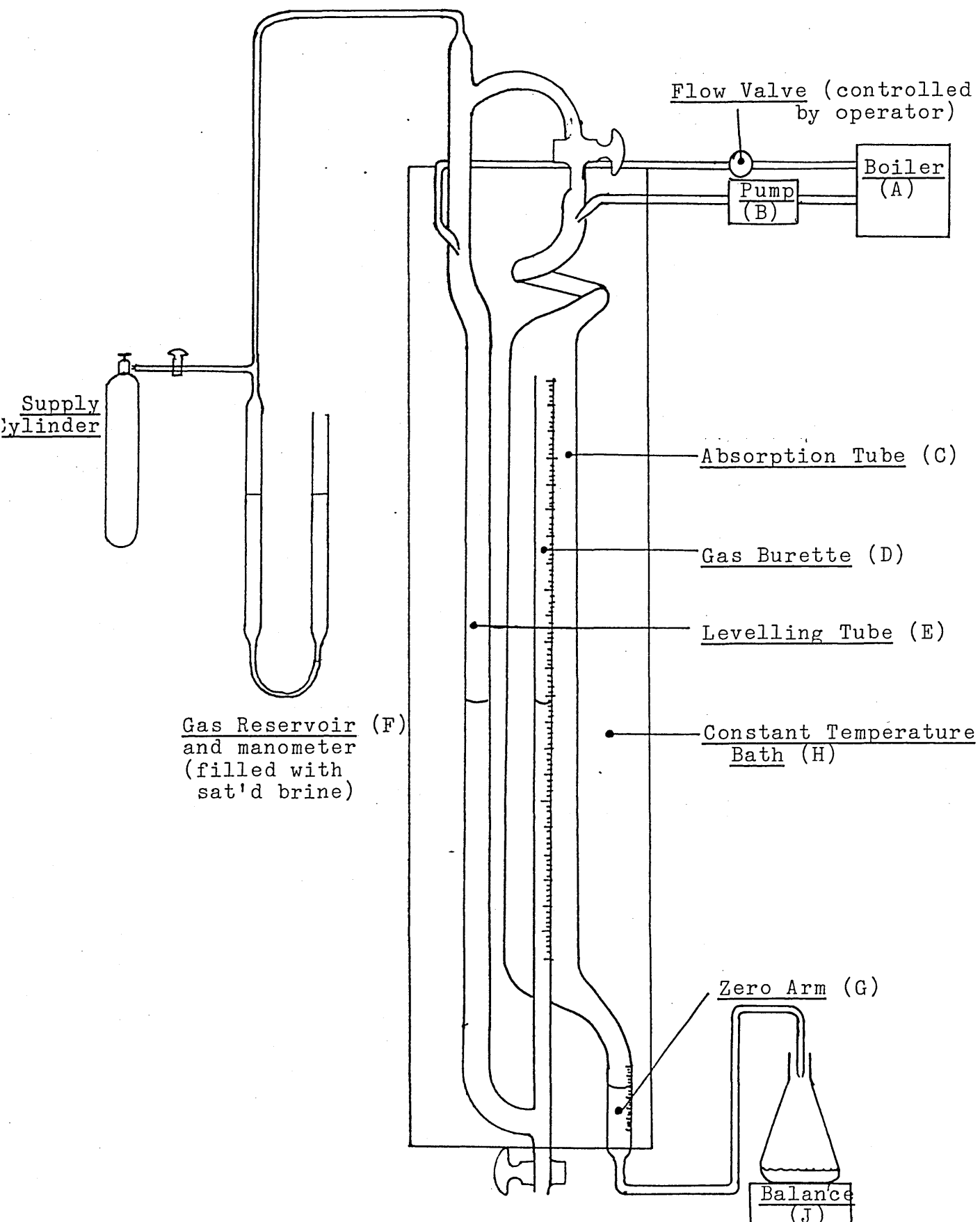
2.4.1 Principle of Operation

With reference to Figure 2.4.1(i) the process is as follows.

A fixed volume of gas is exposed to a thin film of gas-free solvent which runs down the interior of a dissolution chamber, C. The gas is absorbed in the solvent

Figure 2.4.1(i)

Diagram of Apparatus



which is removed at the bottom of the chamber and weighed on a balance, J. The volume of gas absorbed is replaced with gas saturated solvent as it rises in a gas burette, D, under constant pressure conditions. The measurement involves intermittent observations of volume of gas and mass of solvent over a period of several hours.

The apparatus is enclosed in a thermostatted water bath and the procedure can be repeated at various temperatures in the range 4 - 60 °C. Solubility curves are constructed for a series of solvents over a range of composition, in this case up to $x_{alc} \approx 0.4$, until a set is obtained for a given gas-water-alcohol system.

2.4.2 Apparatus: Components and Functions

Figure 2.4.1(i) shows the apparatus as it was used and the components and their functions are given below.

Boiler (A): degasses the solvent and a vapour pump collects a reservoir of gas-free solvent for use.

Peristaltic pump (B): feeds degassed solvent to the (Watson-Marlow MHRE) absorption tube at a steady flow rate. This is a requirement of the technique.

Absorption Tube (C): where the solution of the gas takes place. The solvent runs down the inside surface of the tube in which a sample of the gas is trapped. As the solvent runs down, it dissolves the gas and flows into a flask on a balance (J).

Gas burette (D): open to the absorption tube. Gas saturated solvent is allowed to rise in the burette to take the place of the dissolved gas and the change in level allows the change in gas volume to be measured.

Levelling tube (E): solvent is fed in here dropwise and it becomes saturated with gas. The drop rate is varied by the operator such that the level rises equally with the level in the gas burette i.e. this preserves the condition of constant gas pressure.

Gas Reservoir (F): required to transfer gas from the supply cylinder to the apparatus and also to maintain constant pressure within it.

Zero Arm (G): monitors internal gas pressure variations. The solvent (with gas dissolved in it) collects here before passing over onto the balance (J). This arm has graduations on it and internal pressure fluctuations vary the liquid level position giving the operator information with which to compensate.

Thermostatted Water provides constant temperature
Bath (H): conditions to within 1K.

The chosen experimental conditions resulted in a wide range of solubilities so that the flow rate of solvent through the absorption tube varied from about 20 g per hour (high solubilities) to about 100 g per hour (low solubilities). Under these conditions, the solvent is exposed to the gas for 6 - 10 seconds as it passes down the chamber. During each determination, the volume of gas dissolved varied between 10 and 25 cm³ and the mass of solvent required was 100 - 600 g depending on the magnitude of solubility.

2.5 Recent Modifications

The apparatus of Morrison has had several modifications since its original inception, all of which have, in some way, improved the accuracy of measurement which is presently of the order of 0.5%. It is difficult to improve on this significantly but the remaining major source of error is due to the fluctuating atmospheric pressure and its effect on the volume and partial pressure of the gaseous solute within the apparatus.

It is important that during a run, this partial pressure remains constant and therefore complete isolation from the atmosphere would be advantageous.

The necessary changes in the apparatus in order to accomplish this objective do not alter the well established process devised by Morrison but instead, allow his ideas to be incorporated in a more compact design where, additionally, automation can be introduced.

For the purpose of describing the automated system, a sealed container may serve as a suitable model. Assuming that the contents are gaseous, then for constant temperature conditions, the gas pressure will remain constant regardless of fluctuating external pressure. If two valves are now fitted to the container and a liquid is introduced through one and withdrawn through the other at the same rate, then provided no solution

process takes place, the pressure of the gas will still remain the same. However, if the gas dissolves it will be removed from the container by means of the liquid at the exit and so produce a reduction in internal gas pressure.

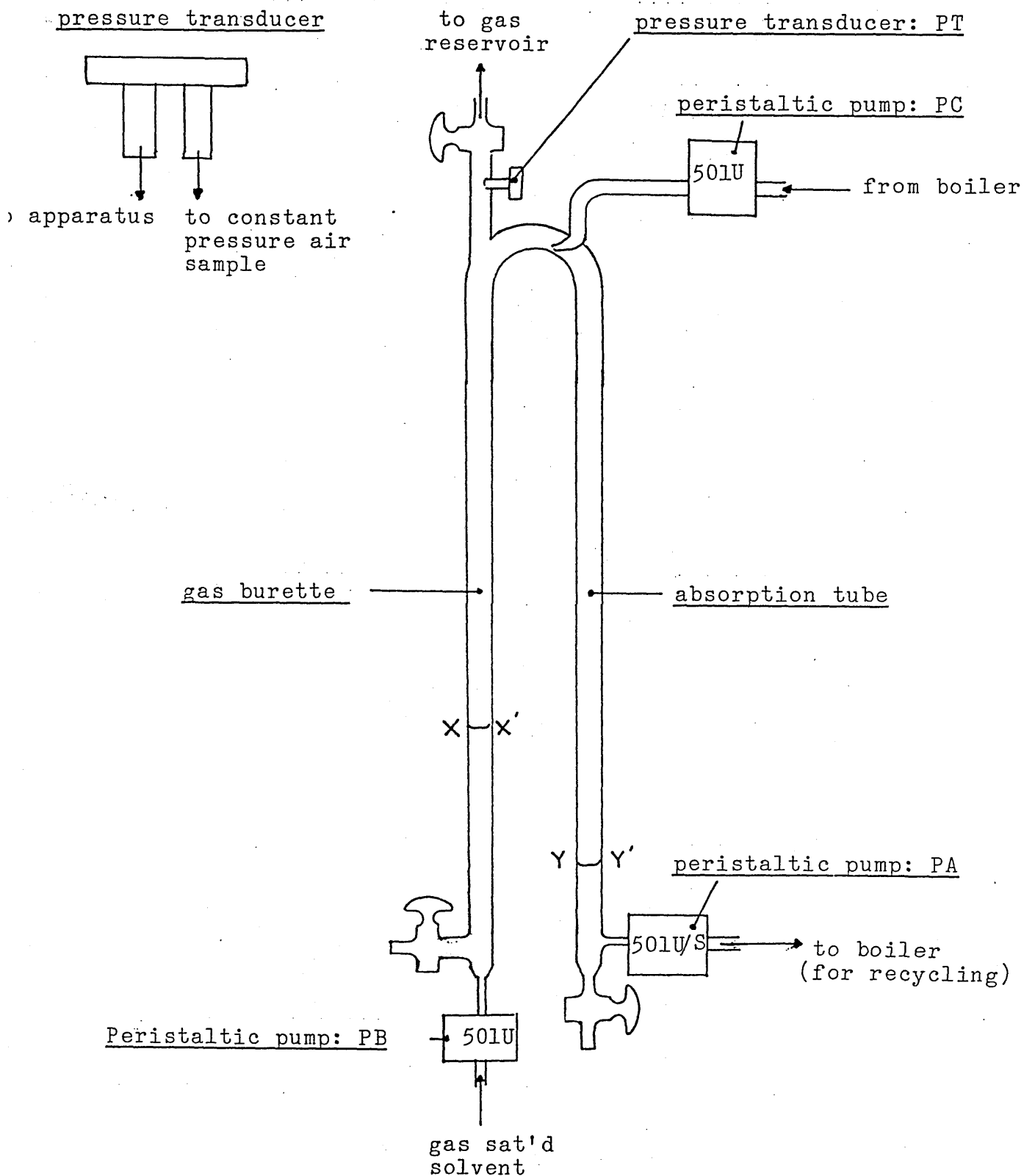
To compensate for this, a third valve may be fitted which would allow passage of gas-saturated liquid into the container at a rate which is exactly equal to the rate of dissolution of the gas. This system could now be described as a constant pressure process and this principle is the basis of the alterations to Morrison's design. The valves referred to above are variable flow peristaltic pumps, all of which can be set manually to a desired flow rate. The third valve is electrically connected to a sensitive pressure transducer which monitors the internal gas pressure so that any deviation in the pressure can be corrected for automatically by electronically increasing or decreasing the speed of the pump. This self-correcting device is shown in Figure 2.5(i).

The principle of operation is as follows:

1. As in the existing system, degassed solvent is supplied via pump PA to the absorption tube where the gas dissolves.

Figure 2.5(i)

Modifications to Existing Apparatus



2. Pump PC removes the solvent with the gas dissolved in it at a rate which maintains the solvent level Y-Y' at a constant vertical position, chosen arbitrarily.
3. Gaseous solute is trapped between solvent levels Y-Y' and X-X' at a constant pressure which is monitored by the transducer PT.
4. Gas saturated solvent is led into the 'gas burette' by pump PB at a rate equal to the rate of solution of the gas. The pump flow rate is electronically controlled by the transducer.

The pumps are of the Watson-Marlow 501 type and all have variable flow facilities.

501 S : manually controlled pump speed

501 U : manually and electronically controlled
pump speed.

The pressure transducer is by National Semiconductors, LX1601D, and is sensitive to the order of 20 mV per mm Hg.

Temperature control is by means of a Techne G-400 circulator in a circuit with the Techne M-1000 heat exchanger.

As it stands, the system is a self supervised dissolution device with no means of making measurements manually. However this is unnecessary because data can be collected electronically from the various pumps as follows.

The information required for solubility determinations is the simultaneous measurement of the volume of gas dissolved, and the mass of solvent required.

The pumps PB and PC produce signals which are proportional to their operating speed. By integrating the signals over a preset time interval, a measurement of volume can be obtained

i.e.
$$\text{Total Volume Throughput} = \frac{\text{pump speed} \times t \times \text{volume for one revolution}}{\text{in time } t}$$

Thus, from pump PB, a measurement of volume of gas dissolved can be made. Similarly the information from PC along with a knowledge of the density of the solvent will yield a measurement of the mass of the solvent required. These measurements may be repeated over a suitable range of volume or mass and the method of least squares²⁵ will determine a value of the solubility.

2.6 Purity of Materials

The aqueous solvents were made up in the laboratory from water (deionised using Fl-streem Cartridge Deioniser) and absolute alcohol (Burroughs; 100%) or 2-methylpropan-2-ol (May and Baker; 99.5% and Aldrich; 99.5%). Solvent composition was checked by density measurements^{2 6} at 20 °C.

The gases propane, butane, 2-methylpropane and 2,2-dimethylpropane were supplied by Air Products and were stated to be at least 99% pure. Cyclopropane and propene were by Matheson and these were stated to be 99% pure.

3. THEORETICAL

3. THEORETICAL

3.1 Symbols

The symbols used in this study have the following significance:

a	activity
<u>a</u> , <u>b</u>	van der Waals coefficients
B	second virial coefficient
C _p	specific heat at constant pressure
f	fugacity
G	Gibbs free energy
H	enthalpy
ln	natural logarithm
log	logarithm to the base 10
m	mass
n	number of moles
P	pressure
R	gas constant
S	entropy
s	solubility measured at temperature, T and pressure P
s ₀	solubility corrected to STP
T	temperature
V _m	molar volume
x	mole fraction
ΔX	change in function X

\bar{X}	partial molar value of X
X°	standard value of function X
X^*	value of function X calculated for a real gas
X_i	value of X for component i in the system
μ	chemical potential
γ	activity coefficient

3.2 Obtaining a Solubility Curve

Numerical data from the apparatus were recorded on a data collection sheet (Appendix I) and corrections were applied. The corrected data were then transferred to a graph of volume vs mass (see Figure 3.2.(i)). The gradient of this line was taken to be the measured solubility s and the adjustments referred to on pages 36 & 37 were applied to determine $\log s_0$.

During the latter part of the project, a micro computer (Apple II Europlus 48K) was employed to perform all these operations. Data were manually fed into the computer which corrected volume and mass terms. These were 'plotted' and the method of least squares²⁵ was employed to evaluate s . The appropriate software is shown in Appendix II.

This second method had several advantages over the first, and consistently gave results comparable with those from the manual method.

Having obtained $\log s_0$, a solubility curve (Figure 3.2(ii)a) was constructed by plotting $\log s_0$ against $1/T$. Usually six or seven data points are required so a suitable set of temperatures between 4 and 60 °C was chosen to correspond to integral values of $10^4/T$ between 30 and 36.

Figure 3.2(i)

Plot of Volume of gas vs Mass of Solvent
for butane-water-ethanol system at 289.2 K
and alcohol mole fraction, $x_c = 0.3$

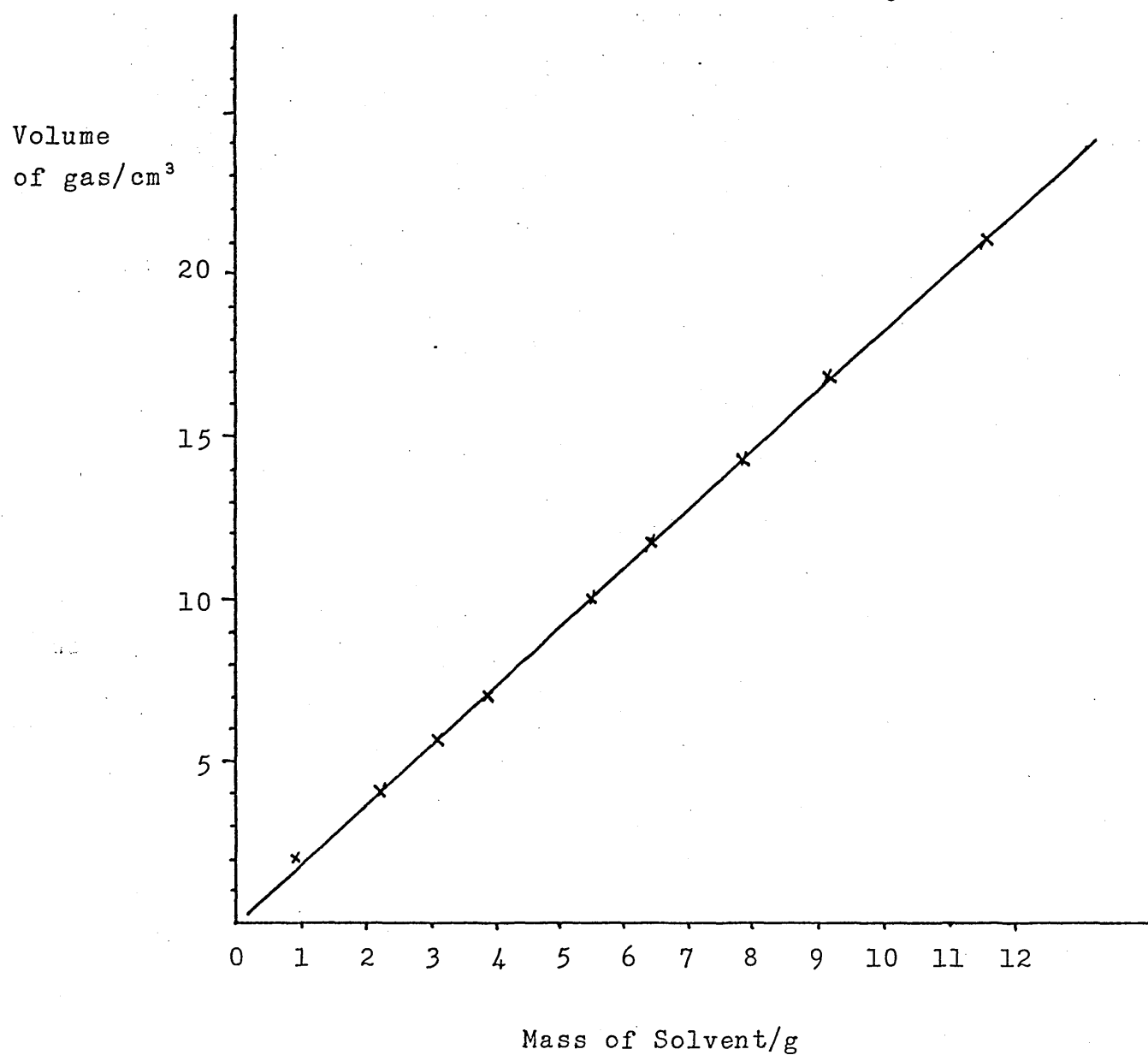


Figure 3.2(ii)a Solubility curve for the system butane-water-ethanol at alcohol mole fraction, $x_c = 0.3$.

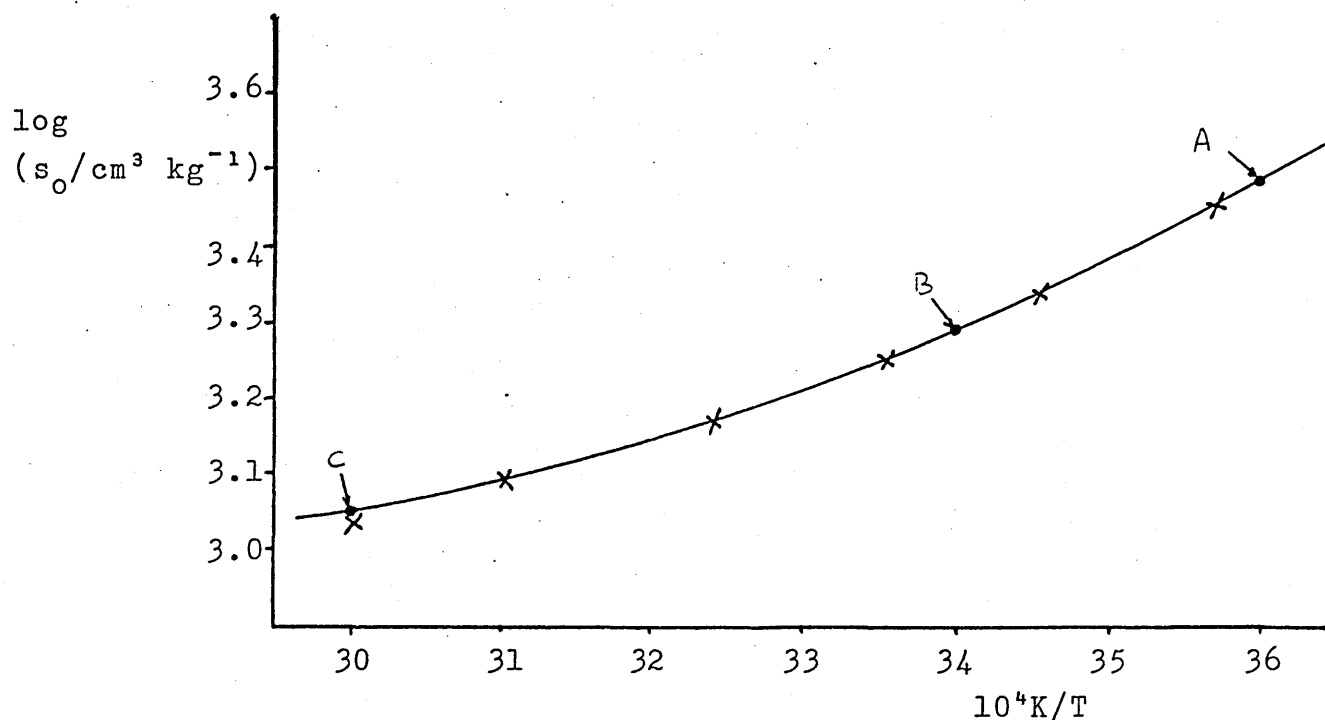
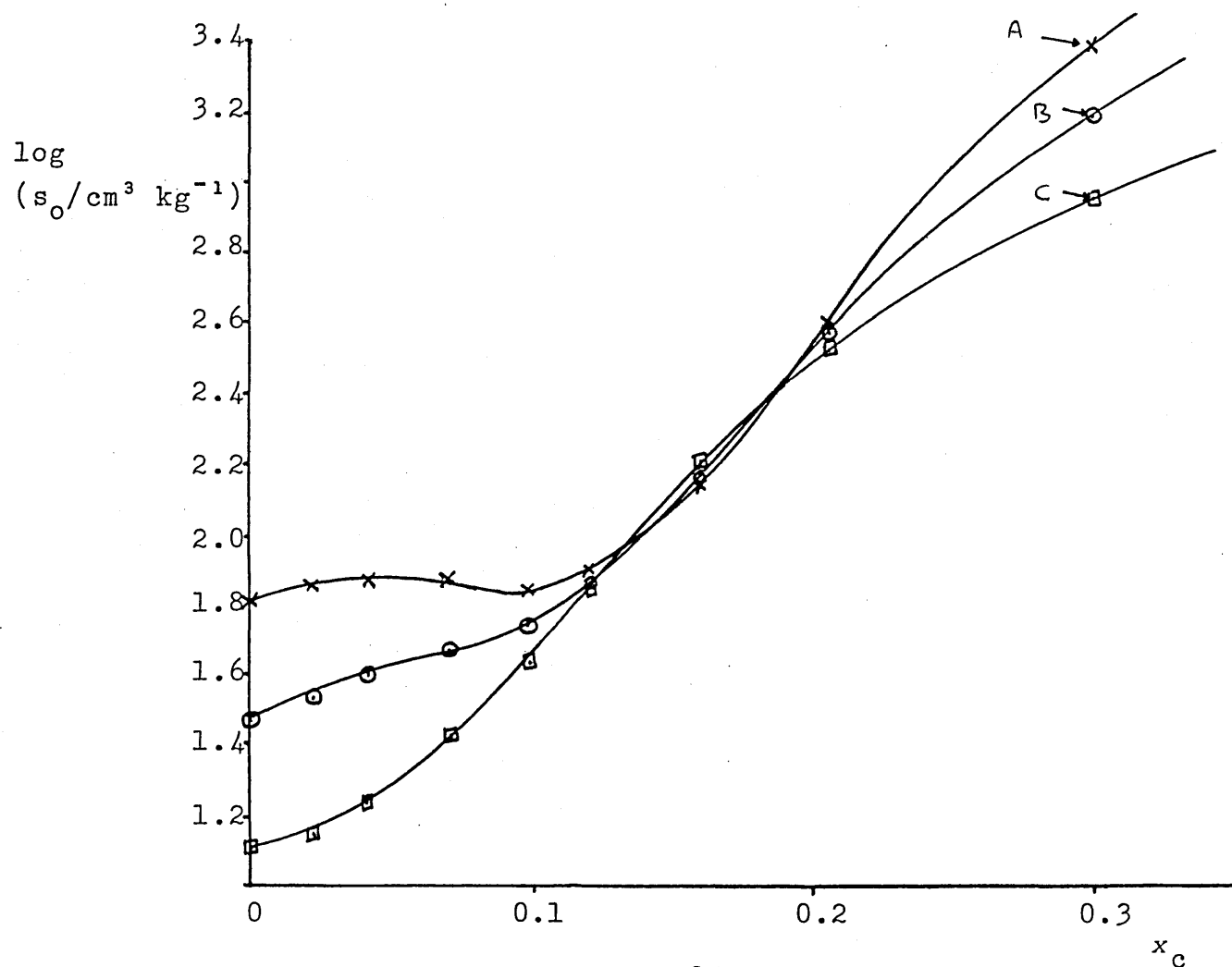


Figure 3.2(ii)b Solubility isotherms for the system butane-water-ethanol at temperatures 4.7(X), 21.0(\circ), and 60.2 $^{\circ}\text{C}$ (\square).



A series of solubility curves is obtained for a given gas-solvent system and these may be supported by the construction of solubility isotherms (Figure 3.2(i)b). These are graphs of $\log s_0$ against solvent composition and the continuity of these isotherms assists in the slight adjustments (within experimental error) sometimes required to obtain a mathematically acceptable curve which is consistent with the experimentally obtained data.

3.3 Units and Treatment for Non-ideality

The measured solubility s' , is defined as the volume of gas in cm^3 (at temperature T and pressure P) dissolved by 1 kg of solvent.

Thus,

$$s/\text{cm}^3\text{kg}^{-1} = \frac{\text{Volume of gas (T,P)}/\text{cm}^3}{\text{Mass of solvent/kg}}$$

This is now adjusted to STP conditions in two stages:

$$(a) \quad s' = \left(s \times \frac{273}{T} \times \frac{P}{760} \right)$$

assuming ideality of the gas. s' is the equivalent STP value of solubility for the gas at its partial pressure p within the apparatus. This may vary from experiment to experiment but always remains constant during a run.

(b) Next, the result is expressed for the gas at a partial pressure of one standard atmosphere using Henry's law (assuming an ideal solution is formed).

$$s_0 = \left(s \times \frac{273}{T} \times \frac{P}{760} \right) \times \frac{760}{P}$$

giving

$$s_0 = s \times \frac{273}{T}$$

Thus s_0 is defined as the volume of gas in cm^3 (corrected to STP) dissolved by 1 kg of solvent under a partial pressure of gas equal to one atmosphere.

For systems previously studied, where the solutes were oxygen²⁷, hydrogen²⁸, helium²⁸ and argon³, it was justifiably assumed that the gases behaved ideally in the gas phase. In the case of the hydrocarbons though, some of which liquefy at pressures and temperatures close to the experimental values, the same assumptions could not be made unless it could be shown that the deviation from ideality was insignificant.

For an ideal gas, the chemical potential is given by

$$\mu(T,P) = \mu^\circ(T,P) + RT \ln \frac{p}{p^\circ}$$

where p is the partial pressure of the gas and p° is the standard unit of pressure (e.g. one atmosphere).

The partial pressure may easily be obtained from experimental measurements and other thermodynamic quantities can then be evaluated.

However, for a real gas,

$$\mu^* = \mu^\circ(T, p) + RT \ln \frac{f}{p} \quad (1)$$

where f is the fugacity. It is clear that the imperfections in the gas are measured in the second term in equation (1) and more precisely in the value of f . The fugacity has the same units as pressure and it plays the same role in a real gas as p does in an ideal gas. It is defined^{2,9} as

$$f \equiv p \exp \left[\frac{1}{RT} \int_0^p \left(v - \frac{RT}{p'} \right) dp' \right]$$

(see also equation (5))

and the limiting behaviour is apparent.

$$\text{i.e. } f \rightarrow p \quad \text{as } p \rightarrow 0.$$

The significance of this is that at low pressures (atmospheric pressure is relatively low), f is approximately equal to p and therefore in equation (1), μ^* is equal to the chemical potential for the real gas.

To investigate further, the non-ideal behaviour in the gas phase however, a more detailed approach may be made as follows.

From first principles,

$$\left(\frac{d\mu}{dp}\right)_T = V$$

$$\therefore \mu = \int_{p^\ominus}^P V dp \quad (2)$$

For an ideal gas,

$$\mu = RT \ln\left(\frac{P}{p^\ominus}\right) + \mu^\ominus \quad \text{since } V = \frac{RT}{P}$$

or $\mu - \mu^\ominus = RT \ln P \quad \text{where } P = \frac{p}{p^\ominus}$

For a real gas we can write

$$\mu - \mu^\ominus = RT \ln f \quad \text{where } f = \frac{f}{p} \quad (3)$$

If (3) is now differentiated with respect to pressure at constant temperature, we obtain

$$RT\left(\frac{\delta \ln f}{\delta P}\right)_T = \left(\frac{\delta \mu}{\delta P}\right)_T = V$$

i.e. $VdP = RTd\ln f \quad (4)$

Integrating (4) gives

$$\int VdP = RT \int d\ln f.$$

Taking P as one of the limits of integration and some very low pressure P' as the other (at which $f = P'$),

$$RT \ln\left(\frac{f}{P'}\right) = \int_{P'}^P VdP$$

Adding $RT \ln\left(\frac{P'}{P}\right)$ to both sides gives

$$\begin{aligned} RT \ln\left(\frac{f}{P}\right) &= \int_{P'}^P V dP - RT \ln P + RT \ln P' \\ &= \int_{P'}^P \left(V - \frac{RT}{P}\right) dP \\ \text{i.e. } RT \ln\left(\frac{f}{P}\right) &= \int_{P'}^P \alpha dP \end{aligned} \quad (5)$$

$$\text{where } \alpha = V - \frac{RT}{P}$$

For a perfect gas, $\alpha = 0$ but for a real gas, it can be calculated from $P - V$ data and the integration carried out graphically. The plot allows the integration to be taken down to zero pressure (by extrapolation) thus giving a true measure of f , now that $P' = 0$.

The equation of state for an ideal gas is given by

$$\lim_{P \rightarrow 0} \frac{PV}{nRT} = 1$$

Although we have substituted f for p in the case of the real gas, we cannot simply apply the above equation. An equation of state valid for all gases is the power series

$$\frac{PV}{nRT} = 1 + \frac{nB}{V} + \frac{n^2C}{V^2} + \dots \quad (6)$$

This is the virial equation of state in which B and C are temperature dependant constants. Using only the first term and an alternative form of (6) we have

$$PV = RT + BP \quad (7)$$

Comparing (7) with (5) we see that

$\alpha = B$ and therefore,

$$RT \ln \left(\frac{f}{p} \right) = \int_0^P B dp = BP$$

Thus the deviation from ideality in the gas phase is given by $RT \ln \left(\frac{f}{p} \right) = BP$

So, for a real gas,

$$\mu^* = \mu + BP \quad (8)$$

By expanding (6) into the van der Waals form, B can be evaluated. i.e.

$$\left(P + \frac{a}{V^2} \right) (V - b) = RT \left(1 + \frac{B}{V} \right)$$

$$\therefore B = b - \frac{a}{RT}$$

Now the deviation from ideality in the gas phase can be evaluated. The effect on experimentally measured quantities is shown below

$$\Delta \bar{G}^\circ = BP - RT \ln p$$

and

$$\Delta \bar{H}^\circ = BP - R \frac{d \ln p}{d \left(\frac{1}{T} \right)}$$

The magnitude of BP for each gas is shown below in Table 3.3.1 and these values represent the difference associated with the calculation of $\Delta \bar{G}^\circ$ and $\Delta \bar{H}^\circ$ using real and ideal gas assumptions.

Table 3.3.1 : Calculation of BP, the deviation from ideality in the gas phase for some gaseous solutes at 277K and 101.3 kPa.

Solute	$\underline{a}/\text{Nm}^4\text{mol}^{-2}$	$\underline{b}/\text{m}^3\text{mol}^{-1}$	$B/J\text{N}^{-1}\text{m}^2$	BP/J
propane ³⁰	0.8664	8.445×10^{-5}	-2.917×10^{-4}	-29.6
butane ³⁰	1.447	12.26×10^{-5}	-5.06×10^{-4}	-51.2
2-methyl-propane ³⁰	1.287	11.42×10^{-5}	-4.45×10^{-4}	-45.0
2,2-dimethyl-propane* ³¹	1.713	14.07×10^{-5}	-6.03×10^{-4}	-61.1
cyclo-propane* ³¹	0.839	7.52×10^{-5}	-2.89×10^{-4}	-29.3
propene ³⁰	0.8379	8.272×10^{-5}	-2.81×10^{-4}	-28.5

The calculation of BP is based on conditions believed to correspond to maximum deviation from ideal behaviour.

These are:

- (a) Conditions of minimum temperature; although B increases with temperature, it increases from negative, through zero to positive quantities. Over the temperature range considered, the maximum deviation would correspond to the minimum temperature;

* \underline{a} and \underline{b} are calculated from critical parameters.^{31, 32}

(b) A partial pressure of gas equal to one atmosphere. This condition is never achieved due to the vapour pressure of the solvent in the apparatus so that the value of P is always less than one atmosphere. Therefore, the calculated value of BP is always an over-estimate.

Let us now consider the solution phase. Important assumptions made in the calculation of solubility require that the solution of the gas behaves ideally. This may not be strictly true but if it can be shown that the deviation is small then to a good approximation, the solution can be considered ideal.

If we now consider the chemical potential of the solute we have

$$\mu_1 = \mu_1^\ominus + RT \ln a_1$$

where a_1 is the activity of component 1 in the solution. The activity is related to mole fraction x_1 through the activity coefficient γ_1 as follows:

$$a_1 = \gamma_1 x_1$$

Thus the chemical potential for the real solution can be expressed in the form

$$\mu_1^* = \mu_1 + RT \ln \gamma_1 \quad (9)$$

Where μ_1 is the chemical potential of component 1 in the real solution. This is similar to equation (1) except that here the deviation from ideality is contained in the

function γ . It now becomes necessary to investigate the characteristics of γ . The activity follows the limiting behaviour

$$a \rightarrow x \text{ as } x \rightarrow 0$$

therefore

$$\gamma \rightarrow 1 \text{ as } x \rightarrow 0$$

Putting $\gamma = 1$ in equation (9) enables the calculation of the chemical potential to be made using the ideal solution relationship

$$\mu = \mu^\circ + RT \ln x$$

Thus the smaller the number of gas molecules in solution compared with the number of solvent molecules, the smaller the probability of solute - solute interactions and deviations from the ideal solution. The relative numbers of solute and solvent molecules can be calculated from solubility data and these are given below in Table 3.3.2.

Table 3.3.2 : Ratio of Solute:Solvent molecules in solution for each gas at conditions of highest solubility.

Solute	Maximum Solubility (x)	Solute:Solvent
propane	2.185×10^{-3}	1:417
butane	7.054×10^{-3}	1:130
2-methylpropane	1.96×10^{-3}	1:629
2,2-dimethylpropane	2.85×10^{-3}	1:437
cyclopropane	4.0×10^{-3}	1:251
propene	2.02×10^{-3}	1:496

These data correspond to gas solubilities measured in water - ethanol solvents. The effect of the ethanol component tends to increase the solubility giving rise to a greater number of solute molecules in solution.

Ben-Naim and co-workers investigated the solubilities of methane, ethane and butane in H_2O and D_2O ³³ and also of methane and ethane in aqueous ethanol⁷ assuming ideal solution characteristics for their thermodynamic treatment. They also measured the solubilities of these gases at reduced pressures and since no significant deviation from Henry's law was found, their assumptions were justified.

Unfortunately, the apparatus used in this study was unable to measure pressure dependence of solubility and such data for each gas dissolving in aqueous ethanol could not be

found in the literature. However, the data in Table 3.3.2 show that all the solutions formed were very dilute and therefore solute - solute interactions are unlikely to occur to any significant extent unless they are caused by an effect due to the nature of the solvent (see section 6.3). The thermodynamic functions have therefore been evaluated using ideal solution assumptions in accordance with the procedure of Ben-Naim^{7 33} for hydrocarbons, and Cargill^{3 27 28} for other gaseous solutes.

3.4 Relationship between $\log s_o$ and the Thermodynamic Functions

For the investigation of liquid state structure many techniques are presently available, most of which have taken advantage of recently developed technology e.g. fast computer modelling, infrared spectroscopy and x-ray diffraction. The process of solubility is less complicated experimentally but the solubility results require to be manipulated into a form which is meaningful in relation to structural changes within the solvent. This requires a detailed description of the thermodynamics of solubility.

Before the functions can be derived however, it is necessary that the choice of standard states is considered.

3.4.1 Standard States

In the gas phase, the standard state is that of the partial pressure of the gas equal to one standard atmosphere (101.3 kN m^{-2}). This is also the standard to which solubility is corrected.

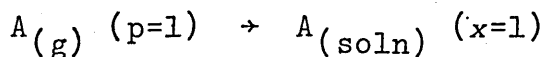
In the solution phase, the standard state is taken as the gas at a mole fraction of unity in the solution. This choice is encouraged by several factors:

- (a) mole fraction is the unit chosen to describe the solvent composition;
- (b) mole fraction is a measure of relative abundancies of molecules in the solution; and
- (c) units of concentration are excluded from calculations.

This standard state for the solution phase, also chosen by others,³³ is not one which would ever occur and indeed the solutions are always extremely dilute. However, the choice is an arbitrary one and for theoretical purposes, allows us to proceed.

3.4.2 Formulation of Thermodynamic Functions

The dissolution of a gas A ($p = 1 \text{ atm}$) in a solvent to form a solution containing A at a hypothetical mole fraction of unity may be represented as follows:



For a real gas (see section 3.3) the chemical potential is given by

$$\mu_{(g)} = \mu_{(g)}^{\ominus} + RT \ln \frac{p}{p^{\ominus}} + BP \quad (10)$$

For a solution of A,

$$\mu_{(soln)} = \mu_{(soln)}^{\ominus} + RT \ln \frac{a}{a^{\ominus}}$$

For a dilute ideal solution of A, this may be rewritten as

$$\mu_{(soln)} = \mu_{(soln)}^{\ominus} + RT \ln \frac{x}{x^{\ominus}} \quad (11)$$

Considering our choice of standard state, and for the gas and solution to be at equilibrium, we can write

$$\Delta \bar{G}^{\ominus} = \mu_{(soln)}^{\ominus} - \mu_{(g)}^{\ominus} = -RT \ln \left(\frac{x}{p} \right) + BP \quad (12)$$

The logarithmic term can be evaluated from

$$\frac{x}{p} = \frac{\text{mole fraction of A in solution phase}}{\text{partial pressure of gas A}}$$

$$= \frac{n_A}{n_A + n_B + n_C}$$

B = water

C = alcohol

because p_A is chosen to be one atmosphere. Since solubility s_0 is defined as the volume of gas at STP dissolved in 1 kg of solvent at $p_A = 1 \text{ atm}$, we can evaluate

n_A , i.e.

$$n_A = \frac{\text{volume of gas}}{\text{molar volume of gas}} = \frac{s_o}{V_m}$$

n_B and n_C are known so $\Delta \bar{G}^\circ$ can be evaluated.

$$\text{i.e. } \Delta \bar{G}^\circ = - RT \ln \left(\frac{n_A}{n_A + n_B + n_C} \right) + BP$$

$$\text{or } \Delta \bar{G}^\circ = 2.3026 RT \left[\log V_m + \log (n_A + n_B + n_C) - \log s_o \right]$$

$$+ BP \quad (13)$$

The Gibbs - Helmholtz equation gives

$$\begin{aligned} \Delta \bar{H}^\circ &= \Delta \bar{G}^\circ + T \Delta \bar{S}^\circ \\ &= \Delta \bar{G}^\circ - T \left(\frac{d\Delta \bar{G}^\circ}{dT} \right) \end{aligned}$$

$$\therefore \frac{\Delta \bar{H}^\circ}{T^2} = \frac{\Delta \bar{G}^\circ}{T^2} - \frac{1}{T} \left(\frac{d\Delta \bar{G}^\circ}{dT} \right)$$

$$\text{but } \frac{\Delta \bar{G}^\circ}{T^2} - \frac{1}{T} \left(\frac{d\Delta \bar{G}^\circ}{dT} \right) = - \frac{d}{dT} \left(\frac{\Delta \bar{G}^\circ}{T} \right)$$

$$\begin{aligned} \therefore \frac{\Delta \bar{H}^\circ}{T^2} &= - \frac{d}{dT} \left(\frac{\Delta \bar{G}^\circ}{T} \right) \\ &= \frac{-d\left(\frac{1}{T}\right)}{dT} \cdot \frac{d}{d\left(\frac{1}{T}\right)} \left(\frac{\Delta \bar{G}^\circ}{T} \right) \end{aligned}$$

$$\therefore \Delta \bar{H}^\circ = \frac{d}{d\left(\frac{1}{T}\right)} \left(\frac{\Delta \bar{G}^\circ}{T} \right)$$

By division and differentiation of (13) we get

$$\Delta \bar{H}^\circ = 2.3026 R \frac{d}{d\left(\frac{1}{T}\right)} (\log s_o) + BP \quad (14)$$

because $n_A \ll (n_B + n_C)$ and so $(n_A + n_B + n_C)$ is approximately constant over the range of $\frac{1}{T}$ considered.

An expression for $\Delta \bar{S}^\circ$ is now obtained directly from the Gibbs - Helmholtz equation

$$\Delta \bar{S}^\circ = \frac{\Delta \bar{H}^\circ - \Delta \bar{G}^\circ}{T} \quad (15)$$

For the purposes of checking, $\Delta \bar{C}_p^\circ$ is also evaluated

$$\Delta \bar{C}_p^\circ = \frac{d\Delta \bar{H}^\circ}{dT}$$

and used in Kirchoff's equation to support $\Delta \bar{H}^\circ$.

$$\text{i.e. } \Delta \bar{H}_1^\circ = \Delta \bar{H}_0^\circ + (T \Delta \bar{C}_p^\circ) \quad \text{where } T = T_1 - T_0$$

In the following section the corrections for non-ideality have been omitted because the value of BP is so small compared to the calculated thermodynamic functions. Examination of Tables 4.5.1 to 4.6.8 shows that for all of the gas - solvent systems studied, typical values for $\Delta \bar{G}^\circ$ and $\Delta \bar{H}^\circ$ were of the order of 25 kJ mol⁻¹ and 15 kJ mol⁻¹ respectively. Comparison of these values with the maximum value of BP equal to 61 J mol⁻¹ (taken from Table 3.3.1) shows that the largest deviation from ideality corresponds to an uncertainty of about 0.25% in $\Delta \bar{G}^\circ$ and 0.4% in $\Delta \bar{H}^\circ$.

These are significantly less than the uncertainty due to experimental error and it is therefore considered unnecessary to complicate the calculations which follow by introducing a non-ideality correction factor.

3.5 Methods of Evaluation

Calculation of values of all the thermodynamic functions was carried out by computer and it was therefore necessary to manipulate some of the expressions further to enable numerical methods to be used. The solubility data in the $\log s_o$ form was treated in the following way. To convert this to s_o , the operation

$$s_o = \exp[2.3026 \log s_o]$$

was used. The number of moles of gas in solution was calculated from this,

$$n_A = \frac{s_o}{V_m} \text{ (in cm}^3\text{)}$$

This leads to the evaluation of x_A , the mole fraction of gas in solution,

$$x_A = \frac{n_A}{n_A + n_B + n_C}$$

from which Henry's Law constant

$$K_H = \frac{1}{x_A} ,$$

and $\Delta \bar{G}^\circ$ are calculated.

$$\Delta \bar{G}^\circ = - RT \ln x_A$$

Then, reference to equation (14) shows that $\Delta \bar{H}^\circ$ can be effectively calculated from the gradients of the solubility curves at temperatures corresponding to values midway between each integral value of $\frac{10^4}{T}$.

The numerical method employed involves taking values of $\log s_o$, corresponding to integral values of $\frac{10^4}{T}$, from a given solubility curve. The difference, $\Delta \log s_o$, between each successive pair is calculated and is related to $\Delta \bar{H}^\circ$ through the equation

$$\Delta \bar{H}^\circ = \frac{\Delta \log s_o}{10^{-4}} \times 2.3026 R$$

Thus, $\Delta \bar{H}^\circ$ values are obtained for temperatures corresponding to those midway between integral $\frac{10^4}{T}$ values. These are plotted against temperature and Kirchoff lines are constructed. The plot usually results in a slight curvature through the points but within experimental error, this can be equated to two straight lines (see Fig 3.5(i)) each of gradients $\Delta \bar{C}_p^\circ$.

These graphs are constructed for all of the solubility curves and from them the values of $\Delta \bar{H}_{290K}^\circ$, $\Delta \bar{H}_{310K}^\circ$, $\Delta \bar{C}_{pT < 300K}^\circ$ and $\Delta \bar{C}_{pT > 300K}^\circ$ are obtained. These are plotted

against solvent composition (see Fig 3.5(ii)) and the best curve through the points is drawn. The most likely values of the above functions are then taken and inserted in Kirchoff's equation in order to calculate $\Delta \bar{H}^\circ$ for each of the integral values of $\frac{10^4}{T}$.

$$\text{i.e. } \Delta \bar{H}_T^\circ = \Delta \bar{H}_O^\circ + \Delta \bar{C}_{p290K}^\circ \quad (T-O)$$

$$\text{or } \Delta \bar{H}_T^\circ = \Delta \bar{H}_O^\circ + \Delta \bar{C}_{p310K}^\circ \quad (T-O)$$

Figure 3.5(i) Plot of $\Delta \bar{H}^\circ$ vs T for the system butane-ethanol-water at mole fraction of alcohol, $x_C = 0.3$.

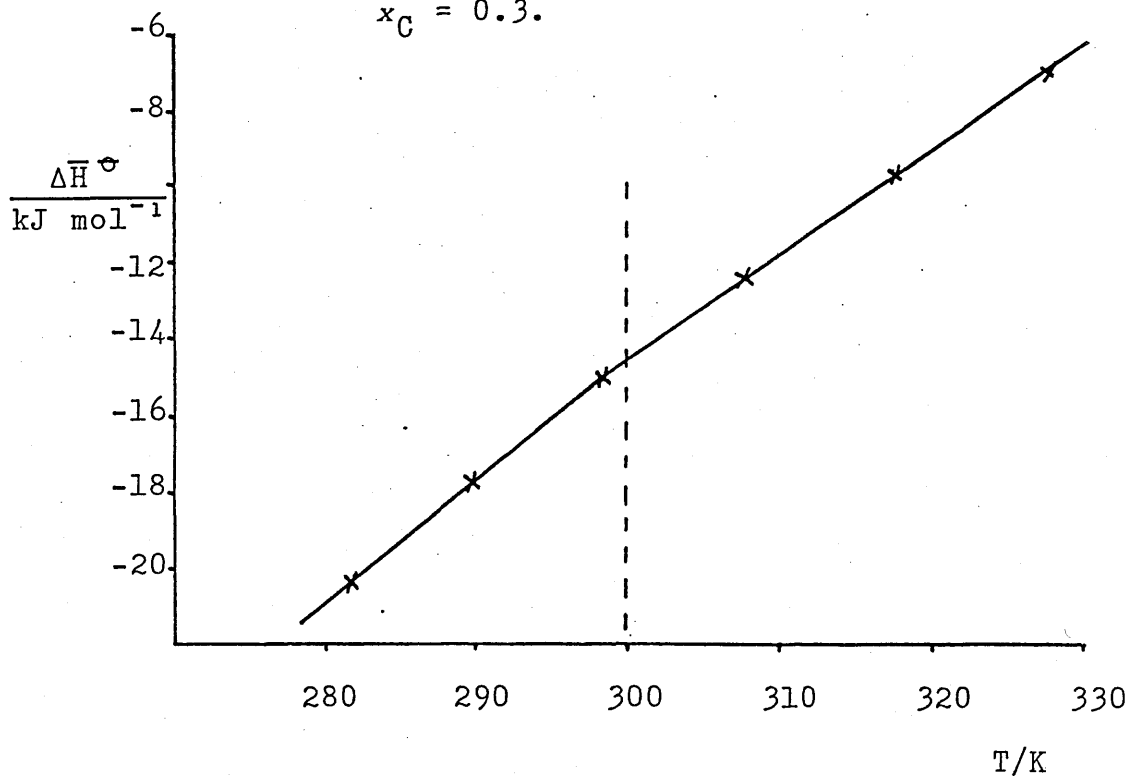
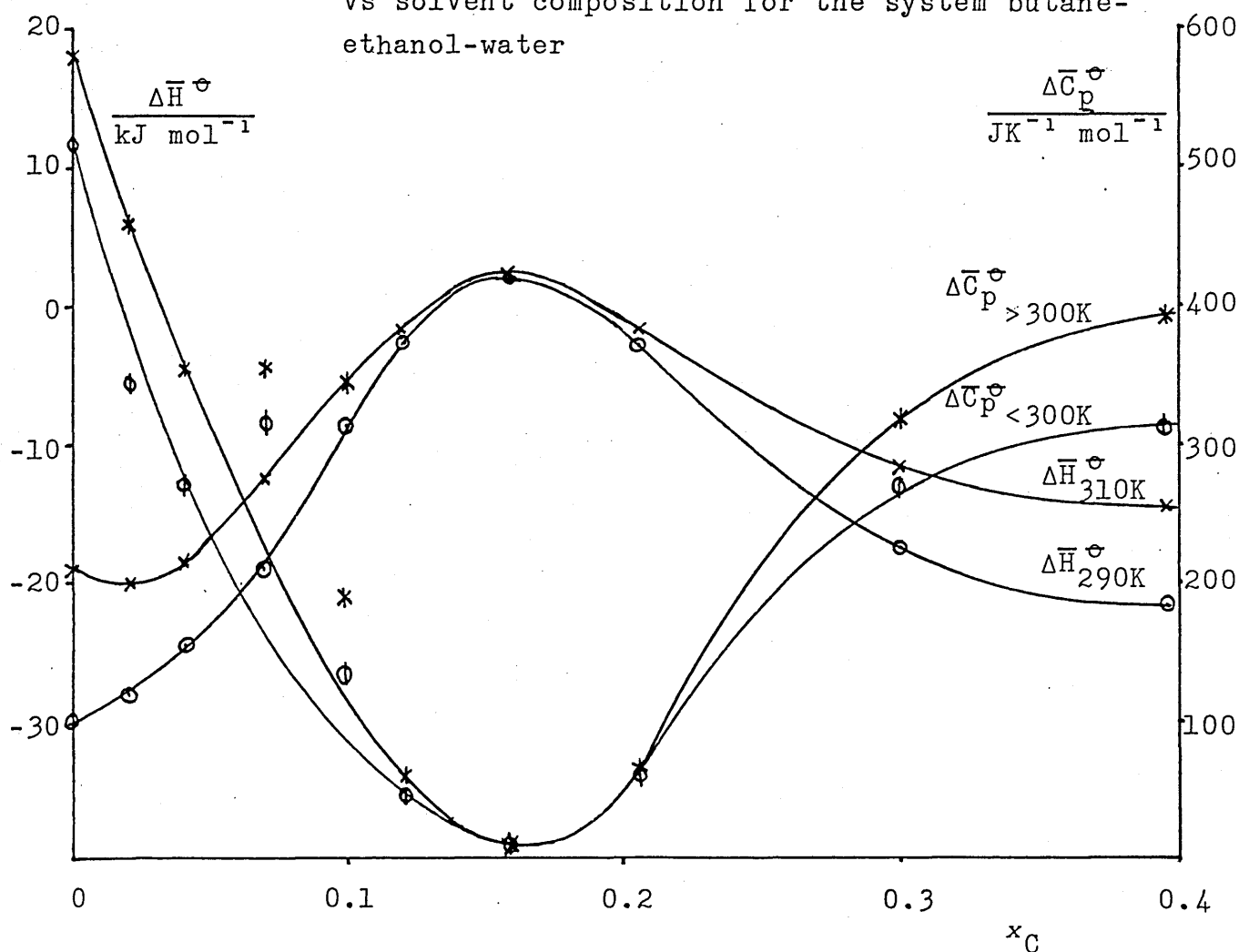


Figure 3.5(ii) Plot of $\Delta \bar{H}_{290\text{K}}^\circ$, $\Delta \bar{H}_{310\text{K}}^\circ$, $\Delta \bar{C}_p^\circ < 300\text{K}$ and $\Delta \bar{C}_p^\circ > 300\text{K}$ vs solvent composition for the system butane-ethanol-water



Now, since the calculation of $\Delta \bar{H}^\circ$ is very dependant on the accuracy of the solubility curve used, some means of checking it must be available. A numerical method exists whereby $\Delta \log s_o$ is calculated as above, then $\Delta \Delta \log s_o$, the difference between successive values of $\Delta \log s_o$ is found. Analysis of Kirchoff's equation shows that this $\Delta \Delta \log s_o$ is proportional to $\Delta \bar{C}_p^\circ$ which was found to remain approximately constant over the range of experimental temperatures. Consider, for example, the case where butane is the solute in an aqueous ethanol solvent of alcohol mole fraction, $x_C = 0.396$. Table 3.5.1 shows the values of $\Delta \log s_o$ and the constant $\Delta \Delta \log s_o$ which confirm the values of $\log s_o$ compatable with experimental observations for this system.

Table 3.5.1 : Numerical Data to confirm the accuracy of a solubility curve.

$\frac{10^4}{T}$	$\log s_o$	$\Delta \log s_o$	$\Delta \Delta \log s_o$
36	3.7750		
35	3.6455	0.1295	0.0165
34	3.5325	0.1130	0.0165
33	3.4360	0.0965	0.0165
32	3.3560	0.0800	0.0165
31	3.2925	0.0635	0.0165
30	3.2455	0.0470	

This numerical method, which was easily adapted to a computer operation (Appendix III(b)), along with curve fitting on the solubility isotherms, gave two methods of checking the solubility curves, allowing considerable confidence to be placed in them.

Finally, $\Delta \bar{S}^\circ$ is calculated directly from the Gibbs - Helmholtz equation using the obtained values of $\Delta \bar{G}^\circ$ and $\Delta \bar{H}^\circ$

$$\text{i.e. } \Delta \bar{S}^\circ = \frac{\Delta \bar{H}^\circ - \Delta \bar{G}^\circ}{T}$$

The software employed for the above calculations is given in Appendices III to VI inclusive.

It should be noted that the error in $\Delta \bar{C}_p^\circ$ may be fairly high due to the second differentiation of $\log s_o$ and might be as high as 10%. However, $\Delta \bar{C}_p^\circ$ data have been used only indirectly in this study, and the accuracy of those functions used more critically is 0.5% in the solubility s_o , and 0.5, 1, and 2.5% respectively in $\Delta \bar{G}^\circ$, $\Delta \bar{H}^\circ$ and $\Delta \bar{S}^\circ$.

4. RESULTS

4.1 RESULTS

The results obtained in this study are now presented in this chapter. To begin with, the experimental solubilities are tabulated for each gas-solvent system in Tables 4.1.1 to 4.1.8 along with temperature and the logarithm of the corrected solubilities. These are then displayed graphically as solubility curves in Figures 4.2.1 to 4.2.8 and as solubility isotherms in Figures 4.3.1 to 4.3.7.

Owing to experimental limitations of the apparatus, very high solubilities could not be accurately determined and for this reason, the most concentrated alcohol solution in water corresponded to a mole fraction of 0.396.

Next, the derived thermodynamic data are presented in Tables 4.4.1 to 4.4.8 and the corresponding isotherms of $\Delta\bar{G}^\circ$, $\Delta\bar{H}^\circ$ and $\Delta\bar{S}^\circ$ are constructed and given in sections 4.5, 4.6 and 4.7 respectively.

It should be noted at this stage however, that with 2-methylpropan-2-ol as co-solvent to water, the solubility measurements at alcohol mole fractions greater than about 0.08 were affected by a phase separation in the solvent. This was particularly noticable in the butane-water-2-methylpropan-2-ol system and further investigation of these solvent systems was not possible.

Table 4.1.1 Experimental Solubility Data for propane in mixtures of water and ethanol

Mole Fraction of ethanol (x_c)	T/K	$s/\text{cm}^3 \text{ kg}^{-1}$	$\log(s_0/\text{cm}^3 \text{ kg}^{-1})$
0.000	277.0	75.7	1.873
	279.3	66.0	1.810
	282.3	60.5	1.767
	284.3	54.7	1.720
	293.1	39.5	1.566
	303.5	30.8	1.443
	313.0	25.7	1.351
	322.2	21.6	1.262
	327.8	20.8	1.240
0.020	279.1	73.0	1.854
	281.6	68.7	1.824
	287.1	53.9	1.710
	293.4	44.8	1.620
	303.3	35.0	1.499
	310.7	30.7	1.431
	313.5	29.4	1.409
	318.3	27.4	1.372
	323.2	24.4	1.314
0.040	331.4	22.5	1.269
	283.9	73.7	1.859
	284.7	62.9	1.780
	291.3	51.6	1.685
	301.1	41.3	1.571
	301.7	40.6	1.566
	312.0	33.5	1.468
	322.7	29.2	1.393
0.069	279.4	71.2	1.842
	279.9	71.4	1.843
	289.0	58.0	1.739
	298.9	49.8	1.658
	309.5	42.2	1.574
	320.4	38.8	1.520
	332.2	37.3	1.487
0.098	278.7	64.0	1.797
	287.1	59.1	1.750
	292.8	54.4	1.705
	304.1	56.0	1.702
	313.3	53.0	1.665
	322.6	52.8	1.650
	333.1	51.2	1.623

Table 4.1.1 (Contd)

Experimental Solubility Data for propane in
mixtures of water and ethanol

Mole Fraction of ethanol (x_c)	T/K	$s/\text{cm}^3 \text{ kg}^{-1}$	$\log(s_o/\text{cm}^3 \text{ kg}^{-1})$
0.120	277.2	72.0	1.851
	283.9	70.3	1.833
	294.7	70.0	1.812
	304.1	70.3	1.800
	312.8	67.3	1.769
	314.5	70.2	1.785
	323.9	67.8	1.757
	332.9	69.7	1.767
0.159	278.3	100.8	1.995
	281.0	103.7	2.004
	290.7	110.4	2.016
	303.0	120.4	2.036
	313.0	125.0	2.038
	322.0	132.0	2.051
0.206	284.6	227.0	2.338
	297.1	236.0	2.336
	306.4	240.0	2.330
	317.3	249.0	2.332
	324.2	247.0	2.319
	324.2	261.0	2.342
0.300	278.6	872	2.932
	289.2	758	2.855
	298.0	695	2.804
	304.0	658	2.772
	322.4	607	2.711
	333.1	583	2.680
0.396	280.3	1771	3.237
	285.6	1620	3.190
	292.9	1373	3.107
	313.3	1185	3.014
	323.7	1162	2.992
	334.1	1047	2.933

Table 4.1.2 Experimental Solubility Data for butane in mixtures of water and ethanol

Mole Fraction of ethanol (x_c)	T/K	$s/\text{cm}^3 \text{ kg}^{-1}$	$\log(s_0/\text{cm}^3 \text{ kg}^{-1})$
0.000	277.1	68.3	1.828
	279.3	57.8	1.752
	282.3	53.0	1.710
	284.3	47.9	1.663
	293.1	34.5	1.507
	303.5	24.3	1.340
	313.0	19.6	1.233
	323.0	17.0	1.159
	327.8	15.9	1.123
	333.1	16.4	1.129
0.020	279.1	67.7	1.821
	281.6	61.7	1.777
	287.1	46.7	1.647
	293.4	37.4	1.542
	303.3	28.2	1.404
	310.7	24.5	1.332
	323.2	18.9	1.203
	331.4	17.2	1.152
0.040	283.9	72.1	1.850
	284.7	58.0	1.745
	291.3	46.0	1.635
	301.7	34.9	1.500
	312.0	28.8	1.387
	322.7	23.8	1.304
0.069	279.4	72.7	1.852
	279.9	72.7	1.851
	298.9	46.0	1.624
	309.5	38.8	1.535
	320.4	35.3	1.479
	332.3	32.8	1.431
0.098	278.7	69.1	1.831
	287.1	62.7	1.776
	292.8	61.0	1.755
	304.1	56.9	1.708
	313.3	53.3	1.667
	322.6	52.7	1.649
	333.6	51.8	1.627

Table 4.1.2 (Contd)

Experimental Solubility Data for butane in
mixtures of water and ethanol

Mole Fraction of ethanol (x_c)	T/K	$s/\text{cm}^3 \text{ kg}^{-1}$	$\log(s_o/\text{cm}^3 \text{ kg}^{-1})$
0.120	277.2	78.7	1.889
	283.9	77.7	1.873
	293.6	80.7	1.875
	302.9	79.0	1.853
	304.1	78.7	1.849
	314.5	79.0	1.836
	323.9	78.7	1.822
	332.9	82.8	1.832
0.159	281.0	160.8	2.147
	290.7	152.5	2.156
	291.5	150.0	2.148
	303.0	164.6	2.171
	313.0	174.6	2.183
	322.0	185.8	2.198
0.206	278.4	406.0	2.600
	286.0	391.0	2.573
	296.5	405.0	2.572
	306.4	424.0	2.577
	317.3	405.0	2.543
	324.2	408.0	2.536
	333.6	421.0	2.537
0.300	279.8	2310	3.353
	289.2	1821	3.236
	298.0	1553	3.153
	308.5	1302	3.062
	322.4	1162	2.993
	333.1	1050	2.935
0.396	280.3	5487	3.728
	284.2	5300	3.707
	292.9	3775	3.547
	313.3	2633	3.361
	323.7	2294	3.287
	334.1	2145	3.244

Table 4.1.3 Experimental Solubility Data for 2-methylpropane
in mixtures of water and ethanol

Mole Fraction of ethanol (x_c)	T/K	$s/\text{cm}^3 \text{ kg}^{-1}$	$\log(s_0/\text{cm}^3 \text{ kg}^{-1})$
0.000	288.4	29.2	1.442
	298.9	21.4	1.291
	307.5	17.5	1.192
	308.9	17.0	1.178
	319.9	13.3	1.052
	328.5	11.2	0.966
0.026	285.5	37.8	1.558
	297.2	27.4	1.401
	306.2	23.7	1.328
	317.4	19.6	1.227
	329.3	18.0	1.173
0.062	284.9	40.8	1.592
	298.3	33.0	1.481
	308.1	28.6	1.404
	317.3	28.5	1.390
	331.1	27.7	1.359
0.100	287.2	41.4	1.595
	294.9	39.8	1.566
	306.5	38.1	1.532
	317.9	36.8	1.500
	330.5	37.7	1.494
0.128	287.2	54.3	1.713
	297.7	59.9	1.740
	307.0	62.4	1.744
	317.8	66.5	1.756
	330.0	70.6	1.767
0.168	286.6	130.4	2.095
	296.8	142.8	2.119
	308.7	162.2	2.157
	317.6	178.0	2.182
	329.3	178.3	2.170

Table 4.1.3 (Contd)

Experimental Solubility Data for 2-methylpropane
in mixtures of water and ethanol

Mole Fraction of ethanol (x_c)	T/K	$s/\text{cm}^3 \text{ kg}^{-1}$	$\log(s_o/\text{cm}^3 \text{ kg}^{-1})$
0.216	285.5	396.8	2.579
	293.7	393.9	2.564
	306.5	379.8	2.529
	317.7	363.5	2.492
	329.9	355.7	2.469
<hr/>			
0.319	285.5	1576	3.178
	297.1	1295	3.076
	305.9	1184	3.024
	319.6	1097	2.972
	327.9	965	2.904

Table 4.1.4 Experimental Solubility Data for
2,2-dimethylpropane in mixtures of water
and ethanol

Mole Fraction of ethanol (x_c)	T/K	$s/\text{cm}^3 \text{ kg}^{-1}$	$\log(s_o/\text{cm}^3 \text{ kg}^{-1})$
0.000	284.9	19.7	1.276
	288.4	16.3	1.189
	298.9	13.0	1.075
	307.5	11.0	0.990
	319.9	8.2	0.842
	328.5	7.4	0.786
0.026	285.5	22.8	1.339
	297.2	17.1	1.197
	306.2	14.9	1.126
	317.4	12.0	1.016
	329.3	10.8	0.954
0.062	284.9	26.4	1.404
	298.3	21.5	1.295
	308.1	18.8	1.222
	317.3	18.3	1.198
	331.1	18.0	1.172
0.1	285.0	30.7	1.469
	287.2	29.1	1.443
	294.9	28.2	1.417
	306.5	26.5	1.373
	317.9	25.9	1.348
	330.5	26.7	1.344
0.128	287.2	42.0	1.602
	297.7	48.1	1.645
	307.0	50.4	1.652
	317.8	54.5	1.671
	330.0	57.0	1.674
0.168	286.6	149.3	2.153
	296.8	147.0	2.131
	308.7	162.7	2.158
	317.6	174.5	2.174
	329.3	174.8	2.161

Table 4.1.4 (Contd)

Experimental Solubility Data for
2,2-dimethylpropane in mixtures of water
and ethanol

Mole Fraction of ethanol (x_c)	T/K	$s/\text{cm}^3 \text{ kg}^{-1}$	$\log(s_0/\text{cm}^3 \text{ kg}^{-1})$
0.216	285.5	492.0	2.673
	293.7	437.6	2.610
	306.5	403.5	2.556
	317.7	398.9	2.533
	329.9	366.6	2.482
<hr/>			
0.319	285.5	2321	3.346
	297.1	1809	3.221
	305.9	1623	3.161
	319.6	1494	3.069
	327.9	1232	3.010

Table 4.1.5 Experimental Solubility Data for cyclopropane in mixtures of water and ethanol

Mole Fraction of ethanol (x_c)	T/K	$s/\text{cm}^3 \text{ kg}^{-1}$	$\log(s_o/\text{cm}^3 \text{ kg}^{-1})$
0.000	279.1	563.2	2.741
	279.8	572.0	2.747
	280.6	523.2	2.707
	289.0	383.0	2.559
	297.9	294.0	2.431
	305.9	237.6	2.327
	308.7	223.0	2.295
	321.8	177.7	2.179
	331.5	153.3	2.102
0.032	278.3	610.9	2.778
	283.1	509.0	2.691
	294.6	361.0	2.525
	305.6	284.0	2.405
	314.4	246.7	2.331
	323.6	210.0	2.249
	332.3	193.0	2.200
0.072	279.1	567.1	2.744
	288.9	449.0	2.628
	294.8	396.8	2.565
	305.3	343.0	2.487
	313.9	306.8	2.426
	330.0	267.1	2.345
0.088	279.5	550.3	2.731
	284.0	484.8	2.669
	289.1	479.4	2.656
	298.9	399.9	2.563
	308.7	357.4	2.500
	320.7	327.8	2.446
	331.1	305.0	2.401
0.119	279.9	593.2	2.763
	285.0	550.5	2.722
	289.3	531.0	2.700
	300.4	478.6	2.639
	310.7	418.5	2.566
	321.1	389.9	2.521
	330.9	377.8	2.494

Table 4.1.5 (Contd)

Experimental Solubility Data for cyclopropane in
mixtures of water and ethanol

Mole Fraction of ethanol (x_c)	T/K	$s/\text{cm}^3 \text{ kg}^{-1}$	$\log(s_o/\text{cm}^3 \text{ kg}^{-1})$
0.148	277.6	763.5	2.876
	283.6	726.3	2.845
	290.0	686.4	2.810
	300.4	646.5	2.769
	310.6	601.9	2.724
	311.3	573.8	2.702
	321.6	580.7	2.693
	321.7	516.8	2.642
	331.9	544.7	2.652
0.186	279.6	1078.5	3.023
	285.1	1010.4	2.986
	285.1	974.2	2.970
	290.4	993.4	2.970
	301.3	930.0	2.926
	311.0	864.7	2.880
	322.1	819.8	2.842
0.226	279.4	1695	3.219
	281.6	1631	3.199
	290.9	1451	3.134
	300.7	1333	3.083
	311.7	1227	3.031
	322.1	1169	2.996
	332.6	1037	2.930
0.322	279.1	3642	3.552
	282.1	3630	3.546
	293.1	3122	3.464
	303.1	2686	3.384

Table 4.1.6 Experimental Solubility Data for propene in mixtures of water and ethanol

Mole Fraction of ethanol (x_c)	T/K	$s/\text{cm}^3 \text{ kg}^{-1}$	$\log(s_o/\text{cm}^3 \text{ kg}^{-1})$
0.000	279.1	246.1	2.382
	279.8	234.8	2.360
	280.6	234.4	2.358
	289.0	176.4	2.222
	297.9	133.7	2.089
	305.9	114.5	2.010
	308.7	104.6	1.967
	321.8	86.7	1.867
	331.5	80.0	1.819
0.032	278.3	262.7	2.411
	283.1	227.4	2.341
	294.6	167.0	2.190
	305.6	135.0	2.082
	314.4	118.4	2.013
	323.6	105.0	1.947
	332.3	98.4	1.908
0.072	279.1	239.7	2.370
	288.9	200.7	2.278
	294.8	173.1	2.205
	305.3	160.7	2.158
	313.9	149.7	2.115
	330.0	138.0	2.058
0.088	279.5	234.6	2.360
	284.0	215.0	2.316
	289.1	213.5	2.305
	298.9	187.3	2.233
	308.7	173.8	2.187
	320.7	167.6	2.155
	331.1	164.3	2.132
0.119	279.5	236.1	2.362
	285.0	236.0	2.355
	289.3	232.2	2.341
	300.4	227.6	2.316
	310.7	218.1	2.283
	321.1	215.4	2.263
	330.9	212.3	2.244

Table 4.1.6 (Contd)

Experimental Solubility Data for propene in
mixtures of water and ethanol

Mole Fraction of ethanol (x_c)	T/K	$s/\text{cm}^3 \text{ kg}^{-1}$	$\log(s_o/\text{cm}^3 \text{ kg}^{-1})$
0.148	277.6	291.8	2.458
	283.6	298.7	2.459
	290.0	307.4	2.462
	300.4	313.8	2.455
	310.6	309.0	2.434
	311.3	311.1	2.436
	321.6	309.1	2.419
	321.7	312.9	2.424
	331.9	304.4	2.399
0.186	279.6	469.5	2.661
	285.1	463.5	2.647
	285.1	475.4	2.658
	290.4	478.0	2.653
	301.3	465.2	2.625
	311.0	453.4	2.600
	322.1	446.2	2.578
	331.9	446.5	2.565
0.226	279.4	769.4	2.876
	281.6	744.2	2.858
	290.9	680.3	2.808
	300.7	681.5	2.792
	311.7	654.9	2.759
	322.1	640.8	2.735
	332.6	606.0	2.697
0.322	279.1	1757	3.235
	282.1	1718	3.221
	293.1	1604	3.175
	303.1	1400	3.101
	312.9	1348	3.070
	323.5	1240	3.020
	333.3	1220	3.000

Table 4.1.7 Experimental Solubility Data for propane in mixtures of water and 2-methylpropan-2-ol

Mole fraction of
2-methylpropan-2-ol
(x_c)

	T/K	$s/\text{cm}^3 \text{ kg}^{-1}$	$\log(s_o/\text{cm}^3 \text{ kg}^{-1})$
0.000	277.0	75.7	1.873
	279.3	66.0	1.810
	282.3	60.5	1.767
	284.3	54.7	1.720
	293.1	39.5	1.566
	303.5	30.8	1.443
	313.0	25.7	1.351
	322.2	21.6	1.262
	327.8	20.8	1.240
0.005	282.2	63.5	1.789
	286.3	51.6	1.690
	290.5	45.7	1.633
	296.9	38.0	1.544
	306.4	29.2	1.416
	317.7	24.0	1.315
	326.2	21.5	1.256
	334.8	20.2	1.218
0.026	280.5	70.6	1.837
	283.0	59.8	1.761
	287.6	51.7	1.691
	295.3	41.6	1.585
	305.7	33.3	1.473
	317.4	28.5	1.390
	326.8	26.7	1.349
	333.6	24.9	1.310
0.038	278.8	63.0	1.790
	282.4	56.2	1.736
	290.5	47.9	1.653
	299.8	41.0	1.572
	309.1	37.1	1.506
	318.9	36.4	1.493
	334.2	35.7	1.736

Table 4.1.7 (Contd)

Experimental Solubility Data for propane in
mixtures of water and 2-methylpropan-2-ol

Mole fraction of
2-methylpropan-2-ol
(x_c)

	T/K	$s/\text{cm}^3 \text{ kg}^{-1}$	$\log(s_o/\text{cm}^3 \text{ kg}^{-1})$
0.050	280.6	50.0	1.687
	285.2	51.3	1.692
	295.7	56.2	1.716
	306.1	61.0	1.736
	326.8	70.9	1.772
	333.6	75.0	1.788
<hr/>			
0.066	278.2	90.7	1.950
	283.2	91.5	1.946
	296.9	114.3	2.022
	306.9	137.1	2.086
	331.2	247.0	2.309
	331.6	268.0	2.344

Table 4.1.8 Experimental Solubility Data for butane in mixtures of water and 2-methylpropan-2-ol

Mole fraction of
2-methylpropan-2-ol
(x_c)

	T/K	$s/\text{cm}^3 \text{ kg}^{-1}$	$\log(s_o/\text{cm}^3 \text{ kg}^{-1})$
0.000	277.1	68.3	1.828
	279.3	57.8	1.752
	282.3	53.0	1.710
	284.3	47.9	1.663
	293.1	34.5	1.507
	303.5	24.3	1.340
	313.0	19.6	1.233
	323.0	17.0	1.159
	327.8	15.9	1.123
	333.1	16.4	1.129
0.005	282.2	58.2	1.751
	290.5	38.6	1.560
	296.9	31.6	1.463
	306.4	22.4	1.301
	316.1	18.4	1.232
	317.7	17.9	1.188
	326.2	16.4	1.137
	334.8	15.5	1.103
0.026	280.5	64.2	1.796
	283.0	52.1	1.701
	295.3	35.9	1.521
	305.7	26.7	1.378
	317.4	23.3	1.303
	326.8	21.4	1.253
	333.6	20.2	1.218
0.038	278.8	56.5	1.743
	282.4	48.8	1.674
	299.8	36.4	1.520
	309.1	32.8	1.452
	318.9	33.6	1.459
	334.2	32.8	1.429
0.050	280.6	55.8	1.735
	285.2	56.9	1.736
	295.7	67.4	1.794
	306.1	76.2	1.832
	326.8	96.0	1.904
	333.6	102.4	1.923

Table 4.1.8 (Contd)

Experimental Solubility Data for butane in
mixtures of water and 2-methylpropan-2-ol

Mole fraction of 2-methylpropan-2-ol (x_c)	T/K	$s/\text{cm}^3 \text{ kg}^{-1}$	$\log(s_o/\text{cm}^3 \text{ kg}^{-1})$
0.080	290.3	1176	3.044
	298.4	823	2.877
	308.8	768	2.832
	319.1	697	2.776
	330.1	605	2.699
	331.1	587	2.685

4.2 Solubility Curves

The solubility curves are now presented for each gas-solvent system as plots of $\log s_0$ against $10^4 K/T$. In the case of the system containing 2,2-dimethylpropane, which liquefies at 9.5°C , the experimental temperature range was restricted and this prevented measurements corresponding to a reciprocal temperature value of $36 \times 10^{-4} \text{ K}^{-1}$. Since this system was investigated simultaneously with the 2-methylpropane-water-ethanol system, the same restrictions applied here also.

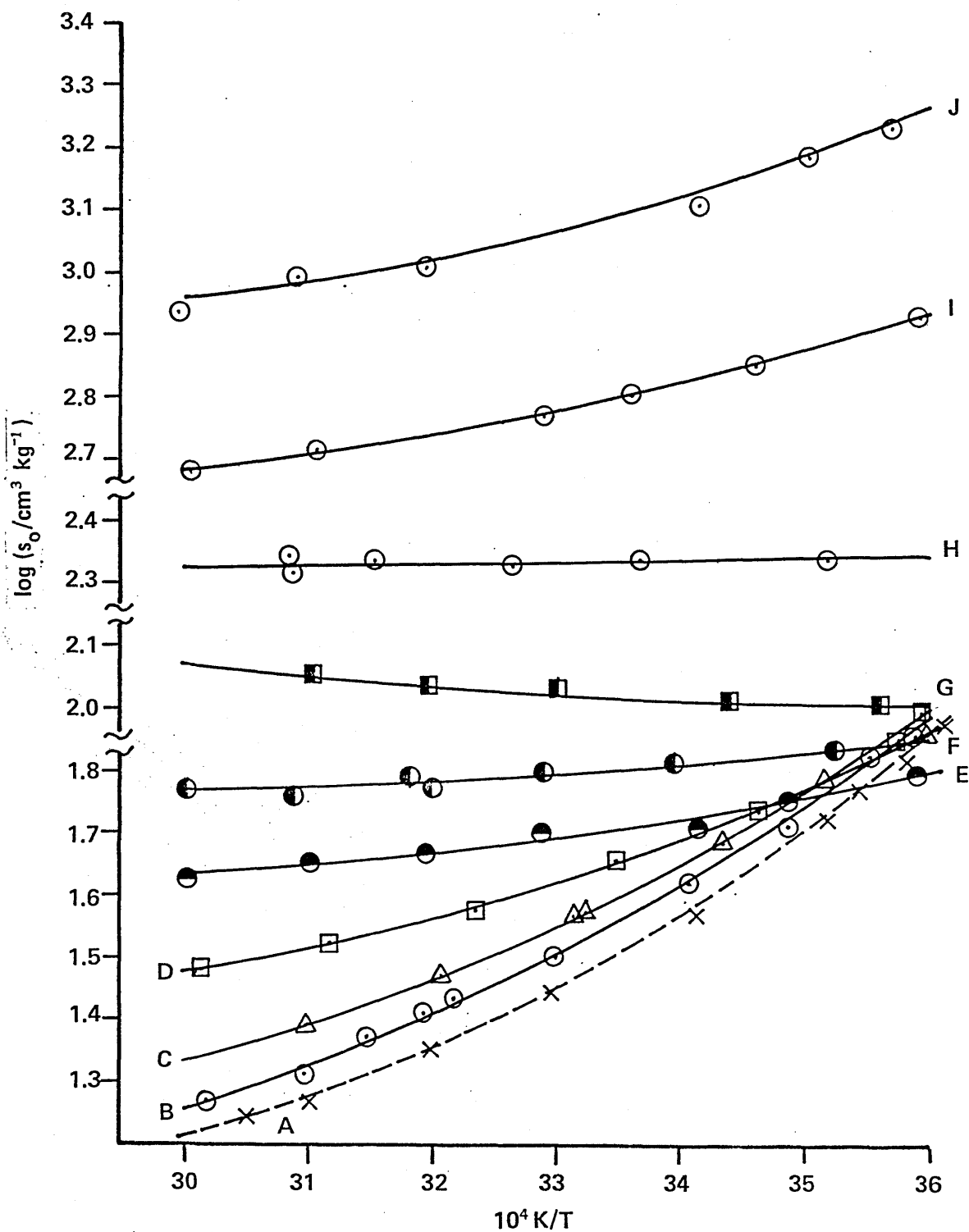


Figure 4.2.1 : Solubility curves for propane in aqueous ethanol of mole fraction:
 A, 0.000; B, 0.02; C, 0.04; D, 0.069;
 E, 0.098; F, 0.12; G, 0.159; H, 0.206;
 I, 0.300; J, 0.396.

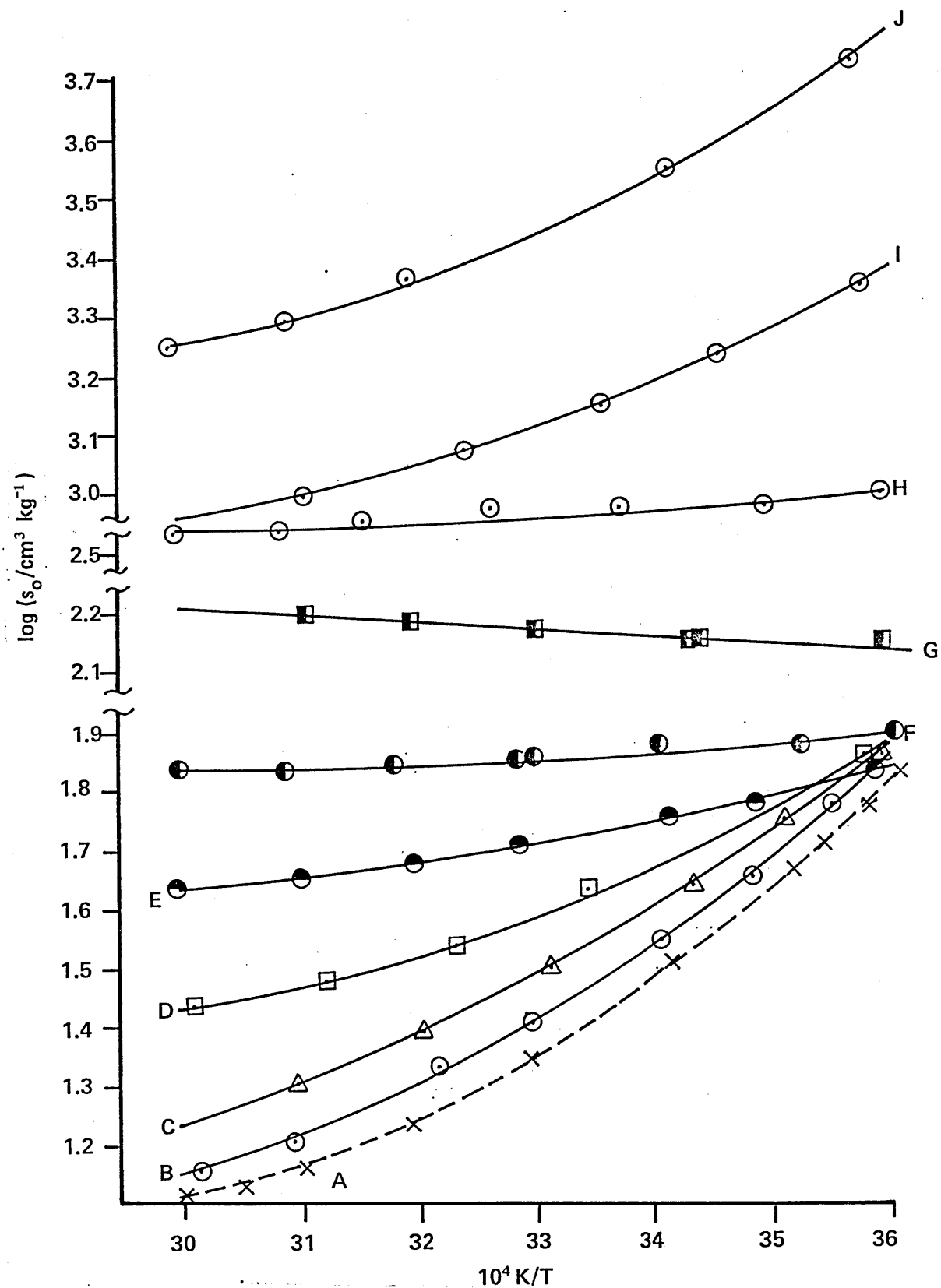


Figure 4.2.2 : Solubility curves for butane in aqueous ethanol of mole fraction:
 A, 0.000; B, 0.02; C, 0.04; D, 0.069;
 E, 0.098; F, 0.12; G, 0.159; H, 0.206,
 I, 0.300; J, 0.396.

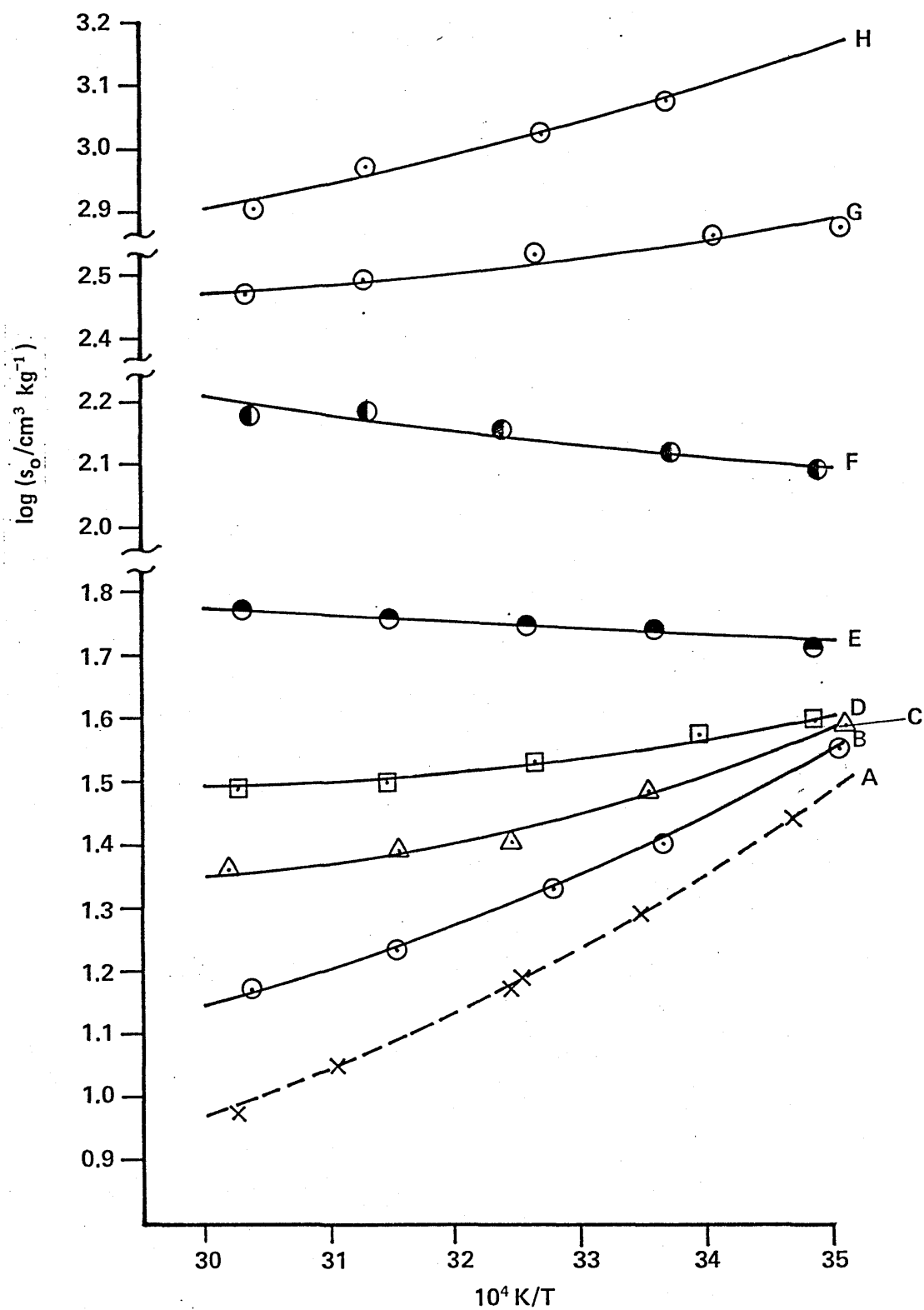


Figure 4.2.3 : Solubility curves for 2-methylpropane in aqueous ethanol of mole fraction:

A, 0.000; B, 0.026; C, 0.062; D, 0.10;
E, 0.128; F, 0.168; G, 0.216; H, 0.319.

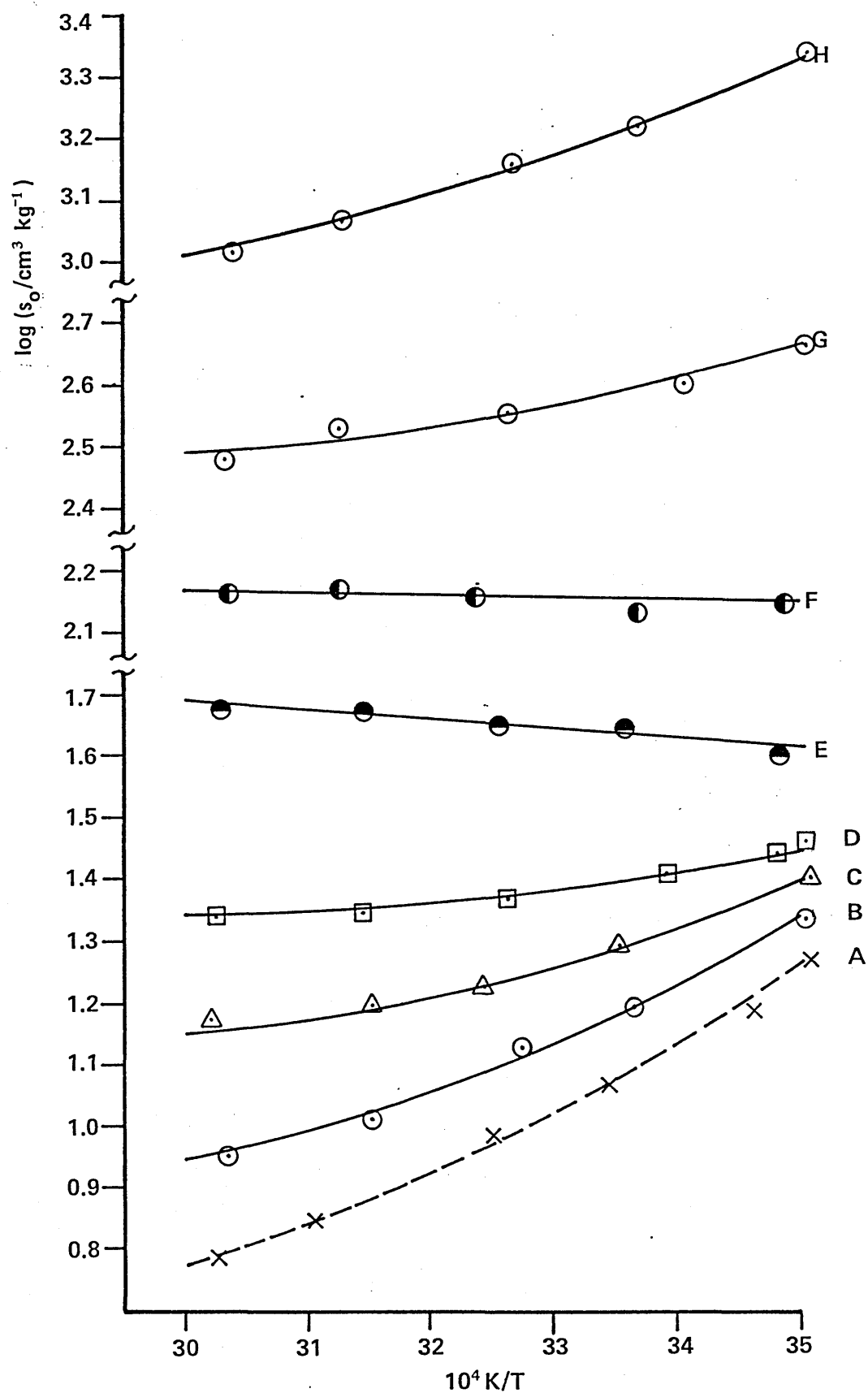


Figure 4.2.4 : Solubility curves for 2,2-dimethylpropane in aqueous ethanol of mole fraction:

A, 0.000; B, 0.026; C, 0.062; D, 0.10;
E, 0.128; F, 0.168; G, 0.216; H, 0.319.

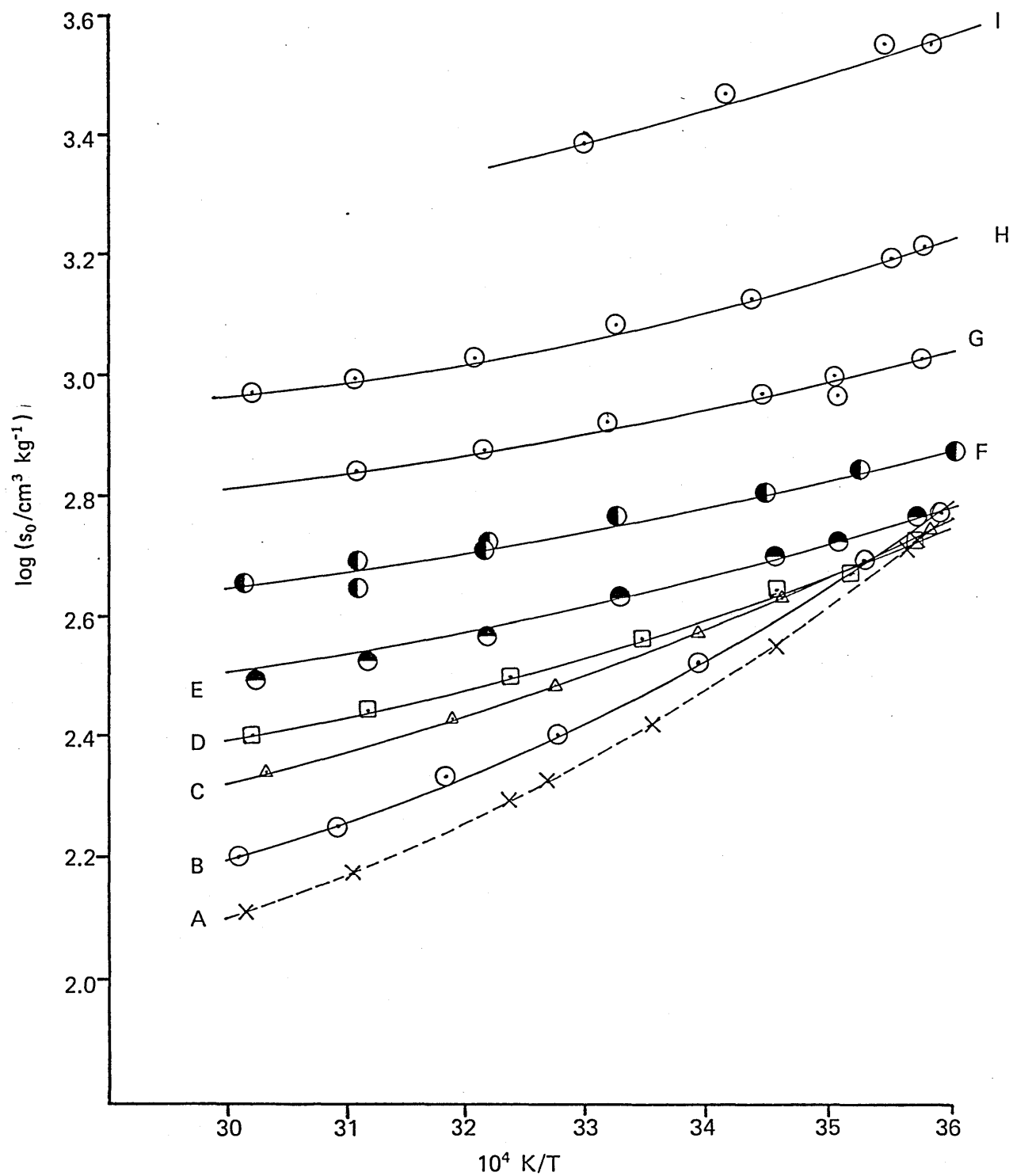


Figure 4.2.5: Solubility curves for cyclopropane in aqueous ethanol of mole fraction:

A, 0.000; B, 0.032; C, 0.072; D, 0.088; E, 0.119; F, 0.148; G, 0.186; H, 0.226; I, 0.322.

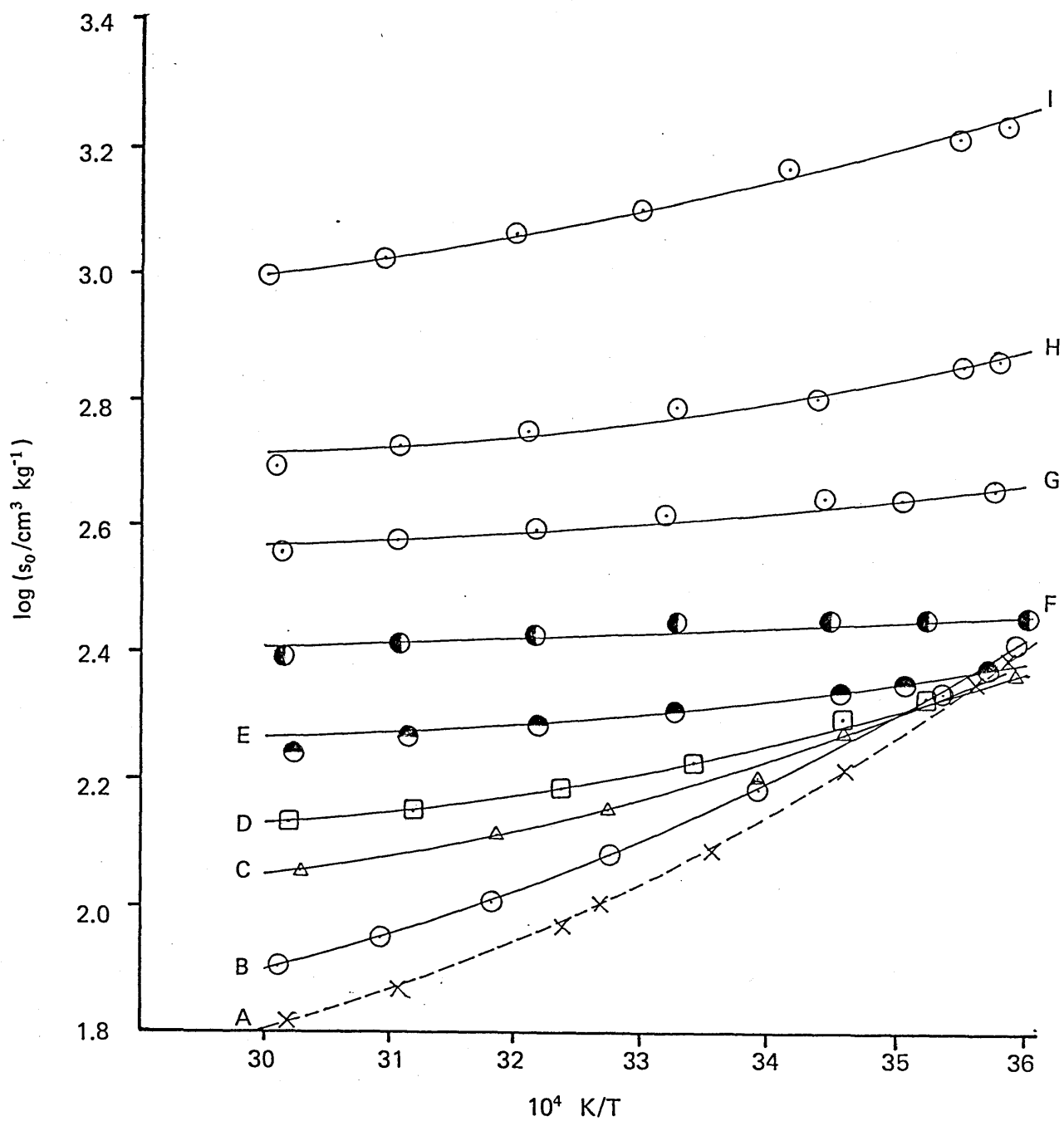


Figure 4.2.6: Solubility curves for propene in aqueous ethanol of mole fraction:
A, 0.000; B, 0.032; C, 0.072; D, 0.088; E, 0.119; F, 0.148; G, 0.186;
H, 0.226; I, 0.322.

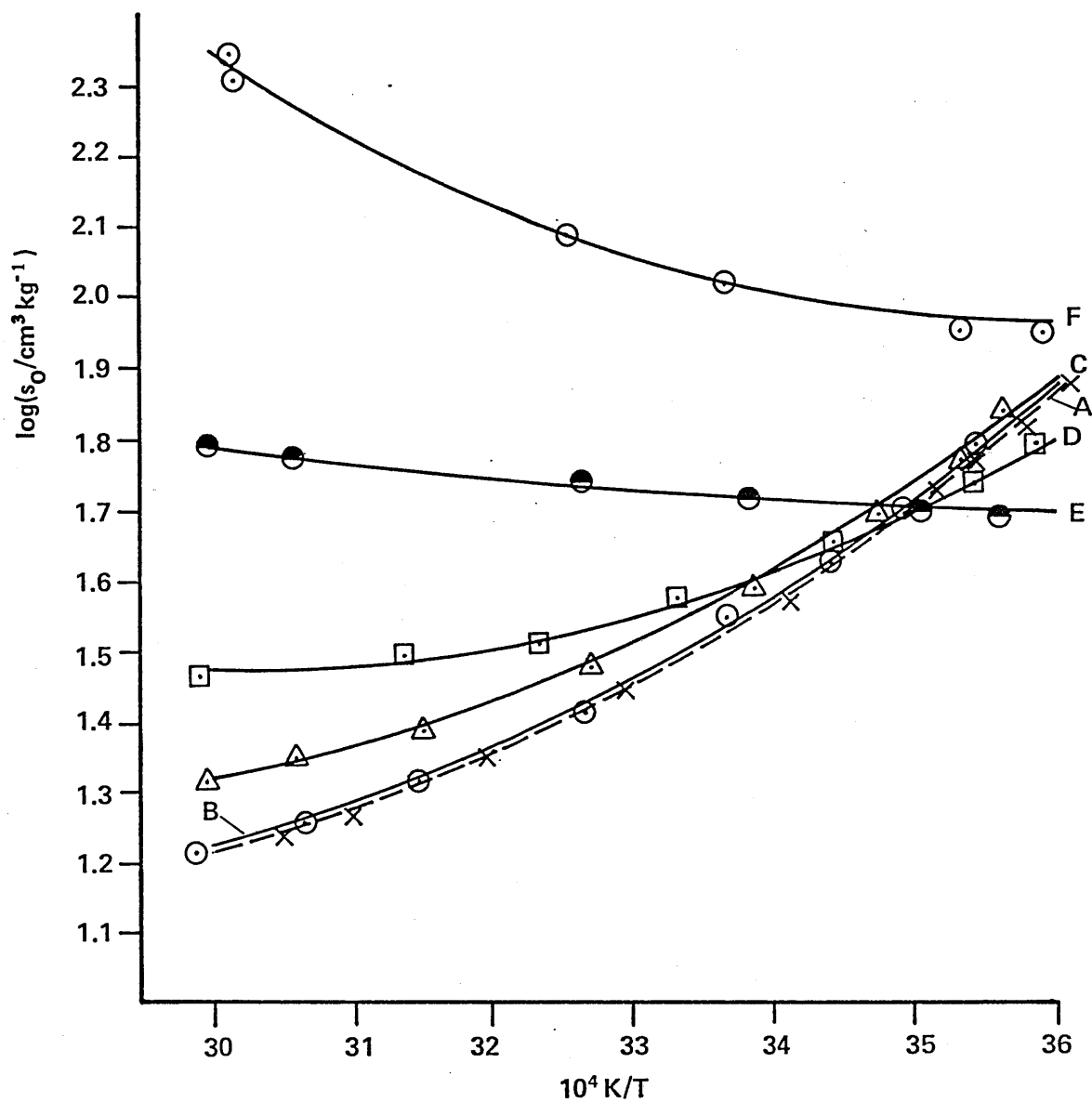


Figure 4.2.7 : Solubility curves for propane in aqueous 2-methylpropan-2-ol of mole fraction:

A, 0.000; B, 0.005; C, 0.026;
D, 0.038; E, 0.050; F, 0.066.

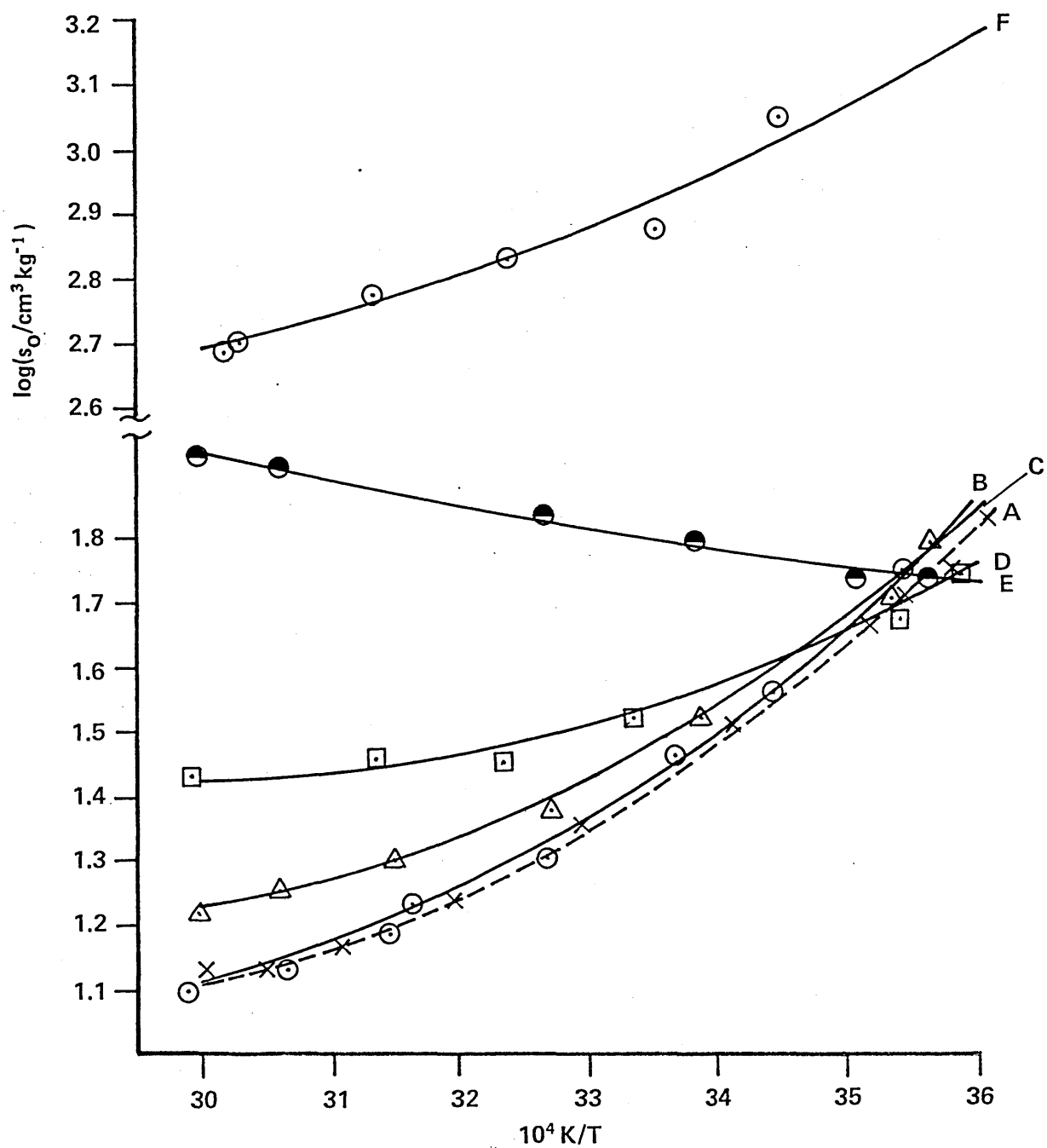


Figure 4.2.8 : Solubility curves for butane in aqueous 2-methylpropan-2-ol of mole fraction:

A, 0.000; B, 0.005; C, 0.026;
D, 0.038; E, 0.050; F, 0.08.

4.3 Solubility Isotherms

These plots of $\log S_0$ against mole fraction of alcohol, x_C show the variation of solubility with solvent composition for each gas-solvent system. Again, the isotherm corresponding to $\frac{1}{T} = 36 \times 10^{-4} \text{ K}^{-1}$ is missing in the cases where 2-methylpropane and 2,2-dimethylpropane are solutes in water-ethanol mixtures.

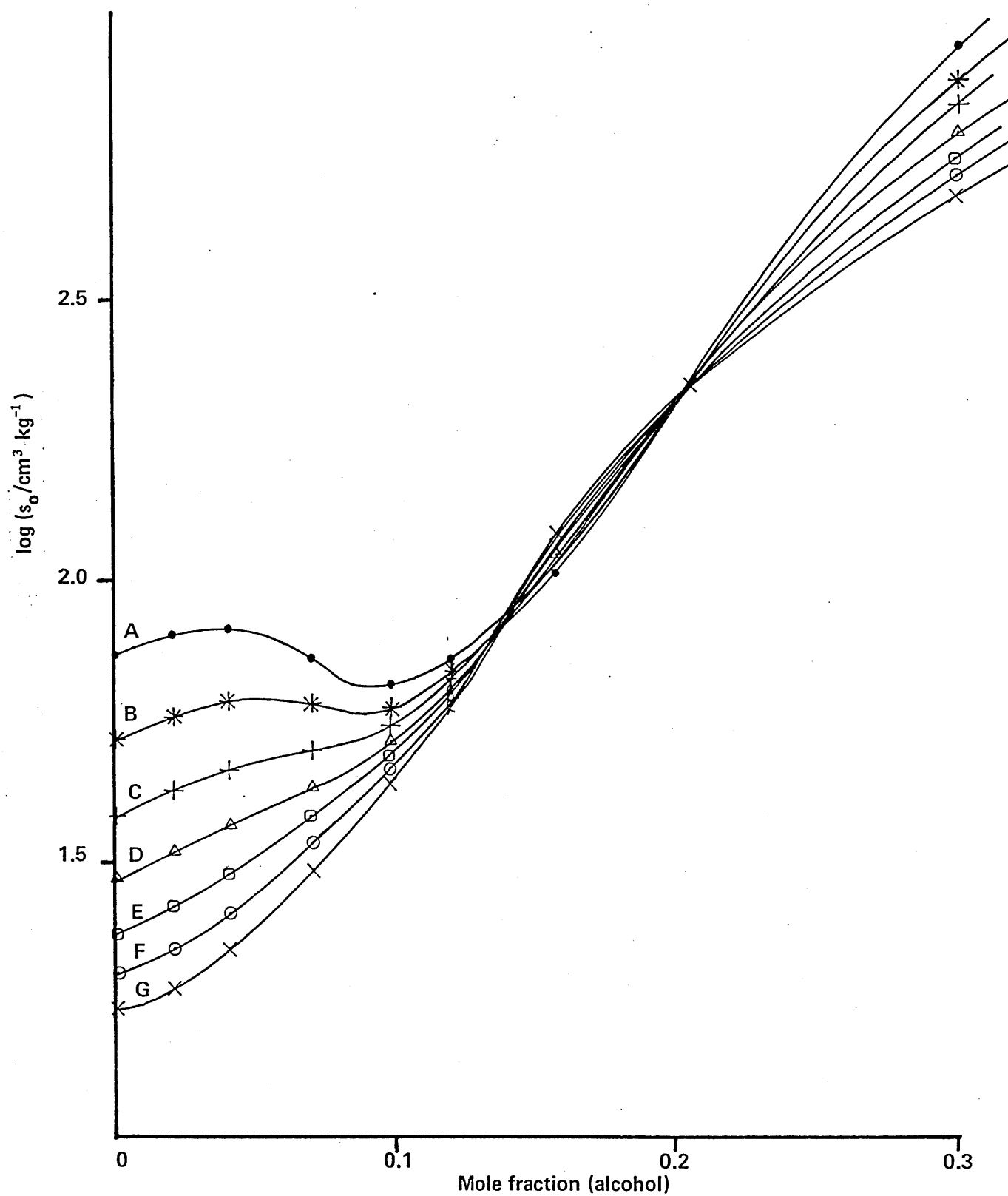


Figure 4.3.1 : Solubility isotherms for propane in water-ethanol mixtures.
 Temperatures: 4.7(A), 12.6(B), 21.0(C), 29.9(D), 39.4(E),
 49.5(F), 60.2°C(G).

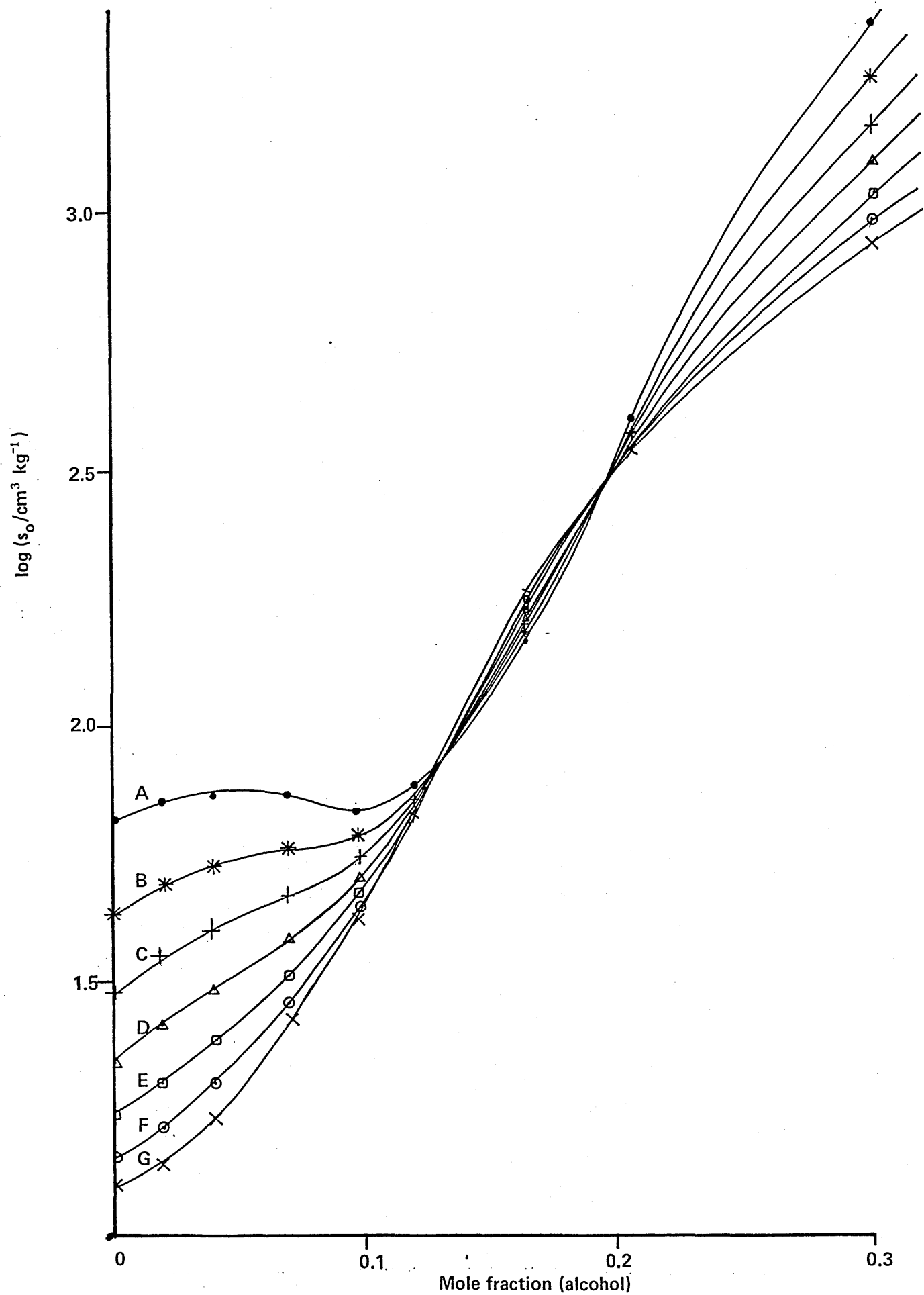


Figure 4.3.2 : Solubility isotherms for butane in water-ethanol mixtures.
 Temperatures: 4.7(A), 12.6(B), 21.0(C), 29.9(D), 39.4(E),
 49.5(F), 60.2 °C(G).

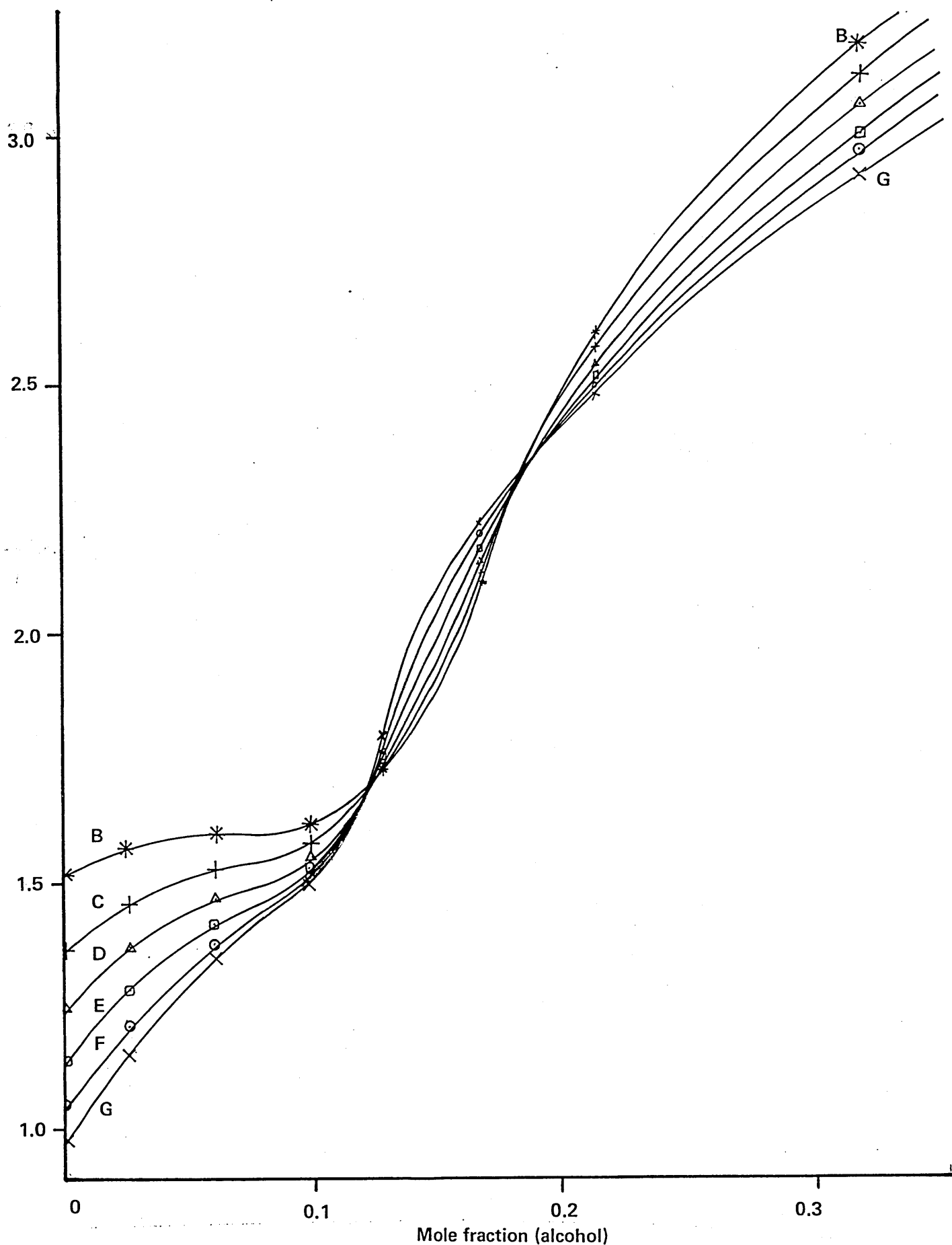


Figure 4.3.3 : Solubility isotherms for 2-methylpropane in water-ethanol mixtures
 Temperatures: 12.6(B), 21.0(C), 29.9(D), 39.4(E), 49.5(F), 60.2 °C(G).

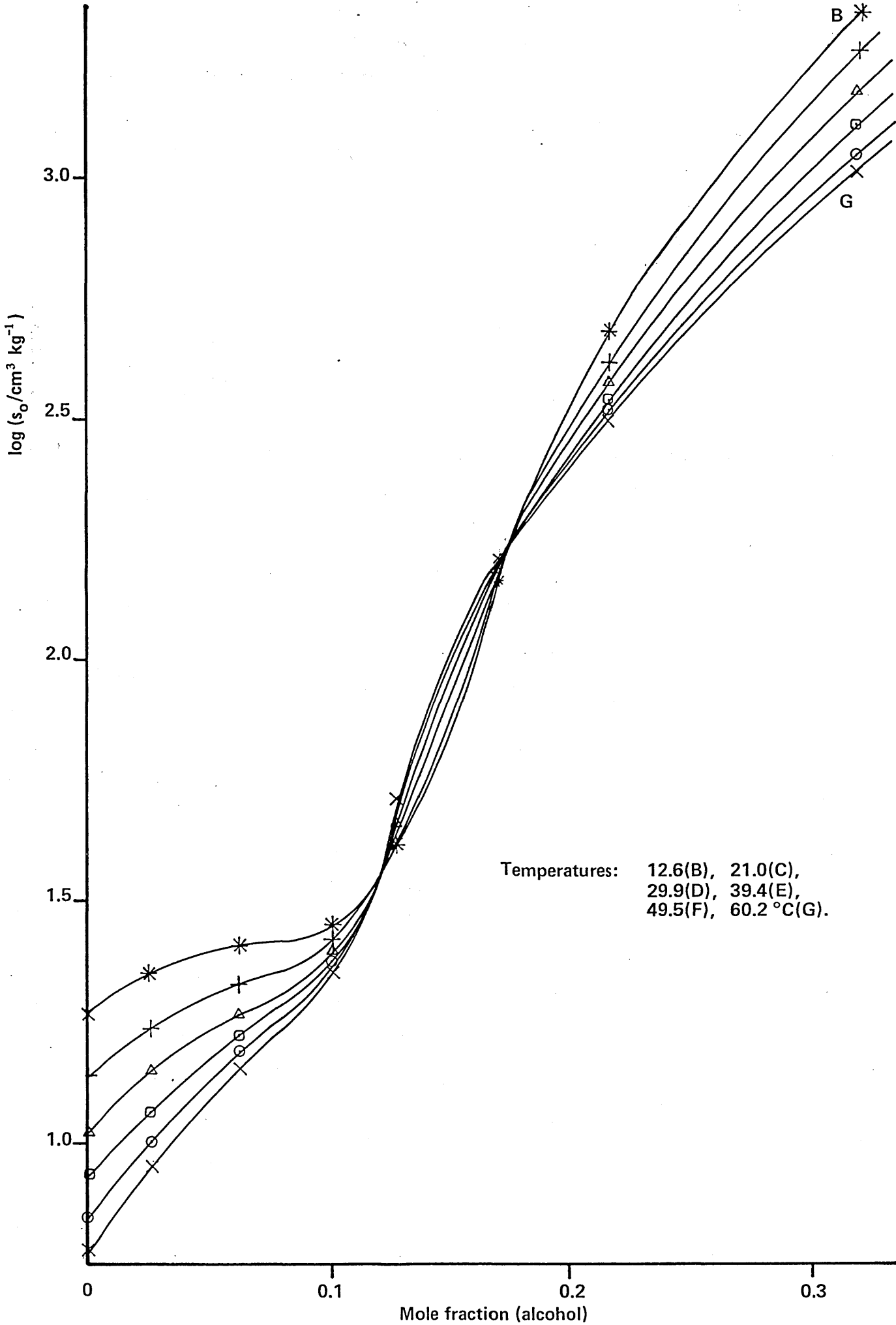


Figure 4.3.4 : Solubility isotherms for 2,2-dimethylpropane in water-ethanol mixtures

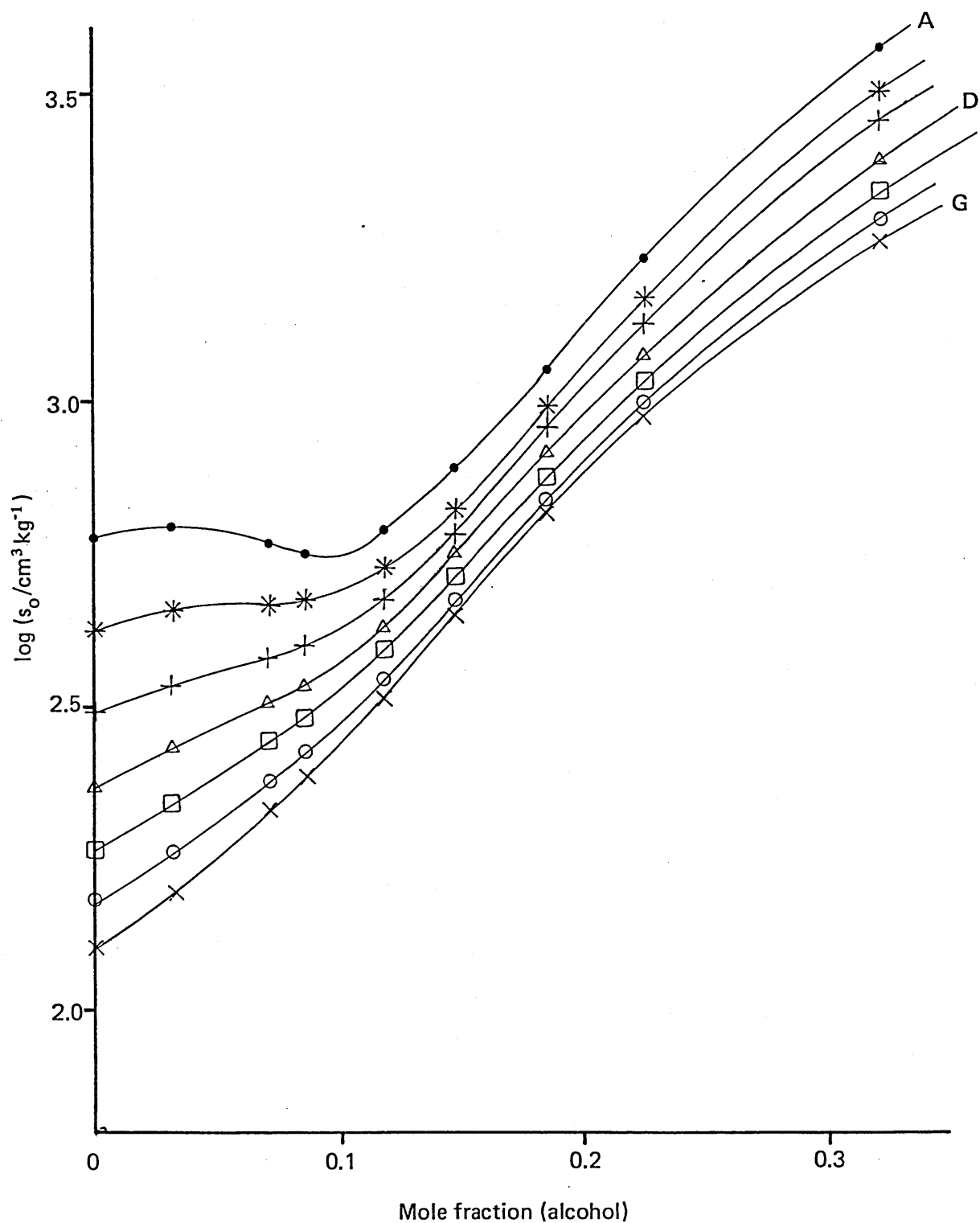


Figure 4.3.5: Solubility isotherms for cyclopropane in water-ethanol mixtures. Temperatures: 4.7(A), 12.6(B), 21.0(C), 29.9(D), 39.4(E), 49.5(F), 60.2 °C(G).

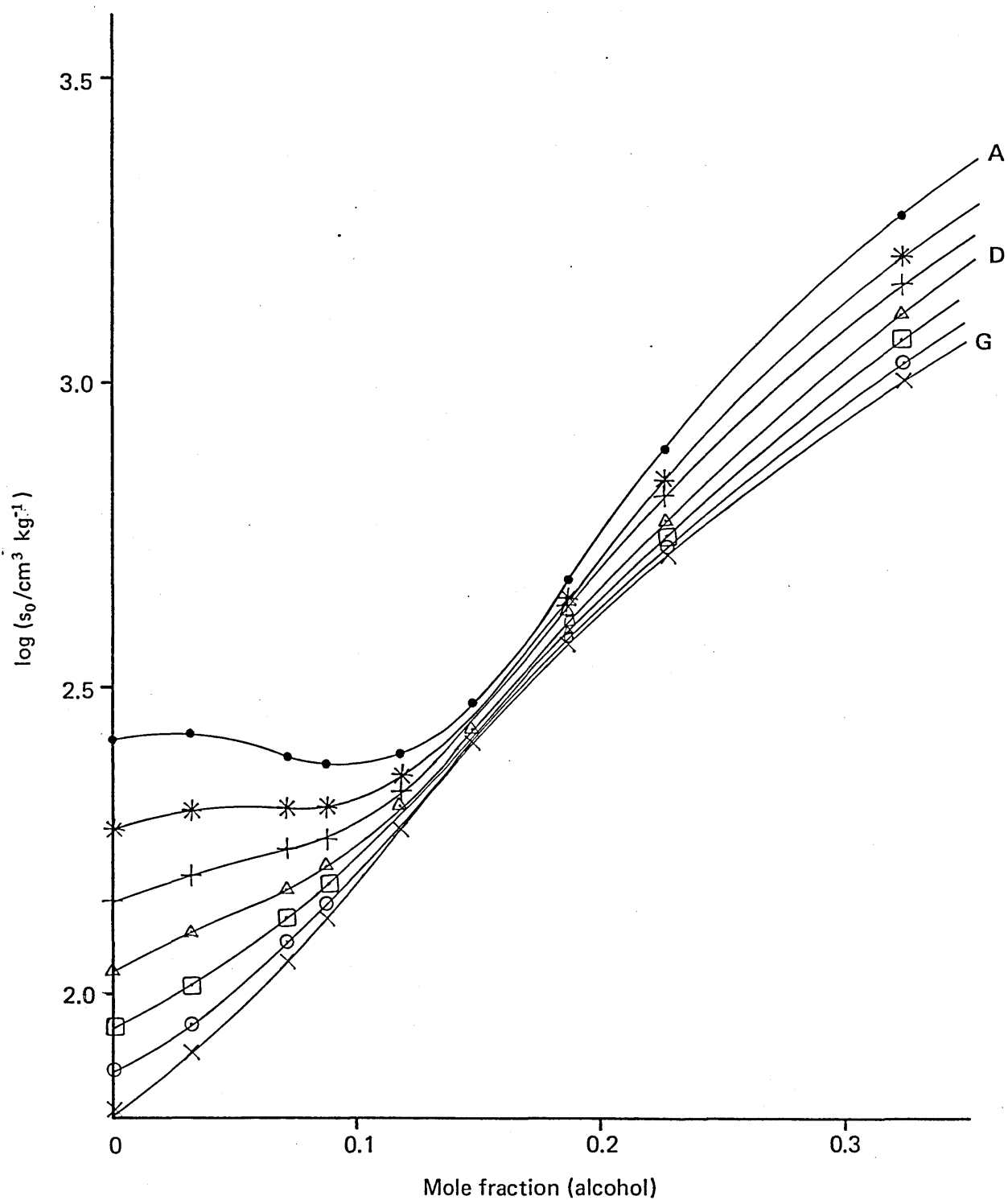


Figure 4.3.6: Solubility isotherms for propene in water – ethanol mixtures.

Temperatures: 4.7(A), 12.6(B), 21.0(C), 29.9(D), 39.4(E), 49.5(F), 60.2 °C(G).

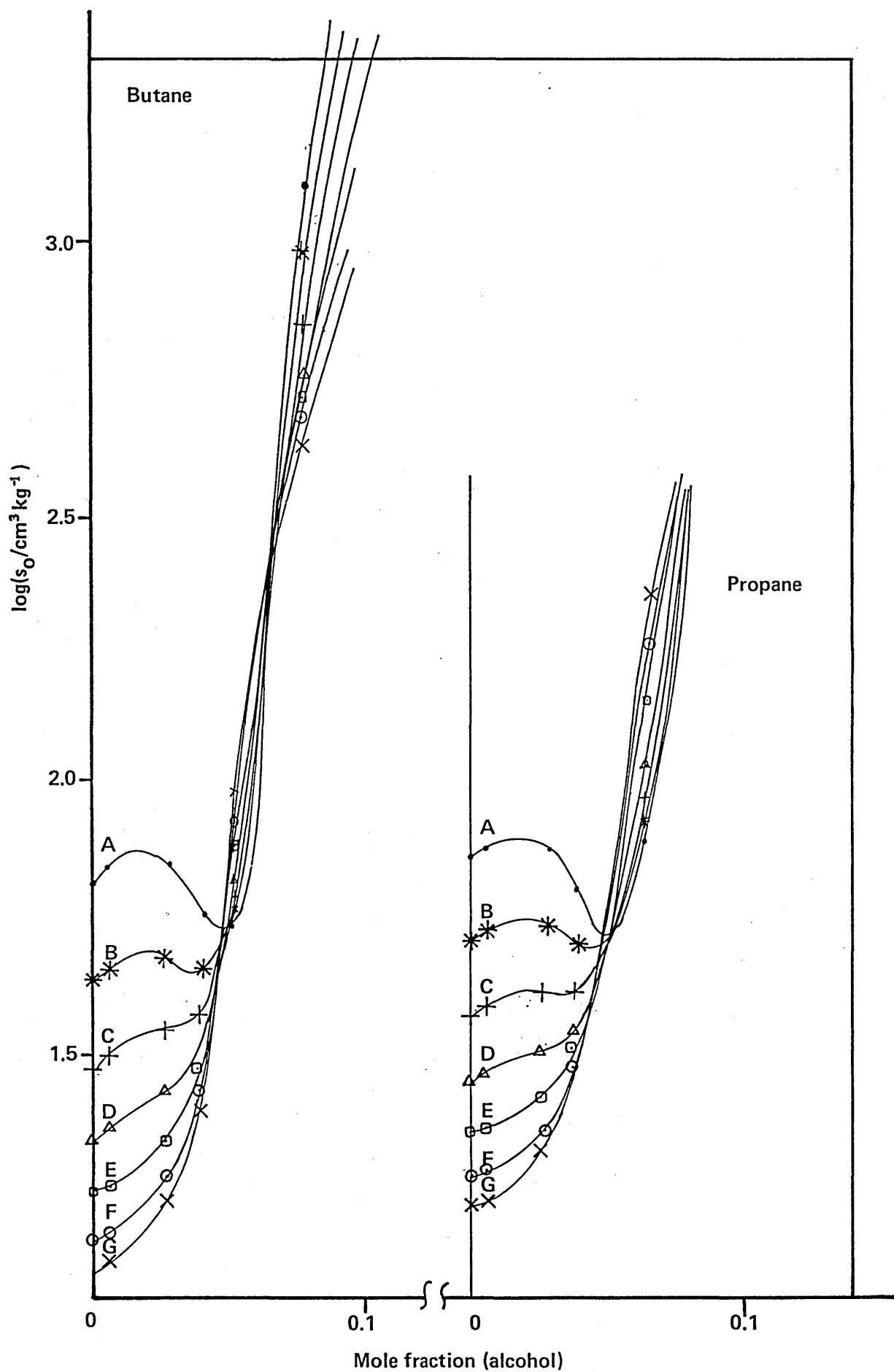


Figure 4.3.7 : Solubility isotherms for butane and propane in water – 2 methylpropan-2-ol mixtures.

Temperatures: 4.7(A), 12.6(B), 21.0(C), 29.9(D), 39.4(E) 49.5(F)
60.2 °C(G)

4.4 Thermodynamic Data

Here, the results of the calculations described in section 3.5 are presented for each gas-solvent system. The alcohol mole fraction, x_c and the reciprocal temperature $1/T$ are tabulated with the logarithm of solubility, $\log s_0$; the mole fraction of gas in the solution phase, x_{gas} ; $\Delta \bar{G}^\circ$, $\Delta \bar{H}^\circ$ and $\Delta \bar{S}^\circ$ of solution and an alternative unit of solubility, Henry's Law constant, K_H .

This has been included to facilitate comparisons with other workers results because although there are several different units of solubility in use all of these are interconvertible.

Table 4.4.1: Tabulated Thermodynamic Data for the solubility of propane in water - ethanol solvents of alcohol mole fraction x_c

x_c	$1/T$	$\log s_o$	$x_{\text{gas}} \times 10^3$	$\frac{\Delta \bar{G}}{\text{kJ}}$	$\frac{\Delta \bar{H}}{\text{kJ}}$	$\frac{\Delta \bar{S}}{\text{JK}^{-1}}$	$K_H/10^3$
0.000	0.0036	1.859	0.058	22.52	-32.9	-199	17.2
0.000	0.0035	1.703	0.041	24.02	-28.8	-185	24.7
0.000	0.0034	1.566	0.030	25.50	-24.5	-170	33.8
0.000	0.0033	1.449	0.023	26.95	-20.3	-156	44.3
0.000	0.0032	1.352	0.018	28.38	-16.8	-144	55.3
0.000	0.0031	1.275	0.015	29.77	-13.0	-132	66.1
0.000	0.0030	1.217	0.013	31.12	-8.9	-120	75.4
0.020	0.0036	1.887	0.064	22.31	-29.7	-187	15.7
0.020	0.0035	1.742	0.046	23.73	-26.4	-175	21.8
0.020	0.0034	1.614	0.034	25.16	-22.9	-163	29.4
0.020	0.0033	1.501	0.026	26.57	-20.0	-154	38.0
0.020	0.0032	1.404	0.021	27.98	-17.1	-144	47.5
0.020	0.0031	1.324	0.017	29.38	-13.9	-134	57.2
0.020	0.0030	1.259	0.015	30.77	-10.6	-124	66.3
0.040	0.0036	1.898	0.068	22.18	-26.5	-175	14.8
0.040	0.0035	1.765	0.050	23.53	-23.8	-166	20.1
0.040	0.0034	1.649	0.038	24.89	-21.0	-156	26.3
0.040	0.0033	1.547	0.030	26.23	-17.6	-145	33.2
0.040	0.0032	1.461	0.025	27.56	-15.3	-137	40.5
0.040	0.0031	1.390	0.021	28.89	-12.8	-129	47.6
0.040	0.0030	1.335	0.019	30.20	-10.1	-121	54.1
0.069	0.0036	1.868	0.066	22.24	-19.2	-149	15.2
0.069	0.0035	1.769	0.052	23.42	-17.4	-143	19.1
0.069	0.0034	1.684	0.043	24.58	-15.4	-136	23.2
0.069	0.0033	1.613	0.037	25.74	-12.0	-124	27.4
0.069	0.0032	1.555	0.032	26.89	-10.4	-119	31.3
0.069	0.0031	1.510	0.029	28.04	-8.7	-114	34.7
0.069	0.0030	1.478	0.027	29.18	-6.9	-108	37.3
0.098	0.0036	1.800	0.059	22.51	-8.5	-112	17.1
0.098	0.0035	1.758	0.053	23.38	-7.4	-108	18.8
0.098	0.0034	1.722	0.049	24.27	-6.3	-104	20.5
0.098	0.0033	1.692	0.046	25.18	-5.5	-101	21.9
0.098	0.0032	1.668	0.043	26.11	-4.7	-99	23.2
0.098	0.0031	1.649	0.041	27.07	-3.8	-96	24.2
0.098	0.0030	1.635	0.040	28.06	-2.9	-93	25.0
0.120	0.0036	1.850	0.068	22.18	-4.2	-95	14.8
0.120	0.0035	1.830	0.065	22.92	-3.4	-92	15.5
0.120	0.0034	1.813	0.062	23.69	-2.6	-89	16.1
0.120	0.0033	1.795	0.060	24.51	-2.0	-88	16.8
0.120	0.0032	1.782	0.058	25.35	-1.4	-86	17.3
0.120	0.0031	1.772	0.057	26.23	-0.8	-84	17.7
0.120	0.0030	1.765	0.056	27.15	-0.2	-82	18.0

4.4.1 (Contd): Tabulated Thermodynamic Data for the solubility of propane in water-ethanol solvents of alcohol mole fraction x_c

x_c	$1/T$	$\log s_o$	$x_{gas} \times 10^3$	$\frac{\Delta \bar{G}}{kJ}$	$\frac{\Delta \bar{H}}{kJ}$	$\frac{\Delta \bar{S}}{JK^{-1}}$	$K_H/10^3$
0.159	0.0036	2.005	0.102	21.24	1.0	-73	9.8
0.159	0.0035	2.010	0.103	21.82	1.2	-72	9.7
0.159	0.0034	2.017	0.104	22.42	1.5	-71	9.6
0.159	0.0033	2.026	0.107	23.04	2.2	-69	9.4
0.159	0.0032	2.037	0.109	23.70	2.4	-68	9.2
0.159	0.0031	2.050	0.113	24.38	2.6	-68	8.9
0.159	0.0030	2.065	0.117	25.10	2.8	-67	8.6
0.206	0.0036	2.345	0.235	19.30	-0.9	-73	4.3
0.206	0.0035	2.340	0.232	19.87	-0.8	-72	4.3
0.206	0.0034	2.336	0.230	20.48	-0.8	-72	4.3
0.206	0.0033	2.331	0.228	21.13	-0.6	-72	4.4
0.206	0.0032	2.329	0.227	21.80	-0.6	-72	4.4
0.206	0.0031	2.326	0.225	22.53	-0.6	-72	4.4
0.206	0.0030	2.324	0.224	23.29	-0.6	-72	4.5
0.300	0.0036	2.938	1.022	15.90	-12.0	-101	1.0
0.300	0.0035	2.878	0.891	16.68	-10.7	-96	1.1
0.300	0.0034	2.825	0.788	17.47	-9.4	-91	1.3
0.300	0.0033	2.779	0.709	18.27	-8.1	-87	1.4
0.300	0.0032	2.739	0.648	19.08	-7.0	-83	1.5
0.300	0.0031	2.706	0.600	19.90	-5.7	-79	1.7
0.300	0.0030	2.680	0.565	20.73	-4.5	-76	1.8
0.396	0.0036	3.266	2.395	13.94	-16.4	-109	0.4
0.396	0.0035	3.186	1.993	14.77	-14.2	-102	0.5
0.396	0.0034	3.118	1.702	15.59	-11.9	-94	0.6
0.396	0.0033	3.060	1.493	16.39	-9.7	-86	0.7
0.396	0.0032	3.015	1.345	17.18	-7.7	-80	0.7
0.396	0.0031	2.981	1.244	17.94	-5.6	-73	0.8
0.396	0.0030	2.958	1.180	18.69	-3.4	-66	0.8

Table 4.4.2: Tabulated Thermodynamic Data for the solubility of butane in water - ethanol solvents of alcohol mole fraction x_c

x_c	$1/T$	$\log s_o$	$x_{\text{gas}} \times 10^3$	$\frac{\Delta \bar{G}}{kJ}$	$\frac{\Delta \bar{H}}{kJ}$	$\frac{\Delta \bar{S}}{JK^{-1}}$	$K_H/10^3$
0.000	0.0036	1.809	0.052	22.78	-37.1	-216	19.2
0.000	0.0035	1.627	0.034	24.42	-32.5	-199	29.2
0.000	0.0034	1.471	0.024	26.02	-27.6	-182	41.8
0.000	0.0033	1.341	0.018	27.56	-22.5	-165	56.4
0.000	0.0032	1.237	0.014	29.04	-17.6	-149	71.6
0.000	0.0031	1.159	0.012	30.46	-12.4	-133	85.7
0.000	0.0030	1.107	0.010	31.81	-6.8	-116	96.6
0.020	0.0036	1.848	0.059	22.50	-33.4	-201	17.0
0.020	0.0035	1.683	0.040	24.04	-29.8	-188	24.9
0.020	0.0034	1.537	0.029	25.57	-25.9	-175	34.8
0.020	0.0033	1.412	0.022	27.08	-22.6	-164	46.5
0.020	0.0032	1.304	0.017	28.56	-18.8	-152	59.5
0.020	0.0031	1.215	0.014	30.04	-14.8	-139	73.1
0.020	0.0030	1.145	0.012	31.49	-10.5	-126	85.9
0.040	0.0036	1.868	0.063	22.32	-29.0	-185	15.8
0.040	0.0035	1.725	0.046	23.75	-26.1	-175	21.9
0.040	0.0034	1.596	0.034	25.16	-23.1	-164	29.5
0.040	0.0033	1.484	0.026	26.58	-20.3	-155	38.2
0.040	0.0032	1.386	0.021	28.00	-17.7	-146	47.9
0.040	0.0031	1.301	0.017	29.42	-14.8	-137	58.2
0.040	0.0030	1.230	0.015	30.86	-11.8	-128	68.4
0.069	0.0036	1.878	0.068	22.17	-21.9	-159	14.8
0.069	0.0035	1.763	0.052	23.44	-20.0	-152	19.3
0.069	0.0034	1.664	0.041	24.68	-18.1	-145	24.2
0.069	0.0033	1.581	0.034	25.91	-13.5	-130	29.3
0.069	0.0032	1.514	0.029	27.12	-11.9	-125	34.2
0.069	0.0031	1.463	0.026	28.31	-10.3	-120	38.4
0.069	0.0030	1.428	0.024	29.48	-8.5	-114	41.7
0.098	0.0036	1.839	0.064	22.29	-10.3	-117	15.5
0.098	0.0035	1.785	0.057	23.22	-9.2	-114	17.6
0.098	0.0034	1.739	0.051	24.16	-8.2	-110	19.6
0.098	0.0033	1.701	0.047	25.11	-6.0	-103	21.3
0.098	0.0032	1.671	0.044	26.08	-5.2	-100	22.9
0.098	0.0031	1.648	0.041	27.06	-4.4	-98	24.1
0.098	0.0030	1.632	0.040	28.07	-3.5	-95	25.0
0.120	0.0036	1.890	0.075	21.95	-3.4	-91	13.4
0.120	0.0035	1.874	0.072	22.67	-3.0	-90	13.9
0.120	0.0034	1.859	0.069	23.41	-2.5	-88	14.4
0.120	0.0033	1.848	0.068	24.19	-1.9	-86	14.8
0.120	0.0032	1.839	0.066	25.00	-1.5	-85	15.1
0.120	0.0031	1.832	0.065	25.84	-1.0	-83	15.3
0.120	0.0030	1.828	0.065	26.73	-0.5	-82	15.5
0.159	0.0036	2.134	0.137	20.54	2.0	-67	7.3
0.159	0.0035	2.144	0.141	21.07	2.1	-67	7.1
0.159	0.0034	2.155	0.144	21.62	2.1	-66	6.9
0.159	0.0033	2.167	0.148	22.21	2.2	-66	6.7
0.159	0.0032	2.179	0.152	22.83	2.3	-66	6.6
0.159	0.0031	2.192	0.157	23.49	2.4	-65	6.4
0.159	0.0030	2.204	0.162	24.19	2.5	-65	6.2

4.4.2 (Contd): Tabulated Thermodynamic Data for the solubility of butane in water-ethanol solvents of alcohol mole fraction x_c

x_c	$1/T$	$\log s_o$	$x_{\text{gas}} \times 10^3$	$\frac{\Delta \bar{G}}{kJ}$	$\frac{\Delta \bar{H}}{kJ}$	$\frac{\Delta \bar{S}}{JK^{-1}}$	$K_H/10^3$
0.206	0.0036	2.600	0.425	17.93	-3.7	-78	2.4
0.206	0.0035	2.582	0.408	18.54	-3.2	-76	2.5
0.206	0.0034	2.567	0.394	19.17	-2.6	-74	2.5
0.206	0.0033	2.555	0.384	19.82	-2.1	-72	2.6
0.206	0.0032	2.546	0.376	20.49	-1.5	-71	2.7
0.206	0.0031	2.540	0.370	21.19	-0.9	-69	2.7
0.206	0.0030	2.537	0.368	21.91	-0.3	-67	2.7
0.300	0.0036	3.384	2.867	13.52	-21.6	-127	0.3
0.300	0.0035	3.278	2.245	14.49	-19.1	-117	0.4
0.300	0.0034	3.185	1.815	15.43	-16.4	-108	0.6
0.300	0.0033	3.106	1.515	16.36	-13.7	-99	0.7
0.300	0.0032	3.042	1.306	17.25	-11.1	-91	0.8
0.300	0.0031	2.991	1.163	18.12	-8.4	-82	0.9
0.300	0.0030	2.955	1.069	18.96	-5.6	-74	0.9
0.396	0.0036	3.775	7.735	11.23	-26.5	-136	0.1
0.396	0.0035	3.646	5.752	12.25	-23.4	-125	0.2
0.396	0.0034	3.533	4.440	13.25	-20.1	-113	0.2
0.396	0.0033	3.436	3.558	14.21	-16.8	-102	0.3
0.396	0.0032	3.356	2.962	15.13	-13.8	-93	0.3
0.396	0.0031	3.293	2.560	16.01	-10.7	-83	0.4
0.396	0.0030	3.245	2.298	16.84	-7.3	-72	0.4

Table 4.4.3: Tabulated Thermodynamic Data for the solubility of 2-methylpropane in water - ethanol solvents of alcohol mole fraction x_c

x_c	$1/T$	$\log s_o$	$x_{\text{gas}} \times 10^3$	$\frac{\Delta \bar{G}}{kJ}$	$\frac{\Delta \bar{H}}{kJ}$	$\frac{\Delta \bar{S}}{JK^{-1}}$	$K_H/10^3$
0.000	0.0035	1.488	0.025	25.14	-26.9	-182	39.5
0.000	0.0034	1.354	0.019	26.64	-24.0	-172	53.8
0.000	0.0033	1.235	0.014	28.13	-21.4	-164	70.7
0.000	0.0032	1.132	0.011	29.63	-18.7	-155	89.8
0.000	0.0031	1.042	0.009	31.14	-15.8	-145	110.4
0.000	0.0030	0.967	0.008	32.66	-12.6	-136	131.2
0.026	0.0035	1.553	0.031	24.69	-22.1	-164	32.7
0.026	0.0034	1.445	0.024	26.03	-19.4	-154	41.9
0.026	0.0033	1.351	0.019	27.37	-17.4	-148	52.1
0.026	0.0032	1.270	0.016	28.70	-14.8	-139	62.8
0.026	0.0031	1.204	0.014	30.04	-12.0	-130	73.1
0.026	0.0030	1.151	0.012	31.37	-9.0	-121	82.5
0.062	0.0035	1.584	0.035	24.40	-15.7	-140	28.9
0.062	0.0034	1.511	0.029	25.53	-13.4	-132	34.2
0.062	0.0033	1.452	0.026	26.64	-11.5	-126	39.2
0.062	0.0032	1.404	0.023	27.76	-9.2	-118	43.7
0.062	0.0031	1.369	0.021	28.88	-6.8	-110	47.4
0.062	0.0030	1.346	0.020	29.99	-4.2	-102	50.0
0.100	0.0035	1.605	0.038	24.16	-7.3	-110	26.1
0.100	0.0034	1.567	0.035	25.08	-5.8	-105	28.5
0.100	0.0033	1.537	0.033	26.02	-4.6	-101	30.6
0.100	0.0032	1.515	0.031	26.96	-3.1	-96	32.1
0.100	0.0031	1.501	0.030	27.92	-1.5	-91	33.2
0.100	0.0030	1.495	0.030	28.89	0.2	-86	33.7
0.128	0.0035	1.727	0.053	23.40	1.1	-78	19.0
0.128	0.0034	1.734	0.053	24.06	1.3	-77	18.7
0.128	0.0033	1.741	0.054	24.74	2.0	-75	18.4
0.128	0.0032	1.752	0.056	25.45	2.3	-74	17.9
0.128	0.0031	1.760	0.057	26.22	2.6	-73	17.6
0.128	0.0030	1.772	0.058	27.01	2.9	-72	17.1
0.168	0.0035	2.100	0.130	21.25	2.9	-64	7.7
0.168	0.0034	2.113	0.134	21.80	3.3	-63	7.4
0.168	0.0033	2.130	0.140	22.36	4.1	-60	7.1
0.168	0.0032	2.150	0.147	22.94	4.5	-59	6.8
0.168	0.0031	2.178	0.157	23.50	5.0	-57	6.4
0.168	0.0030	2.210	0.168	24.09	5.6	-56	5.9
0.216	0.0035	2.592	0.429	18.42	-6.9	-89	2.3
0.216	0.0034	2.558	0.398	19.15	-5.9	-85	2.5
0.216	0.0033	2.530	0.372	19.90	-5.0	-82	2.7
0.216	0.0032	2.505	0.352	20.66	-4.0	-79	2.8
0.216	0.0031	2.485	0.336	21.45	-3.0	-76	3.0
0.216	0.0030	2.470	0.324	22.27	-1.8	-72	3.1
0.319	0.0035	3.170	1.818	14.99	-13.6	-100	0.6
0.319	0.0034	3.103	1.559	15.81	-12.3	-95	0.6
0.319	0.0033	3.043	1.358	16.63	-11.2	-92	0.7
0.319	0.0032	2.990	1.202	17.47	-9.8	-87	0.8
0.319	0.0031	2.944	1.081	18.32	-8.4	-83	0.9
0.319	0.0030	2.905	0.988	19.18	-6.9	-78	1.0

Table 4.4.4: Tabulated Thermodynamic Data for the solubility of 2,2-dimethylpropane in water - ethanol solvents of alcohol mole fraction x_c

x_c	$1/T$	$\log s_o$	$x_{\text{gas}} \times 10^3$	$\frac{\Delta \bar{G}}{kJ}$	$\frac{\Delta \bar{H}}{kJ}$	$\frac{\Delta \bar{S}}{JK^{-1}}$	$K_H/10^3$
0.000	0.0035	1.262	0.015	26.41	-26.1	-184	67.4
0.000	0.0034	1.133	0.011	27.91	-23.2	-174	90.6
0.000	0.0033	1.020	0.009	29.41	-20.4	-164	117.5
0.000	0.0032	0.922	0.007	30.91	-17.4	-155	147.1
0.000	0.0031	0.840	0.006	32.42	-14.3	-145	177.7
0.000	0.0030	0.774	0.005	33.92	-10.9	-135	207.1
0.026	0.0035	1.338	0.018	25.89	-22.3	-169	54.2
0.026	0.0034	1.230	0.014	27.26	-19.4	-159	69.4
0.026	0.0033	1.137	0.012	28.63	-16.6	-149	86.0
0.026	0.0032	1.059	0.010	29.99	-13.7	-140	103.0
0.026	0.0031	0.996	0.008	31.34	-10.7	-130	119.0
0.026	0.0030	0.948	0.008	32.70	-7.4	-120	132.9
0.062	0.0035	1.400	0.023	25.42	-16.3	-146	44.4
0.062	0.0034	1.321	0.019	26.61	-13.8	-137	53.2
0.062	0.0033	1.257	0.016	27.79	-11.4	-129	61.6
0.062	0.0032	1.208	0.014	28.95	-8.8	-121	69.1
0.062	0.0031	1.173	0.013	30.10	-6.1	-112	74.9
0.062	0.0030	1.153	0.013	31.23	-3.2	-103	78.5
0.100	0.0035	1.447	0.027	25.03	-7.8	-115	37.7
0.100	0.0034	1.410	0.024	25.97	-6.3	-110	41.0
0.100	0.0033	1.381	0.023	26.93	-4.2	-103	43.9
0.100	0.0032	1.360	0.022	27.90	-2.7	-98	46.0
0.100	0.0031	1.347	0.021	28.88	-1.2	-93	47.4
0.100	0.0030	1.342	0.021	29.87	0.5	-88	48.0
0.128	0.0035	1.616	0.041	24.01	2.8	-74	24.6
0.128	0.0034	1.630	0.042	24.64	2.8	-74	23.8
0.128	0.0033	1.645	0.044	25.30	2.9	-74	23.0
0.128	0.0032	1.661	0.045	26.00	3.0	-74	22.2
0.128	0.0031	1.676	0.047	26.74	3.1	-73	21.4
0.128	0.0030	1.693	0.049	27.52	3.2	-73	20.6
0.168	0.0035	2.152	0.148	20.95	0.5	-72	6.8
0.168	0.0034	2.155	0.149	21.55	0.5	-71	6.7
0.168	0.0033	2.157	0.150	22.19	0.6	-71	6.7
0.168	0.0032	2.161	0.151	22.86	0.7	-71	6.6
0.168	0.0031	2.165	0.152	23.58	0.8	-71	6.6
0.168	0.0030	2.169	0.154	24.33	0.9	-70	6.5
0.216	0.0035	2.667	0.513	17.99	-9.8	-97	1.9
0.216	0.0034	2.613	0.454	18.82	-8.6	-93	2.2
0.216	0.0033	2.569	0.410	19.65	-7.2	-88	2.4
0.216	0.0032	2.533	0.378	20.48	-6.0	-85	2.6
0.216	0.0031	2.507	0.355	21.30	-4.8	-81	2.8
0.216	0.0030	2.489	0.341	22.12	-3.4	-77	2.9
0.319	0.0035	3.338	2.706	14.04	-17.6	-111	0.4
0.319	0.0034	3.251	2.215	14.95	-15.6	-104	0.5
0.319	0.0033	3.175	1.860	15.84	-13.5	-97	0.5
0.319	0.0032	3.110	1.602	16.72	-11.5	-90	0.6
0.319	0.0031	3.056	1.415	17.59	-9.3	-83	0.7
0.319	0.0030	3.013	1.282	18.46	-6.9	-76	0.8

Table 4.4.5: Tabulated Thermodynamic Data for the solubility of cyclopropane in water - ethanol solvents of alcohol mole fraction x_c

x_c	$1/T$	$\log s_o$	$x_{gas} \times 10^3$	$\frac{\Delta \bar{G}}{kJ}$	$\frac{\Delta \bar{H}}{kJ}$	$\frac{\Delta \bar{S}}{JK^{-1}}$	$K_H/10^3$
0.000	0.0036	2.766	0.469	17.70	-30.3	-173	2.1
0.000	0.0035	2.615	0.331	19.03	-27.4	-162	3.0
0.000	0.0034	2.480	0.243	20.35	-24.3	-152	4.1
0.000	0.0033	2.361	0.185	21.66	-21.5	-142	5.4
0.000	0.0032	2.258	0.146	22.95	-18.4	-132	6.9
0.000	0.0031	2.171	0.119	24.23	-15.1	-122	8.4
0.000	0.0030	2.100	0.101	25.49	-11.5	-111	9.9
0.032	0.0036	2.787	0.517	17.48	-27.3	-161	1.9
0.032	0.0035	2.651	0.378	18.72	-24.6	-152	2.6
0.032	0.0034	2.530	0.286	19.95	-21.7	-142	3.5
0.032	0.0033	2.424	0.224	21.17	-19.1	-133	4.5
0.032	0.0032	2.333	0.182	22.38	-16.2	-124	5.5
0.032	0.0031	2.257	0.153	23.57	-13.2	-114	6.6
0.032	0.0030	2.196	0.133	24.74	-9.9	-104	7.5
0.072	0.0036	2.761	0.516	17.48	-19.3	-133	1.9
0.072	0.0035	2.665	0.413	18.51	-17.4	-126	2.4
0.072	0.0034	2.579	0.339	19.54	-15.4	-119	2.9
0.072	0.0033	2.503	0.285	20.57	-14.0	-114	3.5
0.072	0.0032	2.436	0.244	21.61	-12.2	-108	4.1
0.072	0.0031	2.378	0.214	22.67	-10.3	-102	4.7
0.072	0.0030	2.328	0.190	23.74	-8.3	-96	5.3
0.088	0.0036	2.748	0.512	17.50	-16.0	-120	2.0
0.088	0.0035	2.669	0.426	18.43	-14.4	-115	2.3
0.088	0.0034	2.598	0.362	19.38	-12.8	-109	2.8
0.088	0.0033	2.535	0.313	20.33	-11.5	-105	3.2
0.088	0.0032	2.481	0.276	21.29	-10.0	-100	3.6
0.088	0.0031	2.434	0.248	22.26	-8.3	-95	4.0
0.088	0.0030	2.396	0.227	23.25	-6.6	-89	4.4
0.119	0.0036	2.783	0.578	17.22	-12.1	-106	1.7
0.119	0.0035	2.723	0.503	18.04	-11.0	-102	2.0
0.119	0.0034	2.668	0.444	18.88	-9.8	-98	2.3
0.119	0.0033	2.620	0.397	19.73	-8.9	-94	2.5
0.119	0.0032	2.577	0.360	20.60	-7.7	-91	2.8
0.119	0.0031	2.540	0.331	21.49	-6.4	-86	3.0
0.119	0.0030	2.510	0.308	22.40	-5.0	-82	3.2
0.148	0.0036	2.880	0.750	16.62	-10.3	-97	1.3
0.148	0.0035	2.828	0.666	17.38	-9.3	-93	1.5
0.148	0.0034	2.782	0.599	18.15	-8.3	-90	1.7
0.148	0.0033	2.742	0.546	18.93	-7.4	-87	1.8
0.148	0.0032	2.707	0.504	19.73	-6.3	-83	2.0
0.148	0.0031	2.677	0.470	20.55	-5.2	-80	2.1
0.148	0.0030	2.652	0.444	21.39	-4.0	-76	2.3

Table 4.4.5 (Contd): Tabulated Thermodynamic Data for the solubility of cyclopropane in water - ethanol solvents of alcohol mole fraction x_c

x_c	$1/T$	$\log s_o$	$x_{gas} \times 10^3$	$\frac{\Delta \bar{G}^\circ}{\text{kJ}}$	$\frac{\Delta \bar{H}^\circ}{\text{kJ}}$	$\frac{\Delta \bar{S}^\circ}{\text{JK}^{-1}}$	$K_H/10^3$
0.186	0.0036	3.042	1.142	15.65	-10.2	-93	0.9
0.186	0.0035	2.991	1.015	16.37	-9.3	-90	1.0
0.186	0.0034	2.945	0.913	17.11	-8.3	-86	1.1
0.186	0.0033	2.904	0.831	17.87	-7.4	-83	1.2
0.186	0.0032	2.868	0.765	18.64	-6.4	-80	1.3
0.186	0.0031	2.837	0.712	19.44	-5.4	-77	1.4
0.186	0.0030	2.811	0.671	20.25	-4.3	-74	1.5
0.226	0.0036	3.229	1.842	14.54	-12.1	-96	0.5
0.226	0.0035	3.166	1.592	15.30	-11.1	-92	0.6
0.226	0.0034	3.111	1.401	16.07	-10.1	-89	0.7
0.226	0.0033	3.063	1.256	16.83	-8.7	-84	0.8
0.226	0.0032	3.023	1.147	17.59	-7.6	-81	0.9
0.226	0.0031	2.992	1.067	18.35	-6.5	-77	0.9
0.226	0.0030	2.968	1.011	19.11	-5.4	-73	1.0
0.322	0.0036	3.570	4.469	12.50	-13.5	-94	0.2
0.322	0.0035	3.506	3.859	13.20	-12.2	-89	0.3
0.322	0.0034	3.446	3.363	13.93	-10.8	-84	0.3
0.322	0.0033	3.390	2.957	14.67	-10.0	-81	0.3
0.322	0.0032	3.338	2.624	15.44	-8.7	-77	0.4
0.322	0.0031	3.290	2.350	16.23	-7.3	-73	0.4
0.322	0.0030	3.246	2.124	17.06	-5.8	-69	0.5

Table 4.4.6: Tabulated Thermodynamic Data for the solubility of propene in water - ethanol solvents of alcohol mole fraction x_c

x_c	$1/T$	$\log s_o$	$x_{\text{gas}} \times 10^3$	$\frac{\Delta \bar{G}^\circ}{\text{kJ}}$	$\frac{\Delta \bar{H}^\circ}{\text{kJ}}$	$\frac{\Delta \bar{S}^\circ}{\text{JK}^{-1}}$	$K_H/10^3$
0.000	0.0036	2.410	0.211	19.55	-28.3	-172	4.7
0.000	0.0035	2.269	0.153	20.87	-25.4	-162	6.5
0.000	0.0034	2.145	0.115	22.19	-22.3	-151	8.7
0.000	0.0033	2.037	0.089	23.49	-19.4	-142	11.2
0.000	0.0032	1.944	0.072	24.78	-16.4	-132	13.9
0.000	0.0031	1.868	0.061	26.05	-13.2	-122	16.5
0.000	0.0030	1.807	0.053	27.30	-9.7	-111	19.0
0.032	0.0036	2.421	0.227	19.38	-24.1	-156	4.4
0.032	0.0035	2.302	0.173	20.58	-21.6	-147	5.8
0.032	0.0034	2.196	0.135	21.78	-18.9	-138	7.4
0.032	0.0033	2.103	0.109	22.98	-17.0	-132	9.2
0.032	0.0032	2.023	0.091	24.18	-14.3	-123	11.0
0.032	0.0031	1.956	0.078	25.37	-11.4	-114	12.8
0.032	0.0030	1.902	0.069	26.56	-8.4	-105	14.5
0.072	0.0036	2.387	0.223	19.42	-16.7	-130	4.5
0.072	0.0035	2.303	0.184	20.43	-14.8	-123	5.4
0.072	0.0034	2.231	0.155	21.44	-12.8	-117	6.4
0.072	0.0033	2.169	0.135	22.45	-10.7	-110	7.4
0.072	0.0032	2.119	0.120	23.45	-8.8	-103	8.3
0.072	0.0031	2.079	0.110	24.45	-6.7	-97	9.1
0.072	0.0030	2.051	0.103	25.45	-4.4	-90	9.7
0.088	0.0036	2.371	0.220	19.45	-12.7	-116	4.6
0.088	0.0035	2.308	0.190	20.35	-11.2	-110	5.3
0.088	0.0034	2.255	0.168	21.25	-9.5	-104	6.0
0.088	0.0033	2.211	0.152	22.15	-7.7	-99	6.6
0.088	0.0032	2.176	0.140	23.05	-6.1	-93	7.1
0.088	0.0031	2.150	0.132	23.96	-4.3	-88	7.6
0.088	0.0030	2.133	0.127	24.87	-2.4	-82	7.9
0.119	0.0036	2.387	0.237	19.28	-6.0	-91	4.2
0.119	0.0035	2.355	0.220	20.00	-5.0	-88	4.5
0.119	0.0034	2.328	0.207	20.74	-4.0	-84	4.8
0.119	0.0033	2.306	0.197	21.50	-3.8	-83	5.1
0.119	0.0032	2.289	0.189	22.27	-2.9	-80	5.3
0.119	0.0031	2.277	0.184	23.06	-1.8	-77	5.4
0.119	0.0030	2.270	0.181	23.88	-0.8	-74	5.5
0.148	0.0036	2.469	0.298	18.75	-2.9	-78	3.4
0.148	0.0035	2.455	0.288	19.37	-2.5	-77	3.5
0.148	0.0034	2.443	0.280	20.00	-2.1	-75	3.6
0.148	0.0033	2.433	0.274	20.67	-1.8	-74	3.7
0.148	0.0032	2.425	0.269	21.36	-1.4	-73	3.7
0.148	0.0031	2.419	0.265	22.09	-1.0	-72	3.8
0.148	0.0030	2.415	0.263	22.85	-0.6	-70	3.8

Table 4.4.6 (Contd): Tabulated Thermodynamic Data for the solubility of propene in water - ethanol solvents of alcohol mole fraction x_c

x_c	$1/T$	$\log s_o$	$x_{gas} \times 10^3$	$\frac{\Delta \bar{G}}{kJ}^\circ$	$\frac{\Delta \bar{H}}{kJ}^\circ$	$\frac{\Delta \bar{S}}{JK^{-1}}^\circ$	$K_H/10^3$
0.186	0.0036	2.672	0.498	17.57	-4.4	-79	2.0
0.186	0.0035	2.650	0.473	18.19	-4.0	-78	2.1
0.186	0.0034	2.630	0.452	18.83	-3.6	-76	2.2
0.186	0.0033	2.612	0.433	19.51	-2.8	-74	2.3
0.186	0.0032	2.596	0.418	20.22	-2.4	-72	2.4
0.186	0.0031	2.582	0.404	20.95	-2.0	-71	2.5
0.186	0.0030	2.570	0.393	21.73	-1.5	-70	2.5
0.226	0.0036	2.884	0.850	16.33	-8.4	-89	1.2
0.226	0.0035	2.839	0.766	17.04	-7.6	-86	1.3
0.226	0.0034	2.801	0.702	17.76	-6.8	-84	1.4
0.226	0.0033	2.770	0.654	18.47	-5.6	-79	1.5
0.226	0.0032	2.746	0.618	19.20	-4.8	-77	1.6
0.226	0.0031	2.729	0.595	19.92	-4.0	-74	1.7
0.226	0.0030	2.719	0.581	20.65	-3.1	-71	1.7
0.322	0.0036	3.263	2.255	14.08	-11.9	-94	0.4
0.322	0.0035	3.207	1.983	14.78	-10.5	-88	0.5
0.322	0.0034	3.156	1.764	15.50	-9.0	-83	0.6
0.322	0.0033	3.110	1.587	16.24	-8.0	-80	0.6
0.322	0.0032	3.069	1.444	16.99	-6.6	-76	0.7
0.322	0.0031	3.033	1.329	17.76	-5.1	-71	0.8
0.322	0.0030	3.002	1.238	18.55	-3.5	-66	0.8

Table 4.4.7: Tabulated Thermodynamic Data for the solubility of propane in water - 2-methylpropan-2-ol solvents of alcohol mole fraction x_c

x_c	$1/T$	$\log s_o$	$x_{\text{gas}} \times 10^3$	$\frac{\Delta \bar{G}}{kJ}$	$\frac{\Delta \bar{H}}{kJ}$	$\frac{\Delta \bar{S}}{JK^{-1}}$	$K_H/10^3$
0.000	0.0036	1.859	0.058	22.52	-31.8	-196	17.2
0.000	0.0035	1.703	0.041	24.02	-28.2	-183	24.7
0.000	0.0034	1.566	0.030	25.50	-24.3	-169	33.8
0.000	0.0033	1.449	0.023	26.95	-20.1	-155	44.3
0.000	0.0032	1.352	0.018	28.38	-16.8	-145	55.3
0.000	0.0031	1.275	0.015	29.77	-13.3	-133	66.1
0.000	0.0030	1.217	0.013	31.12	-9.5	-122	75.4
0.005	0.0036	1.865	0.060	22.46	-31.8	-195	16.7
0.005	0.0035	1.709	0.042	23.95	-28.0	-182	23.9
0.005	0.0034	1.574	0.031	25.42	-24.1	-168	32.6
0.005	0.0033	1.458	0.023	26.86	-20.6	-157	42.6
0.005	0.0032	1.361	0.019	28.28	-17.1	-145	53.3
0.005	0.0031	1.281	0.016	29.68	-13.3	-133	64.0
0.005	0.0030	1.220	0.014	31.06	-9.4	-121	73.8
0.026	0.0036	1.875	0.065	22.26	-29.9	-188	15.3
0.026	0.0035	1.730	0.047	23.68	-25.9	-174	21.4
0.026	0.0034	1.606	0.035	25.08	-21.7	-159	28.5
0.026	0.0033	1.503	0.028	26.44	-17.7	-146	36.1
0.026	0.0032	1.420	0.023	27.76	-13.9	-133	43.7
0.026	0.0031	1.359	0.020	29.04	-9.9	-121	50.4
0.026	0.0030	1.317	0.018	30.27	-5.7	-108	55.4
0.038	0.0036	1.799	0.057	22.58	-22.3	-161	17.7
0.038	0.0035	1.693	0.044	23.81	-18.5	-148	22.5
0.038	0.0034	1.607	0.036	24.99	-14.4	-134	27.4
0.038	0.0033	1.542	0.031	26.13	-10.4	-121	31.9
0.038	0.0032	1.497	0.028	27.21	-6.9	-109	35.4
0.038	0.0031	1.473	0.027	28.24	-3.1	-97	37.5
0.038	0.0030	1.467	0.026	29.22	0.9	-85	37.9
0.050	0.0036	1.697	0.046	23.05	0.5	-81	21.6
0.050	0.0035	1.702	0.047	23.68	1.2	-79	21.4
0.050	0.0034	1.710	0.048	24.33	2.0	-76	21.0
0.050	0.0033	1.722	0.049	25.00	2.9	-73	20.4
0.050	0.0032	1.739	0.051	25.68	3.6	-71	19.6
0.050	0.0031	1.760	0.053	26.38	4.3	-69	18.7
0.050	0.0030	1.784	0.057	27.11	5.0	-66	17.7
0.066	0.0036	1.957	0.088	21.57	1.1	-74	11.4
0.066	0.0035	1.972	0.091	22.10	4.7	-61	11.0
0.066	0.0034	2.007	0.099	22.56	8.6	-47	10.1
0.066	0.0033	2.062	0.112	22.93	12.6	-34	9.0
0.066	0.0032	2.136	0.132	23.20	15.9	-23	7.5
0.066	0.0031	2.229	0.164	23.37	19.4	-12	6.1
0.066	0.0030	2.342	0.213	23.43	23.2	-1	4.7

Table 4.4.8: Tabulated Thermodynamic Data for the solubility of butane in water - 2-methylpropan-2-ol solvents of alcohol mole fraction x_c

x_c	1/T	$\log s_0$	$x_{\text{gas}} \times 10^3$	$\frac{\Delta \bar{G}}{\text{kJ}}$	$\frac{\Delta \bar{H}}{\text{kJ}}$	$\frac{\Delta \bar{S}}{\text{JK}^{-1}}$	$K_H/10^3$
0.000	0.0036	1.809	0.052	22.78	-37.6	-217	19.2
0.000	0.0035	1.627	0.034	24.42	-32.7	-200	29.2
0.000	0.0034	1.471	0.024	26.02	-27.4	-182	41.8
0.000	0.0033	1.341	0.018	27.56	-22.4	-165	56.4
0.000	0.0032	1.237	0.014	29.04	-17.7	-149	71.6
0.000	0.0031	1.159	0.012	30.46	-12.7	-134	85.7
0.000	0.0030	1.107	0.010	31.81	-7.3	-117	96.6
0.005	0.0036	1.841	0.057	22.57	-38.0	-218	17.6
0.005	0.0035	1.654	0.037	24.24	-33.2	-201	27.0
0.005	0.0034	1.494	0.026	25.85	-28.1	-183	39.0
0.005	0.0033	1.361	0.019	27.41	-23.0	-166	53.0
0.005	0.0032	1.253	0.015	28.91	-18.4	-151	68.0
0.005	0.0031	1.170	0.012	30.35	-13.5	-136	82.3
0.005	0.0030	1.112	0.011	31.74	-8.2	-120	94.0
0.026	0.0036	1.836	0.060	22.46	-32.9	-199	16.7
0.026	0.0035	1.675	0.041	23.97	-28.5	-184	24.2
0.026	0.0034	1.540	0.030	25.44	-24.0	-168	33.0
0.026	0.0033	1.427	0.023	26.87	-19.3	-152	42.8
0.026	0.0032	1.338	0.019	28.24	-15.1	-139	52.6
0.026	0.0031	1.271	0.016	29.56	-10.7	-125	61.3
0.026	0.0030	1.228	0.015	30.83	-5.9	-110	67.7
0.038	0.0036	1.757	0.052	22.79	-21.6	-160	19.3
0.038	0.0035	1.654	0.041	24.01	-18.0	-147	24.5
0.038	0.0034	1.570	0.034	25.19	-14.1	-134	29.8
0.038	0.0033	1.505	0.029	26.33	-10.3	-121	34.5
0.038	0.0032	1.460	0.026	27.42	-6.9	-110	38.3
0.038	0.0031	1.434	0.025	28.47	-3.3	-98	40.7
0.038	0.0030	1.427	0.024	29.46	0.6	-87	41.3
0.050	0.0036	1.731	0.050	22.86	4.6	-66	19.9
0.050	0.0035	1.757	0.053	23.37	5.1	-64	18.7
0.050	0.0034	1.784	0.057	23.90	5.7	-62	17.6
0.050	0.0033	1.816	0.061	24.44	6.2	-60	16.4
0.050	0.0032	1.849	0.066	25.00	6.7	-58	15.1
0.050	0.0031	1.887	0.072	25.58	7.4	-57	13.9
0.050	0.0030	1.926	0.079	26.18	8.0	-55	12.7
0.080	0.0036	3.176	1.514	15.00	-23.0	-137	0.7
0.080	0.0035	3.063	1.167	16.04	-20.5	-128	0.9
0.080	0.0034	2.963	0.927	17.08	-17.9	-119	1.1
0.080	0.0033	2.876	0.759	18.10	-15.2	-110	1.3
0.080	0.0032	2.802	0.640	19.11	-13.0	-103	1.6
0.080	0.0031	2.740	0.555	20.10	-10.7	-96	1.8
0.080	0.0030	2.690	0.495	21.09	-8.2	-88	2.0

4.5 $\Delta\bar{G}^\circ$ Isotherms

Isotherms of $\Delta\bar{G}^\circ$ have been constructed by plotting $\Delta\bar{G}^\circ$ against x_c , the mole fraction of alcohol and they show the variation of this function with solvent composition in the following Figures 4.5.1 to 4.5.8.

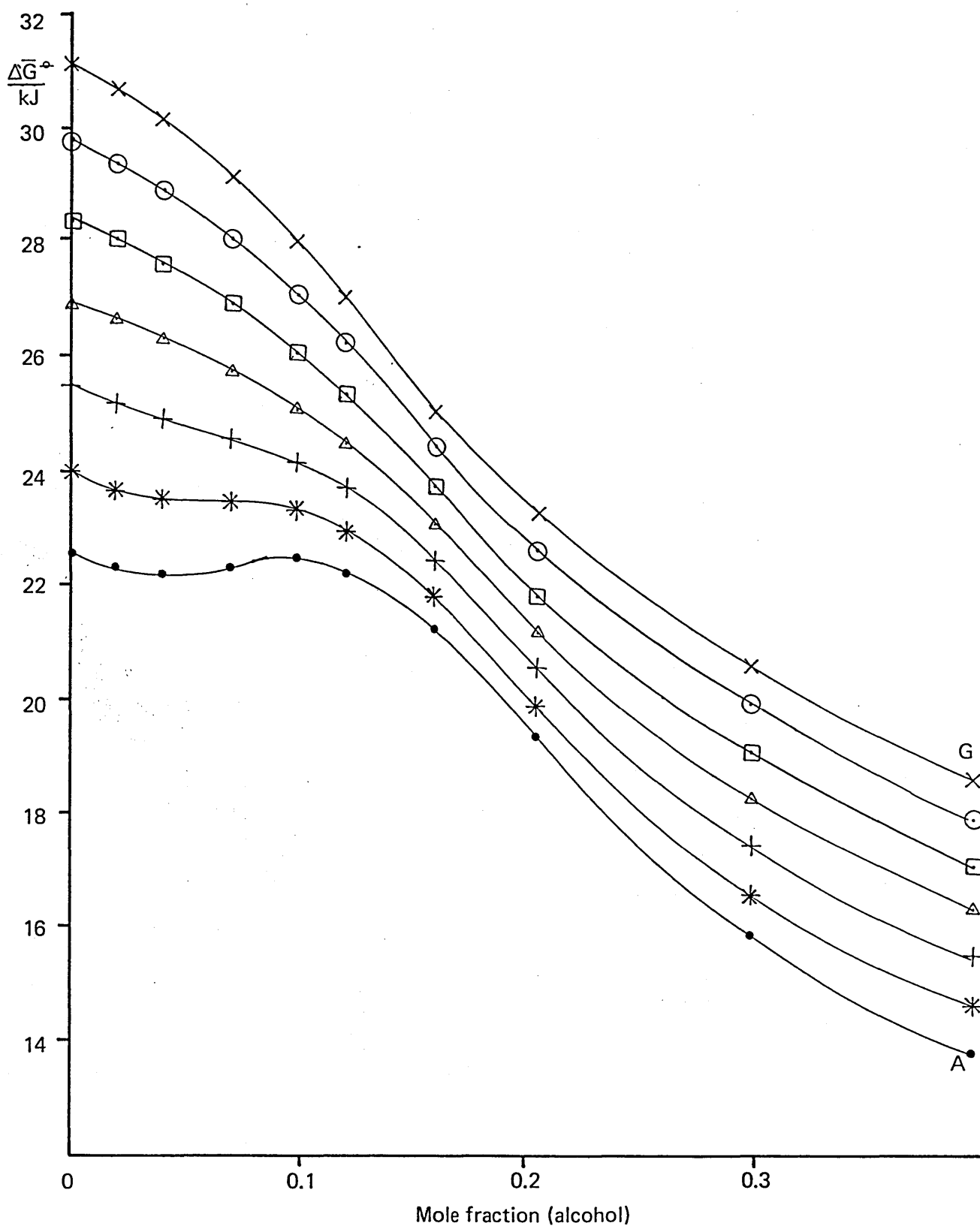


Figure 4.5.1 : ΔG° isotherms for the solubility of propane in mixtures of water and ethanol.
 Temperatures: 4.7(A), 12.6(B), 21.0(C), 29.9(D), 39.4(E), 49.5(F), 60.2°C(G).

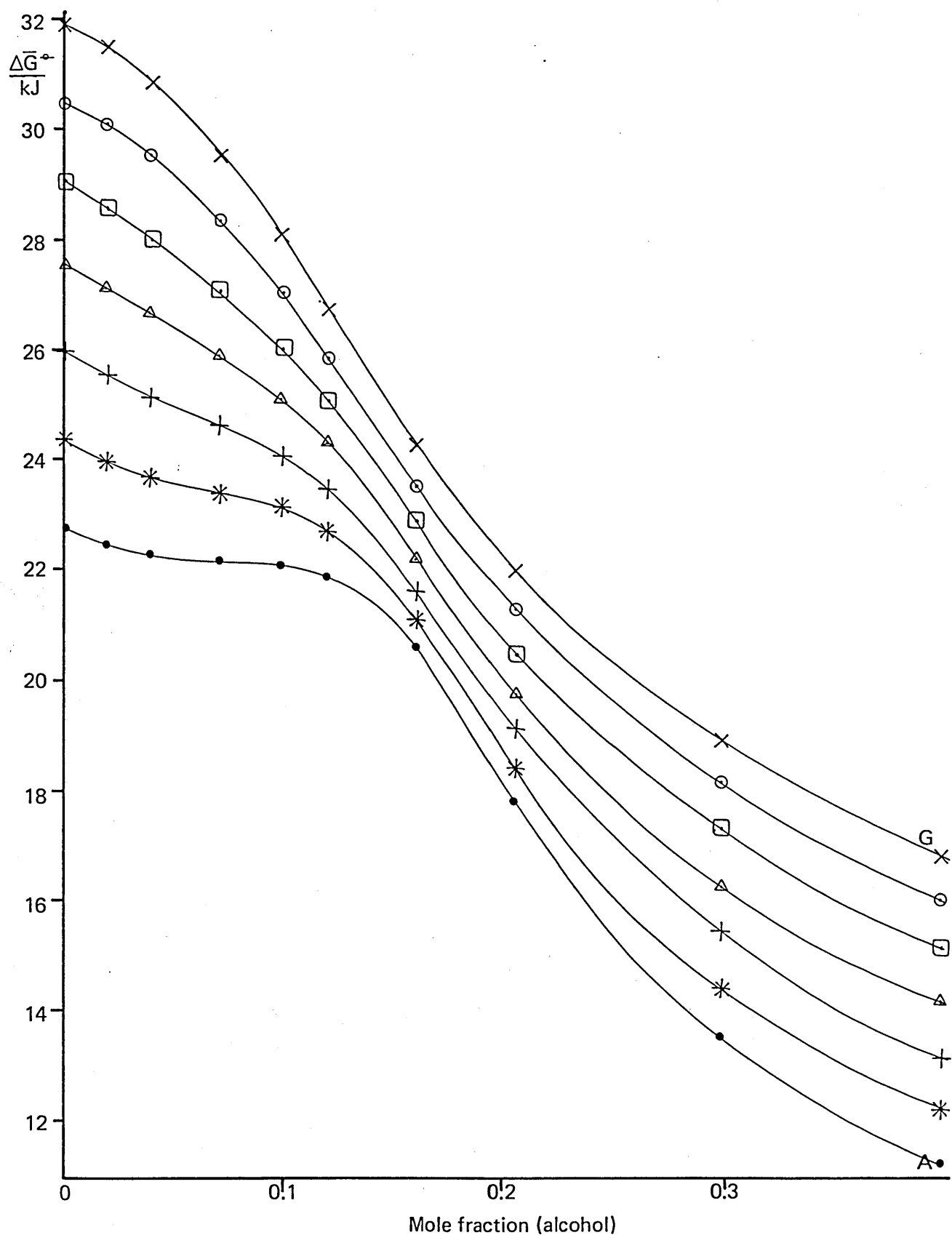


Figure 4.5.2 : $\Delta \bar{G}^\circ$ isotherms for the solubility of butane in mixtures of water and ethanol.
 Temperatures: 4.7(A), 12.6(B), 21.0(C), 29.9(D), 39.4(E), 49.5(F), 60.2°C(G).

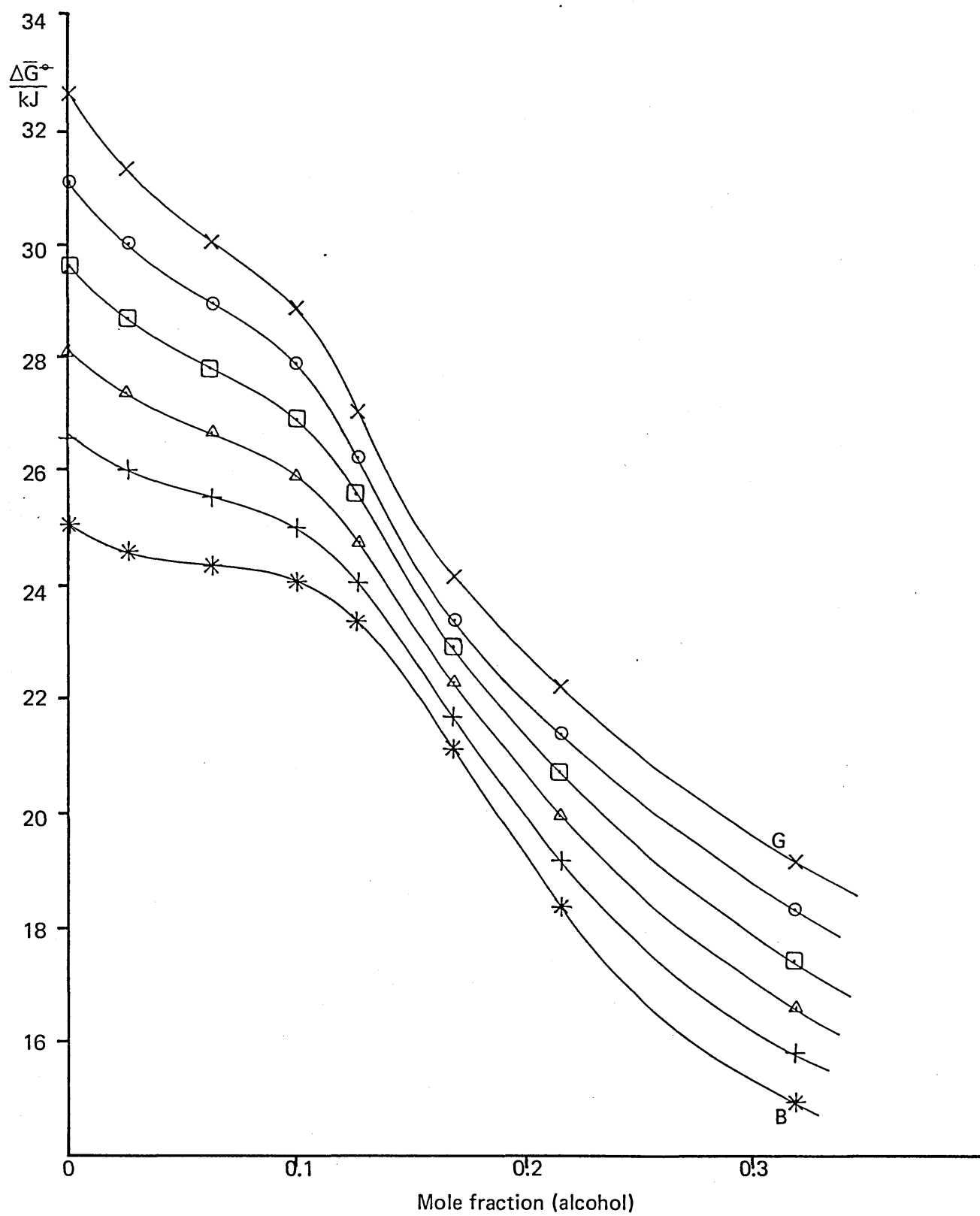


Figure 4.5.3 : ΔG° isotherms for the solubility of 2-methylpropane in mixtures of water and ethanol.

Temperatures: 12.6(B), 21.0(C), 29.9(D), 39.4(E), 49.5(F), 60.2°C(G).

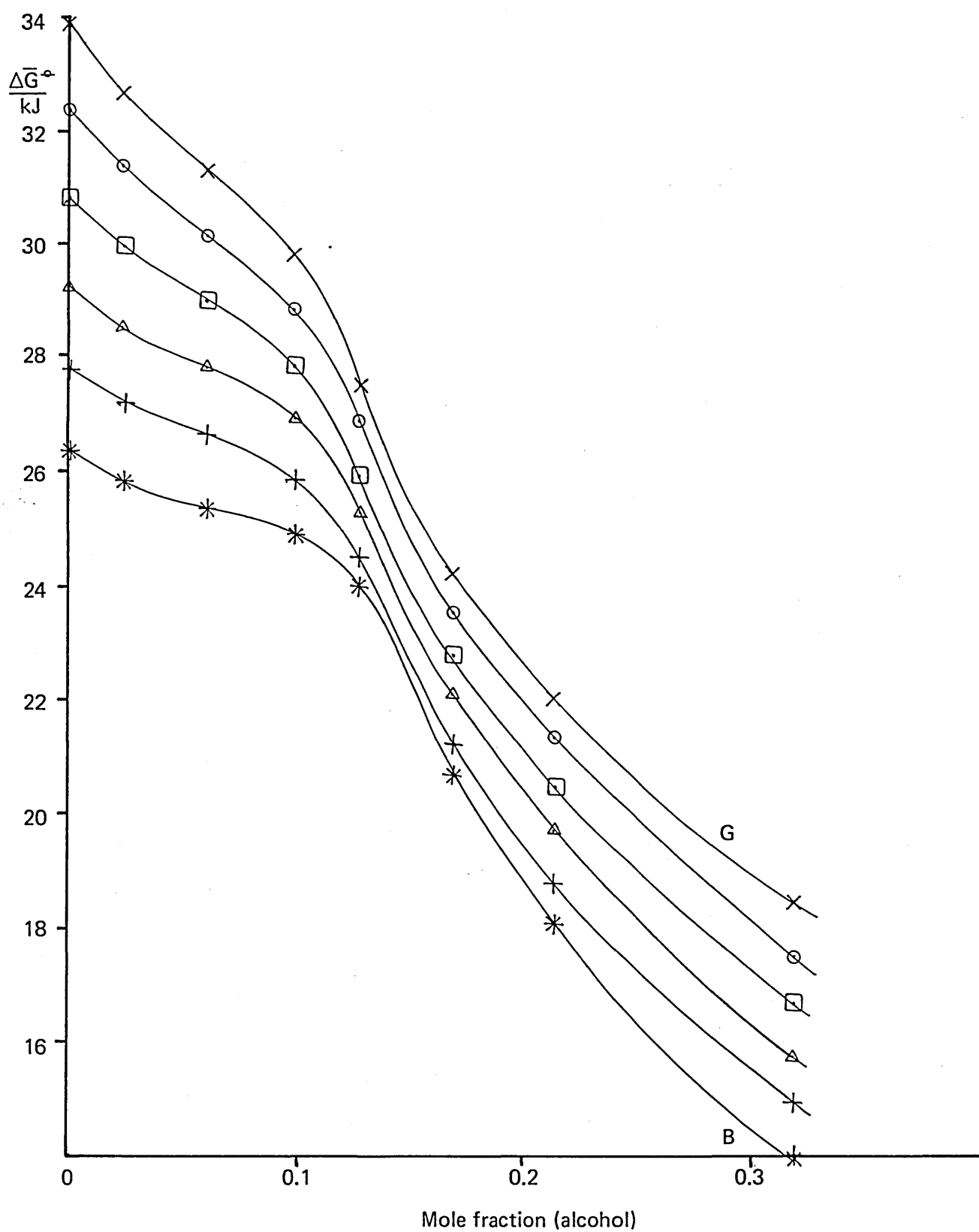


Figure 4.5.4 : ΔG° isotherms for the solubility of 2,2-dimethylpropane in mixtures of water and ethanol.

Temperatures: 12.6(B), 21.0(C), 29.9(D), 39.4(E), 49.5(F), 60.2°C(G).

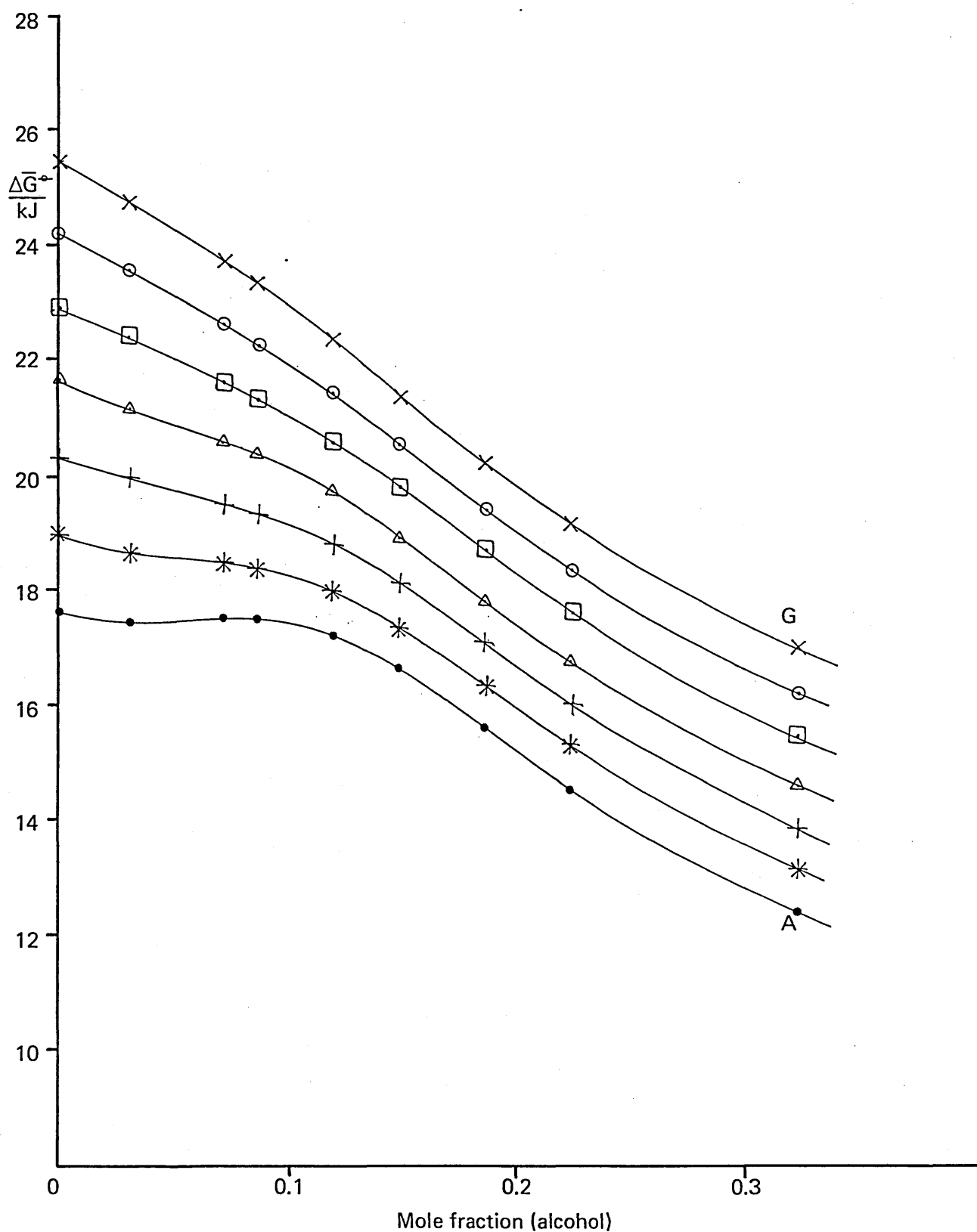


Figure 4.5.5 : $\Delta \bar{G}^{\circ}_{tr}$ isotherms for the solubility of cyclopropane in mixtures of water and ethanol.

Temperatures: 4.7(A), 12.6(B), 21.0(C), 29.9(D), 39.4(E), 49.5(F), 60.2°C(G)

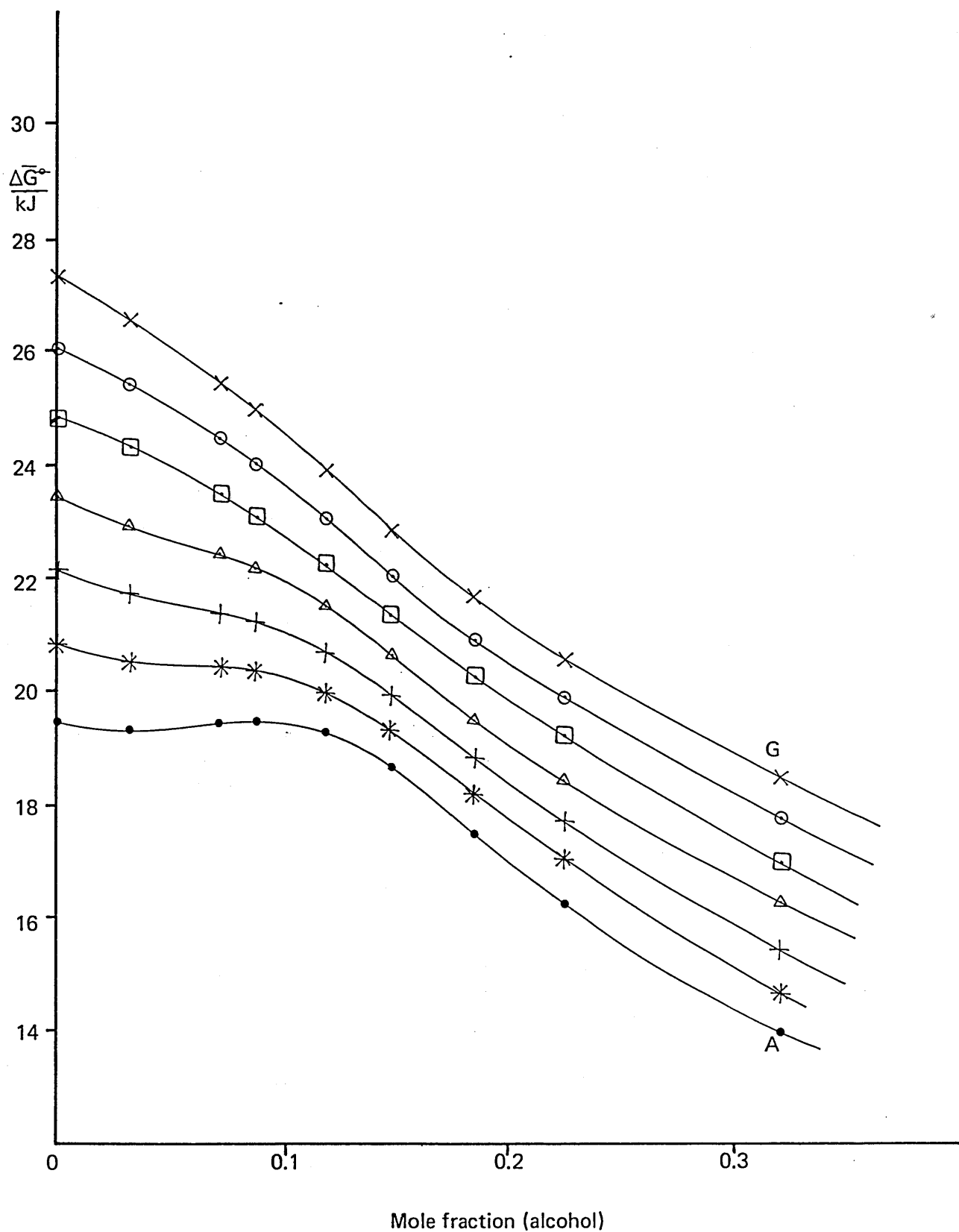


Figure 4.5.6 : ΔG° isotherms for the solubility of propene in mixtures of water and ethanol.

Temperatures: 4.7(A), 12.6(B), 21.0(C), 29.9(D), 39.4(E), 49.5(F), 60.2°C(G)

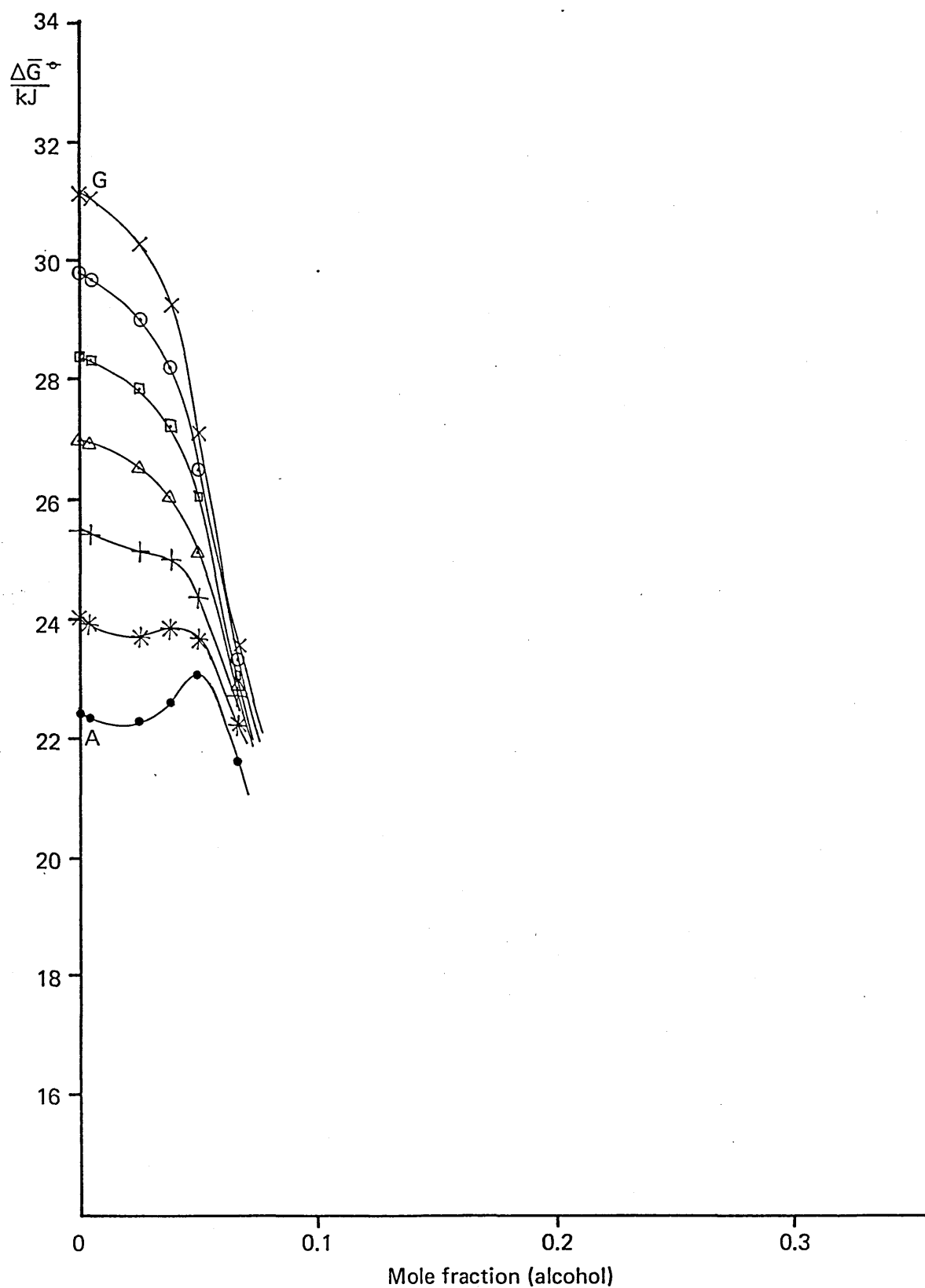


Figure 4.5.7 : $\Delta \bar{G}^*$ isotherms for the solubility of propane in mixtures of water and 2-methylpropan-2-ol.

Temperatures: 4.7(A), 12.6(B), 21.0(C), 29.9(D), 39.4(E), 49.5(F), 60.2°C(G)

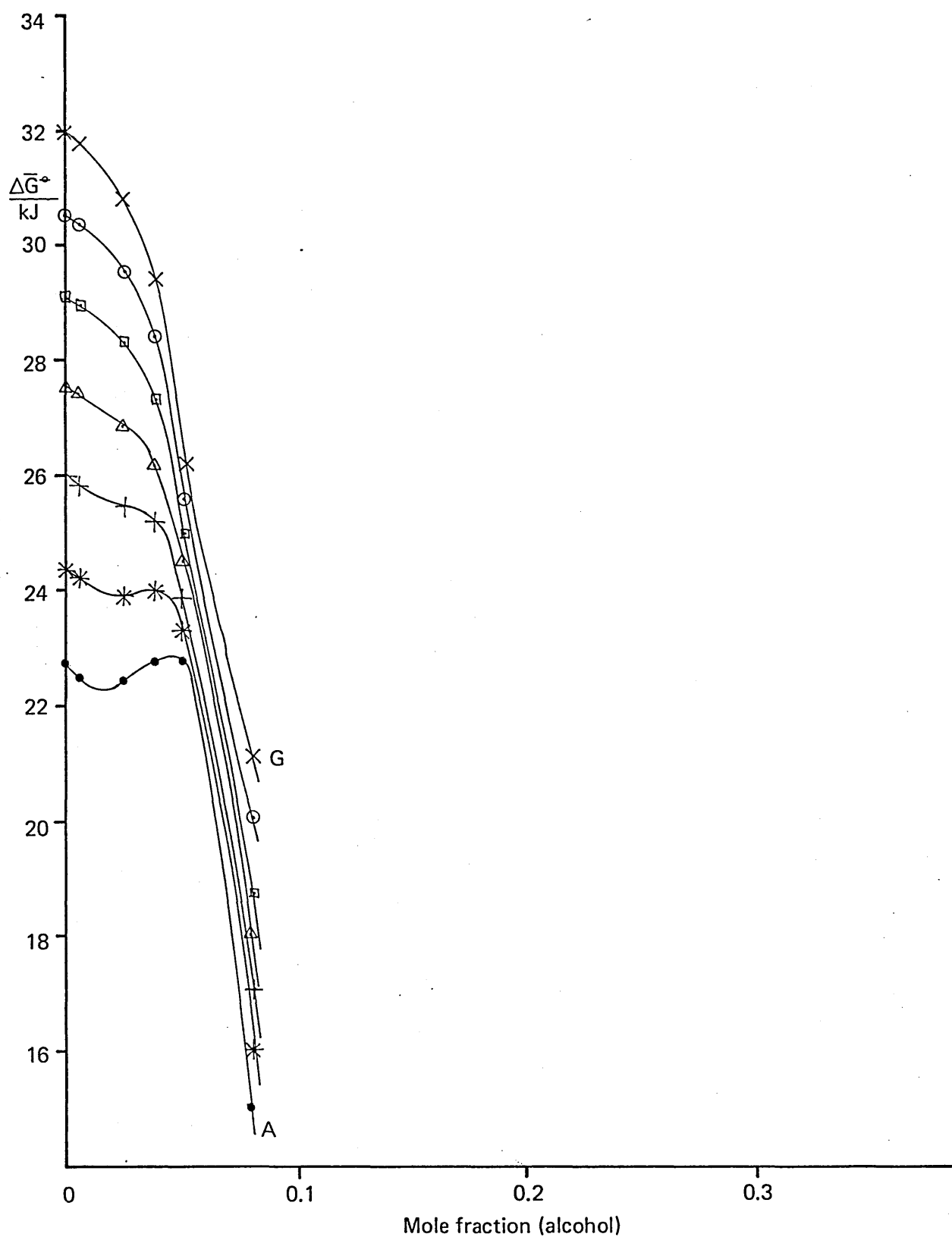


Figure 4.5.8 : $\Delta \bar{G}^\circ$ isotherms for the solubility of butane in mixtures of water and 2-methylpropan-2-ol.

Temperatures: 4.7(A), 12.6(B), 21.0(C), 29.9(D), 39.4(E), 49.5(F), 60.2°C(G)

4.6 $\Delta\bar{H}^\circ$ Isotherms

In this section, $\Delta\bar{H}^\circ$ isotherms have been plotted against solvent composition and the graphs show the variation of $\Delta\bar{H}^\circ$ with increasing x_c . All of the systems involving ethanol as the alcohol component have $\Delta\bar{H}^\circ$ plotted on the same scale. However, for 2-methylpropan-2-ol-water solvents, the magnitudes of $\Delta\bar{H}^\circ$ are too large and a different scale is used.

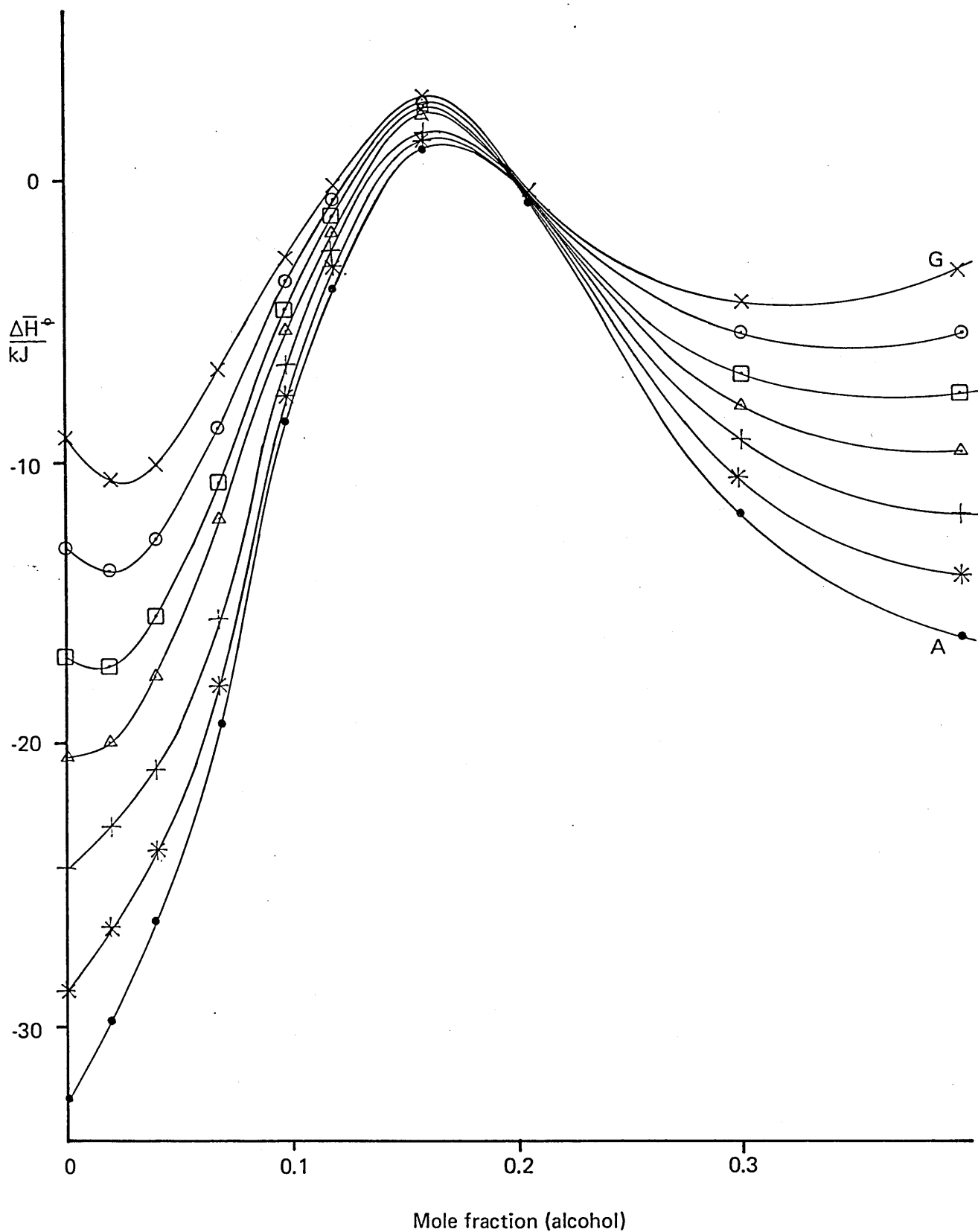


Figure 4.6.1: $\Delta \bar{H}^{\circ}$ isotherms for the solubility of propane in mixtures of water and ethanol.

Temperatures: 4.7(A), 12.6(B), 21.0(C), 29.9(D), 39.4(E), 49.5(F), 60.2°C(G)

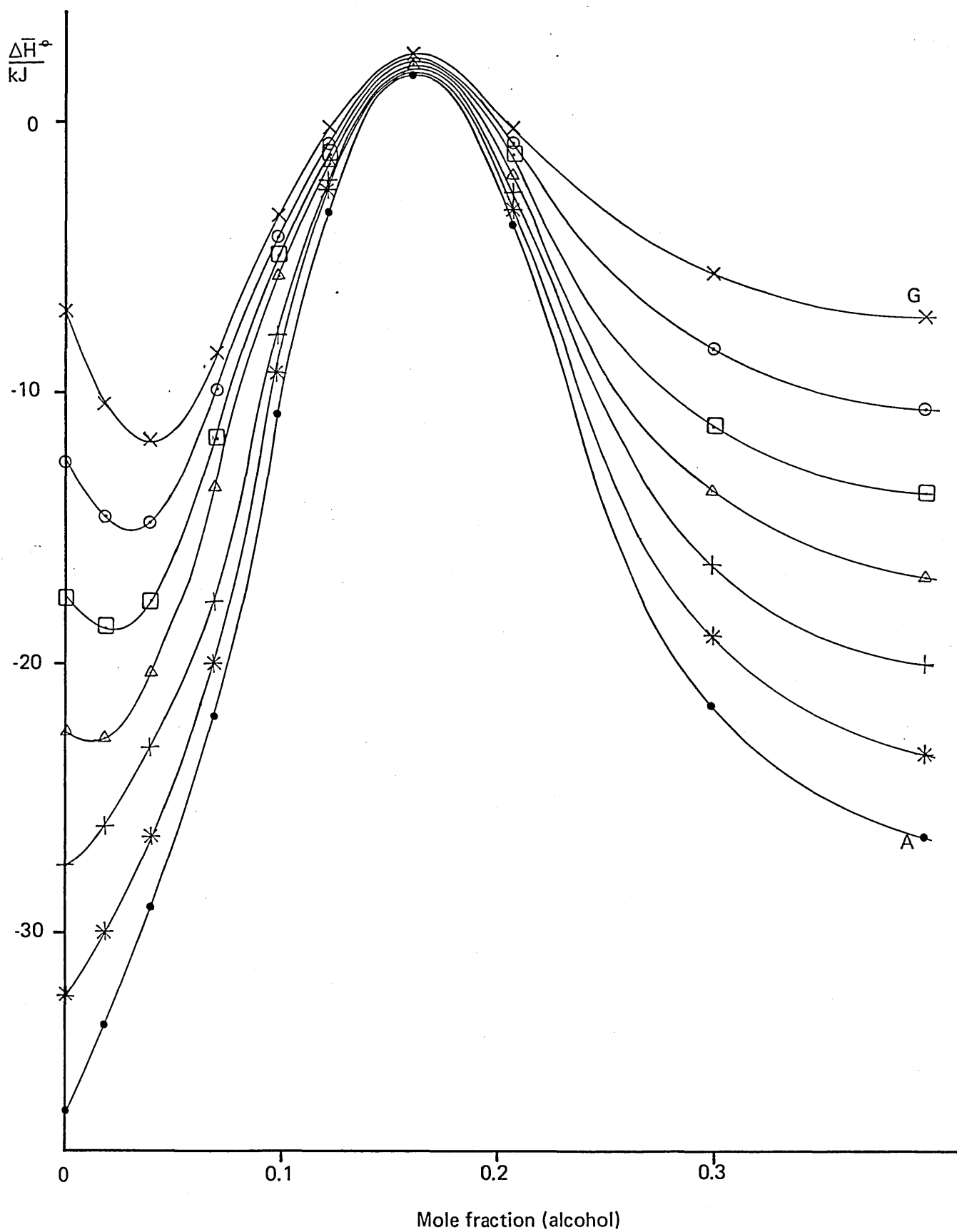


Figure 4.6.2: $\Delta\bar{H}^\circ$ isotherms for the solubility of butane in mixtures of water and ethanol.

Temperatures: 4.7(A), 12.6(B), 21.0(C), 29.9(D), 39.4(E), 49.5(F), 60.2 °C(G).

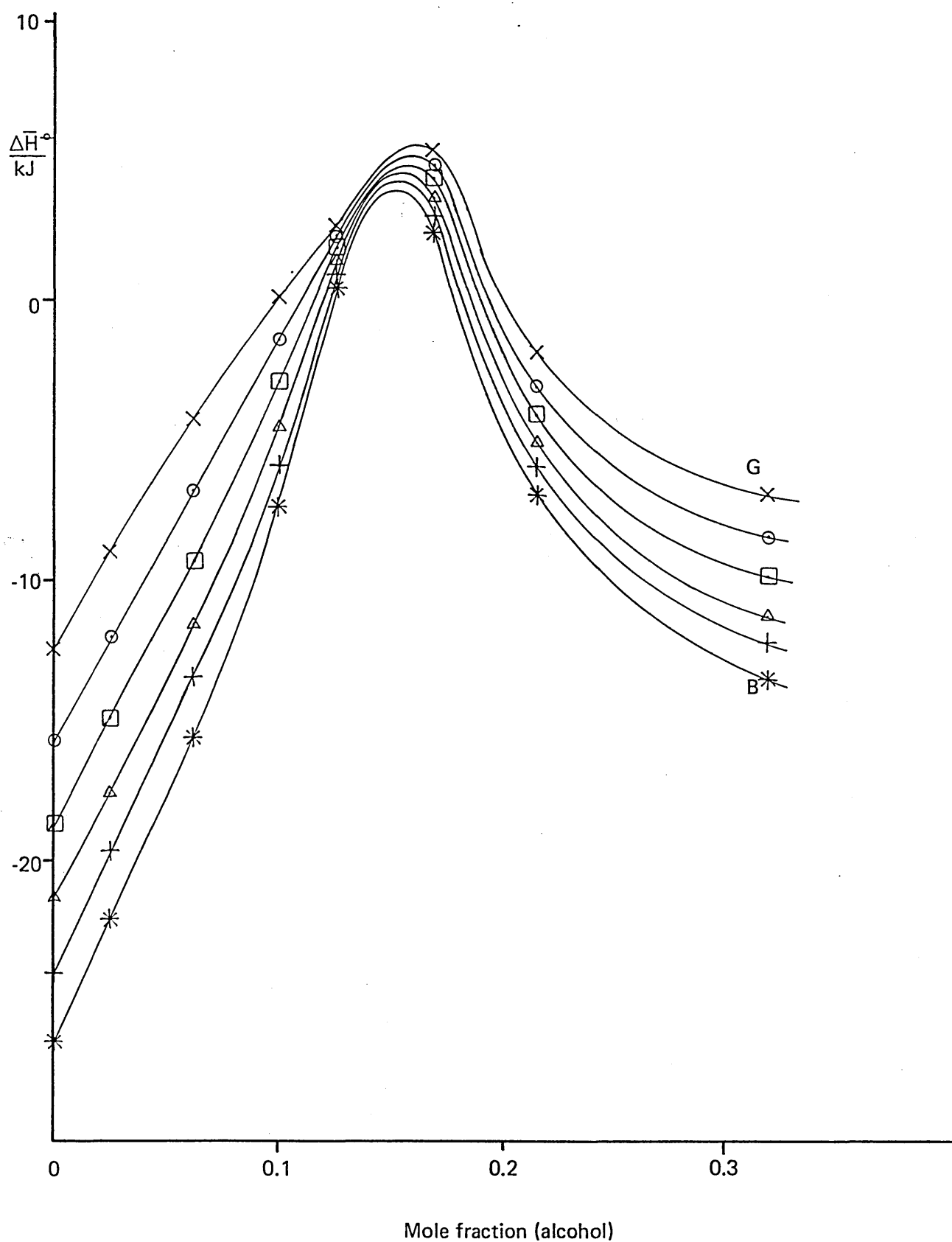


Figure 4.6.3: $\Delta \bar{H}^\circ$ isotherms for the solubility of 2-methylpropane in mixtures of water and ethanol.

Temperatures: 12.6(B), 21.0(C), 29.9(D), 39.4(E), 49.5(F), 60.2°C(G)

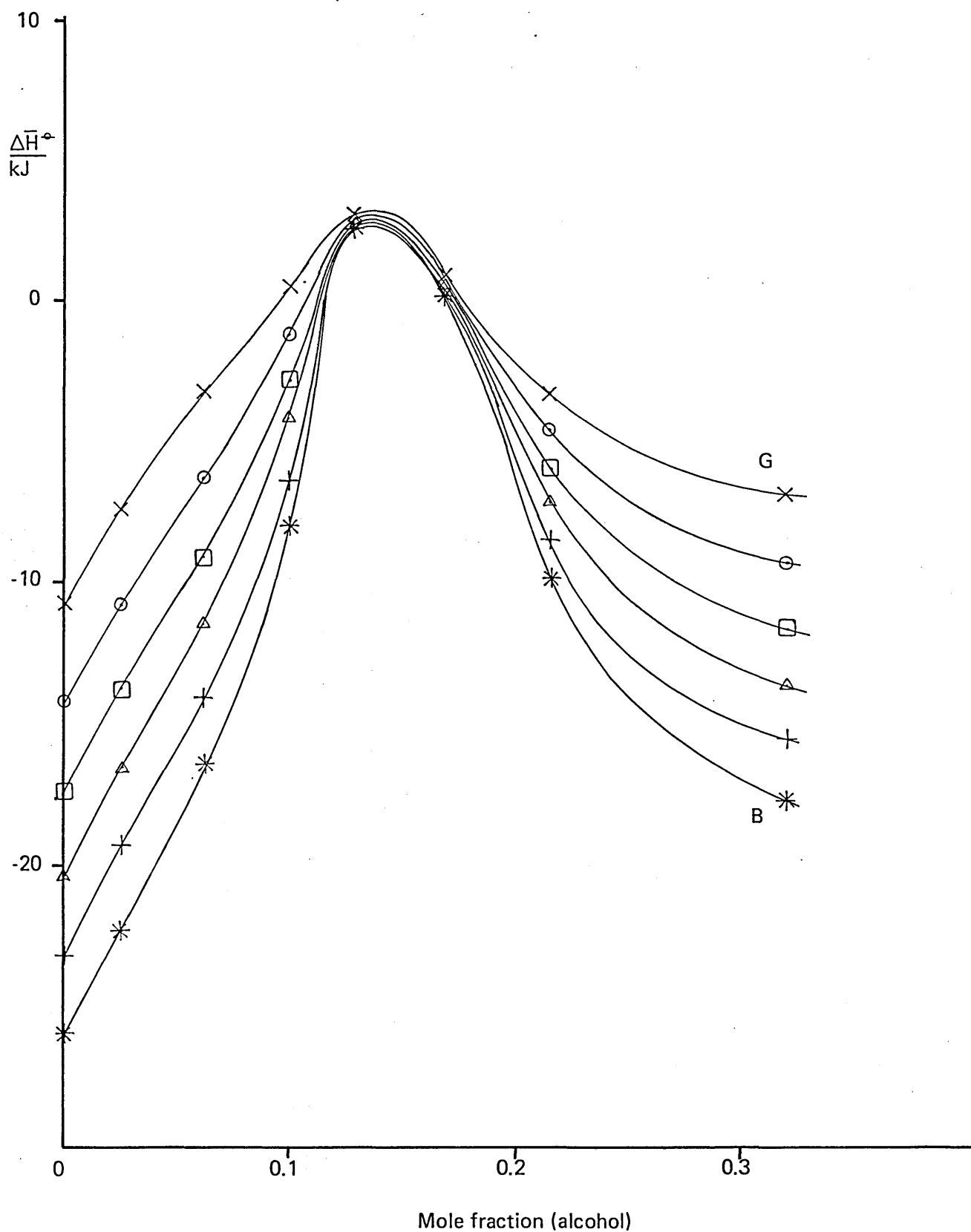


Figure 4.6.4: $\Delta \bar{H}^m$ isotherms for the solubility of 2,2-dimethylpropane in mixtures of water and ethanol.

Temperatures: 12.6(B), 21.0(C), 29.9(D), 39.4(E), 49.5(F), 60.2 °C(G)

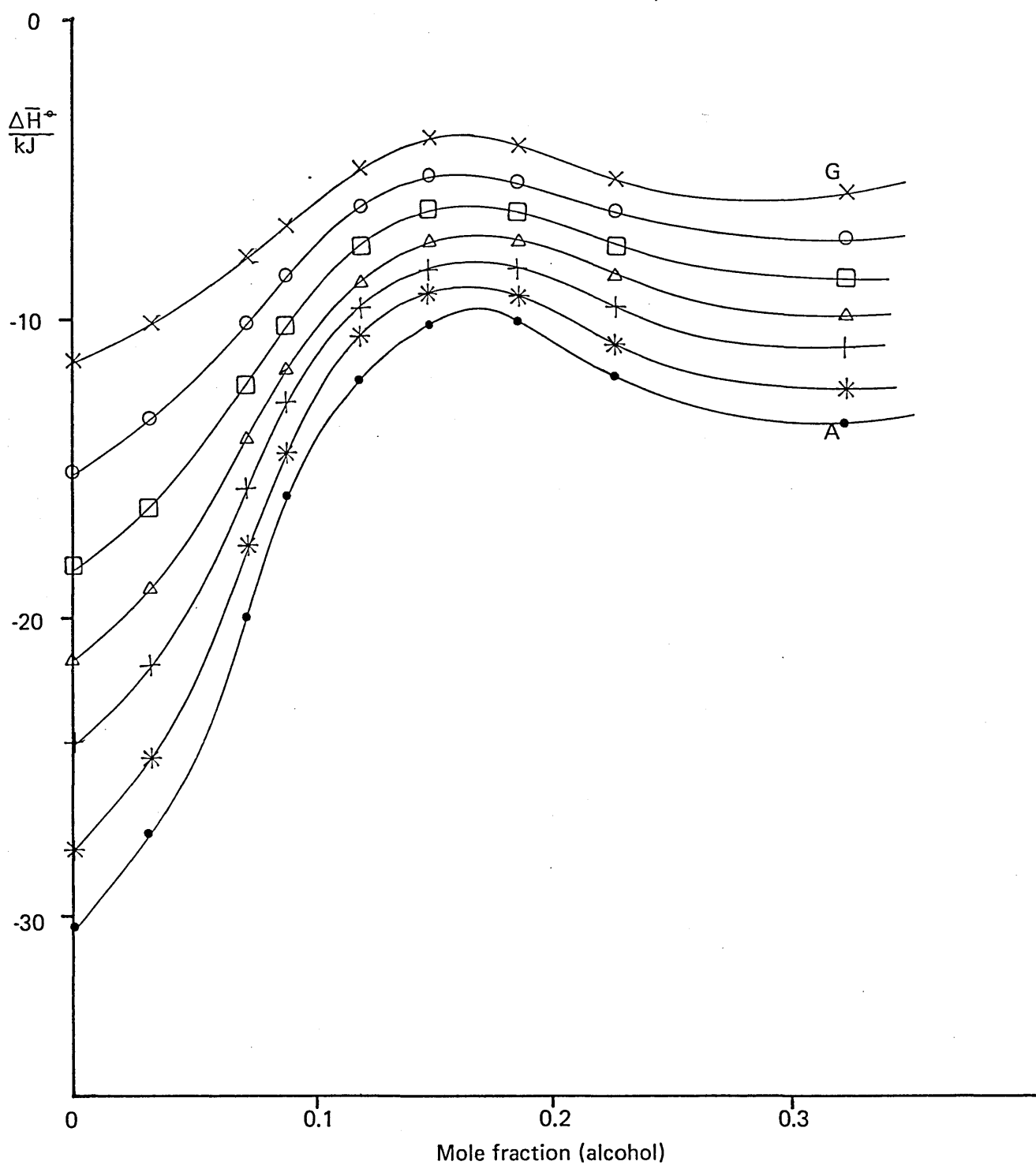


Figure 4.6.5 : $\Delta \bar{H}^+$ isotherms for the solubility of cyclopropane in mixtures of water and ethanol.
 Temperatures: 4.7(A), 12.6(B), 21.0(C), 29.9(D), 39.4(E), 49.5(F), 60.2°C(G).

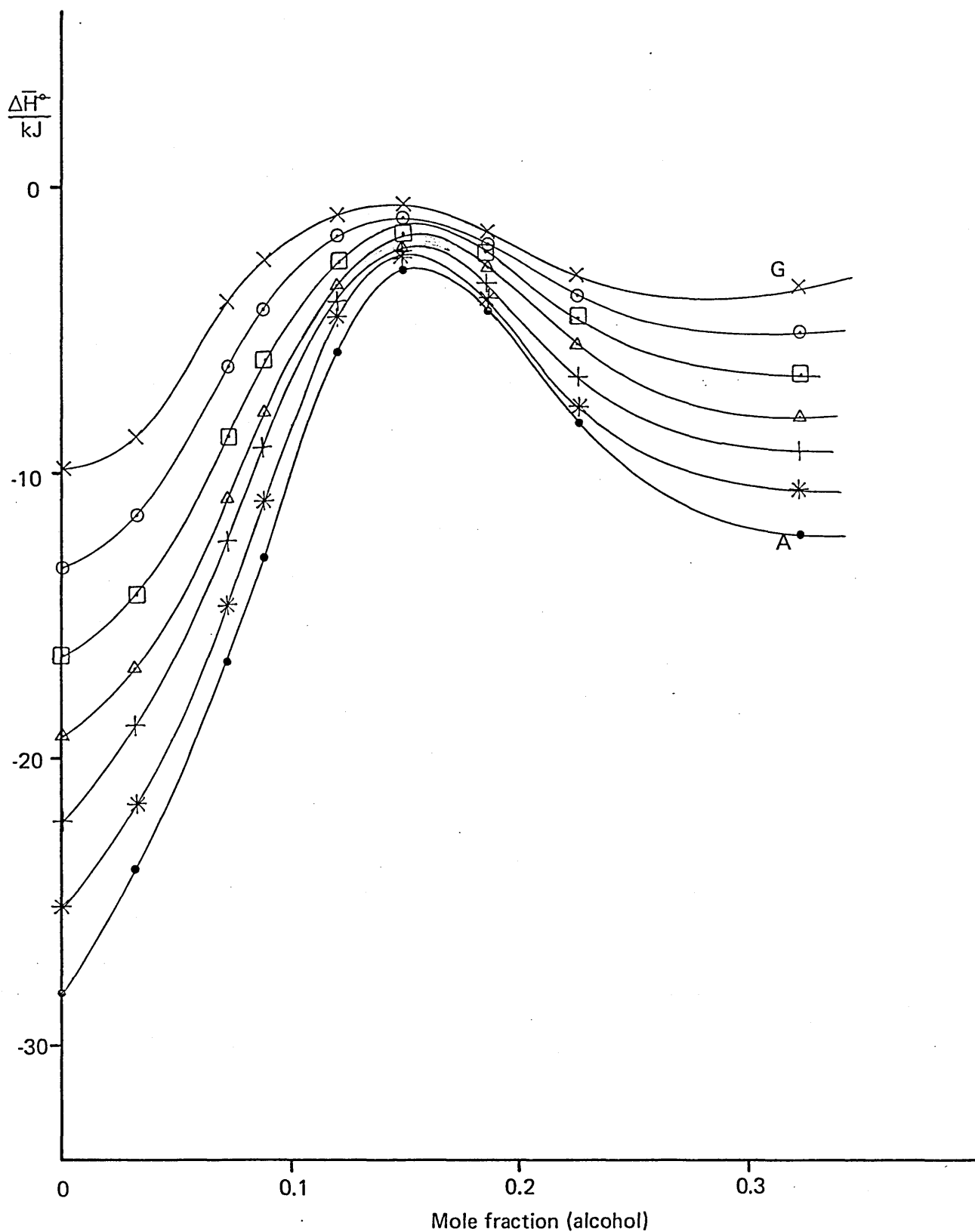


Figure 4.6.6 : $\Delta \bar{H}^0$ isotherms for the solubility of propene in mixtures of water and ethanol.
 Temperatures: 4.7(A), 12.6(B), 21.0(C), 29.9(D), 39.4(E), 49.5(F), 60.2°C(G)

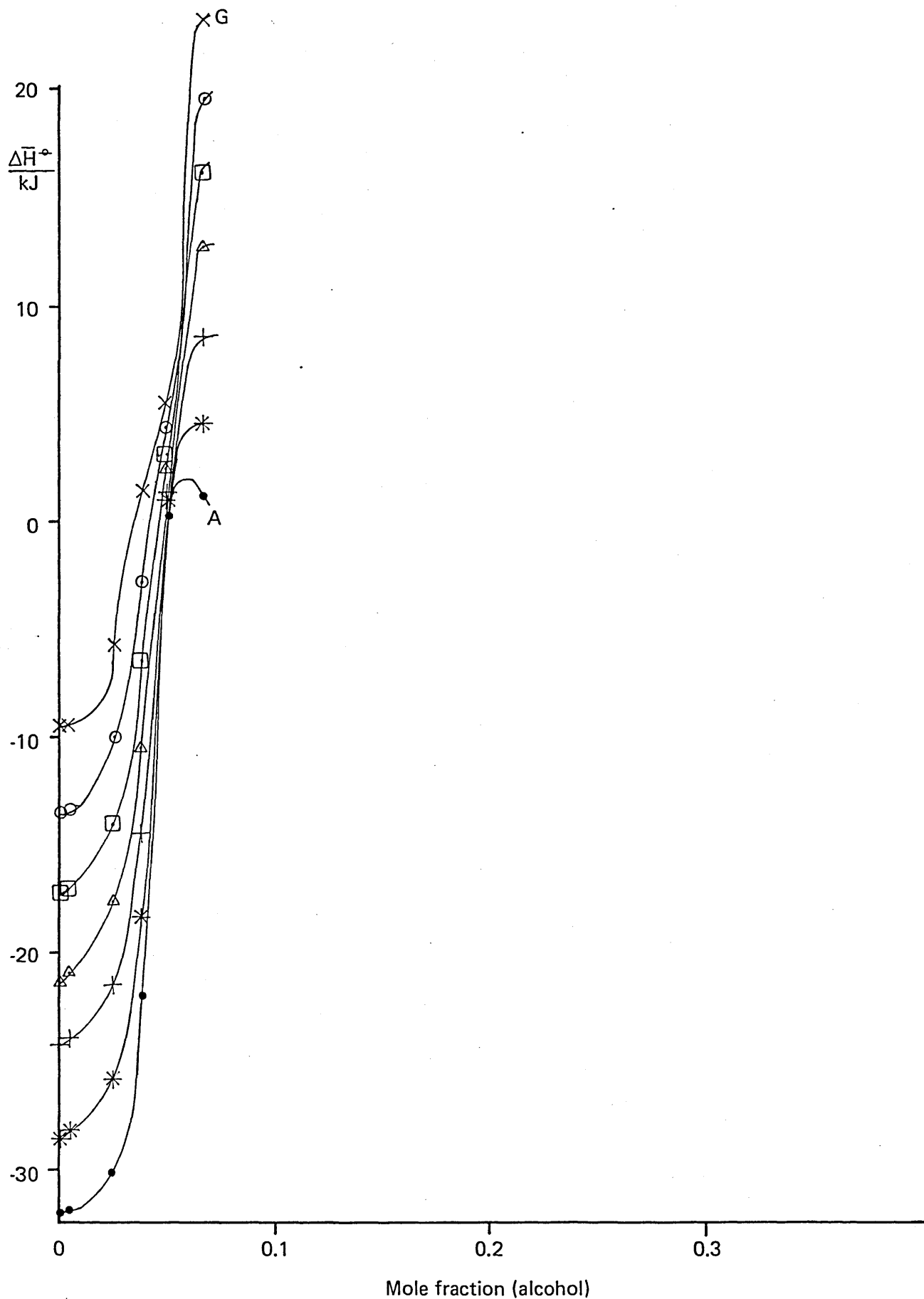


Figure 4.6.7 : $\Delta \bar{H}^\circ$ isotherms for the solubility of propane in mixtures of water and 2-methylpropan-2-ol.

Temperatures: 4.7(A), 12.6(B), 21.0(C), 29.9(D), 39.4(E), 49.5(F), 60.2°C(G).

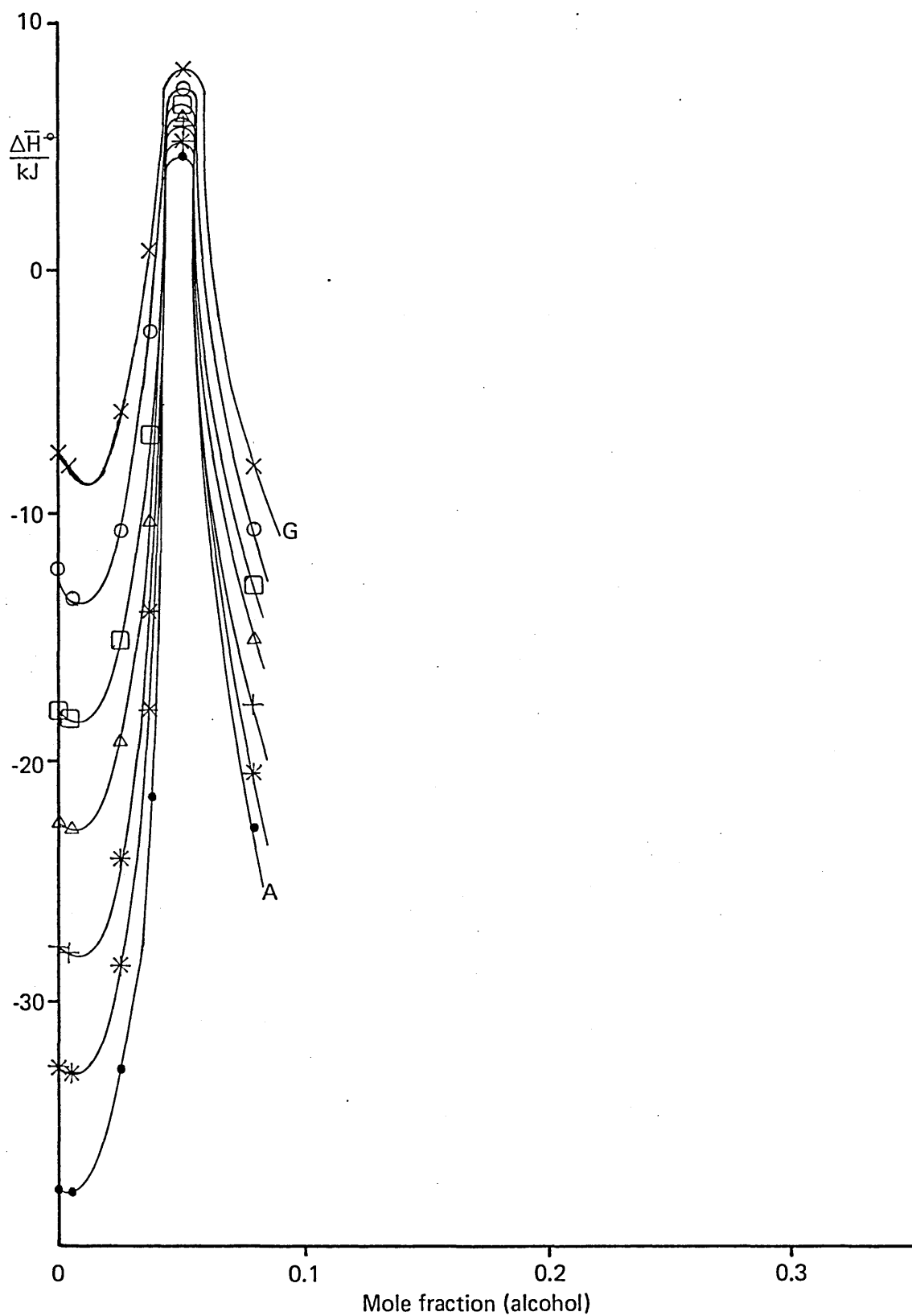


Figure 4.6.8: $\Delta \bar{H}^i$ isotherms for the solubility of butane in mixtures of water and 2-methylpropan-2-ol

Temperatures: 4.7(A), 12.6(B), 21.0(C), 29.9(D), 39.4(E), 49.5(F), 60.2°C(G)

4.7 $\Delta\bar{S}^\circ$ Isotherms

Finally, these isotherms are constructed from plots of $\Delta\bar{S}^\circ$ against mole fraction of alcohol and show the dependence of $\Delta\bar{S}^\circ$ on solvent composition. As in the case of $\Delta\bar{H}^\circ$, all of the graphs corresponding to a solvent including ethanol as a component are drawn on the same scale. A different scale is adopted for this function also for solvents containing 2-methylpropan-2-ol.

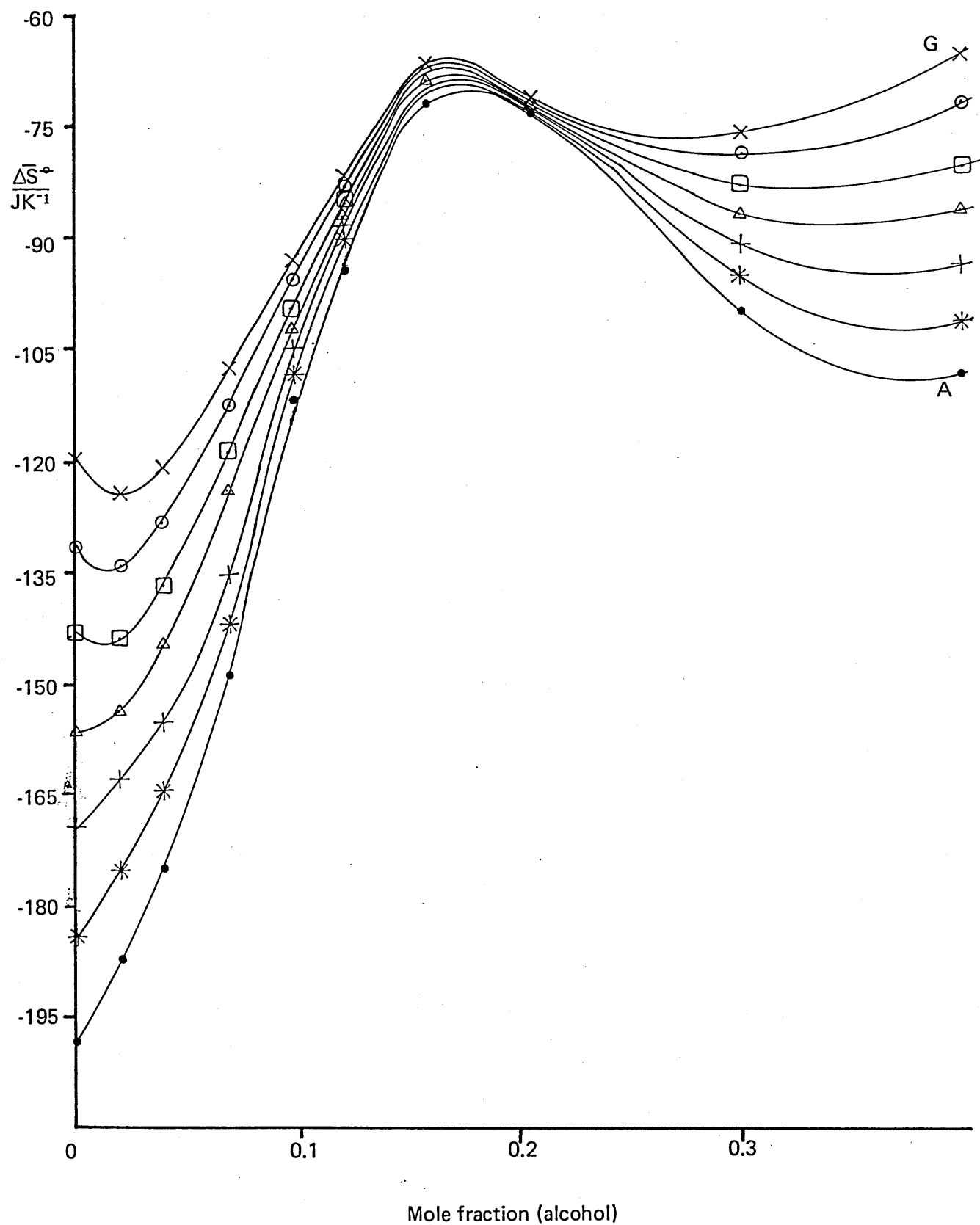


Figure 4.7.1: $\Delta \bar{S}$ isotherms for the solubility of propane in mixtures of water and ethanol.
 Temperatures: 4.7(A), 12.6(B), 21.0(C), 29.9(D), 39.4(E), 49.5(F), 60.2°C(G)

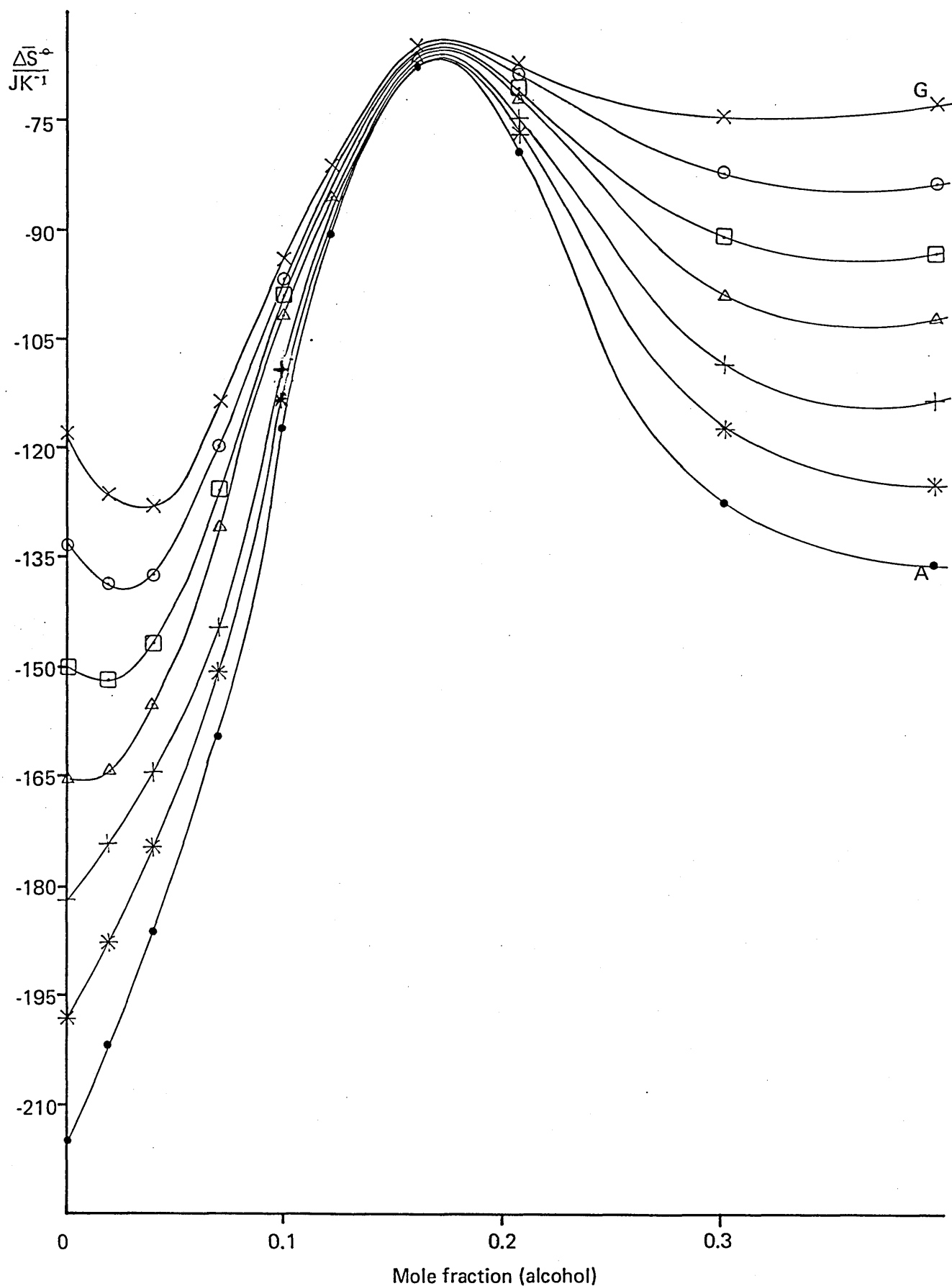


Figure 4.7.2: $\Delta \bar{S}^\circ$ isotherms for the solubility of butane in mixtures of water and ethanol.
 Temperatures: 4.7(A), 12.6(B), 21.0(C), 29.9(D), 39.4(E), 49.5(F), 60.2°C(G)

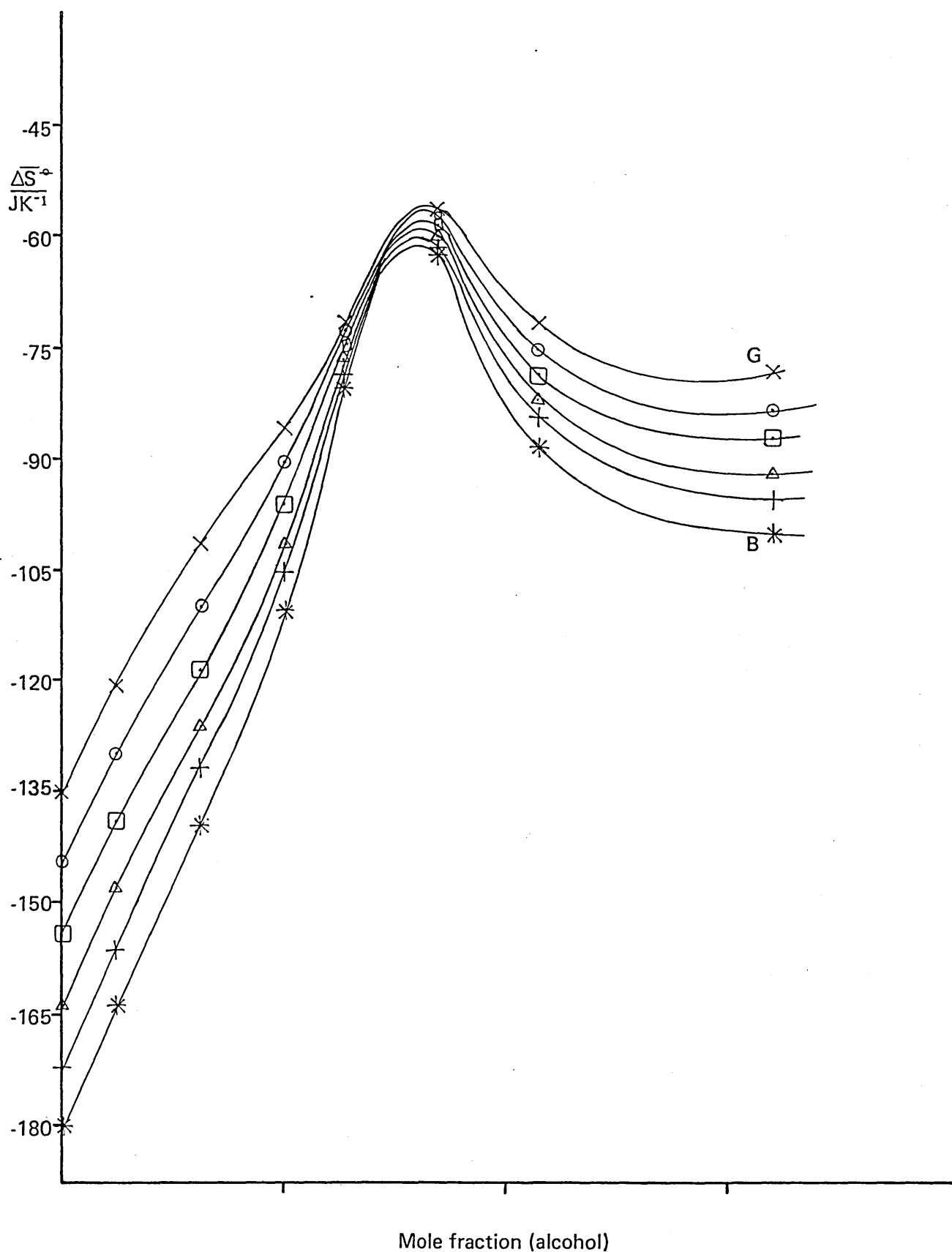


Figure 4.7.3: ΔS° isotherms for the solubility of 2-methylpropane in mixtures of water and ethanol.

Temperatures: 12.6(B), 21.0(C), 29.9(D), 39.4(E), 49.5(F), 60.2°C(G).

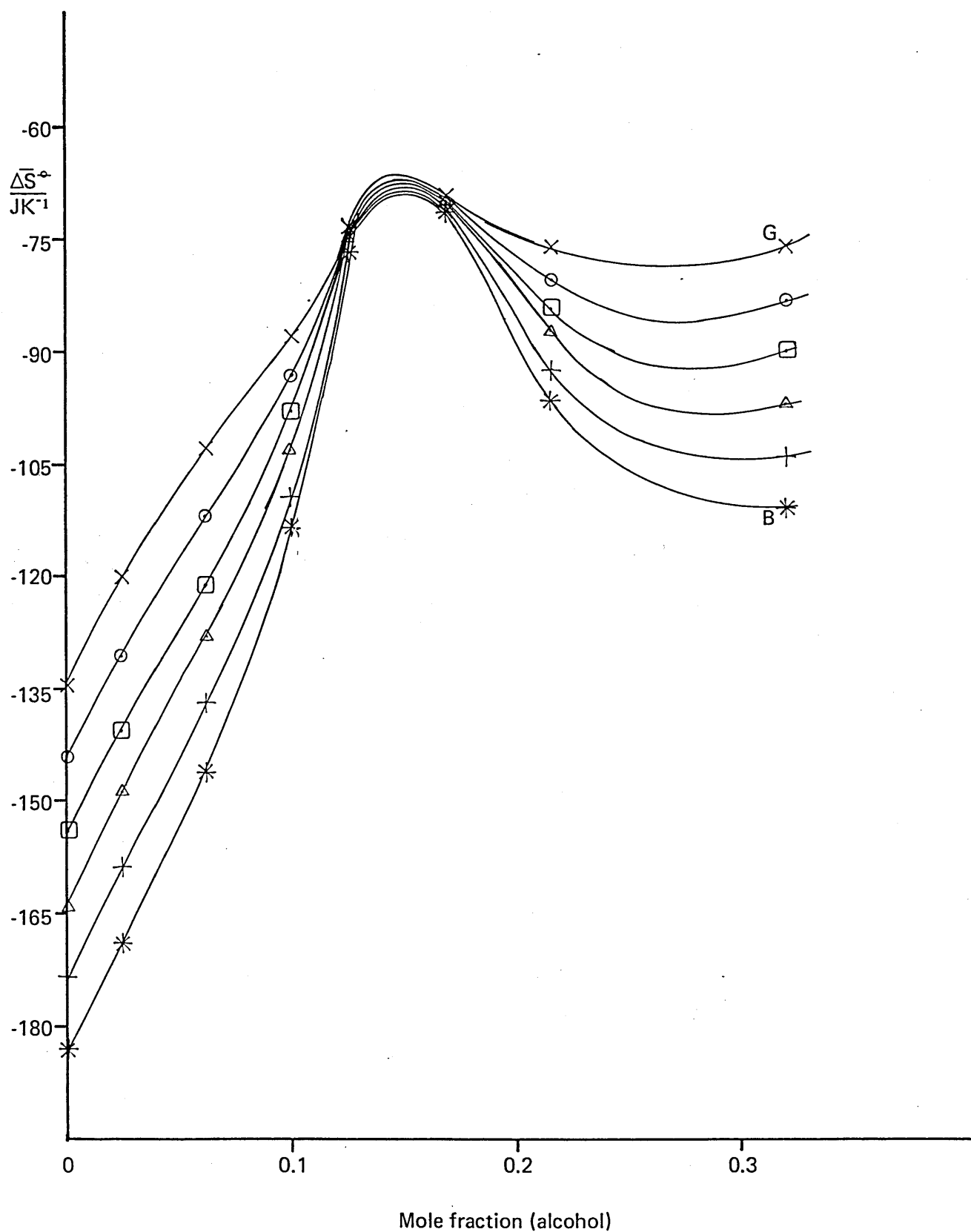


Figure 4.7.4: $\Delta \bar{S}^\circ$ isotherms for the solubility of 2,2-dimethylpropane in mixtures of water and ethanol.

Temperatures: 12.6(B), 21.0(C), 29.9(D), 39.4(E), 49.5(F), 60.2°C(G)

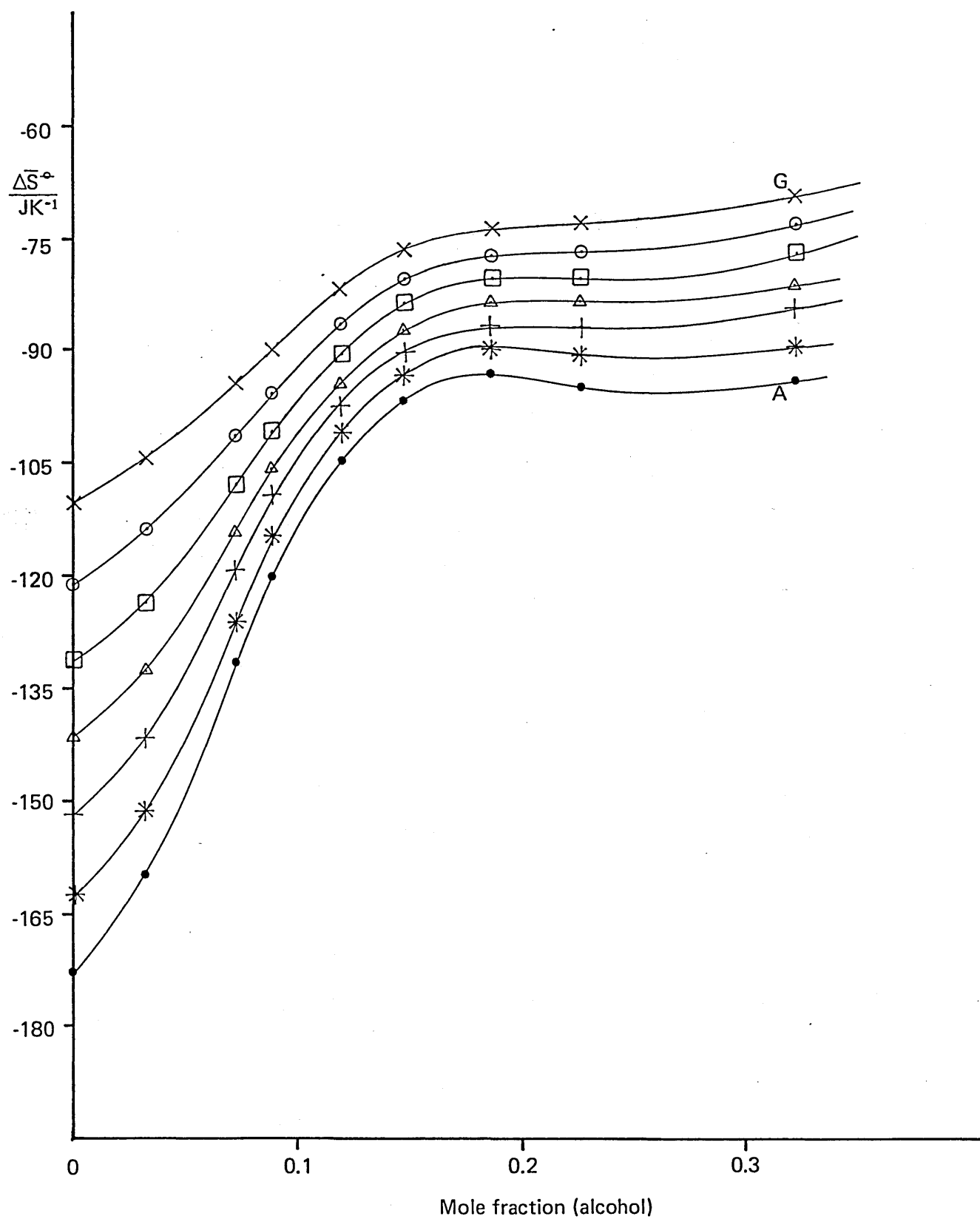


Figure 4.7.5 : $\Delta \bar{S}^\circ$ isotherms for the solubility of cyclopropane in mixtures of water and ethanol.
 Temperatures: 4.7(A), 12.6(B), 21.0(C), 29.9(D), 39.4(E), 49.5(F), 60.2°C(G).

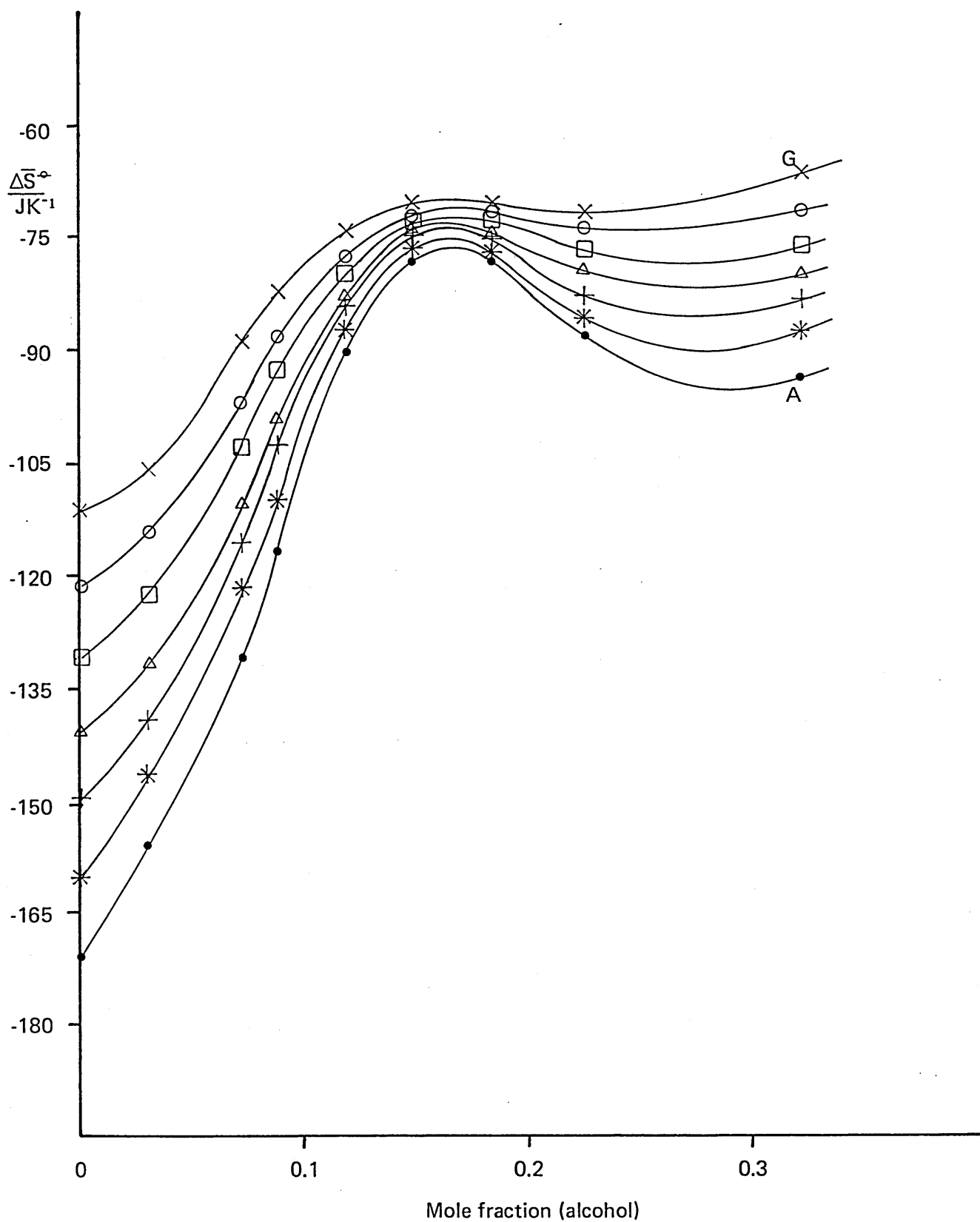


Figure 4.7.6 : $\Delta \bar{S}^\circ$ isotherms for the solubility of propene in mixtures of water and ethanol.
 Temperatures: 4.7(A), 12.6(B), 21.0(C), 29.9(D), 39.4(E), 49.5(F), 60.2°C(G)

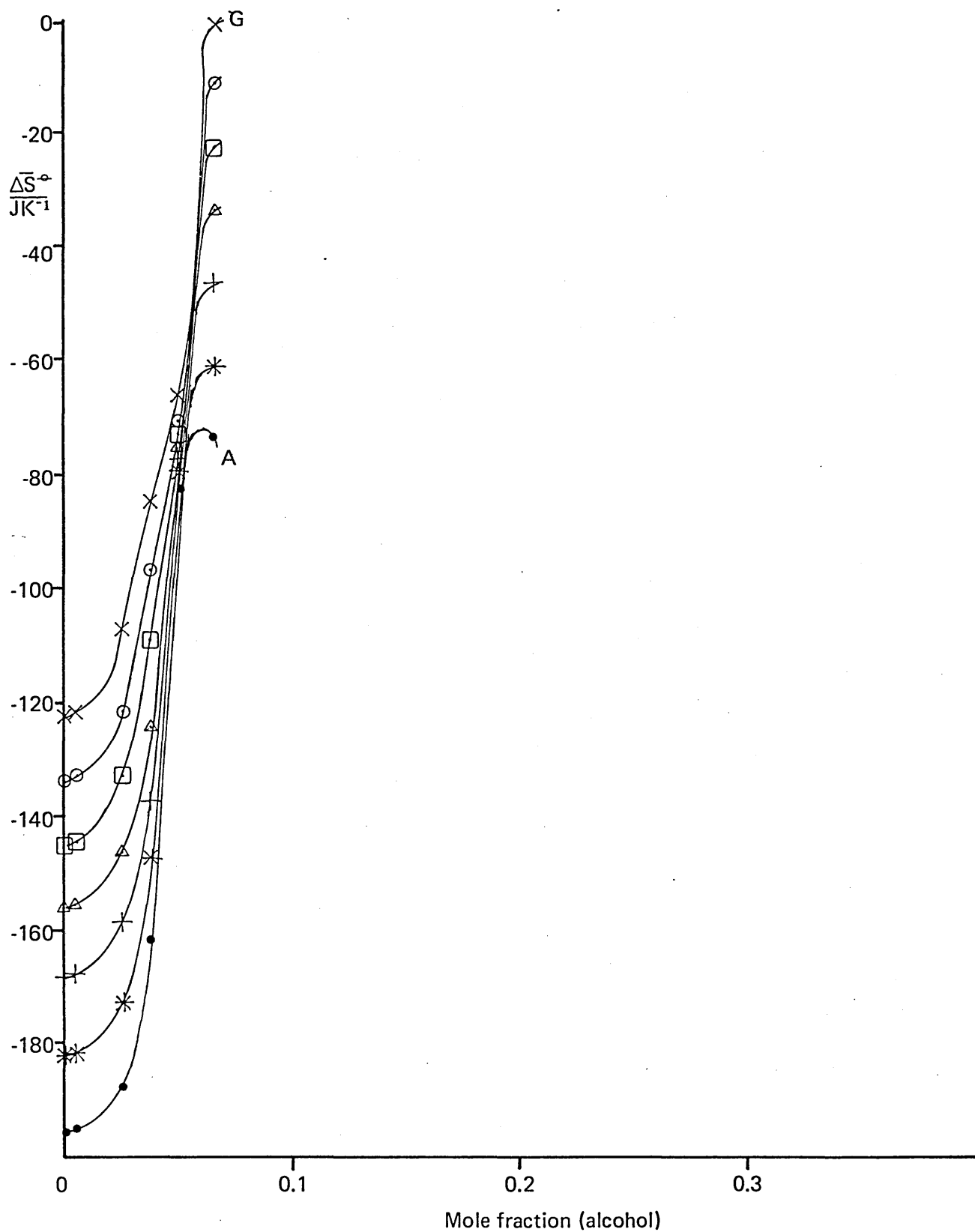


Figure 4.7.7 : $\Delta \bar{S}^\circ$ isotherms for the solubility of propane in mixtures of water and 2-methylpropan-2-ol.

Temperatures: 4.7(A), 12.6(B), 21.0(C), 29.9(D), 39.4(E), 49.5(F), 60.2°C(G)

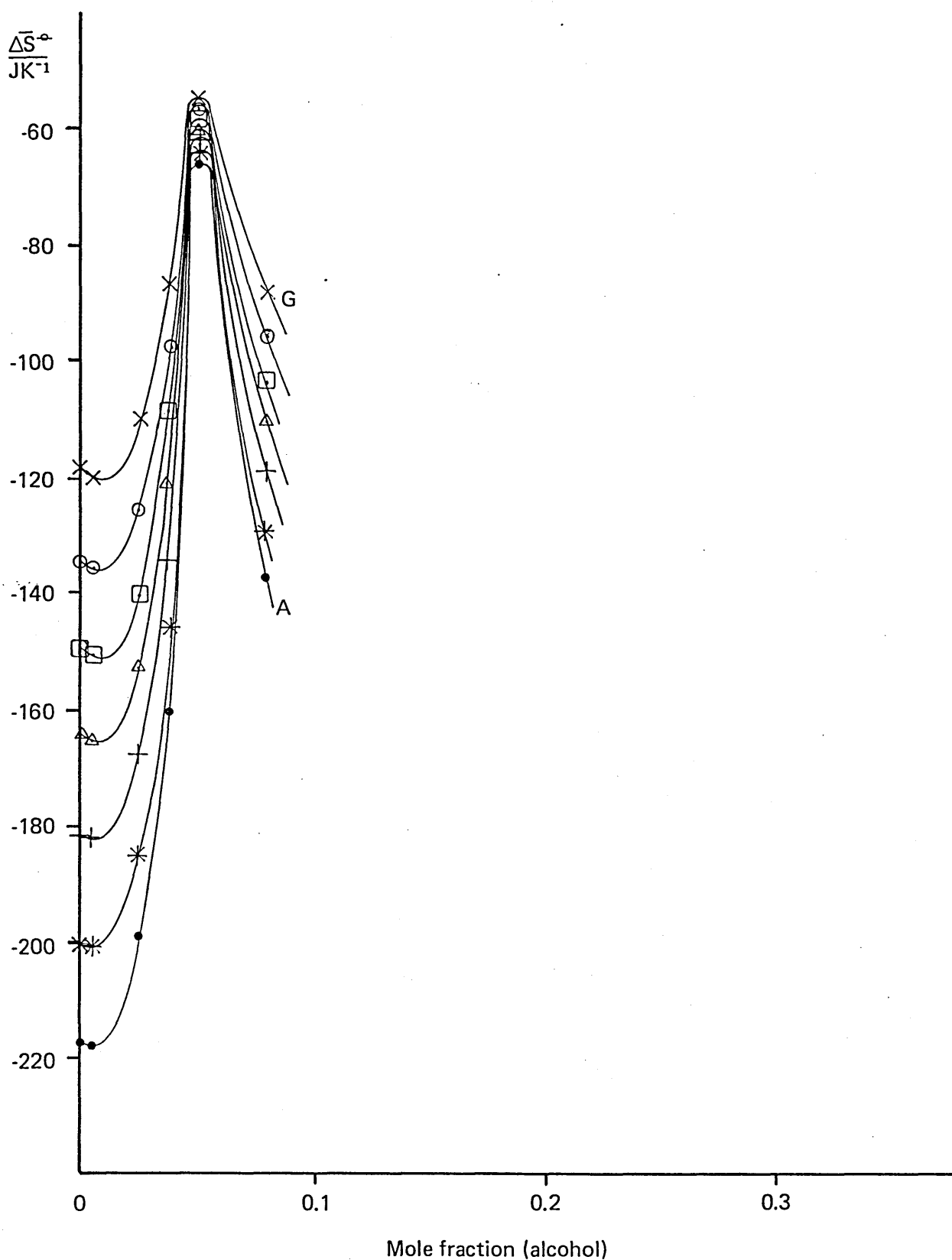


Figure 4.7.8: ΔS° isotherms for the solubility of butane in mixtures of water and 2-methylpropan-2-ol.

Temperatures: 4.7(A), 12.6(B), 21.0(C), 29.9(D), 39.4(E), 49.5(F), 60.2°C(G)

5. OBSERVATIONS

5. OBSERVATIONS

In this chapter, a detailed examination is made of the results presented in Chapter 4. The effect of a solute on the structure of the solvent is reflected in the variation of the thermodynamic functions $\Delta\bar{G}^\circ$, $\Delta\bar{H}^\circ$ and $\Delta\bar{S}^\circ$ of solution and it is important when examining these, plotted against solvent composition, to observe predominant graphical features which may represent positions of structural rearrangements in the solution.

The most profitable approach to an examination of this kind is to draw comparisons between the solubility characteristics of each of the gases in the water-alcohol mixtures and also between the effects of the co-solvents, ethanol and 2-methylpropan-2-ol on solubility.

To begin with, a general inspection of all of the graphs is carried out seeking trends or similarities when comparing each of the gas-solvent systems. Next, attention is directed towards the isotherms of $\Delta\bar{H}^\circ$ and $\Delta\bar{S}^\circ$. These functions are closely related to structural effects in the solution, describing changes in the extent of hydrogen bonding and of structural order respectively caused by the introduction of gaseous solute molecules into the solution phase. From the isotherms of these functions, it is possible to make direct observations of structural changes in the solution as the alcohol concentration is increased.

5.1 General Observations

An extensive examination of all of the graphs presented in Chapter 4 shows that the variation in a given function with solvent composition is remarkably similar when comparing the solutes with each other. Taking the solubility isotherms as an example, we can observe in each case, the shape which now seems to be characteristic to this type of measurement^{3,22,27,28}.

As the alcohol mole fraction in the solvent is increased from zero, the solubility of all of the gases is seen to increase at all experimental temperatures. At low temperatures, this increase is usually more obvious because in most cases, maxima become apparent. As the alcohol concentration is further increased, these maxima give way to minima after which the isotherms are seen to rise smoothly to values representing the corresponding solubilities in alcohol-rich solvents.

The extent of these observed graphical extrema is diminished by increasing temperature and they are eventually replaced by points of inflection at the higher temperatures. However, at higher alcohol concentrations, these high temperature isotherms adopt the characteristics shown by the low temperature ones, rising smoothly as the alcohol concentration is increased. These observations are valid for all of the gas-water-alcohol systems studied here and

elsewhere^{3,22,27,28} but an additional feature noted in some of the isotherms presented here is their crossing-over at alcohol mole fractions beyond the region in which extrema are displayed. Here, the solubility is highest at high temperatures whereas in water, the maximum solubility is observed at low temperatures. However, as alcohol concentration continues to rise, this cross-over is reversed and the isotherms continue to rise smoothly over the remaining experimental range, and the highest solubility is again at lowest temperature.

Measurements of the solubility of 2,2-dimethylpropane at temperatures in the region of 5°C were not possible in this investigation because this gas liquefies at 9.5°C and since the experiments were conducted for two gases simultaneously, the temperature range covered for the solute 2-methylpropane was restricted also. The resulting absence of the 4.7°C isotherm therefore prevents study of extrema for these gases since none exist at higher temperatures.

The isotherms of solubility though are very informative in an experimental sense since the continuity of these justifies the choice of suitable solubility curves (see Chapter 3). The solubility is also closely related to $\Delta\bar{G}^\circ$ through the expression $\Delta\bar{G}^\circ = -RT \ln s_0$ and because of this, the isotherms of this thermodynamic function are also closely similar (although inverted with respect to those for

solubility) when comparing each of the gases.

Thermodynamically, $\Delta\bar{G}^\circ$ describes the degree of ease with which a gas enters the solvent environment. It is derived from the more fundamental functions $\Delta\bar{H}^\circ$ and $\Delta\bar{S}^\circ$. These are of particular importance in a structural study of this kind because they relate to changes in the degree of association and organisation in the solvent caused by the introduction of the solute. Because of their importance in this investigation, these functions and their variation with solvent composition will be discussed in some detail in the following section.

The range of solubilities covered in this study was considerable ($\sim 10 \text{ cm}^3 \text{ kg}^{-1}$ to $\sim 10,000 \text{ cm}^3 \text{ kg}^{-1}$) and in all cases, it was beyond the capability of the apparatus to measure accurately the high solubilities of the gases in solvents with alcohol mole fractions beyond 0.4. In water, the solubilities were low but for a given solvent system, the rate of increase in solubility with increasing alcohol concentration was different for each of the gases studied.

From the solubility isotherms, it can be seen that in water-rich solvents, some gases are more soluble than others but less soluble in alcohol-rich solvents. This means that for a given alcohol, the steepness of the isotherms in the intermediate range of solvent composition

varies with the choice of solute although the magnitudes of solubility are approximately in the same range in all cases. This appears to be due to the suitability of the gas for the solvent. The more soluble it is in water, the less soluble it is in alcohol-rich solvents and vice-versa.

The graphical extrema displayed by these isotherms vary in size for each of the gases studied but all appear to be situated at approximately the same solvent composition for a given alcohol. This observation is best illustrated in Table 5.1.1 where the positions of graphical maxima and minima are tabulated with respect to solvent composition expressed as mole fraction of alcohol.

Table 5.1.1 Positions of graphical extrema on solubility isotherms for some gaseous hydrocarbons as solutes in mixtures of water and ethanol.

Solute	Positions of Maxima		Positions of Minima	
	4.7°C	12.6°C	4.7°C	12.6°C
propane	0.044	0.052	0.094	0.09
butane	0.052	-	0.096	-
2-methylpropane	-	-	-	-
2,2-dimethylpropane	-	-	-	-
cyclopropane	0.035	-	0.09	-
propene	0.035	0.05	0.09	0.085

It is clear from Table 5.1.1 that for a given alcohol, the position of graphical extrema is fairly constant for each of the different gas-solvent systems and it therefore seems that the gas plays very little part in defining these positions.

On the other hand, the effect on these positions of changing the alcohol component is quite dramatic. Table 5.1.2 shows this effect in a comparison of the solubility characteristics for propane and butane between the solvents aqueous ethanol and aqueous 2-methylpropan-2-ol.

Table 5.1.2 Positions of graphical extrema on the solubility isotherms for propane and butane in both aqueous ethanol and aqueous 2-methylpropan-2-ol solvents.

Solvent	Solute	Positions of Maxima		Positions of Minima	
		4.7 °C	12.6 °C	4.7 °C	12.6 °C
water + ethanol	propane	0.044	0.052	0.094	0.09
	butane	0.052	-	0.096	-
water + 2-methylpropan-2-ol	propane	0.022	0.02	0.05	0.042
	butane	0.016	0.018	0.05	0.036

Here also it is seen that the positions, with respect to alcohol mole fraction, are closely similar when comparing the two gases, propane and butane, as solutes in the water + 2-methylpropan-2-ol solvent.

However, more spectacular is the change in position of the extrema due to the different alcohols. This observation was pointed out before³ and it was then shown that, for a given gas, each of the three alcohols, methanol, ethanol and 2-methylpropan-2-ol, were responsible for altering the horizontal positions of graphical extrema by differing extents, effectively compressing the isotherms towards the water rich region as the complexity of the alkyl group on the alcohol increased.

It was felt that this dependence of position on the alcohol component may only be observed because of the way in which solvent composition was expressed. To test this, the results for propane and butane were plotted against volume fraction of the solvents, aqueous ethanol and aqueous 2-methylpropan-2-ol. The resulting isotherms were less different horizontally but the displacement was still apparent for both the propane and the butane sets.

These observations can also be made for the $\Delta\bar{G}^{\circ}$ isotherms and in some cases, these are preferred because they are much more relaxed in character. For this reason, it was decided to attempt curve-fitting in order to examine the possibility of relating the mole fraction of alcohol x_c , by a numerical method, to $\Delta\bar{G}^{\circ}$. This

was only conducted for the systems propane-water-ethanol and butane-water-ethanol where it was found that the isotherms were best described by a fifth order Chebyshev polynomial. Mathematically, this type of polynomial can be truncated with minimal error but when this was attempted for a third order common polynomial (or less), the results were unsatisfactory. However, the Chebyshev polynomial was converted to a fifth order common polynomial of the form

$$\Delta\bar{G}/T = A + B\bar{x}_c + C\bar{x}_c^2 + D\bar{x}_c^3 + E\bar{x}_c^4 + F\bar{x}_c^5$$

and the coefficients are tabulated below for the two systems.

Table 5.1.3 Coefficients for the fifth order polynomial which fits the isotherms of $\Delta\bar{G}^\circ$ for the propane-water-ethanol and the butane-water-ethanol systems.

Propane-water-ethanol

$1/T \times 10^4$	A	B	C	D	E	F
36	0.071	-0.031	-0.008	0.037	0.003	-0.022
35	0.071	-0.030	-0.003	0.032	0.000	-0.018
34	0.071	-0.028	0.001	0.026	-0.002	-0.015
33	0.071	-0.027	0.004	0.022	-0.004	-0.012
32	0.071	-0.026	0.008	0.018	-0.005	-0.01
31	0.071	-0.025	0.010	0.013	-0.007	-0.007
30	0.071	-0.024	0.012	0.009	-0.008	-0.004

Table 5.1.3 (Contd)
Butane-water-ethanol

1/T x 10 ⁴	A	B	C	D	E	F
36	0.066	-0.041	-0.008	0.045	0.003	-0.025
35	0.067	-0.039	-0.002	0.039	0.000	-0.022
34	0.067	-0.036	0.004	0.033	-0.003	-0.019
33	0.067	-0.034	0.008	0.028	-0.006	-0.015
32	0.067	-0.032	0.012	0.021	-0.008	-0.011
31	0.067	-0.031	0.015	0.016	-0.010	-0.007
30	0.067	-0.029	0.018	0.100	-0.011	-0.003

It is important to note that the polynomial is expressed for the arithmetic argument of alcohol mole fraction \bar{x}_c , which is given by the formula

$$\bar{x}_c = \frac{2x_c - (x_{c_{\max}} + x_{c_{\min}})}{(x_{c_{\max}} - x_{c_{\min}})}$$

For this solvent system, this equation can be reduced to

$$\bar{x}_c = (x_c/0.198) - 1$$

where x_c is the experimental alcohol mole fraction.

One final note to make in this section concerns the extent of the graphical extrema on both $\log s_o$ and $\Delta\bar{G}^\circ$ isotherms. The presence of these suggests structural effects, the extent of which are temperature dependant and also dependant on the solute. In Table 5.1.4, the sizes

of these extrema are tabulated along with temperature for each gas, this data obtained from the solubility isotherms.

Table 5.1.4 Extent of graphical extrema measured on the solubility isotherms for the selected solute-solvent systems.

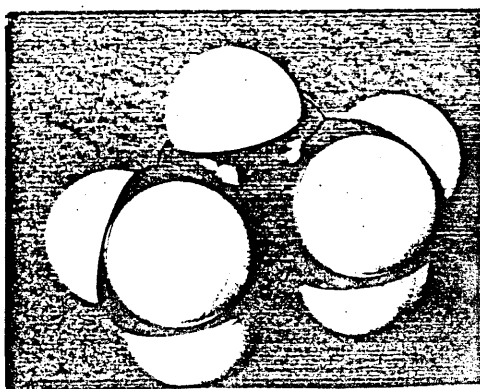
Solvent	Solute	<u>Size of Maxima</u> <u>log(cm³kg⁻¹)</u>	
		4.7 °C	12.6 °C
water and ethanol	propane	0.5	0.3
	butane	0.4	-
	2-methyl- propane	-	-
	2,2-dimethyl- propane	-	-
	cyclopropane	0.3	-
	propene	0.2	0.1
water and 2-methyl propan-2-ol	propane	0.6	0.4
	butane	0.6	0.4

The sizes of these maxima are clearly dependant on temperature and also, it seems, on the alcohol component. Arnett³⁴ refers to 2-methylpropan-2-ol as a favourable alcohol component because it exaggerates the extrema and also, as we have noted here, reduces the amount of alcohol required to produce them.

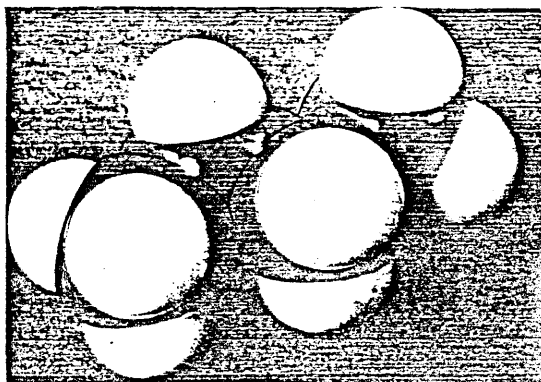
However, the values tabulated in Table 5.1.3 are only estimated from isotherms constructed largely by 'free-hand' drawing and although they represent the solubility characteristics of each of the gases with solvent composition reasonably accurately, it is unwise to place too much emphasis on the accuracy of these tabulated values. Nevertheless it can be seen that the nature of the gas governs the extent of the maxima at both 4.7 and 12.6 °C. They are reduced in size as the complexity of the solute molecules is increased.

5.2 $\Delta \bar{H}^\circ$ and $\Delta \bar{S}^\circ$ Isotherms

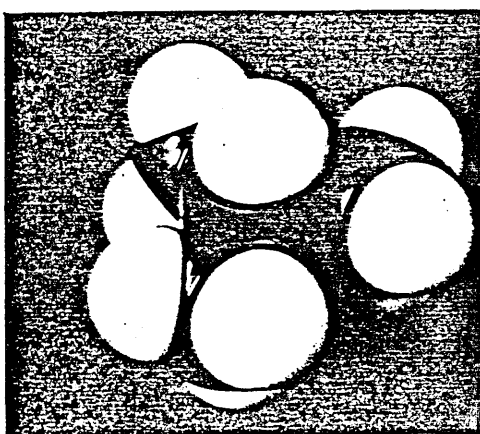
As stated in the previous section, the functions $\Delta \bar{H}^\circ$ and $\Delta \bar{S}^\circ$ describe the immediate consequences of introducing a solute molecule into the aqueous environment. $\Delta \bar{H}^\circ$ conveys information about changes in the degree of hydrogen bonding whilst $\Delta \bar{S}^\circ$ relates to changes in structural order in the solvent. Each of the gas molecules is of different size and shape and, along with the type of interaction between these solutes and water, this must control the ability of the gas to enter the liquid. Figure 5.2.1 shows a scaled representation of each of the solute molecules indicating the type of space which each might require in the solvent.



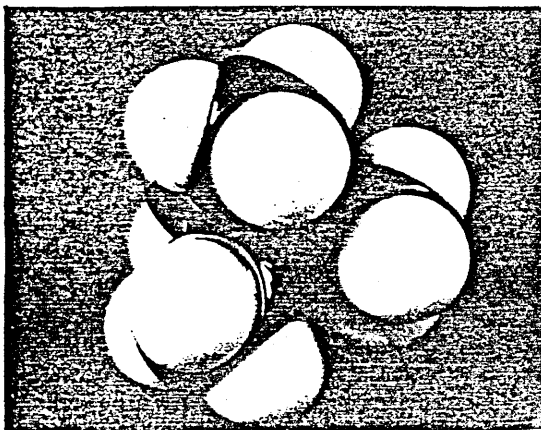
propane



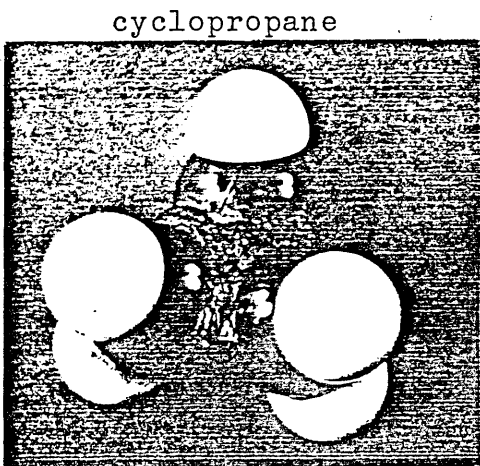
butane



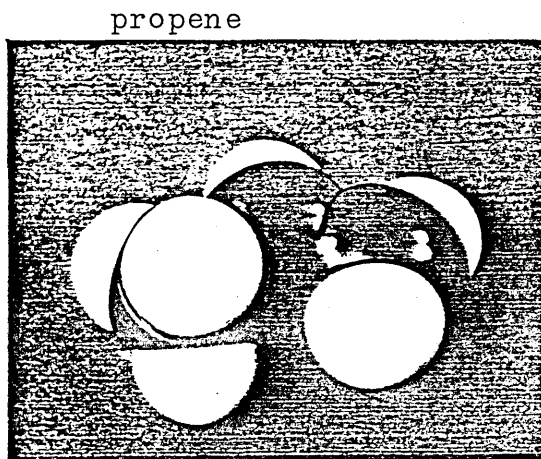
2-methylpropane



2,2-dimethylpropane



cyclopropane



propene

Figure 5.2.1: Models depicting the size and shape of the solute molecules. Each is scaled with respect to the others, the van der Waals' radii of both the methyl and methylene groups representing a distance of 20 nm⁷⁵.

From the above figure, the following observations can be made. Propane and butane, the 'straight chain' hydrocarbons, exist as puckered chains and both have cylindrical dimensions. The branched molecules, 2-methylpropane and 2,2-dimethylpropane are much more bulky and now take on a spherical appearance. Propene is very similar to propane in size and shape while the strained cyclopropane ring 'looks' like a short squat cylinder. All of these molecules repel water because they are hydrophobic. The way in which the solvent molecules rearrange themselves around the solute is therefore not simply a matter of filling available space but is governed by the orientational forces which exist strongly in aqueous solutions. These are reflected in the values of $\Delta\bar{H}^\circ$ and $\Delta\bar{S}^\circ$ and this is why these functions are so important in the elucidation of the liquid structure.

Examination of the isotherms of these functions permits comparisons to be drawn between the structural effects imposed by each of the gases as they enter the solvent and by inspecting each of them, it is possible to see how the increasing alcohol concentration affects the way in which the solvent molecules envelop the solutes.

Due to the close similarity in the appearance of the functions $\Delta\bar{H}^\circ$ and $\Delta\bar{S}^\circ$ for a given gas-solvent system, it is possible to discuss both sets of isotherms together.

It is perhaps surprising that the general appearance of these graphs is also reflected throughout the range of systems studied, where again the effect of the alcohol is noticed only to alter the positions of graphical features with respect to the solvent composition.

In all cases, the variation of the functions with increasing alcohol concentration is the same. Considering the $\Delta\bar{H}^\circ$ set, it is seen that the value of this function increases rapidly at low temperatures, up to an alcohol mole fraction of 0.15-0.18 for ethanol and 0.05 for 2-methylpropan-2-ol, where an obvious deflection is observed. At higher temperatures, this initial rise is less steep and indeed in some cases, the value of $\Delta\bar{H}^\circ$ actually decreases upon addition of the alcohol to water, producing minima. However at all temperatures, the isotherms approach the point of deflection in a smooth and increasing manner as the alcohol concentration is increased.

(These minima, or curvatures which are often present at high temperatures, are thought to be related to the hydrophobic effect and the range of $\Delta\bar{H}^\circ$ for the pure water solvent over the temperature range seems expanded for this reason. These features will therefore be discussed later in this section.)

The nature of the 'deflection', mentioned above, is always displayed as maxima for this function, $\Delta \bar{H}^\circ$. Until now, all of the features discussed above were also true of the $\Delta \bar{S}^\circ$ isotherms, but this is where the first difference arises. In the case of cyclopropane (Fig 4.7.5), the maxima on the $\Delta \bar{H}^\circ$ isotherms are replaced by points of inflection for $\Delta \bar{S}^\circ$ at temperatures above 39.4 °C. This is due to the continuing increase in this function at high temperatures and at alcohol mole fractions above the 'deflection point'. In this region, all similarities between $\Delta \bar{H}^\circ$ and $\Delta \bar{S}^\circ$ are lost and now deviations are observed from the linear plot of $\Delta \bar{H}^\circ$ against $\Delta \bar{S}^\circ$ obtained for alcohol concentrations below the deflection.

Returning to the minima and curvatures observed at high temperatures, it is seen that these exist in all cases except for the two branched hydrocarbons, 2-methylpropane and 2,2-dimethylpropane. In fact an examination of $\Delta \bar{H}^\circ$ isotherms for the work on carbon dioxide²², oxygen²⁷, hydrogen²⁸, helium²⁸, and argon³ shows none of these characteristics either at these temperatures. Definite minima only occur for propane and butane in aqueous ethanol and for butane in aqueous 2-methylpropan-2-ol while for the other cases studied here, prominent curvatures are observed. The effect diminishes with decreasing temperature and as the size of the solute molecule increases, i.e. a deeper minimum is observed for butane

than for propane. It is difficult to tabulate evidence for this phenomenon but Table 5.2.1 attempts to convey the required information where the presence or absence of these curvatures is indicated.

Table 5.2.1: Tabulated Data showing depth in kJ of minima (where present) and the presence (+) or absence of curvature on the $\Delta\bar{H}^\circ$ isotherms.

Solvent: water and ethanol

Solute	4.7°C	12.6°C	21°C	29.9°C	39.4°C	49.5°C	60.2°C
propane				0.1	0.4	1.0	1.8
butane				0.3	1.2	2.8	5.1
2-methylpropane							
2,2-dimethylpropane							
cyclopropane							+
propene				+	+	+	+

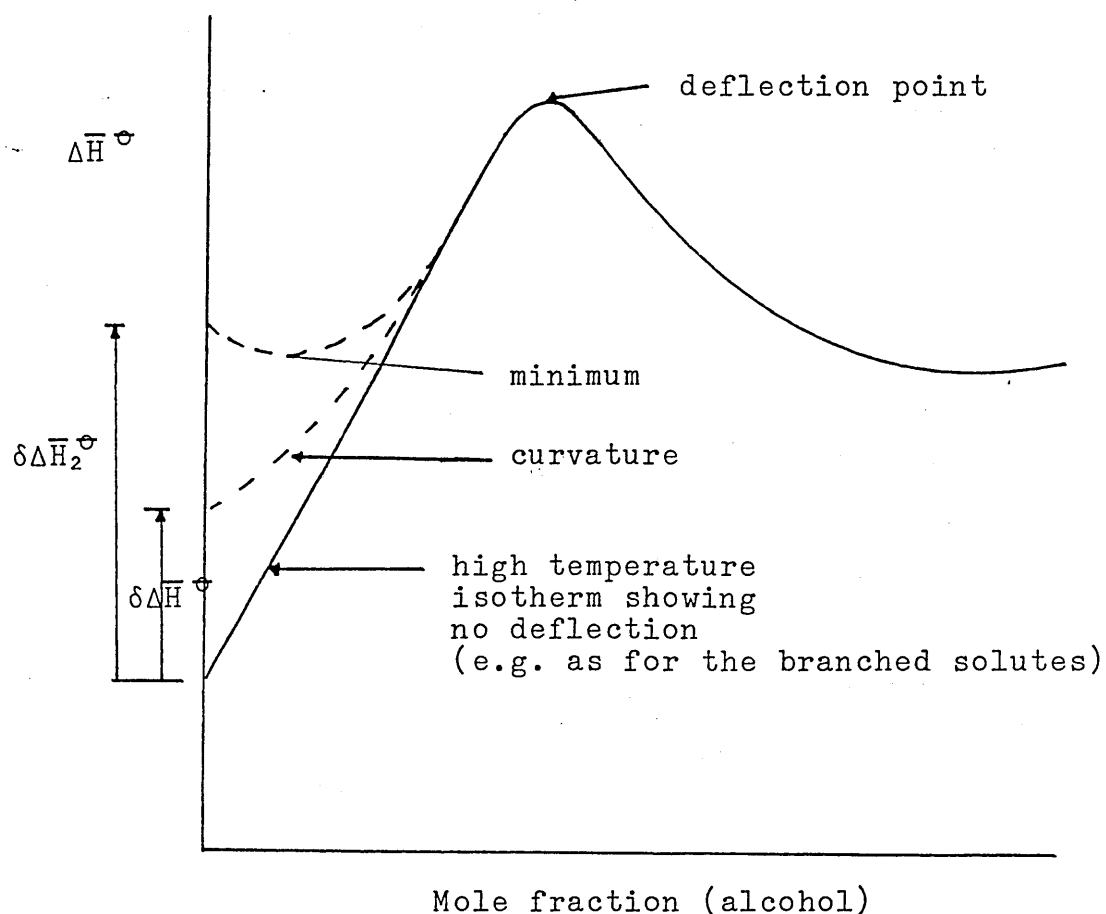
Solvent: water and 2-methylpropan-2-ol

Solute	4.7°C	12.6°C	21°C	29.9°C	39.9°C	49.5°C	60.2°C
propane	+	+	+	+	+	+	+
butane	0.2	0.4	0.4	0.4	1.2	1.4	1.6

This effect seems to be absent for the two branched hydrocarbon solutes and so it is perhaps worthwhile comparing, more closely, the isotherms of these gases

with those of the others. Graphically, the effect of these curvatures is to divert the isotherm concerned to higher values of $\Delta\bar{H}^\circ$ or $\Delta\bar{S}^\circ$ in the water-rich region of the graphs. The greater the curvature, the higher becomes the value of $\Delta\bar{H}^\circ$ in water for a given gas and where minima are present, the deviation is considerable. This observation is best described on Figure 5.2.2.

Figure 5.2.2 The effect of curvature or minima on the isotherms of $\Delta\bar{H}^\circ$.



For a smooth curvature on the isotherm at low alcohol concentrations, the value of $\Delta\bar{H}^\circ$ for the pure water solvent is elevated by the amount $\delta\Delta\bar{H}_1^\circ$. Where minima are present, this increase is represented by the larger quantity $\delta\Delta\bar{H}_2^\circ$. Also observed, is the effect of these features on the values of $\Delta\bar{H}^\circ$ as the alcohol mole fraction in the solvent is increased from zero. The quantities $\delta\Delta\bar{H}_1^\circ$ and $\delta\Delta\bar{H}_2^\circ$ are seen to decrease as alcohol concentration increases suggesting that this effect is diminished by the presence of alcohol molecules, leading to structural rearrangements.

It is also clear from Table 5.2.1 that this effect is dependant on the nature of the gas. Comparison of these results with those for the solution of oxygen²⁷, argon³, hydrogen²⁸, helium²⁸, and carbon dioxide²² in aqueous alcohols shows that minima and curvatures are only apparent for the hydrocarbon solutes. The hydrocarbons are hydrophobic whereas the other gases are not and it is therefore suggested that these minima, and curvatures, are due to hydrophobic interactions in the water-alcohol solvents.

To support this suggestion it is necessary to investigate the possible molecular rearrangements in the solvent, and their effects on the values of $\Delta\bar{H}^\circ$ and $\Delta\bar{S}^\circ$. Section 6 discusses the development of models for water structure

and also of hydrophobicity in solute-solvent systems and this theoretical approach may explain the observed variation in $\Delta\bar{H}^\circ$ and $\Delta\bar{S}^\circ$ with temperature and with solvent composition. It is also expected that the size of $\delta\Delta\bar{H}^\circ$ and $\delta\Delta\bar{S}^\circ$ will be associated with the strength of intermolecular hydrophobic interactions by relating the popular molecular interpretation of these interactions to the observed experimental results.

6. STRUCTURAL THEORIES OF WATER

6. STRUCTURAL THEORIES OF WATER

6.1 The Need for a Model

In order to describe a substance fully at the molecular level, it is necessary to have as much information as possible about the physical properties of the substance. These are known from macroscopic measurements but they are a direct consequence of molecular size, shape and interactions and it is these quantities which are required for the development of a structural model. The real value of the model, provided it is an accurate one, is to allow predictions of further properties of the substance to be made for varying experimental conditions.

The ease with which successful models are arrived at depends of course on the complexity of the substance concerned. Considering the three states of matter, it is clear that the solid state is the one which can be most easily described structurally. In metals for example, atoms are arranged in a lattice and except for occasional defects due to vacancies and interstitial atoms, a high degree of order exists throughout the entire crystal. Most crystalline solids exhibit this type of 'structuredness' and order generally persists over very many interatomic separations.

The opposite extreme describes the gas phase, where molecules or atoms are allowed to rotate, vibrate and translate

with minimum restriction. This results in a high degree of disorder and it is unlikely that any form of long range order exists at all. Some interactions do occur in the gas phase which account for deviations from the theoretical ideal gas. The equation of state given by van der Waals attempts to allow for such interactions when describing the P-V-T characteristics of a real gas.

The liquid state shows varying degrees of complexity. Molecules are much closer to each other than they would be in the gas phase and are also much more restricted. They still, however, retain some freedom and can translate, vibrate and rotate (or librate³⁵) to some extent.

In many cases, a liquid can be described as a mobile solid where the atoms or molecules occupy sites similar to those they might occupy in the solid phase. If however, electrostatic interactions occur, this simple picture disappears and molecular association results. When now the molecules contain hydrogen and electronegative elements or groups, hydrogen bonding can occur and to this has been attributed the anomalously high boiling points and enthalpies of vapourisation of water and hydrogen fluoride when compared with the other Group VI and Group VII hydrides respectively. So this is where the difficulties arise in creating a model, especially for water. This common liquid exhibits many other

peculiar properties such as a maximum density at 277 K, a low density in general (cf 1.84 g cm⁻³ for close packed water molecules³⁶), a minimum in the isothermal compressibility; ($K_T = -\frac{1}{V} \left(\frac{\partial V}{\partial P} \right)_T$), a high dielectric constant, a high specific heat capacity and an initial viscosity reduction upon pressurisation.

It is widely accepted that hydrogen bonding is responsible for many, if not all, of these peculiarities but the extent and nature of these bonds has provoked some controversy. In the development of a model for liquid water, conflicting ideas have led to the emergence of two major theories. These are discussed in the next section along with a more recent computer assisted approach to the problem.

6.2 Models for the Structure of Liquid Water

In 1933, Bernal and Fowler³⁶ postulated a three structures model for water and this survived until 1951 when Pople³⁷ proposed his continuum theory. More recently, further developments in the mixture of structures approach have succeeded in placing the two models in competition. Both can account for some different characteristics of water under certain circumstances but lack explanations in other areas. It is likely that the real structure of liquid water lies somewhere between the

two models and this seems to be the conclusion drawn from the band theory for water structure.

Computer simulation studies have now almost replaced the classical approaches to structure elucidation and a description of these along with the mixture and continuum models is now given.

6.2.1 Mixture Models

6.2.1.1 'Mixture of Structures' model (1933)

This is the model of Bernal and Fowler³⁶ who visualised water as consisting of three types of structure each predominating over different temperature ranges. In an attempt to explain water's maximum density characteristics they assumed that at temperatures below 277 K, water had an ice-tridymite-like structure. This structure is an open one corresponding to a liquid of low density.

Above 277 K, and persisting up to 473 K, a quartz-like structure was envisaged and after this, above 473 K, the close packed ammonia-like structure was proposed. The transitions between structures was considered to be gradual with both types existing together at and around the transition temperatures.

As temperature increased towards 277 K, the ice-tridymite-structure becomes influenced more and more by the denser quartz-like structure consequently increasing the density of the liquid. Above 277 K, normal expansion effects increase the volume and the density begins to decrease with temperature.

6.2.1.2 'Mixture of States' Model (1962)³⁸

This model by Nemethy and Scheraga³⁸ was based on the theory of hydrogen bonding proposed by Frank and Wen³⁹. It virtually replaced Bernal and Fowler's model but retained the idea of organised structure in water. Based on a tetrahedral arrangement of the oxygen atoms, each water molecule was bound by linear hydrogen bonds forming clusters, the size of which was said to be strongly temperature dependent. In a later estimate by Hagler, Scheraga and Nemethy⁴⁰, the suggested cluster size of 273 K was put at 11.2 water molecules, this number decreasing with temperature to 5.6 at 333 K.

The lifetime of such clusters was short due to the continual 'melting' and 'freezing' processes within them and was typically of the order of 10^{-11} s. (based on dielectric relaxation time measurements)⁴¹. This making and breaking of hydrogen bonds resulted in an equilibrium^{42, 43} being established between unbonded and bound water molecules

and the term 'flickering cluster' was used to describe the process.

The extent of hydrogen bonding was investigated and used in an attempt to calculate the physical and thermodynamic properties of water. The number of hydrogen bonds per water molecule in a cluster ranges from a maximum of four, corresponding to the situation in ice, down to one. The case where this number is zero describes monomeric water which can exist within the confines of a cluster as well as in the bulk. Thus five different states of bonding were envisaged for water, each with their own characteristic energy. This was clearly a function of the hydrogen bond energy although the assumption of equal spacing between the energy levels for each state may have been a serious oversimplification⁴⁴. However, the theory did account for the possibility of an unbonded water molecule being encapsulated within a water cluster, and allowed for the van der Waals interaction between it and its surrounding cavity wall.

By adopting an appropriate heat cycle, Nemethy and Scheraga related the energy of a hydrogen bond to interaction parameters, enabling certain thermodynamic and physical parameters to be calculated for water. Some agreement was obtained with experimental data in a description of the temperature dependence for A , the Helmholtz free energy, U ,

the internal energy and S , the entropy although the calculation for C_p was less satisfactory. The calculations were based only on empirical assumptions but the results were encouraging and for this reason, the theory was to play an important role in further developments of models for the structure of aqueous solutions.

In a later paper⁴⁰, Hagler, Scheraga and Nemethy reported the calculated distribution of cluster size as a function of temperature. The results show that the number of water molecules in a cluster decreases with increasing temperature whilst the concentration of small clusters increases. The distribution also shows the presence of monomeric water at all temperatures up to a concentration of $\approx 3\%$ but Conway⁴⁴ suggests that this is likely to be less than 1% .

6.2.1.3 'Mixture of Structures' Model (1965)

A final example of mixture models given here is that of Davis and Litovitz⁴⁵. As temperature increases from the melting point, order in water begins to diminish and hydrogen bonds are broken. This model views each water molecule in the liquid state as being hydrogen bonded to only two others in a near body centred cubic structure with only 18% of the hydrogen bonds being broken on melting. This is regarded structurally as consisting

of six-membered puckered rings which situate themselves above and below each other in the liquid.

Two types of this stacking structure are proposed. The first resembles the open ice structure where the rings are situated "point to point" and held together by varying degrees of hydrogen bonding. In the second type, the rings are "rotated" slightly with respect to each other so that one ring "fits" onto the other in a close packing configuration reducing the distance between nearest water neighbours. Thus an attempt was made to explain the form of the radial distribution function which indicated the presence of a significant proportion of molecules at distances intermediate between first and second nearest neighbours in an ice structure. The calculation of this radial distribution function up to 450pm gave good agreement with experiment as did values of the relaxational components of compressability, expansibility and specific heat.

6.2.2 The Continuum Model³⁷

In contrast to Némethy and Scheraga³⁸, Pople³⁷ considered for his model, the existence of non-linear hydrogen bonds in water. The structure of the liquid is described as consisting of water molecules bound by hydrogen bonds in which there is a continuous distribution of extents of bending. This is due to the various angles of orientation of lone pair orbitals with respect to O-H bonds.

From theoretical calculations, Pople suggested that the bond could be bent up to 25 or 30° from the linear O-H --- O direction and still represent an associative interaction. The extent of bending is dependant on temperature fluctuations within local regions of the liquid and this is proposed to account for many of the peculiar characteristics of liquid water. The concept of bent hydrogen bonds is found elsewhere as intramolecular bonds in salicylic acid and in solid hydrates⁴⁶ and this is considered to support the application of this theory to water.

Pople supposed that in ice all four hydrogen bonds would bend during thermal activity but would remain intact preserving the order of the lattice. On melting a very small percentage of bonds would break but more importantly, each remaining bond would now bend independently of the others in a less rigid structure corresponding to the disordered liquid state. Any broken hydrogen bonds would be considered as those which had exceeded the critical angle of bending.

Calculations based on the model for four successively bonded water molecules showed good agreement with the experimentally obtained radial distribution curve of Morgan and Warren⁴⁷ at high temperatures (83°C), but at low temperatures (1.5°C) the experimental data shows more sub-structure at about 370 pm. This was the feature which

the Davis and Litovitz⁴⁵ model attempted to explain using a close packed stack of hexagonal puckered rings. Here, Pople suggested that these results are due to a 'bending in' of water molecules into the void spaces of the open structure thus producing water molecules at distances corresponding to those intermediate between first and second nearest neighbours. This 'bending in' of water molecules was also used to explain the temperature of maximum density, above which normal temperature effects increased the volume.

6.2.3 The Band Model

This model of Vand and Senior⁴⁸ falls between those describing mixture and continuum theories because it has characteristic features of both models. The idea of energy bands has been introduced to replace the discrete levels proposed by Némethy and Scheraga³⁸ for their five states of bonding in water. Buijs and Choppin⁴⁹ could not support the existence of five different molecular species but found spectroscopic evidence of three, and suggested that these corresponded to water molecules with one OH group bonded, two OH groups bonded and no bound OH groups.

Vand and Senior⁴⁸ developed this idea but showed that the results of Buijs and Choppin⁴⁹ were not consistent with any thermodynamic model of liquid water based on

three molecular species, each associated with a sharp level of positive energy. Instead they proposed the idea of bands of energy to replace the discrete levels envisaged by Némethy and Scheraga³⁸ and applied this idea to give excellent agreement between theoretical and experimental quantities, including the specific heat of water, for which the Némethy and Scheraga model failed.

The association between this and the mixture models is clear but the relationship to the continuum model requires some explanation. Pople's model³⁷ is based on the ability of hydrogen bonds to bend from the linear OH -- O direction up to a maximum angle of 25 - 30°. This must correspond to a series of hydrogen bond energies each corresponding to different degrees of bending, thus forming an energy band as defined in the Vand and Senior explanation.

Merging features of both mixture and continuum models, as in this theory, can serve to advance our understanding of liquid water and indeed such agreement between experimental and calculated thermodynamic functions emphasises that this model probably represents the real structure of liquid water more closely than any other classical approach.

6.2.4 Molecular Dynamics Calculations

These types of calculations have almost replaced the classical approach to structure elucidation and modern computing techniques enable calculations of the interactions between many molecules to be made by considering static and kinetic behaviour. A knowledge of the molecular interactions with respect to molecular separation give some information about the relative positions and orientations of the molecules in the sample and this may be expressed in various forms in an attempt to positively identify its structure.

These types of calculations were applied to water by Stillinger and Rahman⁵⁰ who considered a "sample" of 216 rigid molecules with a total density of 1 g cm^{-3} . The pairwise molecular interaction was modified slightly from that of Ben-Naim and Stillinger⁵¹ and consisted of a "6-12" Lennard-Jones potential energy function and an electrostatic calculation based on a quadrupole of charges placed tetrahedrally, 100 pm from the centre of the O nucleus for the protons and 80 pm for the negative charges. Without this electrostatic term, the molecules would neglect any directional associative interaction and the full extent of hydrogen bonding would be ignored.

The calculations gave excellent agreement with the X-ray scattering intensities observed by Narten⁵² and therefore with the radial distribution function for water. The structural explanation from calculated pair-pair correlation functions shows⁵³ water to be a random, defective and highly strained network of hydrogen bonded molecules and shows no evidence of long range order in the liquid even at low temperatures. However, it should be noted that the predicted temperature of maximum density was calculated to be 27 °C⁵⁰ instead of the observed value of 4 °C and this was attributed to the use of classical rather than quantum mechanical calculations. For the same reason, a disagreement also exists between calculated and actual values of C_v , the specific heat at constant volume.

Hirata and Rossky⁵⁴ recently applied computer simulated study to the so called "V" structure for liquid water. Using an experimental sampling time of 0.2 ps for the basis of their calculations, an average over the translational and rotational vibrations was taken and this showed that basically the same hydrogen bonded network existed as was found for the instantaneous or "I" structure approach. However, the study produced no new evidence for the existence of a mixture of distinguishable molecular species in water.

The molecular dynamics techniques were also applied to describe the effect of a non-polar solute on the structure of water⁵⁵. The calculations supported existing models of hydrophobic hydration (see next section) deduced from spectroscopic and thermodynamic experimental observations. The inert solutes were supposed to be surrounded by water cages whose orientational structure was similar to clathrates. However, these water molecules in the hydration shell were said to retain almost all of their mobility and this is not the case in solid crystalline hydrates.

6.3 The Hydrophobic Interaction

For some time now, the characteristics of aqueous solutions have been examined with interest and it was probably Kauzmann⁵⁶ in 1959 who was first to suggest a solvent induced association of solutes in the liquid. He used the term "hydrophobic bonding" to describe the apparent aggregation of non-polar groups in aqueous environments and advanced the theory that the existence of these "bonds" explained the tendency for water to stabilise the folded configurations of protein structures. The immense research in biochemistry and physical chemistry which followed has, as yet however, failed to give a satisfactory account of this mysterious "hydrophobic interaction" and indeed the exact nature of the phenomenon is still largely a matter for discussion.*

**Faraday Symposium No.17: "The Hydrophobic Interaction"*
(December 1982)

This section is intended to give a brief description of presently accepted theories of hydrophobic interaction which is of particular relevance to the solution of hydrocarbons in aqueous alcohols.

The first attempts to quantify hydrophobicity on a molecular basis were those of Nemethy and Scheraga^{57, 58} who calculated the free energy associated with the approach to pairwise contact of two non-polar species in terms of certain postulated changes in the aqueous environment. Based on their structural model for water³⁸ (see Section 6.2), they showed that the net intermolecular energies of interaction for the solute with non-hydrogen bonded water molecules differ from those for the solute with water molecules which are hydrogen bonded into clusters. The differences are reflected in a change of the coordination number of the hydrogen bonded molecules in the region of the solute. The result is increased order and the formation of partially encapsulating "cages".

This is in agreement with the suggestions of Frank and Evans⁵⁹ who as early as 1945 had introduced the concept of "iceberg" formation around non-polar solutes and proposed that the high partial molar heat capacities were due to the "melting" of these local structures. Further support is gained from the existence of crystalline

gas hydrates. These consist of a network of hydrogen bonded water molecules arranged such that cavities of various sizes exist. Inclusion of a "guest" molecule of suitable dimensions in such a cavity stabilises this structure and it is a similar situation which is envisaged for the liquid phase. Here, water molecules are supposed to arrange themselves in a hydrogen bonded network around part of the non-polar solute, interacting with it only by van der Waals forces.

The 'cage' may be incomplete for several reasons:

- (a) in the case of large solute molecules, the formation of a complete cage may be sterically prevented;
- (b) in the dilute solution, no cooperative effect exists because the solutes are too far apart; and
- (c) due to local thermal fluctuations, the formation of even moderately sized cavities is unlikely.

However, these partial cages are considered to form from the interaction of the solute with an existing water cluster (see Figure 6.3.1). In the case of a large solute molecule, two or more clusters may be involved rather than a single cage extending around most of the solute surface. The cages, together with the clusters, of which they are part, are formed and melted through local energy fluctuations therefore the extent of cage

Figure 6.3.1 Schematic cross-section of a hydrogen-bonded water cluster near a hydrocarbon solute molecule, indicating the formation of a partial cage around the solute. The O-H---O hydrogen bonds are represented by broken lines. The heavy lines correspond to the surfaces defined by the van der Waals contact radii for the molecules involved. (from Nemethy and Scheraga - reference 57).

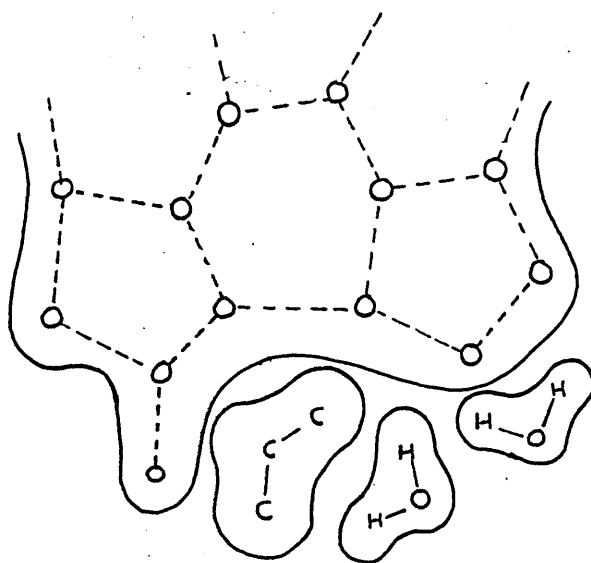
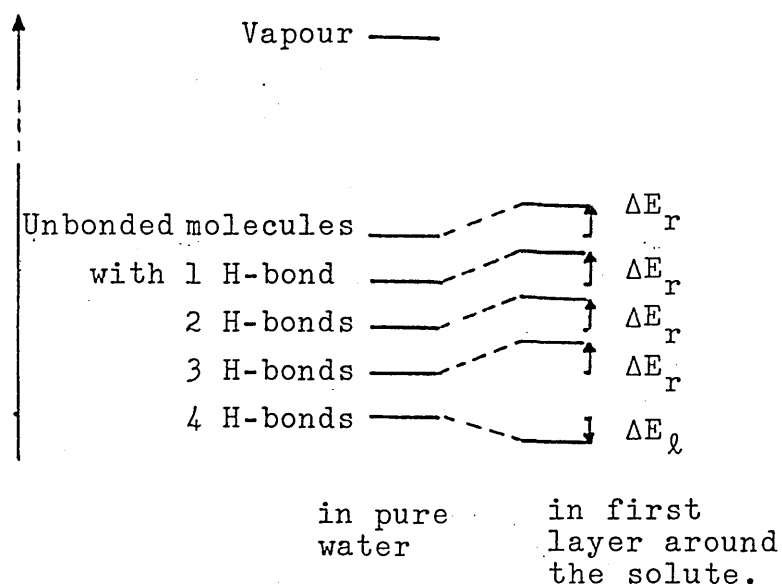


Figure 6.3.2 Schematic representation of the energy level changes occurring on transfer of water from the pure liquid to the structure next to a non-polar solute. These correspond to water molecules in the first layer around the solute only (from Nemethy and Scheraga - reference 57).



formation around the solutes is variable and even the number of clusters touching a given solute molecule changes.

The solute-water interactions are treated by Nemethy and Scheraga in terms of the energy levels they proposed for the five states of bonding in water. The effect on these energy levels is shown in Figure 6.3.2 where only the molecules in the water layer nearest to the solute are represented. The energy depression, ΔE_l , experienced by the water molecule with four hydrogen bonds, is a consequence of the van der Waals interaction between it and the solute. Water molecules in all other states of bonding experience an increase in energy ΔE_r corresponding to the difference between (a) the energy lost in decreasing the dipole interactions of the molecules with their neighbours when one of the neighbours is removed and (b) the energy gained from the interaction with the new hydrocarbon solute. These energy changes are related to the interaction energies E_{RW} (solute-water) and E_{dip} (water-water) through the following equations

$$\Delta E_l = \frac{1}{2}E_{RW}$$

and

$$\Delta E_r = \frac{1}{2}E_{RW} - E_{dip}$$

For aliphatic hydrocarbons, the values used were

$$\Delta E_{\ell} = -0.130 \text{ kJ mol}^{-1} \text{ and } \Delta E_r = 1.276 \text{ kJ mol}^{-1}.$$

This model of "hydrophobic hydration" was extended to cater for the introduction of proteins to water where the non-polar side chains on the protein are situated within a close distance of each other. It was considered that a "hydrophobic bond" was formed when two or more of these groups came into contact, thereby reducing the extent of interaction with the surrounding water. The existence of these "bonds" is mainly due to the entropy change connected with changes in the water structure around the side chains and the endothermicity of 'bond' formation makes them stronger with increasing temperature. The process is described as a partial reversal of solution but the magnitudes of the changes in thermodynamic parameters of "bond formation" must be less than those for solution because, in general, the side chains are not completely removed from the aqueous environment. The term 'hydrophobic bond' used by Kauzmann⁵⁶ and Nemethy and Scheraga^{57,58} is perhaps an unfortunate one as no bond as such exists between the non-polar species. The more precise term hydrophobic interaction, describes an effect induced by the nature of the solvent where the interaction between two (or more) solute molecules is preferred to that between the solute and water.

Ben-Naim⁶⁰ used a statistical mechanical approach to define the hydrophobic interaction. He postulated that the work required to bring two simple solute molecules together in a solvent is the sum of three terms. The first of these depends only on the properties of the solvent molecules, the second on the pairwise interaction between the solute molecules and the third on both solvent-solvent and solvent-solute interactions. He⁷ and co-worker also attempted to calculate the indirect part of the free energy of solution associated with the bringing of two non-polar solutes from infinite separation in an aqueous solvent to within a close distance of each other. The energy cycle depicted in Figure 6.3.3 describes the process involved which is carried out at constant temperature and pressure.

The required process is represented in the bottom half of the figure, where the two solute particles, denoted by a and b are brought from infinite separation to some close distance (σ_1). The free energy change for this process is ΔG_{a+b}^L . An equivalent process is also shown in the figure which involves the following steps: First, the two solute particles are transferred from the liquid to the gaseous phase where they are brought to within a close distance (σ_1) of each other. The combined pair is then replaced by a single new particle denoted by a, b which is introduced into the liquid and

Figure 6.3.3 Cyclic process used to obtain an approximate relation between hydrophobic interaction and experimental quantities. The process required is depicted at the bottom of the figure, i.e. two solutes *a* and *b* are brought from infinite separation to a close distance. The corresponding work is ΔG_{a+b}^l . An alternative 'route' is also shown (from Yaacobi and Ben-Naim - reference 7).

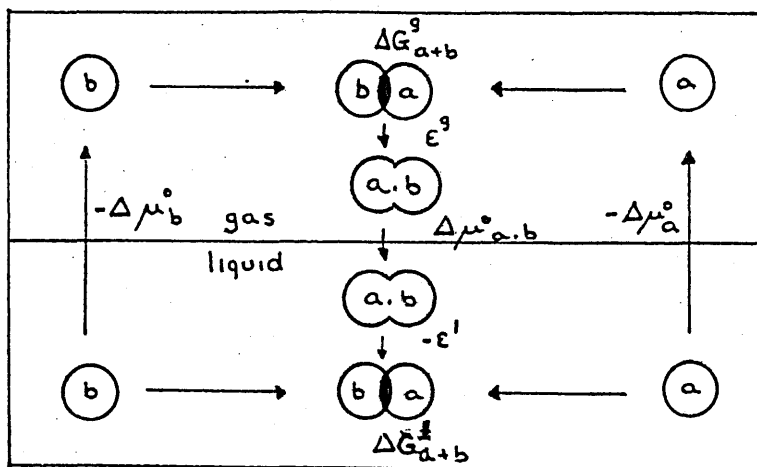
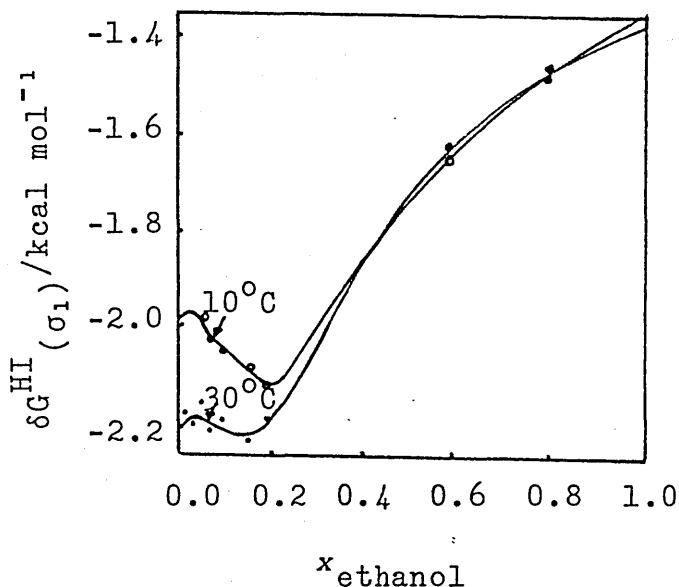


Figure 6.3.4 Variation of the hydrophobic interaction ($\delta G_{(\sigma_1)}^{HI}$)/kcal mol⁻¹), between two methane molecules, with the mole fraction of alcohol at two temperatures (from Yaacobi and Ben-Naim - reference 7).



finally replaced by the pair of solutes $a + b$. This final state is the same as that produced by the more direct route and the total balance of work for the whole cycle is

$$\Delta G_{a+b}^{\ell}(\sigma_1) = -\Delta\mu_a^{\oplus} - \Delta\mu_b^{\oplus} + \Delta G_{a+b}^g(\sigma_1) + \epsilon^g + \Delta\mu_{a.b}^{\oplus} - \epsilon^{\ell} \quad (16)$$

In the gas phase, it is assumed that the interaction between a and b is represented simply by a pair potential $U(\sigma_1)$,

Therefore

$$\Delta G_{a+b}^g(\sigma_1) = U(\sigma_1) \quad (17)$$

and from the definition of the hydrophobic interaction,

$$\delta G^{HI}(\sigma_1) = \Delta G_{a+b}^{\ell}(\sigma_1) - U(\sigma_1) \quad (18)$$

Therefore,

$$\delta G^{HI}(\sigma_1) = \Delta\mu_{a.b}^{\oplus} - \Delta\mu_a^{\oplus} - \Delta\mu_b^{\oplus} + \epsilon^g - \epsilon^{\ell} \quad (19)$$

The assumption involved in the theory is that

$$\Delta\epsilon = \epsilon^g - \epsilon^{\ell} \approx 0$$

and so

$$\delta G^{HI}(\sigma_1) = \Delta\mu_{a.b}^{\oplus} - \Delta\mu_a^{\oplus} - \Delta\mu_b^{\oplus} \quad (20)$$

All of the terms on the right hand side of equation (20) are experimentally obtained quantities. Yaacobi and Ben-Naim⁷ applied these calculations to solubility data for methane and ethane. Treating the solutes *a* and *b*, from the energy cycle, as two methane molecules, and the combined species *a.b* as an ethane molecule, δG^{HI} was calculated from the equation

$$\delta G_{(\sigma_1)}^{\text{HI}} = \Delta \mu_{\text{ethane}}^{\circ} - 2\Delta \mu_{\text{methane}}^{\circ} \quad (21)$$

for the approach of two methane molecules to a separation of $\sigma_1 = 153.3$ pm in an aqueous ethanol solvent. The variation of $\delta G^{\text{HI}}(\sigma_1)$ with solvent composition is shown in Figure 6.3.4.

This approach had been previously taken by Ben-Naim⁶¹ when he considered the interactions between different solutes in water. The free energy associated with the bringing together of methane and a range of non-polar solutes at 25°C was calculated and a similar treatment was applied to account for the attachment of ethyl or larger groups to various molecules.

Using an equation similar to (21), the effect of mutual approach of several methane molecules was investigated. As the number of methane molecules, *n* increased, values of $|\delta A^{\text{HI}}|/n$ increased with *n* and seemed to approach a limiting value for large *n* values. δA_n^{HI} is

the Helmholtz free energy associated with the hydrophobic interaction between n methane molecules. Also for a given value of n , the value of δA_n^{HI} seemed to be unaffected by the configuration of the molecules but it was stated that because of insufficient precision of data, conclusions as to the effect of branching in molecules on δA^{HI} , could not be made.

Before leaving this approach by Ben-Naim, it is important to emphasise that the pairwise interaction between the two solutes (e.g. methane-methane) does not correspond to the formation of a bonded "dimer" (e.g. ethane) but rather, represents the separation of the 'methanes' in a hypothetical ethane molecule.

An alternative description of the hydrophobic interaction has been proposed by Friedman and Krishnan⁶² whereby lower monohydric alcohols are used as hydrophobic probes. Here, the work required to bring two molecules up to one another in a solvent medium is formulated in terms of a repulsive contribution and a "Gurney" contribution. This latter effect is concerned with the overlap of hydration spheres due to the close approach of the hydrated solute molecules. The repulsive effect is that which is assumed to apply in vacuum as well as in solution and is similar to the energy term ΔG_{a+b}^G in the Ben-Naim model. The Gurney contribution is estimated by calculating

the volume of overlap of the hydration spheres and assigning to each mole of solvent expelled from this volume a free energy A_{xx} known as the Gurney coefficient. This is derived from experimental measurements of osmotic pressures, excess energies and excess volumes. However, Franks *et al*⁶³ criticise the use of alcohols as hydrophobic probes and note that some specification of the hydration spheres must be given in order to evaluate the volume of overlap. Also, a knowledge of solvent density would be required to convert this volume to a number of solvent molecules displaced from it. A slight modification⁶³ to the core potential (repulsive interaction) allowed calculations to be made using the Lennard-Jones formulation producing an attractive as well as repulsive interaction between the solutes. The Gurney term was now made to correspond with Ben-Naim's definition⁶⁰ of the hydrophobic interaction making the proposed parameters of Freedman and Krishnan easier to relate to experimental data.

The strength of hydrophobic interaction both in water and heavy water was investigated by Ben-Naim, Wilf and Yaacobi³³ in 1973. Using equation (20) values of δG^{HI} were obtained for the interactions: 2(Ethane) \rightarrow n-Butane; 2(Methane) \rightarrow Ethane; 4(Methane) \rightarrow n-Butane and 2(benzene) \rightarrow Biphenyl. As in a previous paper⁷, ΔH^{HI} and ΔS^{HI} were obtained from the following equations.

$$\delta S^{HI} = -(\delta \delta G^{HI} / \delta T)_p \quad (22)$$

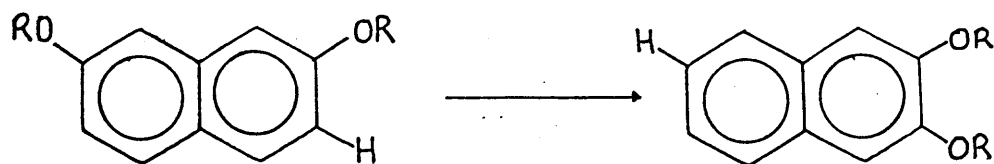
$$\text{and } \delta H^{HI} = \delta G^{HI} + T \delta S^{HI} \quad (23)$$

For the first three "reactions", hydrophobic interaction is stronger in H_2O compared with D_2O but in the last case, this trend is reversed. The values of δH^{HI} and δS^{HI} are all positive and this may be attributed to the decrease in the "structure of the water" as the two solutes approach each other to within a close distance. Detailed explanations for these characteristics are sketchy due to the unknown nature of hydrophobic interactions in these solvents but the properties suggested above are supported by the earlier experimental work of Kresheck, Schneider and Scheraga⁶⁴.

Moving on to look at intramolecular interactions between side groups on larger molecules, Wilf and Ben-Naim⁶⁵ examined the hydrophobic characteristics of 2,3- and 2,7-dialkoxynaphthalenes in aqueous solutions. The process involves the transfer of a non-polar group from one position on a carrier molecule (naphthalene here) some distance from another non-polar group to a second position where it is close to the second non-polar group. Here it was possible only to calculate the change in strength of the intramolecular hydrophobic interaction in the aqueous mixture and in pure water, between the two alkyl groups on the carrier molecule. The process is schematically represented in Figure 6.3.5 and this

system along with others referred to in the paper provided the authors with the conclusion that intramolecular hydrophobic interaction is stronger in water than in D_2O , ethanol, ethylene glycol and n-hexane.

Figure 6.3.5 Schematic process for the exchange of the alkoxy group with the hydrogen atom in which a 2,3-dialkoxynaphthalene is obtained from a 2,7-dialkoxynaphthalene (from Wilf and Ben-Naim - ref 33)



Intramolecular hydrophobic interaction in proteins describes the association, suggested by Kauzmann⁵⁶, between apolar side chains when introduced into an aqueous environment, and indeed Nemethy and Scheraga⁵⁸ also applied their model of hydration to protein solutions. Recently, Rupley⁶⁶ et al reviewed the hydration of globular proteins and described how the macromolecule-water interaction influenced folding, enzymatic activity and other biological properties. Hydration is described as the incremental addition of water to dry macromolecules until a dilute solution is obtained. At some level, there is sufficient

water to completely hydrate the molecule, any additional water only serving to further dilute the system. Some measure of this 'endpoint' of hydration can be obtained from heat capacity measurements⁶⁷ as at full hydration, the value of this experimentally measured parameter corresponds to that for the dilute solution.

Using this method, the quantity of water required to fully hydrate the protein lysozyme was found to be 0.38g/g corresponding to 0.2 nm² of the protein surface area being covered by a single water molecule. This is twice the effective area associated with a water molecule in the bulk liquid. This feature is attributed to the protein-water interaction through which the protein imposes a structure on its neighbouring water molecules in order to gain maximum surface coverage. Thus minimum contact between water and the protein is assumed; hence the folding of the protein, which minimises exposure of non-polar groups and maximises exposure of polar and in particular ionisable groups to the solvent. Since the protein with a monolayer of hydration water fits without perturbation into the bulk solvent, it is also assumed that no significant amount of 'multilayer' water can exist due to the effect of the protein surface on the structure of the surrounding water.

To complete this section, a final view of hydrophobic interaction is taken with respect to the presence of

cavities in the hydrogen bonded liquid. This has already been discussed in the treatment of Nemethy and Scheraga⁵⁷ and Friedman and Krishnan⁶² but the calculation of the energy associated with the formation of a small cavity is difficult to perform with any reliability because of the uncertainty in the extent of bonding in the liquid. However, the cavity energy may be estimated from the product of cavity surface area and specific surface free energy (i.e. surface tension, γ_T)⁶⁸. Considering the molecular interpretation of hydrophobic interaction, a comparison of the sizes of a joint cavity, for a 'combined' pair of solutes, and two single cavities will indicate the magnitude and sign of the free energy for the process of bringing the two cavities together. That is, if the sum of the cavity sizes for the two isolated cavities is less than the size of the joint cavity then the sign of the free energy of hydrophobic interaction will be negative. The magnitude of this function is given by

$$\Delta G^{HI} = \gamma_T \Delta A$$

where ΔA is the loss of cavity area in 'dimer' association and is given by

$$\Delta A = 4\pi r_h^2 (r/r_h - 1)$$

r and r_h correspond to the solute and cavity radius respectively. ΔA is always negative when $r_h > r$ which is the case for a real solvent with finite sized particles.

A consequence of this approach is the ability to relate the strength of hydrophobic interaction to the shape of the solute molecule.

For large spherical molecules, the change in cavity area will be smaller than for long cylindrical solutes interacting side by side. Thus, the hydrophobic interaction associated with the bringing of two large spherical solutes together will be a small effect compared with that for cylindrical molecules.

Several methods are described above from which the strength of the hydrophobic interaction can be measured. The effect is clearly one which is dependant on the physical characteristics of water and since some doubt still exists as to the exact structure of this liquid, the exact molecular interpretation of the hydrophobic interaction is still largely theoretical. In this study though, it is hoped that the solubility characteristics of the hydrocarbons in aqueous solutions will reveal some features which can be attributed to the hydrophobic interaction and in turn assist in the clarification of some of the mysteries associated with the structure of water and aqueous solutions.

7. DISCUSSION OF RESULTS

7. DISCUSSION OF RESULTS

The development of a theoretical model for the structure of liquid water is necessarily based on experimental data from which trends and similarities may be observed and related to physical processes occurring within the liquid. The theories of 'iceberg formation' and 'hydrophobic interactions', caused by the introduction of 'molecular probes' to water, are based on the thermodynamics of solution, observed as changes in such functions as $\Delta\bar{G}^\circ$, $\Delta\bar{H}^\circ$ and $\Delta\bar{S}^\circ$. The extent of these changes depends on variations in experimental conditions of temperature and solvent composition, on the choice of solute and on the choice of co-solvent, and it is the purpose of this discussion to relate the observed thermodynamic changes to structural rearrangements in the solvent.

The three major factors to influence the structure of liquid water in this study are temperature, the concentration and nature of the alcohol co-solvent, and the gaseous solute itself. These will now be discussed in turn with reference made to the theories of structure discussed in Chapter 6.

7.1 The Effect of Temperature

The effect of temperature is clearly noticeable in the experimental results. The solubility measurements

themselves are strongly temperature dependent and because of this, so too are the calculated thermodynamic functions of solution. This dependence was discussed throughout Chapter 5 where particular reference was made to the isotherms of $\Delta\bar{H}^\circ$ and $\Delta\bar{S}^\circ$. As mentioned previously, these functions are closely related to structural effects and changes in these provide information regarding alterations in the structure of the solvent.

The isotherms of $\Delta\bar{H}^\circ$ and $\Delta\bar{S}^\circ$ are now to be used to estimate the effect of temperature on the structure of liquid water since it has been assumed³ that at the deflection point (see section 5.2), all of the organised structures in the liquid have been destroyed by the influence of the alcohol. Since $\Delta\bar{H}^\circ$ and $\Delta\bar{S}^\circ$ for gas solubility indicate the amount of structure present in the solvent, (see section 5) the change in the value of these functions along an isotherm from alcohol mole fraction $x_c = 0$ up to the deflection point, will be a measurement of the amount of structure which was present in liquid water at that temperature.

This technique was used by Cargill²⁸ and data from his investigations^{3 22 27 28} are now presented in Table 7.1.1 where the changes $\Delta(\Delta\bar{X}^\circ)$ are tabulated against temperature. Also included for each gas are the ratios of $\Delta(\Delta\bar{X}^\circ)$ at temperature T to the $\Delta(\Delta\bar{X}^\circ)$ value at 4.7 °C. These are

inserted at the bottom right of each element in the table, expressed as a percentage.

Table 7.1.1 $\Delta(\Delta\bar{X}^\circ)$ values, and corresponding percentages, from the data of Cargill^{3 22 27 28}.

Solute	$\Delta(\Delta\bar{H}^\circ)/\text{kJ}$				$\Delta(\Delta\bar{S}^\circ)/\text{JK}^{-1}$			
	4.7°C	21°C	39.4°C	60.2°C	4.7°C	21°C	39.4°C	60.2°C
hydrogen ²⁸	115 100	10 87	82 71	7 61	48 100	40 83	34 71	31 65
helium ²⁸	11 100	10 91	78 71	6 54	48 100	40 83	32 67	25 52
argon ³	16 100	14 87	11 69	8 50	63 100	51 81	42 67	32 51
oxygen ²⁷	17 100	14 82	11 65	8.4 49	63 100	53 84	43 68	33 52
carbon dioxide ²²	114 100	98 86	87 76	7.9 69	425 100	37 87	34 80	30.5 72
Average %	100	87	70	57	100	84	71	58

The values of $\Delta(\Delta\bar{X}^\circ)$ are shown at the top left of each element in the table and for each gas are seen to be inversely related to the temperature. The calculated percent values shown at the bottom right of each element do not vary much for a given temperature and an average is taken for inclusion at the bottom of the table. There is good agreement between the 'average %' values at a

given temperature for both the $\Delta(\Delta\bar{H}^\circ)$ and $\Delta(\Delta\bar{S}^\circ)$ analysis and from these, the destructive influence of temperature on water structure has been calculated, the results showing that in the temperature range 4.7 to 60.2 °C, up to 40% of the organised structure in water has been destroyed.

This analysis can now be repeated for the solution of the hydrocarbons and the appropriate data are included in the table below.

Table 7.1.2 $\Delta(\Delta\bar{X}^\circ)$ values, and the corresponding percentages for the hydrocarbon solutes used in this study.

Solute	$\Delta(\Delta\bar{H}^\circ)/\text{kJ}$				$\Delta(\Delta\bar{S}^\circ)/\text{JK}^{-1}$			
	4.7°C	21°C	39.4°C	60.2°C	4.7°C	21°C	39.4°C	60.2°C
propane	347 100	272 78	194 56	12 35	130 100	102 78	77 59	55 42
butane	388 100	30 77	20 51	94 24	148 100	118 80	85 57	53 36
2-methyl-propane	316† 100	283 89	241 76	18 57	138† 100	112 81	97.5 70	80 58
2,2-dimethyl-propane	292† 100	26 89	206 70	141 48	117† 100	105 89	87 74	68 58
cyclopropane	208 100	164 79	122 59	7.7 37	80 100	65 81	52 65	37 46
propene	276 100	204 74	152 55	94 34	97 100	77 79	60 62	42 43
Average %*	100	77	55	32	100	79	61	42

* Not including percentage values for 2-methylpropane or 2,2-dimethylpropane.

† Projected values using 'average %' data from Table 7.1.1 and the higher temperature values in Table 7.1.2.

Since no 4.7 °C isotherm was available for the gases 2-methylpropane and 2,2-dimethylpropane, the entries for these were initially ignored and the remaining data were used to calculate 'average %' values. Again the percentage values do not vary much for a given temperature but this time, these 'average %' results are consistently lower than those in Table 7.1.1.

In order to obtain $\Delta(\bar{X}^{\circ})$ values at 4.7 °C for 2-methylpropane and 2,2-dimethylpropane, the following method was used. Inspection of the data available at 21.0, 39.4 and 60.2 °C for these gases, showed that these did not correspond to the ratio of 77:55:32 as given in the 'average %' row of Table 7.1.2. However, they were approximately of the ratio 87:70:57 which is the ratio shown in the 'average %' row of Table 7.1.1. On the basis of the assumption that these two gases did behave like those of Table 7.1.1, the value of $\Delta(\bar{X}^{\circ})$ for each at 4.7 °C was taken to correspond to 100% based on the above ratio.

To compare the stabilising influence of each type of solute against temperature, it is useful to examine the theoretical approach of Nemethy and Scheraga³³, where the

effect of temperature on the mole fraction of unbound molecules in pure water was calculated. These data can now be used with the 'average %' values in Tables 7.1.1 and 7.1.2 to calculate the mole fraction of hydrogen bonded molecules in water as a function of temperature. Referring to Table 7.1.3, these values represent the mole fraction of structured water remaining in (a) pure water, as given by Nemethy and Scheraga³³, (b) in water containing solutes like those used by Cargill^{3 22 27 28} and (c) in water containing solutes like the non-branched hydrocarbons used here at various temperatures, each calculated on the basis of Nemethy and Scheraga's estimate of $x_b = 0.756$ at 0 °C.

Table 7.1.3 Calculated mole fractions of structured water as a function of water temperature.

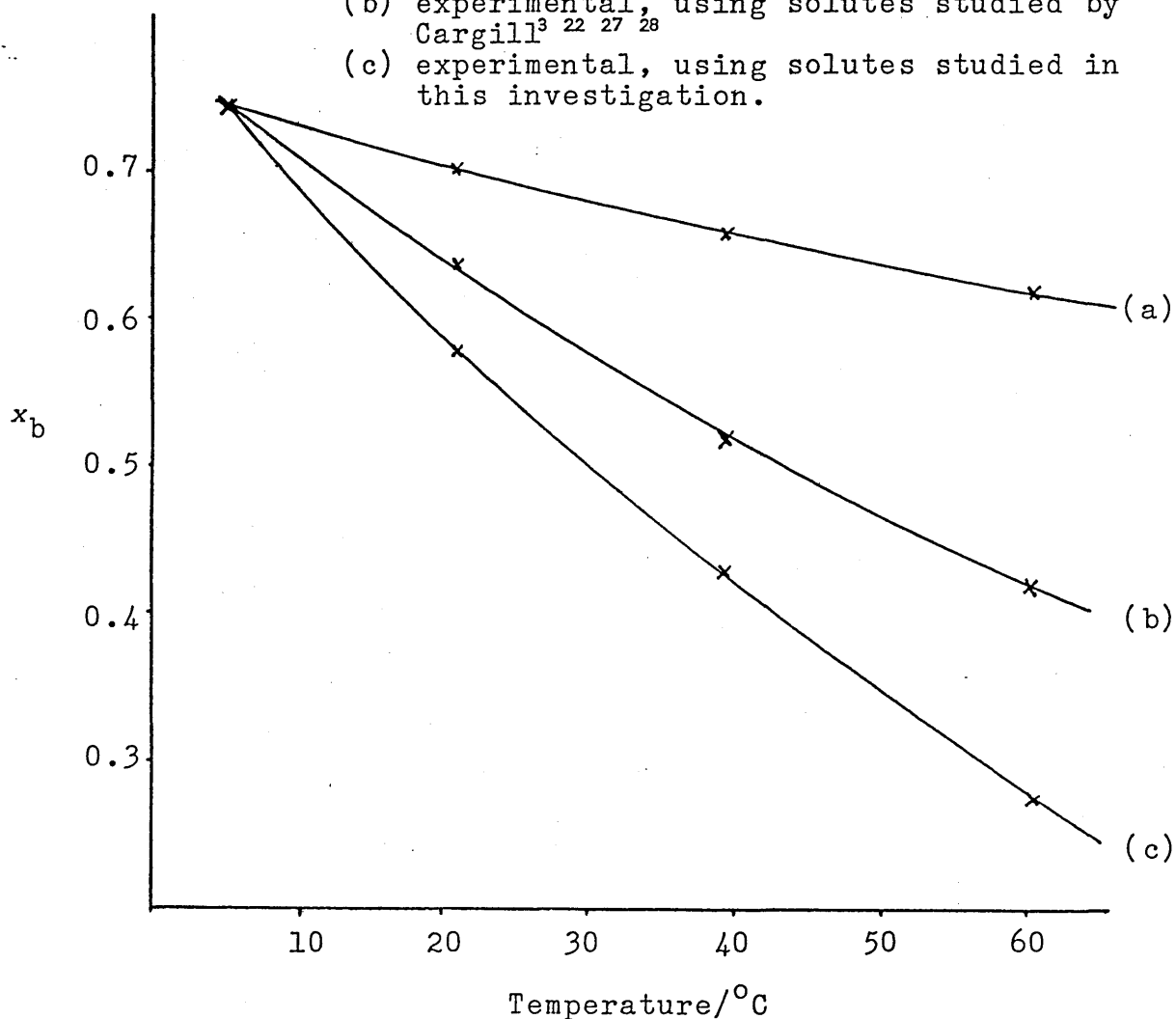
Temp/°C	x_b		
	(a)	(b)	(c)
4.7	0.744	0.744	0.744
21.0	0.703	0.640	0.580
39.4	0.661	0.521	0.431
60.2	0.622	0.424	0.275

Table 7.1.3 clearly shows the effect of temperature on the mole fraction of hydrogen bonded water molecules in the liquid but it also shows that the presence of a gaseous solute considerably reduces the ability of organised structures to

resist the destructive influence of temperature. This is illustrated graphically in Figure 7.1.1 where smooth lines are produced for each of the situations described in Table 7.1.3, each with a slight upward curvature indicating, by extrapolation, that up to the boiling point, there still remains some degree of organisation in the liquid although for the branched hydrocarbon solutes this is found to be as low as about 10% of the maximum.

Figure 7.1.1 Graphical illustration of the destructive influence of temperature on water structures as calculated from:

- (a) theoretical approach³⁸
- (b) experimental, using solutes studied by Cargill^{3 22 27 28}
- (c) experimental, using solutes studied in this investigation.



Comparing the two types of solute discussed here ((b) and (c) above), the presence of the non-branched hydrocarbons seems to assist temperature in the destruction of ordered water to a greater extent than the other gases and from Figure 7.1.1, this appears to be most obvious at high temperatures. In Chapter 5, unusual features were also observed on the isotherms of $\Delta\bar{H}^\circ$ and $\Delta\bar{S}^\circ$ for only these unbranched chain hydrocarbons at high temperatures whereas no such features were present for 2-methylpropane, 2,2-dimethylpropane or for any of the solutes used by Cargill^{3 22 27 28}. At that time, these characteristics were attributed to the hydrophobic effect and this will now be considered in relation to the elevation of $\Delta\bar{H}^\circ$ and $\Delta\bar{S}^\circ$ values, as discussed in Chapter 5, and the apparently destructive influence of these solutes towards water.

From a structural point of view, this effect is considered to influence solute molecules in the way described diagrammatically in Figure 7.1.2.

Figure 7.1.2 Structural interpretation of the hydrophobic interaction.

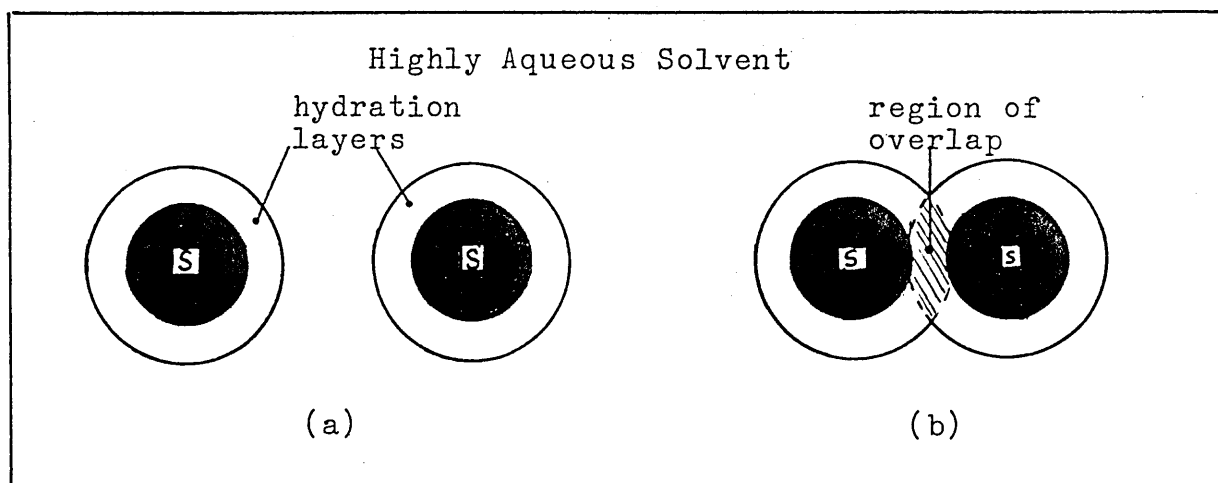


Figure 7.1.2 (a) shows the two solutes s , each of hydrophobic nature and fully hydrated with a layer (or layers) of structured water molecules. In an attempt to reduce the surface area of the solute species exposed to liquid water, the solvent pushes the two solutes towards each other causing the hydration layers to overlap, as shown in Figure 7.1.2 (b). When this occurs, the structured water in the region of overlap is expelled and destroyed causing an increase in the values of functions $\Delta\bar{H}^\circ$ and $\Delta\bar{S}^\circ$. As we have seen, the effect of increasing temperature is destructive towards water structure and will assist in the breaking up of hydrogen bonded groups of molecules expelled from the region of overlap. This explains the endothermicity of the 'hydrophobic bond' observed by Nemethy and Scheraga³³ and can be used to explain the trends observed from the results of this study.

To begin with, the elevation $\delta\Delta\bar{X}^\circ$ as observed in Chapter 5 on the isotherms of $\Delta\bar{X}^\circ$ is believed to be caused by hydrophobic interactions in the solution. The size of $\delta\Delta\bar{X}^\circ$ obeys the same temperature dependence as does the strength of this effect and its sign implies a structural change consistent with the theory of hydrophobic interactions given above. The value of $\Delta(\Delta\bar{X}^\circ)$, as calculated earlier, is also dependent on the size of $\delta\Delta\bar{X}^\circ$ and this is illustrated when comparisons are drawn between the entries in the 'average %' rows of Table 7.1.2 and Table 7.1.1. The increasingly destructive effect of hydro-

phobic interactions on water structure as temperature rises is seen in the smaller percentages in this row of Table 7.1.2. (These were calculated by omitting the data for the branched hydrocarbon solutes.)

The similarity between the 'percentage' data for 2-methylpropane, 2,2-dimethylpropane and the non-hydrophobic solutes used in references 3, 22, 27 and 28 suggests that these branched hydrocarbons do not display the hydrophobic effect. This is supported by the absence of the unusual graphical features found on the isotherms of $\Delta\bar{H}^\circ$ and $\Delta\bar{S}^\circ$ for the other gases, and by the theory discussed by Conway⁸⁸. These branched chain hydrocarbons have bulky molecules which, from the photographs in Figure 5.2.1, display almost spherical dimensions. According to Conway⁸⁸, the strength of the hydrophobic effect can be estimated from a knowledge of the surface tension of the solution and the change in cavity area caused by the interaction of the two solutes (see section 6.3). If the two solutes are spherical, the overlap region would be small compared with that for cylindrical solutes, and therefore the strength of the hydrophobic effect for these two branched hydrocarbons will be small compared with that for the likes of propane or butane.

So these will tend to behave in solution like hydrogen, helium, argon, oxygen and carbon dioxide showing hardly any destructive properties towards water other than as a

result of normal temperature effects. The solutes which do show the hydrophobic effect are forced to destroy the structure in water by the solvent itself in its efforts to isolate the hydrophobic molecules from unnecessary contact with other water molecules. Table 7.1.3 shows that up to a further 20% of structure can be destroyed in this way and although dependent on temperature the strength of this effect also varies with the choice and concentration of co-solvent and as we have seen, the size and shape of the molecule of the hydrophobic solute. These factors will now be discussed in detail.

7.2 The Effect of the Alcohol

The influence of the alcohol on the structure of liquid water is perhaps first observed in the isotherms of solubility where all of the gases studied here possess a very similar variation in solubility with increasing alcohol concentration. There is also a close resemblance between the isotherms presented here and the ones presented by Cargill for the solution of the gases argon³, carbon dioxide²², oxygen²⁷, hydrogen²⁸ and helium²⁸ in the same aqueous solvents, which encourages the assumption that the structural interpretation of this variation in solubility, discussed in reference 28, is valid for this study also.

From the isotherms of solubility and also of $\Delta\bar{H}^\circ$ and $\Delta\bar{S}^\circ$, this might be a fair assumption although there are some minor differences, especially in the position, with respect to alcohol mole fraction, of graphical features which are considered to represent positions of major structural alterations in the solvent. These alterations can be described in the following way.

The addition of small amounts of alcohol to water is observed to increase the solubility of a gas at low temperatures. This implies that to some extent the alcohol stabilises the organised structures associated with the solute although the isotherms of $\Delta\bar{H}^\circ$ and $\Delta\bar{S}^\circ$, in the appropriate region of alcohol concentration, do not always indicate an increase in structural organisation. For example, a decrease in the values of $\Delta\bar{H}^\circ$ and $\Delta\bar{S}^\circ$ is observed for the solution of carbon dioxide in aqueous ethanol²² and for butane in aqueous 2-methylpropan-2-ol, and here the alcohol appears to assist in further structure promotion. Elsewhere, the increase in solubility at low alcohol mole fractions is not accompanied by this evidence for structure promotion and it may be that the effect of the alcohol is to break up outer layers of large hydrating clusters, the fragments forming new clusters around other solute molecules resulting in higher solubility with the steady increase in $\Delta\bar{H}^\circ$ and $\Delta\bar{S}^\circ$ in this region showing that the structure-breaking process is the dominant one.

This would be a logical process as the isotherms of solubility approach their maxima, where now, the alcohol begins to destabilise the structured water closest to the solute. The solubility of the gas then begins to fall as the increasing alcohol concentration continues to break up the organisation in liquid water. Over this region, the values of $\Delta\bar{H}^\circ$ and $\Delta\bar{S}^\circ$ are still rising indicating the continued destruction of order in the liquid. At the minima on the $\log s_0$ isotherms the solubility of the gas is now more controlled by the alcohol component and rises steadily at this point, the structured species in water becoming much more scarce until finally they have disappeared at the alcohol concentration corresponding to the deflection point (see Chapter 5) on the $\Delta\bar{H}^\circ$ and $\Delta\bar{S}^\circ$ isotherms.

At higher temperatures, most of these structural alterations are absent because of the increasingly destructive influence of higher temperatures (see section 7.1) and the smaller cluster sizes present. However, at these temperatures, different effects begin to manifest themselves in the form of hydrophobic interactions, which have been shown to be strongest at higher temperatures. The effect of the alcohol on these will be discussed later.

Beyond the deflection point on the $\Delta\bar{H}^\circ$ and $\Delta\bar{S}^\circ$ isotherms, the variation in $\Delta\bar{H}^\circ$ and $\Delta\bar{S}^\circ$ becomes due to the interactions between the solute and the strongly

alcoholic solvent. The hydrophobic solute molecules will find the hydrophobic part of the alcohol molecules to be easily approachable in contrast to their repulsive interaction with water molecules. This is reflected in the very high solubilities of the hydrocarbon gases in alcohol rich solvents which prevented solubility measurements being made over the complete range of solvent composition. This was particularly obvious when 2-methylpropan-2-ol was the co-solvent. In fact during some experiments butane was found to remove this alcohol component from water and formed a two-phase mixture in the apparatus, rendering further solubility measurements impossible.

So the range of solvent composition studied has been covered and the likely structural effects have been outlined in relation to increasing alcohol concentration. As before³, the choice of the alcohol significantly alters the positions of graphical features and again this will be discussed in relation to structural effects. More importantly however, the differences between this work and the previous work of Cargill^{3 22 27 28} will now be analysed, where possible, attempting to provide structural explanations and the implications of these in relation to liquid water.

The first differences occur in the positions of extrema on the solubility isotherms. These are tabulated below for the solution of several gases in the aqueous ethanol solvents where comparisons can be made between the

results of this and other work²⁸.

Table 7.2.1 Mole fractions of ethanol for positions of extrema on the solubility isotherms for several gases.

Solute	Maxima			Minima		
	4.7°C	12.6°C	21.0°C	4.7°C	12.6°C	21.0°C
helium ²⁸	0.030	0.035	0.045	0.140	0.125	0.105
hydrogen ²⁸	0.035	0.035	0.040	0.135	0.110	0.095
argon ^{3 28}	0.035	0.040	0.045	0.135	0.125	0.100
oxygen ^{27 28}	0.030	0.035	0.040	0.140	0.125	0.095
propane*	0.044	0.052	-	0.094	0.090	-
butane*	0.052	-	-	0.096	-	-
cyclopropane*	0.035	-	-	0.090	-	-
propene*	0.035	0.050	-	0.090	0.085	-

* From Figures 4.3.1, 4.3.2, 4.3.5 and 4.3.6 respectively.

From Table 7.2.1, it is seen that when propane and butane are solutes in aqueous ethanol, more alcohol is required to begin the final stages of destabilising the hydrating clusters, at 4.7 °C, than for any of the other gases considered. At 12.6 °C, this is still true for propane and now also for propene. At higher temperatures the structure of water can no longer resist the destabilising influence of both the alcohol, and temperature, and therefore no solubility maxima appear for the other

hydrocarbon gases. The hydrophobicity of each of these gases may explain the absence of maxima at 21.0 °C, which were found on the solubility isotherms of the non-hydrophobic gases used by Cargill^{3 27 28}. This hydrophobicity may have assisted in the destabilisation of water clusters.

The positions of minima are affected in the opposite direction. This may be a direct consequence of the preferred interaction between solute and alcohol molecules causing the solubility of the gas to become increasingly influenced by the alcohol as the structure of liquid water breaks down. This situation is also found in the solution properties of propane and butane in aqueous 2-methylpropan-2-ol. It has been previously noticed^{3 34} that the large alkyl group of this alcohol moves the positions of graphical extrema towards the water end of the solvent composition axis. This has been observed here also and again these positions differ slightly for the different types of gaseous solutes.

This compression of the isotherms with respect to alcohol mole fraction, caused by changing the alcohol component from ethanol to 2-methylpropan-2-ol, is due to the size of the alkyl group. Much less alcohol is now required to bring about the structural rearrangements discussed above and this is perhaps because the larger alcohol molecule is more destructive towards water clusters.

Where decreases in the values of $\Delta\bar{H}^\circ$ and $\Delta\bar{S}^\circ$ are observed in relation to small concentrations of this alcohol in the solvent, it is possible that some structure forming interaction between the hydrophobic methyl groups of the alcohol and water is taking place in the same way as this is found for the hydration of the hydrophobic molecules discussed in the next section. This would not be so apparent for ethanol due to its reduced size and reduced hydrophobicity.

When the effect of temperature on the structure of water was dealt with in section 7.1, only solvents containing ethanol were considered and the total destruction of organised water clusters was due to the increasing amounts of ethanol in the solvent. Using aqueous 2-methylpropan-2-ol as solvent for propane and butane, Table 7.2.2 was constructed, employing the same $\Delta(\Delta\bar{X}^\circ)$ analysis as before, and quite surprising results were obtained.

Table 7.2.2 $\Delta(\Delta\bar{X}^\circ)$ data, and corresponding percentages, for the solution of propane and butane in aqueous 2-methylpropan-2-ol.

Solute	$\Delta(\Delta\bar{H}^\circ)/\text{kJ}$				$\Delta(\Delta\bar{S}^\circ)/\text{JK}^{-1}$			
	4.7°C	21°C	39.4°C	60.2°C	4.7°C	21°C	39.4°C	60.2°C
propane	322	36	33	325	124	123	123	120
	100	112	102	101	100	99	99	97
butane	422	332	247	155	152	120	94	62
	100	78	58	36	100	79	62	41

For the solution of butane, the 'percent' data agree very well with the 'average %' row of Table 7.1.2 for the non-branched hydrocarbon solutes but for propane, quite unusual structural effects appear to be occurring in the solvent. For propane, the isotherms of $\Delta\bar{X}^\circ$ show almost equal amounts of structure demolition at all temperatures up to the 'apparent deflection point'. Due to some practical problems, experimentation at higher alcohol mole fractions failed to provide reliable data and some doubt exists as to the actual position of this deflection, and this may account for the anomolous $\Delta(\Delta\bar{X}^\circ)$ values presented above for propane. However, until more satisfactory data can be obtained for this region of solvent composition, no real attempt to explain these results is being made.

However, the data for butane provide good support for earlier calculations, the results of which were given in section 7.1 to describe the effect of temperature on water structure. At that time, the rather low values in the 'average %' row of Table 7.1.2 were attributed to an additional destructive effect due to hydrophobic interactions and the data for butane given in Table 7.2.2 will be used later (section 7.3) to find $\delta\Delta\bar{X}^\circ$, the extent of this effect in pure water.

By comparing the $\Delta\bar{X}^\circ$ isotherms for the non-branched hydrocarbons with those for the solutes used by Cargill,^{22 27 28}

the effect of increasing alcohol concentration on the value of $\delta\Delta\bar{H}^\circ$ can be seen.

Figure 7.2 Typical $\Delta\bar{H}^\circ$ isotherm for high temperature showing effect of hydrophobic interactions.

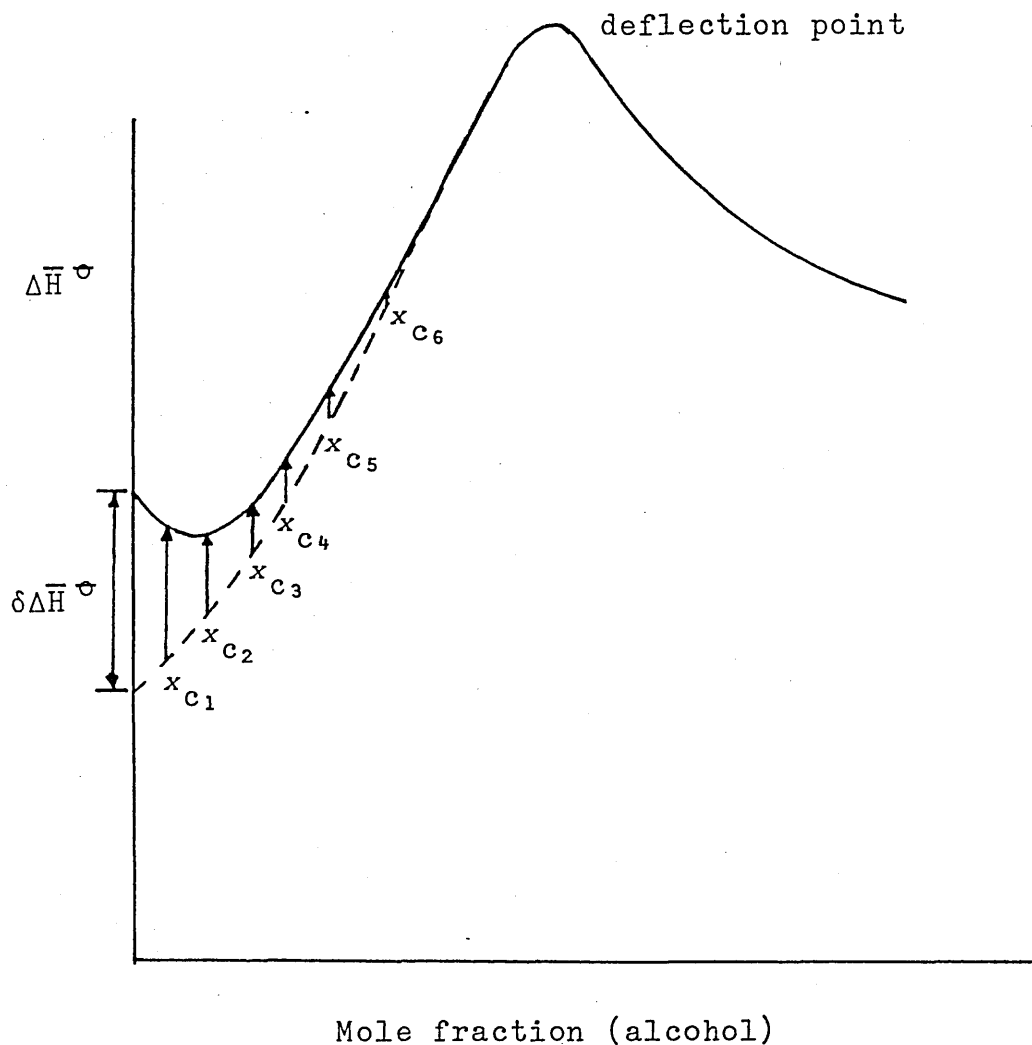


Figure 7.2 shows a typical high temperature isotherm for the solution of a solute displaying the hydrophobic effect. If the extent of hydrophobic interactions in water were known, then the value of $\delta\Delta\bar{H}^\circ$ could be subtracted from the observed $\Delta\bar{H}^\circ$ value allowing the construction of an

isotherm approximately to represent the solution of a gas which does not display the hydrophobic effect. This is shown in Figure 7.2 where the arrows at alcohol mole fractions $x_{c_1} \rightarrow x_{c_6}$ illustrate the diminishing strength of hydrophobic interactions as the alcohol concentration is increased. This can only be an estimate however as it is not clear from this work at what alcohol concentration the hydrophobic effect is negligible. Yaacobi and Ben-Naim⁷ consider this to persist over the complete range of solvent composition, giving the value of δG^{HI} in pure ethanol as -5.8 kJ mol^{-1} but there is no evidence from this work to suggest that the effect persists beyond the region of the 'deflection point' ($\Delta \bar{H}^\circ$ and $\Delta \bar{S}^\circ$).

7.3 The Effect of the Solute

Before a detailed discussion begins relating the strength of hydrophobic interactions to the properties of individual solutes, it is worth noting the magnitudes of $\Delta(\Delta \bar{X}^\circ)$, as calculated in section 7.1, for the gases used in this study. Comparing $\Delta(\Delta \bar{X}^\circ)$ values in Tables 7.1.1 and 7.1.2 shows that when introduced to water at 4.7°C the hydrocarbon solutes are responsible for promoting up to three times the amount of structure more than the non-hydrocarbon solutes. This is at first surprising considering the hydrophobic characteristics of these solutes but perhaps the unfavourable interaction between water and these molecules initiates the formation

of enveloping barriers more readily than these are formed for the other gases. At this temperature, the destructive influence of the hydrophobic effect is small and it may be that water molecules try to reduce the surface area of the solute exposed to the bulk by covering it in a fashion similar to that described by Rupley⁶⁶, where maximum effort is directed towards isolating the hydrophobic solute from further interaction with the solvent.

Energetically, this would be easier if an encapsulating cavity were formed around the solute held together by hydrogen bonds and exhibiting a high degree of order in the vicinity of the solute. The destruction of this order must be responsible for the values of $\Delta(\Delta\bar{X}^{\circ})$ at 4.7 °C with a smaller contribution possibly from the breaking up of some organised structures in bulk water. The size of the solute molecules is a deciding factor in the formation of encapsulation cavities but total coverage must take place since the solutes are indeed dissolved in the solvent and there may be co-operative effects existing between small clusters in order to accomplish this.

To illustrate the effects of each gas on the structure of water, it is useful to compare the values of $\Delta(\Delta\bar{X}^{\circ})$ in Table 7.1.2, where it is shown that the largest degree of structure promotion is exhibited by butane with an

enthalpy change of 38.8 kJ involved in the total destruction of these water clusters. It is not suggested that this energy change is due completely to the destruction of hydration layers of structured water but it is assumed that any organised structures present in bulk water will exist to the same extent regardless of the choice of solute for this temperature. We can now look at these $\Delta(\Delta\bar{X}^\circ)$ values as a percentage of those for butane.

Table 7.3.1 Comparison of structure promoting ability of several solutes in water at 4.7 °C.

Solute	$\Delta(\Delta\bar{H}^\circ)/\text{kJ}$	%	$\Delta(\Delta\bar{S}^\circ)/\text{JK}^{-1}$	%	Average %
butane	38.8	100	148	100	100
propane	34.7	89	130	88	88.5
2-methyl-propane	31.6	81	138	93	87*
2,2-dimethyl-propane	29.2	75	117	79	77*
propene	27.6	71	97	65	68
cyclopropane	20.8	54	80	54	54

* Based on the projected values in Table 7.1.2.

The average % column in Table 7.3.1 provides a comparison of the structure promoting ability of each gas with that of butane but does not imply that butane promotes 100% structure in liquid water.

An interesting observation from the table is the difference between the structuring abilities of propane and propene. The photographs in Figure 5.2.1 show that these two molecules would occupy cylindrical volumes of similar dimensions but it appears that the presence of the double bond in propene inhibits to some extent the ability to promote the formation of hydration layers. This would appear to be due to the difference in polarisability between the two molecules more than the absence of a hydrogen atom from the methyl group of propane.

The remaining data from the table provide no real surprises from a theoretical point of view. Although basically similar in shape, the propane molecule is shorter in length than the butane molecule and therefore requires a smaller number of water molecules to hydrate it. The 'average percent' entries for the branched hydrocarbons, 2-methylpropane and 2,2-dimethylpropane, although based on projections, show the expected trend with the larger 2,2-dimethylpropane molecule being less easy to hydrate due to its size. For cyclopropane, the data show this molecule to be least hydrated amongst the gases studied although this would have been difficult to predict theoretically. We have seen in any case (a) that these hydration layers of structured water are destroyed by the increasing concentration of alcohol molecules in the solvent; and (b) that the hydrophobic effect is also destructive. Now the extent of this interaction will be discussed in relation to each of the chosen solutes.

It has been shown that the gases 2-methylpropane and 2,2-dimethylpropane do not exhibit the hydrophobic effect (see section 7.1) and indeed these tend to behave like the solutes studied by Cargill^{3 22 27 28}. The remaining hydrocarbon gases used here are influenced by the solvent to different extents and a useful way to explore these solvent-induced interactions is to make use, once again, of the data in Tables 7.1.1 and 7.1.2.

If we assume that the differences observed in the 'average percent' rows of Tables 7.1.1 and 7.1.2 are due only to hydrophobic interactions then the amounts by which the isotherms of $\Delta\bar{H}^\circ$ and $\Delta\bar{S}^\circ$ are elevated in the pure solvent can be evaluated. These amounts correspond to the quantities $\delta\Delta\bar{H}^\circ$ and $\delta\Delta\bar{S}^\circ$ discussed in Chapter 5 and may be calculated in the following way. The 'average %' rows of Table 7.1.1 and 7.1.2 are given below along with the differences between them. The fact that these differences are greater for $\Delta(\Delta\bar{H}^\circ)$ than for $\Delta(\Delta\bar{S}^\circ)$ lends support to the idea that this is an indication of hydrophobic interactions in the solution according to the theory of Abraham⁶⁹ which suggests it is more of an enthalpy than an entropy effect for the *n*-alkanes.

	$\Delta(\Delta\bar{H}^\circ)/\text{kJ}$				$\Delta(\Delta\bar{S}^\circ)/\text{JK}^{-1}$			
	4.7°C	21°C	39.4°C	60.2°C	4.7°C	21°C	39.4°C	60.2°C
Table 7.1.1	100	87	70	57	100	84	71	58
Table 7.1.2	100	77	55	32	100	79	61	42
'Difference'	0	10	15	25	0	5	10	16

Using the values in the 'difference' row of the above table, and the values of $\Delta(\Delta\bar{X}^\circ)$ at 4.7 °C given in Table 7.1.2, $\delta\Delta\bar{H}^\circ$ and $\delta\Delta\bar{S}^\circ$ can be obtained from the relationship

$$\delta\Delta\bar{X}^\circ = \Delta(\Delta\bar{X}^\circ)_{4.7^\circ\text{C}} \times \frac{\text{'difference'}}{100}$$

These $\delta\Delta\bar{X}^\circ$ values are tabulated below.

Table 7.3.2 Calculated values of $\delta\Delta\bar{H}^\circ$ and $\delta\Delta\bar{S}^\circ$ for selected solutes in water.

Solute	$\delta\Delta\bar{H}^\circ/\text{kJ}$			$\delta\Delta\bar{S}^\circ/\text{JK}^{-1}$		
	21°C	39.4°C	60.2°C	21°C	39.4°C	60.2°C
propane	3.47	5.20	8.67	6.50	13.00	20.80
butane	3.88	5.82	9.70	7.40	14.80	23.68
cyclo- propane	2.08	3.12	5.20	4.00	8.00	12.80
propene	2.76	4.14	6.90	4.85	9.70	15.52

Using the same analysis for butane as solute in water + 2-methylpropan-2-ol, corresponding data for $\delta\Delta\bar{H}^\circ$ were 3.8, 5.1 and 8.9 kJ respectively and for $\delta\Delta\bar{S}^\circ$ were 7.6, 13.7 and 25.8 JK^{-1} respectively. Considering the possible error in $\Delta(\Delta\bar{X}^\circ)$, these results compare very well with those provided in Table 7.3.2 for butane. This implies that the minima observed at low temperatures and low alcohol concentrations on the isotherms of $\Delta\bar{H}^\circ$ and $\Delta\bar{S}^\circ$ for butane in aqueous 2-methylpropan-2-ol, are not linked with hydrophobic interactions but more likely

indicate increased structure promotion due to the stabilising influence of the alcohol at these concentrations. At higher temperatures, the effect imposed by water (hydrophobic interactions) is seen to affect the solubility characteristics of butane in the same way from the analysis of both the aqueous ethanol and aqueous 2-methylpropan-2-ol solvent systems and the influence of this in water is observed in Table 7.3.2.

The functions $\delta\Delta\bar{H}^\circ$ and $\delta\Delta\bar{S}^\circ$ describe the change in the extent of hydrogen bonding and structural order respectively, induced by hydrophobic interactions in the solvent and from Table 7.3.2, it is clear that their values depend greatly on the solute itself. Referring to the typical isotherm in Figure 7.2, it can be seen that application of these $\delta\Delta\bar{X}^\circ$ to the actual isotherms of $\Delta\bar{X}^\circ$ (e.g. for butane as solute in aqueous ethanol, see Figures 4.6.2 and 4.7.2) would give a pattern of $\Delta\bar{X}^\circ$ which the gas-solvent system would possess if the gas did not display the hydrophobic effect.

Such a pattern is indeed similar to that found experimentally for the solution of solutes such as 2,2-dimethylpropane which does not display these hydrophobic effects in this solvent (see Figures 4.6.4 and 4.7.4).

It is important however to remember the origin of these data. Based largely on estimates they are included here only to provide a rough indication of the extent to which the isotherms of $\Delta\bar{H}^\circ$ and $\Delta\bar{S}^\circ$ deviate at low alcohol concentrations. Normally, they would lead to values for $\delta\Delta\bar{G}^\circ$ which would be much more useful in terms of identifying the strength of the interaction but the uncertainty in $\delta\Delta\bar{S}^\circ$ particularly, prevents further analysis in this direction.

To look at the comparative effect for each of the gases, Table 7.3.2 and the relevant $\Delta\bar{H}^\circ$ and $\Delta\bar{S}^\circ$ sets of isotherms will be useful. The theory discussed by Conway⁶⁸ is again applicable and the case of each gas can be discussed in terms of this. Molecular models of the gases, pictured in Figure 5.2.1 show that the non-branched molecules all have cylindrical shapes of different lengths and radii. From a theoretical point of view, the strength of interaction which pushes two butane molecules towards each other should be the greatest compared to the others since the length of the overlapping cylindrical hydration layers would be greatest here. This is what we observe experimentally over the temperature range considered. To draw theoretical comparisons between propane and propene is not so easy because of the similarity in size and of their shape. From an examination of the isotherms of $\Delta\bar{H}^\circ$ and $\Delta\bar{S}^\circ$ for the two gases, there appears to be a difference

which is also tabulated in Table 7.1.2 for the range of functions covered. The extent of curvature and minima on these, however, produce similar magnitudes of $\delta\Delta\bar{H}^\circ$ and $\delta\Delta\bar{S}^\circ$ and this agrees with the theoretical expectations. Table 7.3.2 also shows that both propane and propene have less hydrophobicity than butane, as would be expected from their shorter molecules.

Finally, cyclopropane, the most different of the solutes studied in this series, is a cyclic molecule which may also be regarded as having cylindrical shape. Using the ring itself as the circumference, a cylinder is produced of short length and large diameter, making it more like a disc. The data in Table 7.3.2 show that hydrophobic interactions between two cyclopropane molecules is the weakest of those studied here (after the branched chain hydrocarbons), and this is most likely due to the reduced length of hydration layer contact. This relationship between length of molecule and strength of interaction was also observed by Ben-Naim⁶¹ who used several methane molecules which, under the influence of the hydrophobic effect, were brought together with an increasing energy as the number of molecules involved was increased.

As was pointed out by Franks⁶³ *et al*, the volume of overlap would be difficult to ascertain but if more confidence could be placed in the values of $\delta\Delta\bar{H}^\circ$ and $\delta\Delta\bar{S}^\circ$,

as obtained from this study, then a versatile method of investigating hydrophobic interactions would be available. The trends observed here are consistent with accepted theories of hydrophobic interaction and the procedure does not involve complex mathematical analysis. The large temperature range used has undoubtedly highlighted the hydrophobic effect, producing deflections on the high temperature isotherms of $\Delta\bar{H}^\circ$ and $\Delta\bar{S}^\circ$. The restricted temperature ranges used by other workers⁷ may have prevented earlier development of this technique.

8. CONCLUSIONS AND FUTURE DEVELOPMENTS

8. CONCLUSIONS AND FUTURE DEVELOPMENTS

During the course of this investigation, a substantial array of solubility data has been obtained and the solubilities of six gaseous hydrocarbons in water and in selected aqueous alcohol solvents are now available for temperatures in the range 4-61 °C. The accuracy of experimentation is reflected in the close agreement between the results of this study and those of Morrison and Billett⁵ and of Wetlaufer⁶ *et al*, for the solubilities of propane, butane, 2-methylpropane and 2,2-dimethylpropane in water, allowing considerable confidence to be placed in these and subsequent measurements for water and water-alcohol solvents using this technique.

The thermodynamics of solution have once again provided much information regarding the influence of the solute on the solvent and can be used, as before^{3 22 27 28}, to describe rearrangements in the solvent structure. The structure of bulk liquid water, as discussed in Chapter 6, is extremely complex and investigative techniques, such as the one used here, cannot be applied directly to study the structure of pure water. Instead, a solute is introduced which disturbs this structure and it is this perturbation which is monitored in the experimental results. These show that 'structure' is promoted by the introduction of the solute molecule to water and this is interpreted

as the formation of hydration layers or encapsulating shells around the solute molecule. This structure promotion is particularly marked when the solute molecule is a hydrocarbon. These have hydrophobic molecules and the interaction between them and water is very much less preferred than that for water molecules with each other. Because of this, the hydrophobic solute molecule is surrounded completely to prevent unnecessary water-hydrocarbon interactions.

The formation of these hydration layers necessarily involves associative interactions between the participating water molecules. The extent of this hydrogen bonding, as monitored in this study, shows the destructive influence of temperature and increasing alcohol concentration on these hydration layers and thus provides the investigator with some indication of the properties of organised water structures in the vicinity of the solute molecule.

If it can be assumed that the same properties are exhibited by organised structures in bulk liquid water (i.e. with no solute molecules present) then some attempt to explain the macroscopic properties of water might be made. In this respect and with reference to the discussion of models (Chapter 6) and of results (Chapter 7), it is clear that the results obtained are, as before^{3 22 27 28}, inclined to support the mixture models for water structure.

This is seen primarily from the analysis of the temperature effect on water structure (see Tables 7.1.1 and 7.1.2) which shows that a considerable amount of structure in water is destroyed with increasing temperature. The fact that some structured water still remains clearly proves that more than one type of structure exists in liquid water at a given time which is the foundation on which the mixture models is based.

So it is to be concluded that the use of these hydrocarbons as gaseous solutes does not alter the conclusions drawn from previous studies on water structure^{3 22 27 28} and, in general, their behaviour as solutes is not too different from that of the other gases used. However, one very important difference was observed between the two different types of solutes and this permitted a detailed investigation of 'the hydrophobic effect', a solvent induced association as described in section 6.3, to be carried out.

The unusual variations in $\Delta \bar{H}^\circ$ and $\Delta \bar{S}^\circ$ observed at low alcohol concentrations and high temperatures for the solution of most of the chosen hydrocarbon gases, are attributed to this hydrophobic effect. The structural interpretation of this, as discussed throughout Chapter 7, considers the interaction between the hydration layers of two (or more) hydrated solute molecules which results in the breaking up of structured water in the region of

interaction. This theory, which has provided an explanation for the apparently non-hydrophobic characteristics of the branched hydrocarbon molecules, is consistent with the calculated $\Delta\bar{H}^\circ$ and $\Delta\bar{S}^\circ$ values and their dependence on temperature and alcohol concentration.

The methods employed here to estimate the magnitude of the hydrophobic effect are only approximate however and a considerable increase in the accuracy of determining $\Delta\bar{H}^\circ$ and $\Delta\bar{S}^\circ$ would be required before the strength of these interactions (expressed as $\delta\Delta\bar{G}^\circ$) could be evaluated. It is doubtful whether improvements in this technique could provide accuracy in these functions to the required extent but the use of alternative methods to measure $\Delta\bar{H}^\circ$ directly would provide not only a check on the results obtained here but also provide sufficient confidence to proceed with the determination of $\delta\Delta\bar{G}^\circ$, the strength of the hydrophobic interactions. Sufficiently high accuracy can be achieved in the determination of $\Delta\bar{H}^\circ$ using calorimetric techniques and the use of these on the hydrocarbon-water-alcohol systems as studied here, would provide support to the existing data and the accuracy required for the further analysis of the hydrophobic effect.

The strength of this effect is in any case derived from $\delta\Delta\bar{H}^\circ$ and $\delta\Delta\bar{S}^\circ$ and the problem has recently been approached⁶⁹ by investigating the incremental effects associated with the methyl and methylene components of

the molecules under investigation. Abraham⁶⁹ showed that the hydrophobic effect associated with a methylene group on a straight chain alkane molecule is primarily an enthalpic one while hydrophobic contributions, for flexible alkane molecules, to their entropies of solution are small and comparatively unimportant. These conclusions were drawn from comparisons between the solution properties of gases which displayed the hydrophobic effect and gases which do not (as was the case in this study) and from these, the methylene contribution to the total hydrophobic effect for the whole molecule was given as 2.1 kJ mol^{-1} in $\Delta \bar{H}^\circ$ and $0.462 \text{ kJ mol}^{-1}$ in $T\Delta \bar{S}^\circ$.

Furthermore, Abraham also showed that the methyl group contribution was entropically dominated with virtually no enthalpic effects arising from the methyl group-solvent interaction at all. Due to the possible errors associated with the calculation of $\delta \Delta \bar{H}^\circ$ and $\delta \Delta \bar{S}^\circ$ as given in Table 7.3.2, it would not be acceptable to use the data obtained here to support or criticise these conclusions but the smaller entropic part of the analysis coupled with the proposed structural interpretation of the hydrophobic effect does tend to suggest that the presence of methylene groups and their number on the molecules of propane and butane contributes significantly to their appreciable hydrophobic characteristics.

Spink and Colgan⁷⁰, who also used an incremental approach in the treatment of $\Delta\bar{G}^\circ$, $\Delta\bar{H}^\circ$ and $\Delta\bar{S}^\circ$ of solution, stated that the methyl groups on the hydrocarbon chain are the main contributors to the hydrophobic effect as displayed by these molecules and suggest that about ten methylene groups would be required to accomplish the same entropic contribution as for one methyl group. This may be considered in relation to the interaction of a methyl group (as part of a complete molecule) with the surrounding solvent structure. The surface area exposed by this group is three times that for the methylene (0.96 nm² against 0.31 nm²⁷¹) and this is considered⁷⁰ to account for the large negative entropies of transfer associated with the hydration of aliphatic hydrocarbon molecules and the entropically controlled hydrophobic effect.

It is seen however, that the work of Abraham⁶⁹ agrees with that of Spink⁷⁰ et al in the allocation of molecular components to their dominating hydrophobic contributions but whereas Spink⁷⁰ sees the entropy as being the dominant contribution, Abraham⁶⁹ favours the enthalpy and methylene group to dominate.

The results of this study however, can not provide definite support for either choice but whilst this approach is only important theoretically, the end results can only be meaningful in the consideration of whole molecules

and their interactions in aqueous solvents. The structural interpretation of the hydrophobic effect, as given here to account for the experimental results, is based on simple concepts and although complete agreement is obtained between theoretical expectations and experimental observations, it may be possible that some alternative explanation will serve equally well. It would therefore be appropriate to investigate the validity of the theory using different experimental approaches.

The theory requires that at least two solute molecules are in solution and that these are within a close distance of each other (close enough for interaction between the hydration layers). Whether or not any solute-solute interactions are involved is not known but measurements to check this possibility could be made as part of a future extension to this study. One such procedure would be to monitor the depression of the freezing point caused by the presence of the gaseous hydrocarbon solute in water. Simple calculation of the solute's molecular weight would show any tendency for dimerisation.

An alternative approach would require the repetition of experiments conducted during the present investigation but this time at reduced pressures. The resulting drop in solubility would produce even more dilute solutions than encountered in this study and the probability of dimerisation would be greatly reduced. If dimerisation

of solute molecules was the cause of the unusual graphical features attributed to hydrophobic interactions then these would not be observed on the results of the new study. If however, they were still to be observed, then the theory of hydrophobic interactions as proposed here would not be valid as it requires the presence of at least two solute molecules at close separation.

There are still many questions to be answered in relation to the structural interpretation of the hydrophobic effect. If the distance between the two hydrated solute molecules were known then some idea of the strength of solute-solute interactions could be calculated in relation to that between the solute and solvent molecules and between the solvent molecules themselves. It is suspected that the solute molecules would prefer mutual contact instead of contact with the solvent and the 'squeezing' effect imposed by the solvent would tend to assist this interaction. However, without further information, it is fruitless to speculate and continual research in this area can only assist in the advancement of structural models and theories which may, one day, unravel the mysteries of liquid water and hydrophobic interactions.

Further measurements of gas solubility may reveal other interesting solution properties and several gas-aqueous solvent systems are of particular industrial interest.

In the purification of natural gas, the impurities carbon dioxide and hydrogen sulphide are removed from the hydrocarbons by the 'gas sweetening' processes, which involve the passing of the gas through countercurrent gas-liquid absorbers which contain an aqueous solution of an alkanolamine. A weak complex is formed, between the acidic gases and the alkanolamine, which decomposes on heating allowing the solvent to be regenerated by steam stripping. Although some data are available for the solution of carbon dioxide and hydrogen sulphide, together, or as individual solutes, in aqueous solutions of monoethanolamine^{72 73}, diethanolamine^{72 73} and diisopropanolamine⁷⁴, a complete survey of these systems would be of great benefit to the industry. It would therefore also be useful to investigate the solubility of the lower hydrocarbons in these solvent systems as well.

In the same industrial area, the ethylene glycols are used to remove water vapour from the gas stream and it would be interesting to use aqueous mixtures of monoethylene glycol, diethylene glycol and triethylene glycol as solvents for all of the gases present in a natural gas pipeline.

From a theoretical point of view, the use of gas-solvent systems to investigate the solvent structure can be extended both by varying the gas and by varying the co-solvent. Already, acetone has been used, with water,

in the study of carbon dioxide's solubility where, as for the aqueous alcohol solvents, changes in the extent of hydrogen bonding in the solution could be monitored with experimental conditions. Possible co-solvents for water in future work could be amines, sugars, or carboxylic acids. In the last case, ionisation of the acid would seriously affect the structure in liquid water by breaking up organised clusters of molecules in the vicinity of the ions. This was shown to occur when the acidic gas, carbon dioxide was dissolved in water²². Although the degree of ionisation was small, the electrostatic effect of the ions on the 'stable' configuration of water clusters was apparent in the experimental results. The suitability of the co-solvent however, depends on its own physical properties and its miscibility with water over the complete range of composition. It must be stable through the process of degassing the solvent and the composition of the mixture must be determined with high accuracy.

The choice of solute can be made now with two directions of research in mind. The size and shape of its molecule can be considered in relation to the formation of encapsulating water shells or its interaction with water in relation to the hydrophobic effect. The use of other hydrophobic gases such as carbon tetrafluoride, or sulphur hexafluoride could produce experimental observations, similar to those from this work, when dissolved in

aqueous ethanol, and perhaps even more interesting results would be obtained using the other co-solvents suggested above. With more available data and refinements in the analysis, solubility measurements could in the future become an important method for investigating hydrophobic interactions in the solution.

APPENDICES

Appendix I

The following page shows a completed data collection sheet typical of those used during the research project. The results shown relate to the solubility of butane in a water-ethanol solvent of alcohol mole fraction $x_c \approx 0.02$.

1/12/80

GAS SOLUBILITIES: butane in aqueous ethanol

 $x_A \approx 0.002$

AS ml.	SOLVENT g.	ZERO ml.	CORRECTIONS		GAS VOLUME ml.	SOLVENT WEIGHT g.
			ZERO ml	PRESS. mm		
3	100	3.3	Time = 9.45 am		Flow Rate = 650	
2.5	119.9	3.5	-0.2		0.85	19.7
	131.8	3.25	+0.05		1.35	31.85
7	143.5	3.15	+0.15		1.75	43.65
1.05	180	3.25	+0.05		3.3	80.05
2.45	189.9	3.45	-0.15		3.7	89.75
2.75	204.6	3.5	-0.2		4.35	104.4
5.5	214.3	3.35	-0.05		4.7	114.25
8.6	246.5	3.05	+0.25		5.95	146.75
7.75	258.7	3.3	—		6.55	158.7
6.65	274.2	3.7	-0.4		7.25	173.8
5.45	294.5	3.2	+0.1		7.95	194.6
5.7	314.1	3.15	+0.15		8.75	214.25
4.45	333	3.45	-0.15		9.7	232.85
4.15	342.5	3.5	-0.2		9.95	242.3
2.6	378	3.45	-0.15		11.55	277.85
1.7	401.8	3.5	-0.2		12.4	301.6
1.5	411.2	3.3	—		12.8	311.2
12/80						

Density:
(100g/20°C)0.9886

Temperature: 20.5°C

+ 273.1

T = 293.6 K

log T = 2.4677

- 2.4364

 $\frac{1}{T} = 34.06 \times 10^{-4}$

Solubility:

s = 41.2 ml kg⁻¹

log s = 1.6149

- 0.0313

log s₀ = 1.5836

Time =

Flow Rate = g/hr.

1/12/80

4.25	100	3.3	Time =		Flow Rate = 650	
4	112.5	3.15	+0.15		0.4	12.65
3.5	121.1	3.3	—		0.75	21.1
2.8	138.8	3.4	-0.1		1.35	38.7
1	190.8	3.7	-0.4		2.85	90.4
0.75	218.9	3.3	—		3.5	118.9
0.5	235.6	3.15	+0.15		3.9	135.75
7	289.2	3.15	+0.15		5.4	189.35
3.2	321.6	3.1	+0.2		6.25	221.8
0.25	386.7	3.15	+0.15		8.15	286.85
4.4	446.3	3.35	-0.05		9.8	346.25
3.8	467.3	3.3	—		10.45	367.3
2.45	515.9	3.35	-0.05		11.75	415.85
1.4	550	3.4	-0.1		12.75	449.9
1	567.7	3.3	—		13.25	467.7
0.4	578.3	3.45	-0.15		13.7	478.15
2.7	605.1	3.2	+0.1		14.65	505.2
Time =						
Flow Rate =						

Density:
(100g/20°C)0.9891

Temperature: 30.2°C

+ 273.1

T = 303.3 K

log T = 2.4819

- 2.4364

 $\frac{1}{T} = 32.97 \times 10^{-4}$

Solubility:

s = 28.17 ml kg⁻¹

log s = 1.4498

- 0.0455

log s₀ = 1.4043

Time =

Appendix II : Applesoft program - 'GRAPH' - to determine the experimental solubility.

```

5  HOME
10  PRINT "THIS PROGRAM USES DATA FROM"
11  PRINT "THE SOLUBILITY APPARATUS AND"
12  PRINT "COMPUTES THE 'BEST STRAIGHT LINE'"
13  PRINT "THROUGH THE POINTS"
14  PRINT : PRINT
15  PRINT "THE DATA GIVEN ALLOWS LIMITED"
16  PRINT "EDITING TO ACCOUNT FOR ANY"
17  PRINT "POINTS WHICH ARE IN ERROR"
18  PRINT : PRINT : PRINT "THESE CAN BE SEEN FROM THE"
19  PRINT "COLUMN HEADED '% VOL DEV'"
20  PRINT : PRINT "PRESS ANY KEY TO CONTINUE": GET A$
100 HOME
200 INPUT "WHAT IS THE OPERATING TEMPERATURE?(/C) ";T:T = T + 273.1
220 PRINT : INPUT "SOLUTE? ";AA$: PRINT
250 RT = INT (1 / T * 10 ^ 4 * 100 + .5) / 100
280 LT = (1 / 2.303) * LOG (T):DLT = LT - 2.4364
300 INPUT "HOW MANY SETS OF DATA? ";B
310 B = B + 20
320 DIM A(B),C(B),V(B),M(B),ZV(B),QV(B),S(B),Y(B),E(B),P(B),H(B),YV
(B),SO(B),Z(B),VOL(B),MASS(B),ZERO(B)
321 DIM SE(B)
322 B = B - 20
325 HOME
330 PRINT "TYPE STARTING VALUES..V,M,Z"
340 INPUT V1,M1,Z1
345 PRINT
350 FOR I = 1 TO B: INPUT "DATA ";V(I),M(I),Z(I)
360 NEXT I
362 FOR I = 1 TO B:VOL(I) = V1 - V(I):MASS(I) = M(I) - M1:ZERO(I) =
Z1 - Z(I)
364 A(I) = VOL(I) + ZERO(I):C(I) = MASS(I) + ZERO(I)
366 NEXT I
367 F = 1
368 HOME
370 PRINT " VOL MASS"
372 FOR I = F TO B:A(I) = INT (A(I) * 100 + .5) / 100:C(I) = INT
(C(I) * 100 + .5) / 100: PRINT A(I),C(I): NEXT I
374 GET A$
400 HOME
440 HGR : COLOR= 3: FOR I = 1 TO 159: HPLLOT 0,I: NEXT I: FOR I = 0
TO 279: HPLLOT I,159: NEXT I
500 FOR I = F TO B: HPLLOT C(I) / 2,160 - A(I) / 0.16: NEXT I
600 VTAB 24: PRINT "PRESS ANY KEY TO CONTINUE"
900 GET A$
1000 TEXT
1050 HOME
1400 V = 0:M = 0
1450 FOR I = F TO B
1500 V = V + A(I): NEXT I:AV = V / (I - F): FOR I = F TO B
1510 M = M + C(I): NEXT I:AM = M / (I - F)
1520 AV = INT (AV * 100 + .5) / 100
1530 AM = INT (AM * 100 + .5) / 100
1540 FOR I = F TO B:A(I) = INT (A(I) * 100 + .5) / 100
1550 C(I) = INT (C(I) * 100 + .5) / 100: NEXT I
1560 FOR I = F TO B:ZV(I) = (C(I) - AM) * (A(I) - AV)
1570 ZV = ZV + ZV(I): NEXT I
1580 FOR I = F TO B:QV(I) = (C(I) - AM) ^ 2
1582 YV(I) = (A(I) - AV) ^ 2:YV = YV + YV(I)
1590 QV = QV + QV(I)
1592 NEXT I

```

Appendix II (Contd)

```

1600 CO = ZV / QV
1601 RV = ZV / ( SQR (QV * YV)):RV = INT (RV * 10000 + .5) / 10000
1602 S = 0: HOME : PRINT " "AA$: PRINT
1603 PRINT "VOL      MASS      %VOL DEV      V*1000/M"
1604 ZV = 0:QV = 0:YV = 0:SE = 0
1605 FOR I = F TO B
1608 SD(I) = INT ((A(I) * 1000 / C(I)) * 100 + .5) / 100
1610 Y(I) = CO * (C(I) - AM) + AV
1611 CE = CO * (O - AM) + AV
1612 S(I) = ((Y(I) - CE) * 1000) / C(I):S = S + S(I)
1615 Y(I) = INT (Y(I) * 100 + .5) / 100:S(I) = INT (S(I) * 100 + .5) / 100
1616 P(I) = INT (((Y(I) - A(I)) * 100 + .5) / A(I))
1617 SE(I) = (Y(I) - A(I)) ^ 2
1618 PRINT A(I) TAB( 10)C(I) TAB( 22)P(I) TAB( 32)SD(I)
1620 SE = SE + SE(I): NEXT I:SD = INT (((SE / B) ^ 0.5) * 10000 + .5) / 10000
1621 PRINT : PRINT "CORREL.COEFFICIENT= ";RV: PRINT : PRINT "AVERAGE ERROR= ";SD;" CC"
1622 PRINT : INPUT "OMIT DATA?(Y/N) ";Z$
1623 IF Z$ = "Y" THEN GOSUB 3000: GOTO .368
1626 PRINT
1628 PRINT "T= ";T;" 1/T*10^4= ";RT: PRINT : PRINT
1630 PRINT : PRINT "AVERAGE SOLUBILITY= "; INT (S / (I - F) * 100 + .5) / 100
1680 LSO = ((1 / 2.303) * LOG (S / (I - F))) - DLT
1700 PRINT : PRINT "LOG SOLUBILITY= "; INT (LSO * 1000 + .5) / 1000
1710 PRINT : INPUT "RETURN TO EDIT?(Y/N) ";B$
1712 HOME
1714 IF B$ = "Y" THEN GOTO 1622
1800 PRINT : INPUT "MORE DATA?(Y/N) ";M$: PRINT
1805 IF M$ = "Y" THEN GOSUB 2500: GOTO 362
1810 END
2500 B = B + 1: INPUT "DATA ";V(B),M(B),Z(B)
2550 HOME
2600 RETURN
3000 PRINT : PRINT "TYPE NUMBER OF SETS TO BE OMITTED"
3100 INPUT L:F = L + 1
3200 RETURN

```

J

Appendix III (a) : Applesoft program - 'MAKE CURVE' - to
calculate a possible solubility curve.

```

-----
0 D$ = CHR$ (4): PRINT "OPEN          DATA"
5 HOME
10 PRINT "CHOOSE THREE RELIABLE POINTS IN A ROW"
20 PRINT "COUNT FROM THE LEFT AND LET N BE THE"
30 PRINT "MIDDLE ONE": PRINT : INPUT "N = ";B
40 N = B
50 PRINT : PRINT "NOW TYPE IN THE VALUES OF THE POINTS"
60 PRINT "CORRESPONDING TO N-1,N AND N+1"
100 INPUT LS(N - 1),LS(N),LS(N + 1)
200 X(N - 1) = LS(N) - LS(N - 1)
300 X(N) = LS(N + 1) - LS(N)
400 X(N + 1) = X(N) + (X(N) - X(N - 1))
500 LS(N + 2) = LS(N + 1) + X(N + 1)
600 IF B > 2 THEN GOSUB 6900: GOTO 880
780 IF N = 8 THEN GOTO 880
800 N = N + 1: GOTO 200
880 PRINT : PRINT
890 PRINT : PRINT : PRINT "1/T*10^4      LOG S0": PRINT
900 FOR I = 1 TO 7: S = 29: S = S + I: PRINT S, INT (LS(I) * 10000 +
.5) / 10000: NEXT I
905 PRINT : INPUT "IF THIS DATA IS OK, TYPE OK ";OK$
906 IF OK$ = "OK" THEN GOTO 1000
910 PRINT : PRINT "TO CHANGE LS("B") TYPE NEW VALUE"
920 INPUT "HERE ";A
925 N = B
930 LS(N) = A: HOME : GOTO 200
1000 D$ = CHR$ (4): PRINT D$;"OPEN DATA"
1100 FOR I = 1 TO 7: LL(I) = LS(8 - I): NEXT I
1200 PRINT D$;"WRITE DATA"
1300 FOR I = 1 TO 7: PRINT LL(I): NEXT I
1400 PRINT D$;"CLOSE DATA"
1410 PRINT : PRINT "YOUR DATA IS NOW IN A TEXT FILE": PRINT
1450 PRINT : PRINT : PRINT "YOU CAN CHECK THIS CURVE"
1460 PRINT "BY RUNNING PROG. 'CURVE TEST'"
1470 PRINT : INPUT "DO YOU WANT TO DO THIS?(Y/N) ";Z$
1480 IF Z$ = "Y" THEN PRINT D$;"RUN CURVE TEST"
5000 END
6900 IF N = 6 THEN X(4) = X(N) - 2 * (X(N) - X(N - 1)):LS(4) = LS(5
) - X(4):N = N - 1
7000 IF N = 5 THEN X(3) = X(N) - 2 * (X(N) - X(N - 1)):LS(3) = LS(4
) - X(3):N = N - 1
7250 IF N = 4 THEN X(2) = X(N) - 2 * (X(N) - X(N - 1)):LS(2) = LS(3
) - X(2)
7300 IF N = 4 THEN X(6) = X(5) + (X(N) - X(N - 1)):LS(7) = LS(6) +
X(6):N = N - 1
7500 IF N = 3 THEN X(1) = X(N) - 2 * (X(N) - X(N - 1)):LS(1) = LS(2
) - X(1)
7550 IF N = 3 THEN X(5) = X(4) + (X(N) - X(N - 1)):LS(6) = LS(5) +
X(5):X(6) = X(5) + (X(N) - X(N - 1)):LS(7) = LS(6) + X(6)
7600 RETURN

```

Appendix III (b) : Applesoft program - 'CURVE TEST' - to check
the curve proposed by (a).

```

100 HOME
110 IF S$ = "Y" THEN S$ = "N"
150 INPUT "IS YOUR DATA IN A TEXT FILE?(Y/N) ";W$
160 IF W$ = "Y" THEN 920
180 PRINT : PRINT
200 PRINT "TYPE IN CORRESPONDING VALUES OF"
300 PRINT "LOG SO FROM THE SOLUBILITY CURVE"
350 PRINT : PRINT : PRINT
380 INPUT "36      ";A(1)
400 INPUT "35      ";A(2)
500 INPUT "34      ";A(3)
600 INPUT "33      ";A(4)
700 INPUT "32      ";A(5)
800 INPUT "31      ";A(6)
900 INPUT "30      ";A(7)
910 GOTO 1000
920 D$ = CHR$(4): PRINT D$;"OPEN DATA"
930 PRINT D$;"READ DATA"
940 FOR I = 1 TO 7: INPUT A(I): NEXT I
950 PRINT D$;"CLOSE DATA"
1000 DL(1) = A(1) - A(2)
1100 DL(2) = A(2) - A(3)
1200 DL(3) = A(3) - A(4)
1300 DL(4) = A(4) - A(5)
1400 DL(5) = A(5) - A(6)
1450 DL(6) = A(6) - A(7)
1500 DD(1) = DL(1) - DL(2)
1600 DD(2) = DL(2) - DL(3)
1700 DD(3) = DL(3) - DL(4)
1800 DD(4) = DL(4) - DL(5)
1900 DD(5) = DL(5) - DL(6)
3900 HOME
3950 PRINT "1/T      LOG SO      DLSO      DDLSO"
3955 PRINT : PRINT
3957 DEF FN A(X) = INT (A(X) * 10000 + .5) / 10000
3960 DEF FN DL(X) = INT (DL(X) * 10000 + .5) / 10000
3965 DEF FN DD(X) = INT (DD(X) * 10000 + .5)
3980 FOR X = 1 TO 7:A(X) = FN A(X): NEXT X
4000 PRINT "36      "A(1)
4100 HTAB 16: PRINT FN DL(1)
4200 PRINT "35      "A(2) TAB( 25) FN DD(1)
4300 HTAB 16: PRINT FN DL(2)
4400 PRINT "34      "A(3) TAB( 25) FN DD(2)
4500 HTAB 16: PRINT FN DL(3)
4600 PRINT "33      "A(4) TAB( 25) FN DD(3)
4700 HTAB 16: PRINT FN DL(4)
4800 PRINT "32      "A(5) TAB( 25) FN DD(4)
4900 HTAB 16: PRINT FN DL(5)
5000 PRINT "31      "A(6) TAB( 25) FN DD(5)
5001 HTAB 16: PRINT FN DL(6)
5002 PRINT "30      "A(7)

```

Appendix III (b) (Contd)

```
5005 PRINT : PRINT
5008 IF S$ = "Y" THEN PR# 0: PRINT : GOTO 5100
5010 INPUT "CHANGE DATA?(Y/N) ";T$
5020 IF T$ < > "Y" THEN 5280
5030 PRINT : PRINT "TO ALTER DATA,TYPE SET NUMBER (1-6)"
5040 INPUT S
5050 PRINT : INPUT "NEW LSO= ";Y
5060 A(S) = Y: PRINT : GOTO 1000
5090 PRINT : INPUT "DO YOU WANT A PRINTED COPY?(Y/N) ";S$
5095 IF S$ = "Y" THEN PR# 1: GOTO 3955
5100 PRINT : INPUT "USE PROGRAM AGAIN?(Y/N) ";X$
5200 IF X$ = "Y" THEN GOTO 100
5250 IF W$ = "Y" THEN PRINT D$;"DELETE DATA"
5260 END
5280 PRINT : INPUT "DO YOU WANT A PRINTED COPY?(Y/N) ";S$
5285 IF S$ = "Y" THEN PRINT : INPUT "SOLUTE IS ";AA$
5290 IF S$ = "Y" THEN PR# 1: PRINT AA$: GOTO 3955
5300 PRINT : GOTO 5100
```

]

Appendix IV : Algol program - 'FINDH' - to evaluate $\Delta \bar{H}^\circ$ for
temperatures midway between integral values of
 $10^4/T$.

```

00100 BEGIN INTEGER N,X,T;
00200 INPUT(2,"DSK");SELECTINPUT(2);OPENFILE(2,"NEO.DAT");
00300 READ (N);
00400 BEGIN ARRAY LC1:N+1,1:7,1:2];
00500 OUTPUT (1,"TTY");SELECTOUTPUT(1);
00600 WRITE ("CHECK DH
00700 X      289.9      298.5      307.7      317.5      327.9");
00800 FOR T:=1 STEP 1 UNTIL 7 DO
00900 FOR X:=1 STEP 1 UNTIL N+1 DO
01000 READ (LCX,T,1]);
01100 FOR X:=2 STEP 1 UNTIL N+1 DO
01200 FOR T:=2 STEP 1 UNTIL 6 DO
01300 LCX,T,2]:=191.44*(LCX,T+1,1]-LCX,T,1]);
01400 FOR X:=2 STEP 1 UNTIL N+1 DO
01500 BEGIN NEWLINE;
01600 PRINT (LCX,1,1],1,3); SPACE(3); FOR T:=2 STEP 1 UNTIL 6 DO
01700 BEGIN PRINT (LCX,T,2],2,2); SPACE(4); END
01800 END
01900 END;
02000 END;

```

Appendix V : Applesoft program - 'CHECK DH' - to numerically determine values of $\Delta \bar{H}_{290}^{\circ}$, $\Delta \bar{H}_{310}^{\circ}$, $\Delta \bar{C}_{pT}^{\circ} < 300$ and $\Delta \bar{C}_{pT}^{\circ} > 300$.

```

100 HOME
150 INPUT "HOW MANY TEMP. VALUES? ";K: PRINT
200 PRINT "TYPE IN TEMP. VALUES": PRINT
300 FOR I = 1 TO K: INPUT T(I): NEXT I
350 PRINT : INPUT "HOW MANY CURVES? ";B
355 PRINT : PRINT "TYPE IN MOLE FRACTION VALUES"
360 FOR I = 1 TO B: INPUT XA(I): NEXT I
400 PRINT : PRINT "NOW TYPE IN DH VALUES...."
410 PRINT "ONE ROW AT A TIME. PRESS RETURN AFTER EACH ENTRY"
500 DIM A(K,B)
600 FOR J = 1 TO B: FOR I = 1 TO K: INPUT A(I,J): NEXT I: NEXT J
620 PRINT : PRINT : PRINT
630 PRINT " XA          DCP          DH"
640 PRINT
650 A = 1: C = 2: F = 290
700 FOR I = A TO C: TT = TT + T(I): NEXT I
800 OT = TT / (I - 1): OT = INT (OT * 10 + .5) / 10
900 FOR J = 1 TO B: FOR I = A TO C: LL(J) = LL(J) + A(I,J)
1000 NEXT I: NEXT J
1100 FOR J = 1 TO B: AL(J) = LL(J) / (I - 1): AL(J) = INT (AL(J) * 10 + .5) / 10: NEXT J
1200 FOR J = 1 TO B: FOR I = A TO C: BT(J) = (T(I) - OT) * (A(I,J) - AL(J)): BT(J) = INT (BT(J) * 10 + .5) / 10
1300 DT(J) = (T(I) - OT) ^ 2: DT(J) = INT (DT(J) * 10 + .5) / 10
1400 XT(J) = XT(J) + BT(J): YT(J) = YT(J) + DT(J)
1500 NEXT I: NEXT J
1600 FOR J = 1 TO B: CO(J) = XT(J) / YT(J)
1700 Y(J) = CO(J) * (T(I) - OT) + AL(J)
1800 CE(J) = CO(J) * (O - OT) + AL(J)
1900 S(J) = CO(J) * F + CE(J)
1920 S(J) = INT (S(J) * 10 + .5) / 10
1950 CO(J) = INT (CO(J) * 10000 + .5) / 10000
2000 PRINT XA(J) TAB( 14)CO(J) * 1000 TAB( 26)S(J)
2100 NEXT J
2150 PRINT : IF A = 3 THEN GOTO 2400
2200 A = 3: C = K: F = 310
2300 GOTO 700
2400 END

```


Appendix VI : Algol program - 'HYDRAL' - to evaluate $\Delta \bar{G}^\circ$, $\Delta \bar{H}^\circ$, $\Delta \bar{S}^\circ$, K_H and x_{gas} .

```

00100      BEGIN  INTEGER N,X,T;
00200          INPUT(2,"DSK");SELECTINPUT(2);OPENFILE(2,"BBOL.DAT");
00300          READ( N);
00400      BEGIN  ARRAY LC1:N+1,1:12,1:8;
00500          OUTPUT(1,"TTY");SELECTOUTPUT(1);
00600          WRITE('BASIC FUNCTIONS
00700      X      1/T      S(CC/KG)      LOG S      DCP1      DCP2      DG(KJ)
          DH(KJ)      DS(J/K)      XGAS*1000      KH/1000
00800      ');
00900          FOR T:=1 STEP 1 UNTIL 12 DO
01000          FOR X:=1 STEP 1 UNTIL N+1 DO
01100          READ( LCX,T,1);
01200          FOR X:=2 STEP 1 UNTIL N+1 DO
01300      BEGIN  LCX,9,2]:=-LCX,11,1]*1000-290*LCX,9,1];
01400          LCX,10,2]:=-LCX,12,1]*1000-310*LCX,10,1];
01500          LCX,1,2]:=1000/(LC1,1,1]*LCX,1,1]/(1-LCX,1,1])+18);
01600          LCX,1,3]:=LCX,1,1]*LCX,1,2]/(1-LCX,1,1]);
01700          FOR T:=2 STEP 1 UNTIL 4 DO
01800          LCX,T,7]:=(LCX,9,2]+LCX,9,1]/LC1,T,1])/1000;
01900          FOR T:=5 STEP 1 UNTIL 8 DO
02000          LCX,T,7]:=(LCX,10,2]+LCX,10,1]/LC1,T,1])/1000;
02100      FOR T:=2 STEP 1 UNTIL 8 DO
02200      BEGIN  LCX,T,2]:=EXP(2.3026*LCX,T,1)];
02300          LCX,T,3]:=LCX,T,2]/LC1,9,1];
02400          LCX,T,4]:=1000*LCX,T,3]/(LCX,T,3]+LCX,1,2]+LCX,1,3)];
02500          LCX,T,5]:=1/LCX,T,4];
02600          LCX,T,6]:=-8.314*LN(LCX,T,4]/1000)/(LC1,T,1]*1000);
02700          LCX,T,8]:=((LCX,T,7]-LCX,T,6])*LC1,T,1])*1000;
02800          NEWLINE;
02900          PRINT(LCX,1,1],1,3);SPACE(1);PRINT(LC1,T,1
],1,4);SPACE(2);
03000      PRINT(LCX,T,2],4,0);SPACE(6);PRINT(LCX,T,1],1,3);SPACE(4);PR
INT(LCX,9,1],3,0);
03100      SPACE(4);PRINT(LCX,10,1],3,0);SPACE(3);
03200      PRINT(LCX,T,6],2,2);SPACE(5);PRINT(LCX,T,7],2,1);SPACE(5);PR
INT(LCX,T,8],3,0);
03300      SPACE(6);PRINT(LCX,T,4],2,3);SPACE(5);PRINT(LCX,T,5],2,3);
03400          END;
03500      NEWLINE;
03600          END;
03700      END;
03800          END;

```

REFERENCES

References

1. Fox, C.S., 'Water', (The Technical Press (London)),
21, (1952).
2. Ben-Naim, A., and Baer, S., Trans. Far. Soc., 59,
2735, (1964).
3. Cargill, R.W., and Morrison, T.J., J.Chem. Soc. Far.
Trans. I., 71, 618, (1975).
4. McAuliffe, C., J. Phys. Chem. 70, 1267, (1966).
5. Morrison, T.J., and Billett, F., J. Chem. Soc.,
2033, (1948); 3819, (1952).
6. Wetlaufer, D.B., Malik, S.K., Stoller, L., and Coffin,
R.L., J. Am. Chem. Soc., 86, 508, (1964).
7. Yaacobi, M., and Ben-Naim, A., J. Soln. Chem.,
2, 425, (1972).
8. Winkler, L.W., Ber., 22, 1764, (1889).
9. Klotz, C.E., and Benson, B.B., J. Marine Res.,
21, 48, (1963).
10. Bohr, N., Ann. Physik, 68, 500, (1899).
11. van Slyke, D.D. and Neill, J.M. J. Biol. Chem., 61, 523,
(1924).
12. Burrows, G., and Preece, F.H. J. Appl. Chem., (London),
3, 451, (1953).
13. Cook, M.W., and Hanson, D.N., Rev. Sci. Instr.,
28, 370, (1957).
14. Gerrard, W., 'The Solubility of Gases in Liquids',
(Plenum), 3, (1976).
15. Cosgrove, B.A., and Walkley, J., J. Chromatog., 216,
161, (1981).
16. Brown, I., Ann. Rev. Phys. Chem., 16, 147, (1965).
17. Markham, A.E., and Kobe, K.A., Chem. Revs., 519, (1941).
18. Battino, R., and Clever, H.L., Chem. Revs., 66, 395,
(1966).
19. Henry, W., Phil. Trans. Roy. Soc. (London), 29, 274,
(1803).
20. Bunsen, R.W., Phil. Mag., 9, 116, 181, (1855).
21. Ostwald, W., 'Manual of Physico-Chemical Measurements',
(The Macmillan Company, (London)), 172-5, (1894).
22. Cargill, R.W., and Macphee, D.E., J. Chem. Research,
(M), 2743, (1981).

References (Contd)

23. Tokunaga, J., J.Chem. Eng. D., 20, 41, (1975).
24. Cseko, G., Chem. Abstr., 56, 5449, (1962).
25. Tippet, L.H.C., 'Technological Applications of Statistics', (Williams and Norgate Ltd (London)), 148, (1952).
26. International Critical Tables, Vol III, (McGraw-Hill Book Company Inc., (New York and London)), 112 and 116-117, (1928)
27. Cargill, R.W., J.C.S. Far. Trans. I, 72, 2296, (1976).
28. Cargill, R.W., J.C.S. Far. Trans. I, 74, 1444, (1978).
29. Berry, R.S., Rice, S.A., and Ross, J., 'Physical Chemistry', (Wiley), 743, (1980).
30. 'Handbook of Chemistry and Physics', 56th Edition, (Chemical Rubber Co.), D178, (1975-76).
31. Braker, W., and Mossman, A.L., 'Matheson Gas Data Book', (Matheson Gas Products), 73, 167, 225, 331, 489, 497, (1971).
32. Caldin, E.F., 'Chemical Thermodynamics', (Oxford Univ. Press) 99, (1958).
33. Ben-Naim, A., Wilf, J., and Yaacobi, M., J. Phys. Chem, 77, 95, (1973).
34. Arnett, E.M., 'Physico-Chemical Processes in Mixed Aqueous Solvents', Ed. Franks, F. (Heinemann Educational Books Ltd, (London)), 117, (1969).
35. Rossky, P.J., and Zichi, D.A., 17th Faraday Symposium, (4); (1982).
36. Bernal, J.D., and Fowler, R.H., J.Chem. Phys., 1, 515, (1933).
37. Pople, J.A., Proc. Roy. Soc. London, A205, 163, (1951).
38. Nemethy, G., and Scheraga, H.A., J.Chem. Phys., 36, 3382, (1962).
39. Frank, H.S., and Wen, W.Y., Disc. Far. Soc., 24, 133, (1957).
40. Hagler, A.T., Scheraga, H.A., and Nemethy, G., J.Phys. Chem., 76, 3229, (1972).
41. Conway, B.E., 'Ionic Hydration in Chemistry and Biophysics', (Elsevier), 291, (1981).
42. Walrafen, G.E., J.Chem. Phys., 44, 1546, (1966).
43. Holba, V., Coll. Czech. Chem. Comm., 47, 2484, (1982).
44. Conway, B.E., 'Ionic Hydration in Chemistry and Biophysics', (Elsevier), 37 & 38, (1981).

References (Contd)

45. Davis, C.M., and Litovitz, T.A., J.Chem. Phys., 42,
2563, (1965).
46. Baur, W.H., Acta. Cryst., 19, 901, (1965).
47. Morgan, J., and Warren, B.E., J.Chem. Phys., 6, 666,
(1938).
48. Vand, V., and Senior, W.A., J.Chem. Phys., 43, 1869,
1873, 1878, (1965).
49. Buijs, K., and Choppin, G.R., J.Chem. Phys., 39, 2035,
(1963).
50. Stillinger, F., and Rahman, A., J.Chem. Phys., 60,
1545, (1974).
51. Ben-Naim, A., and Stillinger, F., 'Water and Aqueous
Solutions' (Ed. Horne), 295, (1972).
52. Narten, A.H., and Levy, H.A., J.Chem. Phys., 55, 2263,
(1971).
53. Lemberg, H.L., and Stillinger, F., J.Chem. Phys.,
62, 1677, (1975).
54. Hirata, F., and Rossky, P.J., J.Chem. Phys., 74, 6867,
(1981).
55. Geiger, A., Rahman, A., and Stillinger, F., J.Chem.
Phys., 70, 263, (1979).
56. Kauzmann, W., Adv. Prot. Chem., 14, 1, (1959).
57. Nemethy, G., and Scheraga, H.A., J.Chem. Phys., 36,
3401, (1962).
58. Nemethy, G., and Scheraga, H.A., J.Phys. Chem., 66,
1773, (1962).
59. Frank, H.S., and Evans, M.W., J.Chem. Phys., 13, 507,
(1945).
60. Ben-Naim, A., J.Chem. Phys., 54, 1387, (1971).
61. Ben-Naim, A., J.Chem. Phys., 57, 5257, (1972).
62. Friedman, H.L., and Krishnan, C.V., J.Soln. Chem.,
2, 119, (1973).
63. Clark, A.H., Franks, F., Pedley, M.D., and Reid, J.,
J.C.S. Far. I, 290, (1977).
64. Kresheck, G.C., Schneider, H., and Scheraga, H.A.,
J.Phys. Chem., 69, 3132, (1965).
65. Wilf, J., and Ben-Naim, A., J.Phys. Chem., 83, 3209,
(1979).
66. Rupley, J.A., Gratton, E., and Careri, G., 'Trends
in Biological Sciences', 18, January (1983).

References (Contd)

67. Rupley, J.A., Yang, P.H., and Tollin, G., 'Water in Polymers', A.C.S. Symposium No. 127, Ed. Rowland, S.P., 111, (1980).
68. Conway, B.E., 'Ionic Hydration in Chemistry and Biophysics' (Elseveir), 523, (1981).
69. Abraham, M.H., J.Am. Chem. Soc., 104, 2085, (1982).
70. Spink, C.H., and Colgan, S., J.Phys. Chem., 87, 888, (1983).
71. Amidon, G.L., and Anik, S.T., J.Phys. Chem., 84, 970, (1980).
72. Lawson, J.D., and Garst, A.W., J.Chem. Eng. D., 21, 20, (1976).
73. Lee, J.I., Otto, F.D., and Mather, A.E., J.Chem.Eng. D., 17, 465, (1972); 20, 161, (1975).
74. Isaacs, E.E., Otto, F.D., and Mather, A.E., J.Chem. Eng. D., 22, 71, (1977).
75. 'Handbook of Chemistry and Physics', 61st Edition, (Chemical Rubber Co.), D 194, (1980-81).